

FACILITY FORM 802

269-38618	
(ACCESSION NUMBER)	
291	
(PAGES)	
NASA CR# 101931	
(NASA CR OR TMX OR AD NUMBER)	
	(THRU)
	1
	(CODE)
	28
	(CATEGORY)

A-1080

FINAL REPORT

VOLUME 3

APOLLO SM-LM RCS ENGINE DEVELOPMENT  
PROGRAM SUMMARY REPORT

Contract NAS 9-7281

EDITED BY:

*J. F. Foote*  
J. F. Foote  
Project Engineer

APPROVED BY:

*D. C. Sund*  
D. C. Sund  
Senior Project Engineer  
*L. R. Bell, Jr.*  
L. R. Bell, Jr.  
Chief Engineer

*C. A. Kerner*  
C. A. Kerner  
Program Manager

TABLE OF CONTENTS

VOLUME 1

Preface

Chapter 1 Marquardt R-4D Engine Development

VOLUME 2

Chapter 2 Thermal Management

Chapter 3 Space Ignition Characteristics

Chapter 4 Gas Pressurization Effects

Chapter 5 Contamination Control

Chapter 6 System Dynamic Effects

VOLUME 3

Chapter 7 Structural Design

Chapter 8 Material Selection

Chapter 9 Propellant Valve Design

Chapter 10 Injector Design

Chapter 11 Thrust Chamber Design

VOLUME 4

Chapter 12 Test Facilities and Instrumentation

Chapter 13 Test Data Analysis

Chapter 14 Flight Test Experience

Chapter 15 Reliability

# TABLE OF CONTENTS

	<u>Page</u>
I INTRODUCTION	7-1
II STRUCTURAL DESIGN CRITERIA	7-1
III MAJOR COMPONENTS	7-5
Bell	7-5
Combustion Chamber-Bell Joint	7-5
Combustion Chamber	7-7
Combustion Chamber Attach Hardware	7-9
Propellant Valves	7-11
Injector	7-14

LIST OF ILLUSTRATIONS

<u>Figure Number</u>	<u>Title</u>	<u>Page</u>
1	R-4D Engine	7-2
2	Typical Vibration Requirement	7-4



LIST OF TABLES

<u>Table Number</u>	<u>Title</u>	<u>Page</u>
I	Table of Critical Structural Criteria	7-3
II	Bell Analysis Table of Margins	7-6
III	Joint-Combustion Chamber to Bell Table of Margins	7-8
IV	Combustion Chamber (228128) Minimum Margins of Safety & Allowable Pressures	7-10
V	Attach Hardware Soak Back - Space Operation	7-12
VI	Attach Hardware Rocket Engine - Reaction Control Structural Evaluation	7-13
VII	Stress Analysis of the Fuel and Oxidizer Valves Minimum Margins of Safety	7-15
VIII	Injector Head Table of Minimum Margins of Safety	7-18

## I. INTRODUCTION

The Marquardt R-4D engine is a bipropellant rocket engine of 100 lbs. nominal thrust. It is used for attitude control or  $\Delta V$  applications and as such it must be able to structurally withstand the stresses imposed by space and launch and the stresses of its own operation. The engine (Figure 1) is radiation cooled. It is mounted outside the spacecraft where it is free to radiate to space but it may also be exposed to the air loads during launch. It also feels the vibration loads during launch and in space when other larger  $\Delta V$  engines fire. Few structural problems occurred during the development of the engine primarily because of the structural analysis of the engine design. The engine was also tested to confirm structural integrity of the engine. For example, tests were made to simulate the vibration loads during launch and in space. Engine tests were also made to confirm that the engine imposed stresses (thermal and ignition) would not damage the engine.

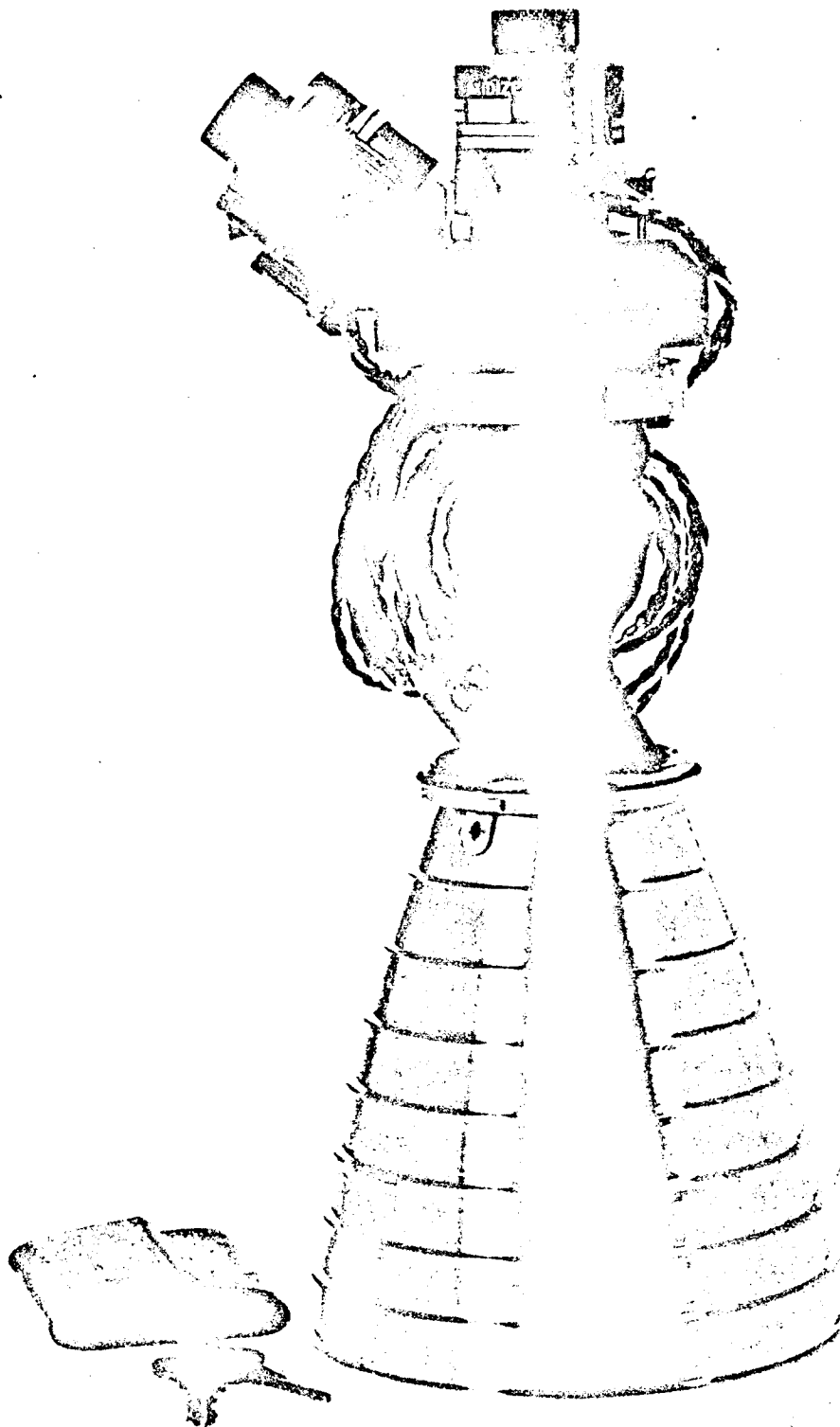
## II. STRUCTURAL DESIGN CRITERIA

The engine must be designed to withstand several different environments and its own operating loads. It must be designed for boost, space, the loads it applies to itself when it operates, and special specification requirements, for example, the propellant supply pressures. The critical structural criteria for the engine components are shown in Table I.

During boost the engine may be exposed to air loads (Apollo Service Module) in addition to vibration from the booster. Once in space, the engine will experience vibration from the spacecraft thrusters. These conditions are critical to the design of the combustion chamber, combustion chamber-bell joint, bell, chamber injector attach hardware, injector head and valves. Figure 2 shows the vibration spectrum for both space and boost. Boost vibration is more severe than space but in space the engines may be operating at the same time as the spacecraft thrusters and the engines may be hot or cold. Both cases were considered in the design.

Tests were made to confirm that the engine would withstand the structural loads. For example, during the qualification tests five engines successfully completed the boost vibration test and three engines successfully completed the space vibration test. One engine also completed a static load limit test simulating the loads during boost. During the Off-Limit tests, one engine successfully completed a vibration test with three times the vibration loads of the boost conditions.

The structural design of the major components of the engine are discussed in the following sections.



R-4D ENGINE

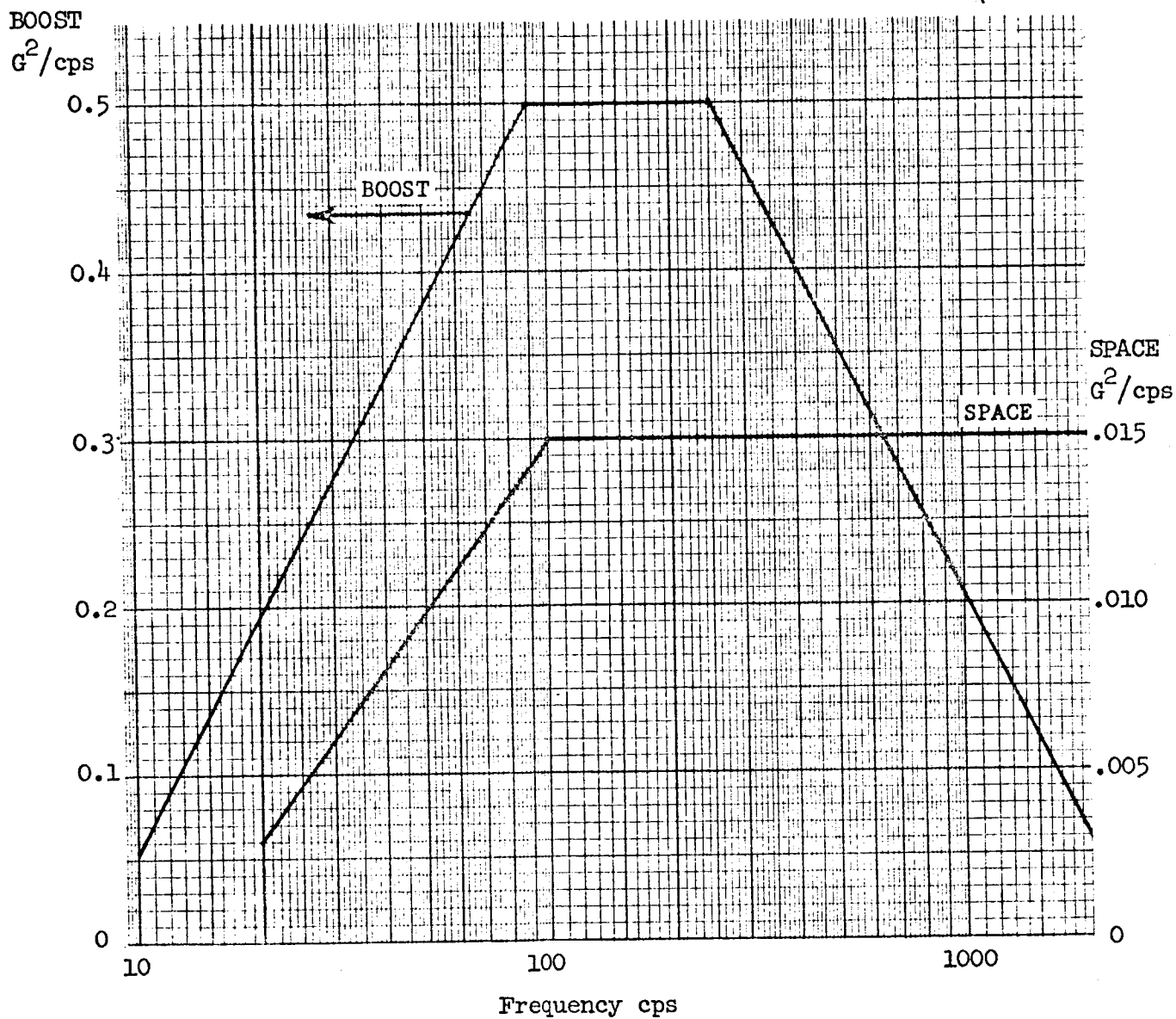
FIGURE 1

The critical structural criteria for the various components are shown below:

TABLE I  
TABLE OF CRITICAL STRUCTURAL CRITERIA

COMPONENTS	CRITERIA
Combustion Chamber	<ol style="list-style-type: none"> <li>Maximum Spike Pulse During Starts <ol style="list-style-type: none"> <li>Spike - Uniform Pressure . . . . .</li> <li>Non-Uniform Spike. . . . .</li> </ol> </li> <li>Boost Condition - Airloads + Vibration = 9.9 psi + 116 "g" . . . . .</li> <li>Space Vibration - Hot &amp; Vibrating = 19.5 "g". . . . .</li> <li>Temperatures Assumed. . . . .</li> </ol>
Two-Piece Joint (attachment nut)	<ol style="list-style-type: none"> <li>Boost Condition - Airload + Vibration - G Loads . . . . .</li> <li>Space Operation - Hot Vibration - G Loads . . . . .</li> <li>Temperatures. . . . .</li> </ol>
Bell	<ol style="list-style-type: none"> <li>Boost Condition - Airloads + Vibration Loads. . . . .</li> <li>Space Operation - Hot Vibration - Loads . . . . .</li> <li>Temperatures. . . . .</li> </ol>
Attach Hardware	<ol style="list-style-type: none"> <li>Preload Stresses . . . . .</li> <li>Boost Condition - Airloads + Vibration . . . . .</li> <li>Space Operation - Thermal Increments . . . . .</li> </ol>
Injector Head	<ol style="list-style-type: none"> <li>Insert Shrink Fits - Pressure Spike Capability</li> <li>Explosion Pressures of 15000 psi in Standoff Area</li> <li>Explosion Pressures of 50000 psi in Injector Tubes</li> <li>Operational Temperatures &amp; Pressures</li> <li>Boost Condition - Engine Flange Bending - Valve Attach Flanges Bending</li> </ol>
Valves	<ol style="list-style-type: none"> <li>Boost Vibration</li> <li>Burst Pressure - 700 psig ULT. Ref. Spec. . . . .</li> <li>Explosion on Valve Poppet Seat - Dynamic Loads</li> <li>Installation Loads - Bolt Installation . . . . .</li> </ol>

# TYPICAL VIBRATION REQUIREMENT



### III. MAJOR COMPONENTS

#### A. Bell

The separate bell for this design was chosen because of the handling and fabrication problems associated with a thin-walled molybdenum nozzle. After coating and recrystallization, the thin walled moly nozzle was very brittle. Most nozzles can be made very thin to withstand the gas forces alone. However, if made to such thicknesses, handling problems become of great significance.

The bell is made of L-605 alloy and is of a ribbed configuration for minimum weight. The principal load and design condition is the Boost condition. This condition imposes high asymmetrical pressures on the bell from the air loads as well as large vibratory forces. The critical failure mode is Rib Bending for the unsymmetrical airload. The rib reacts the airload on the skin. The method of analysis was based on the summation of local loads on a ring.

The rib design was chosen on the basis of minimum weight. A uniformly thick-walled bell would be approximately twice as heavy for the same strength.

The High Temperature Operational condition in space is not critical in comparison because the vibratory loads are low and the internal pressure loads are negligible. The most critical portion of the bell is adjacent to and downstream of the joint. Temperatures can be very high in this locality. For the Space Operation condition, the longitudinal bending stresses in the skin were computed for the vibratory loads.

Table II shows the margin of safety for the different boost and space conditions.

#### B. Combustion Chamber-Bell Joint

The bell is joined to the combustion chamber by means of a clamping nut. The loads are transmitted to the nut by the threaded end of the bell. The nut serves to maintain sufficient clamping force between the combustion chamber and the bell to prevent opening during Boost and Space Operation. Prevention of opening is desired so that the coated molybdenum will not be subjected to impact loads.

The nut is made of Waspaloy, heat treated in order to obtain high strength during Boost and at the high temperatures existing during Space Operation. In addition, Waspaloy has sufficient ductility to withstand the many thermal cycles of wide load variation experienced during the mission duty cycle.

The nut acts as a flexible, flanged ring with a clamping lip. The nut is loaded at the inner edge of the lip, causing radial bending on the lip and tangential stresses in the ring (of the nut). The radial bending stresses predominate and are almost uniform throughout the lip. If the lip thickness was very large, the ring could have been analyzed as a torus. The design chosen was done to save weight.

TABLE II

BELL ANALYSIS  
TABLE OF MARGINS

PART & PART #	MATERIAL	Temp. (°F)	Type of Loading	Actual Stress (ksi)	Allow. Stress (ksi)	Margin of Safety
<u>BELL (228101):</u>						
Ring- 2.976 aft of joint.	L-605	250	Boost (pressure)	37.0 lmt.bend & compression	37.4 Yield	+ .01
Bell-Skin .837-1.584	L-605	250	Boost (pressure & vibra.)	32.2 lmt.bend and tension.	37.4 Yield	+ .16
Bell-Skin at the exit	L-605	250	Boost (pressure)	28.0 lmt.bend	37.4	+ .33
Bell-Skin .837-1.584	L-605	2200	Space Operation vibration.	.54 lmt.bend	1.75 Fatigue	2.35

The critical loading condition is Boost. The nut is preloaded so as not to open under the maximum combined airload plus vibration, i.e., required clamp load = 241 pounds per inch, minimum preload = 294 pounds per inch. The Space Operation Margin is based on a maximum temperature of 1800°F for the 1.25 G load and the residual clamping load. The 3 G vibration load results in a higher margin based on Short Time Allowable.

Relaxation of the nut at high temperature was based on TMC tests. The relaxation strength, at the end of a 20 minute period of maximum temperature, was used to calculate the clamping force remaining after relative thermal expansion had taken place. The remaining clamping force was in excess of the maximum vibratory load. The calculated values are:

Clamping Force = 17.4 pounds per inch circumferential nut vs  
11.5 pounds per inch applied force from the  
3 G vibration.

The application of the nut clamping load caused shear on the threads of the bell and rotation of the flange of the bell. The bell threads are more critical than the nut threads because the L-605 is much weaker than the Waspaloy. Even so, the Margin of Safety in shear on the threads is large. The rotation of the flange due to the clamping loads results in circumferential stresses. An example of the Margins of Safety Table is shown in Table III.

### C. Combustion Chamber

The combustion chamber of the RCS Engine is made of pure molybdenum coated with Durak-B disilicide. The chamber is designed to withstand Boost loads as well as Operational loads and stresses. Boost loads result in high bending stresses at the throat and at the main attach flange. Stresses near the main flange were based on discontinuity effects which are chiefly due to the axial loads. Discontinuity effects were calculated by equating the rotation and deflection of the flange and two short cylinders under the applied loads.

The principal operational stresses are those due to transient ignition spikes. Since these can occur cold, when the lack of ductility causes an effective loss of strength, the chamber has the lowest margins for this condition. Although the chamber ribbed wall was originally designed to reduce deflections resulting from unsymmetrical pressures, it was analyzed for symmetrical pressures. The ribs were analyzed for thermal effects as well as pressure, due to the  $\Delta T$  across the chamber wall. Thick walled cylinder equations were used for these stresses.

The symmetrical starting pressure of 1500 psi was the maximum ignition overpressure expected with the preigniter operation. For this pressure, the Margin of Safety at the first valley was based on discontinuity effects. Hot Operational pressures are also taken from Design Criteria, and coupled with Space Vibration, produce fluctuating stresses to determine short time and fatigue margins of safety.



JOINT - COMBUSTION CHAMBER-TO-BELL  
TABLE OF MARGINS

PART & PART NO.	MATERIAL	ACTUAL STRESS (limit ksi) AND TYPE OF STRESS	TEMP. (°F)	ALLOWABLE STRESS		MARGIN OF SAFETY
				Yield or Creep (ksi)	Ult. or Rupture ÷ 1.5 ksi	
Nut-Bell Attach 228103G	Waspaloy	94.5 meridional	250	110.0	---	+1.16
	AMS	80.0 meridional	250	67.6 ①	---	+1.18
	5707B	1.29 meridional	1,800	4.7 ②	---	+2.64
Nut-Bell Attach 228103G	Waspaloy	66.5 circumfer.	250	110.0	106.0	+1.60
	AMS 5707B	3.17 circumfer.	1,800	4.7 ③	---	+1.48
Nut-Bell Attach 228103G	Waspaloy	4.44 thrd. shr.	250	---	64.0	Large
	AMS 5707B	1.66 thrd. shr.	1,800	---	8.0	Large
Washer - Thrust Chamber 228102B	L-605	21.6 bearing	250	59.9	---	+1.77
	AMS 5759	4.6 bearing	1,800	9.6	---	+1.09
Bell - Thrust Chamber 228101L thrds.	L-605	4.44 thrd. shr.	250	---	22.5	Large
	AMS 5759	1.66 thrd. shr.	1,900	---	7.6	Large
Bell - Thrust Chamber 228101L flange	L-605	33.40 tension + bending	250	37.4	---	+1.12
	AMS 5759	8.5 tension + bending	1,800	10.2	---	+1.20
Bell - Thrust Chamber 228101L wall near joint	L-605	27.2 tension + bending	250	37.4	---	+1.37
	AMS 5759	1.46 tension + bending	1,880	12.0 Endur.	---	Large
Bell - Thrust Chamber 228101L Flange - upstrm. edge	L-605	28.5 circumfer.	250	37.4	---	+1.31
	AMS 5759	1.53 circumfer.	1,900	12.0	---	Large
Combustion Chmbr 228128F Wall Section	Unalloyed	32.9 tension + bending	250	50.0	38.6	+1.18
	Moly Forging MMS-2205 Type II	1.63 tension + bending	1,880	----	10.0 ①	Large
Combustion Chmbr 228128F Flange at Joint at downstream end of combustor	Unalloyed Moly	5.63 circumfer	250	50.0	38.6	Large
		16.00 bearing	250	---	62.0	+2.87
		.278 circumfer	1,880	----	10.0 ①	Large
		8.12 bearing	1,880	16.0	----	+1.97

1 & 2 - Stress at which the joint faces would separate.

3 - Limiting stress taken equivalent to relaxation stabilizing stress after 20 minute period.

Fatigue allowables at high temperatures are based on a comparison with those shown in the Moly Data Brochure of Climax Moly Company, 1960. The latter showed the Endurance Limit to be approximately .50 times the Ultimate Tension Strength for high temperatures. For this analysis, Fatigue Allowable was taken to be .75 times the Creep Rupture Strength because of the small number of cycles corresponding to 3  $\sigma$  stresses. Fatigue Margin for the overall mission is made desirably high.

For the combined steady and alternating stress condition, the pressure stresses, the thermal stresses, and the 3  $\sigma$  vibratory stresses were considered. The 3  $\sigma$  stresses were applied according to the Rayleigh Distribution, 1.2% of the time under random vibration at the basic natural frequency of the chamber.

In any combustion chamber, creep and rupture stresses should be calculated for the cumulative life required at high temperatures. Then margins of safety should be determined based on Test Data from reliable sources. Allowable Creep may be based on acceptable structural deformation, say 1% over the total time period, or some lesser value based on performance degradation due to Throat Diameter increase.

The margins of safety for the different stress conditions are shown in Table IV.

#### D. Combustion Chamber Attach Hardware

The stress analysis of the attach hardware for the combustion chamber of the RCS Engine is based on the following. The attach hardware consists essentially of a clamping ring, fitting over the flange of the combustion chamber, and six (6) bolts to connect the clamping ring to the injector head of the engine. The clamping ring is made large in order to slide over the flange of the combustion chamber. Therefore, an intermediate split ring is inserted between the flange and the main clamping ring. In order to insulate the combustion chamber flange from the aluminum head and to provide a seal as well as a bearing surface, an L-605 material washer is used between the combustion chamber flange and the head. The clamping ring, split ring, and bolts are made of Rene 41 for high strength at Boost temperatures and for Operational temperature margin.

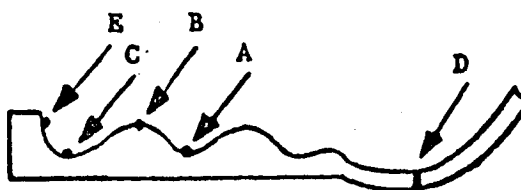
The principal loading conditions are Boost, with airloads plus vibration dictating the required preloads on the bolts, and the Space Operational condition which adds thermal loads to the high preload. The high preloads are required to avoid repeated separation and impact of the moly flange of the combustion chamber on the injector heat seal under vibratory conditions.

The preload, therefore, is set as a minimum equal to the maximum bolt tension load anticipated during Boost. This load is found by applying the total maximum Boost moment of the head to the bending section consisting of four (4) bolts as tension

TABLE IV

COMBUSTION CHAMBER (228128)

MINIMUM MARGINS OF SAFETY & ALLOWABLE PRESSURES



MATERIAL: Recrystallized Coated Molybdenum

LOCATION	TYPE OF STRESS AND LOADING	TEMP. (°F)	ALLOW. (ksi)	STRESS (ksi)	ALLOWABLE PRESSURES (psi)	MARGIN OF SAFETY
Point "C" Flange Joint	flange discontinuity, circumferential bending & hoop - uniform spike pressure.	-50	42 ult.	36.6 ult	1,720 limit 2,580 ult. uniform	+0.15 (ult.)
Point "C" Flange Joint	Boost (airload & vibration)	250	FTU = 58 Fend=43.5	---	---	+0.13 Endur. & mean stress
Point "A" Valley	Hoop stress - uniform chamber pressure	-50	42 ult.	24 ult.	2,630 limit 3,945 ult.	+0.75 (ult.)
Point "A" Valley	Hot operation axial combined stress (p=120 psi limit, $\Delta T=18^{\circ}\text{F}$ , 19.5 "g"s limit.)	2,900	4.8 ult.	2.53 ult	---	+0.90 (ult.)
Point "B" Hump	Hoop stress and bending non-uniform pressure.	-50	42 ult.	13.35 ult	4,700 limit 7,050 ult.	+2.1 (ult.)
Point "B" Hump	Hot operation axial combined stress (p=120 psi limit, $\Delta T=50^{\circ}\text{F}$ , 19.5 "g"s limit)	2,900	4.8 ult.	2.76 ult	---	+0.74 (ult.)
Point "E" Flange	flange to split ring bearing	650	69.6 (ult.)	69.6 (ult.)	---	0.0
Point "D" Throat	Hot operation axial combined stress ( $\Delta T=50^{\circ}\text{F}$ , 19.5 "g"s limit)	2,900	4.8 ult.	2.78 ult	---	+0.73

members and a small portion of the seal ring as the compression member.

The maximum preload results from necessary installation tolerance. It is this maximum preload, when added to the loads resulting from differential expansion during soakback after operation, that causes the critical loading conditions on the attach hardware. The thermal incremental load is approximately 30% of the maximum preload and occurs when the components are hottest, at their lowest strength point. This condition may result in low margins on the bearing surfaces of the split ring, the attach ring, and the moly flange, because of the small amount of bearing area available to react the clamp loads.

The attach ring and split ring may have comparatively large margins in bending under the maximum loads. Because of the great variation in attach loads due to thermal expansion, it is desirable to incorporate some form of spring or constant loading device in the attach hardware to reduce these thermal load variations. For the engine noted herein, wave springs were previously used under the bolt heads. But in the interest of reproducibility of results and greater design simplicity, small diameter, flexible bolts were used as equivalent springs. Of course, this necessitated very close control at the bolt design, fabrication and installation.

Bolt stresses are also critical for maximum installation preload and torque. The allowable preload installation and allowable installation torque on the bolt, including running torque combine to produce high stresses. However, after installation, the torque on the bolt shank drops off to approximately 30% of the installation value and the combined stresses reduce greatly. Since the installation stresses are only momentary, they do not reduce the load-carrying capacity of the bolts.

Maximum flight loads on the bolts occur during soakback, when the thermal increment adds to the maximum preload. A minimum margin for this condition may occur for combined bending plus tension. Bending on bolts occurs because of attach ring rotation under load.

An example of the thermal stress calculations is shown in Table V and the minimum margin of safety in Table VI.

#### E. Propellant Valves

The stress analysis of the engine valves is based on the following. The valves consist of a spool-shaped body, around which coils of wire are wrapped, a cover to enclose the wiring and provide the structural attachment to the head, a spring-loaded armature and valve seat with a Teflon seal on which the conical nose of the armature seals off the flow.

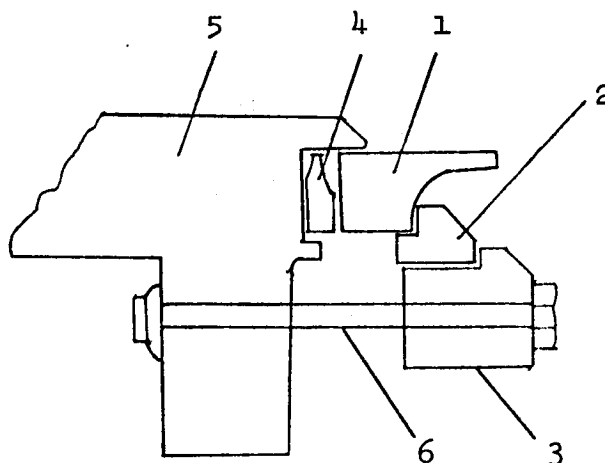
The principal structural elements of the valve are the body (made of 446 CRES), which contains the pressurized fluid; the flange of the body, which transmits the hold-down and dynamic impact forces to the cover; the cover (made of 446 CRES), which retains the valve body and transmits the holddown and dynamic forces to the attach

TABLE V

ATTACH HARDWARE

SOAK BACK - SPACE OPERATION

THERMAL LOAD ON THE ATTACH BOLT



Item	Material	Temperature	Coeff. of Thermal Expansion	Effect Length	Thermal Expansion
1. Chamber	Moly	650°F	$2.9 \times 10^{-6}$	0.25 in.	$420 \times 10^{-6}$
2. Split Ring	Rene 41	480°F	$6.9 \times 10^{-6}$	0.15 in.	$424 \times 10^{-6}$
3. Attach Ring	Rene 41	430°F	$6.9 \times 10^{-6}$	0.17 in.	$422 \times 10^{-6}$
4. Spacer	L-605	490°F	$7.45 \times 10^{-6}$	0.095 in.	$297 \times 10^{-6}$
5. Head	Aluminum	325°F	$13.3 \times 10^{-6}$	0.510 in.	$1729 \times 10^{-6}$
6. Bolt	Rene 41	350(Ave)	$6.8 \times 10^{-6}$	1.18 in.	$2247 \times 10^{-6}$
					$3292 \times 10^{-6}$

$$\text{Tension Bolt} = \frac{e E}{l} = \frac{(3292 - 2247) \times 10^{-6} \times 30.5 \times 10^6}{1.18} = 27,000 \text{ psi}$$

$$P = (\sigma_{\text{Tension}})(A_{\text{Bolt}}) = 27,000 (0.785 \times 12^2) = 305\#/bolt$$

TABLE VI

ATTACH HARDWARE

ROCKET ENGINE - REACTION CONTROL STRUCTURAL EVALUATION

TABLE OF MINIMUM MARGINS OF SAFETY

Item	Part	Material	Temp (°F)	Actual Stress (ksi)	Allow. Stress (ksi)	Margin of Safety
1.	Attach Bolts (228105)	Rene 41 AMS5712	350	$R_t = .804 R_b = .345$ Tension & Bending	198 (ult)	+ .01
2.	Attach Ring (228117)	Rene 41 AMS5713	430	84.0 (ult.) Tension & Bending	168.2 (ult)	+1.0
	Attach Ring (228117)	Rene 41 AMS5713	480	269 (ult.) Bearing	269 (ult)	0
3.	Split Ring (228116)	Rene 41 AMS5713	480	48.01 (ult.) Bending	168.2 (ult)	2.5
	Split Ring (228116)	Rene 41 AMS5713	480	269 (ult.) Bearing	269 (ult)	0
4.	Clinch Nut (228192)	A-286 AMS5737	325	43.9 (ult.) Shear	81.6 (ult)	+ .86
	Clinch Nut (228192)	A-286 AMS5737	325	89.5 (limit) Bending	92 (ult)	+ .03*
5.	Chamber Flange (228128)	Moly	650	69.6 (ult.) Bearing	69.6 (ult)	0
6.	Injector Head (228168)	6061-T6	325	48.3 (ult.) Bearing	67.8 (ult)	+ .40
7.	Seal (227947)	L-605 AMS5759	150	19.8 (limit) Bearing	64 (yield)	2.2
(*) = Bending modulus is used.						

bolts; the attach bolts (made of A-286 for the oxidizer hold-down and 6Al-4V for the fuel hold-down), which retain the valve to the head for static and dynamic loads.

The critical loading conditions for these structural elements are as follows:

1. The body is most highly stressed for the loads applied through the body flange, resulting from maximum preload and Boost vibration. These loads cause flange bending which is resisted by local bending on the body wall and the seat back-up area. Stress analysis is made by considering the body as composed of many plate and cylinder elements and solving for the edge shears and moments necessary to provide joint deflection and slope continuity.
2. The body flange is most highly stressed for the attachment preloads and Boost vibration loads from the bolts. Bending stresses at the body junction are most critical.
3. The cover is loaded by the attach bolts which cause bending stresses in the lugs and shell and bearing stresses at the flange retaining undercut.
4. The bolts are most highly stressed for the preload required to prevent separation of the valves from the injector head under soakback conditions plus additional loads due to Boost vibration. Another critical condition is installation, in which the maximum allowable preload and installation torque result in high combined stresses in the bolt shank. Minimum margin may be during installation.

Other loading conditions to be investigated are proof and burst internal pressures and explosion pressures at the valve seat resulting in dynamic impact forces through the valve body, flange and bolt system. The spring which forces the poppet closed must be analyzed for fatigue stresses due to the required loads and cycles of operation.

The margins of safety are shown in Table VII.

#### F. Injector

The head consists of a 6061 aluminum alloy plate with a pre-combustion chamber and fuel and oxidizer manifold of A-286 steel. Other fuel manifolds and injector holes are drilled directly into the aluminum head.

The head also serves to mount the combustion chamber by means of six (6) attach bolts. Each of the valves is mounted on the head by three (3) screws and the

TABLE VII

STRESS ANALYSIS OF THE FUEL & OXIDIZER VALVES  
MINIMUM MARGINS OF SAFETY

Part & Part No.	Material	Temp.	Type of Loading	Actual Stress (ksi)	Allow. Stress (ksi)	Margin of Safety
Seat (228180)	AM-355	Room Temp.	467 psi pressure	7.12 ult.bend	170 F <sub>TU</sub>	Lrg.
			467 psi pressure	3.69 ult.shr.	102 F <sub>SU</sub>	Lrg.
			preload & vibra.	141.4 ult.bend	170 F <sub>TU</sub>	+.20
			preload & vibra.	166.7 ult.bear	305 F <sub>BRU</sub>	+.83
			preload & vibra.	16.5 ult.shr.	102 F <sub>SU</sub>	Lrg.
Body (227818)	446 Stainless	Room Temp.	467 psi pressure	8.7 limit bend and tension	45 F <sub>TY</sub>	Lrg.
			467 psi pressure	2.46 lmt.shr.	27 F <sub>SY</sub>	Lrg.
			preload & vibra.	38.3 lmt.bend	45 F <sub>TY</sub>	+.17
			preload & vibra.	11.0 lmt.shr.	27 F <sub>SY</sub>	+1.46
Body (Dynatube)	446 Stainless	Room Temp.	Dynatube install. Torque	13.6 lmt.shr.	27 F <sub>SY</sub>	+1.0
Bolt-Fuel Valve (228183)	6AL-4V	Room Temp.	preload & vibra.	95.2 ult.tens.	150 F <sub>TU</sub>	+.58
			installation	83.7 ult.shr.	90 F <sub>SU</sub>	+.08
Bolt-Oxid. Valve (228188)	A-286	Room Temp.	preload & vibra.	57.7 lmt.tens.	85 F <sub>TY</sub>	+.47
			installation	68.8 ult.shr.	85 F <sub>SU</sub>	+.23
			preload & vibra.	50.8 ult.shr. out.	85 F <sub>SU</sub>	+.67
Lock Insert (SP234F142L) (Fuel Valve)	A-286 6061-T6 (Housing)	Room Temp.	preload & vibra.	50.8 ult.shr. out.	85 F <sub>SU</sub>	+.67
			preload & vibra.	18.3 ult.hsg. shear.	27 F <sub>SU</sub>	+.47
Lock Insert (SP234F142L) (Oxid. Valve)	A-286 6061-T6 (Housing)	Room Temp.	preload & vibra.	50.8 ult.shr. out.	85 F <sub>SU</sub>	+.67
			preload & vibra.	18.3 ult.hsg. shear	77 F <sub>SU</sub>	+.47



TABLE VII (continued)

STRESS ANALYSIS OF THE FUEL & OXIDIZER VALVES  
MINIMUM MARGINS OF SAFETY

Part & Part No.	Material	Temp.	Type of Loading	Actual Stress (ksi)	Allow. Stress (ksi)	Margin of Safety
Cover (228195) (Spacer- Fuel 228187) (Spacer- Oxid. 228194)	446 Stainless	Room Temp.	preload & vibra.	50.8 lmt.bear	72 F <sub>BRY</sub>	+.42
Cover, Ear (228195)	446 Stainless	Room Temp.	preload & vibra. preload & vibra. preload & vibra.	35.7 lmt.bend 36.7 lmt.bend 38.8 lmt.bear	45 F <sub>TY</sub> 45 F <sub>TY</sub> 72 F <sub>BRY</sub>	+.26 +.23* +.85
Spring (227827)	Inconel-X	150	Installation	127.5 shear	132 shr.	+.04
Body (227818) Interference with Plug (227824)	446 Stainless	Room Temp.	installation interference	39.3 lmt.bend	45 F <sub>TY</sub>	+.5

\*bending modulus used.

standoff manifold. The head also serves as the main mounting element of the total engine. The outer flange of the head has inserts for the main attach bolts to the vehicle cluster.

The critical structural conditions are those associated with explosion pressures in the head and those concerned with dynamic loads from the chamber and valves. It is estimated that pressures of 15,000 to 50,000 psi may be developed internally. The housing of the head has fairly high interference stresses resulting from installation. When possible explosion pressure effects are added to the interference stresses, minimum margins in circumferential tension may result, for example, Margin of Safety = .01 Yield at the fuel valve standoff press fit in the housing for 15,000 psi.

The fuel and oxidizer manifolds (standoffs) are likewise critical for explosion effects. Contributing loading conditions are the preloads from the valve screws due to the necessity of preventing separation of the valve and standoff because of relative thermal expansion. Maximum stress for this case is due to axial compressive plus bending at the pressed-in end.

The fuel and oxidizer inlet tubes are also critical for possible internal explosions. The failure mode here is bending and compression from installation at the section between window holes. Torsion stresses due to installation should also be investigated at such critical sections.

The phenolic insulator for the standoffs is most highly stressed because of installation interferences causing high local compression. Stresses are high because of the short available length for interference deformation results is high local strain. Boost loads impose additional compressive loads on the spacer because of side shear from the valve ball seat.

The threaded inserts for the various attach screws or bolts should show adequately high margins for the loads resulting from preloads plus Boost vibration.

The Margins of Safety are shown in Table VIII.

TABLE VIII  
INJECTOR HEAD  
TABLE OF MINIMUM MARGINS OF SAFETY

ITEM	PART or LOCATION	MATERIAL	TEMP (°F)	ACTUAL STRESS (ksi) or LOAD (#)	ALLOWABLE STRESS (ksi) or LOAD (#)	MARGIN of SAFETY
1	Oxidizer Insert (228258-3)	A-286	RT	31.1 ksi limit interference stress	88 ksi yld	+1.82
		A-286	250	17.5 ksi limit interference stress	86.2 ksi yield	Large
		A-286	250	1,524 # ultimate push-out loads	6,120 # ultimate	+3.0
		A-286	35	101 ksi ultimate pressure stress	140 ksi ultimate	+38
		A-286	30	24.1 ksi ultimate pressure stress	140 ksi ultimate	Large
2	Fuel Standoff (228170)	A-286	RT	$R_b = .70, R_c = .50$ pressure & preload	140 ksi ultimate	+0.02
		A-286	RT	128.8 ksi ultimate preload & boost	135 ksi ultimate	+0.05
		A-286	RT	166 ult. bearing preload & boost	200 ksi ultimate	+0.20
3	Ring (228258-7)	6061-T6	RT	31.1 ksi limit interference stress	35 ksi yield	+0.13
		6061-T6	350	17.5 ksi limit interference stress	28 ksi yield	+0.60
		6061-T6	350	2,570 # ultimate push-out loads	5,730 # ultimate	+1.23
4	Housing (228168)	6061-T6	RT	18.9 ksi limit interference stress	35 ksi yield	+0.85
		6061-T6	350	11.6 ksi limit interference stress	28 ksi yield	+1.4
		6061-T6	RT	41.6 ksi ultimate explosion stress	42 ksi ultimate	+0.01

TABLE VIII (continued)

ITEM	PART OR LOCATION	MATERIAL	TEMP (°F)	ACTUAL STRESS (ksi) or LOAD (#)	ALLOWABLE STRESS (ksi) or LOAD (#)	MARGIN of SAFETY
4	(Continued) Housing (228168)	6061-T6	150	10.6 ksi ultimate	40 ksi ult.	+2.76
		6061-T6	RT	11.0 ksi ultimate engine mount attach	27 ksi ult. shear	+1.46
		6061-T6	RT	18.3 ksi ultimate Valve attachment	27 ksi ult. shear	+0.47
5	Oxidizer Inlet Tube (228251)	A-286	35	130 ksi ultimate bursting pressure	140 ksi ultimate	+0.07
		A-286	35	108 ksi ultimate preload	140 ksi ultimate	+0.30
		A-286	35	477 # ult. shear preload & pressure thread shear	2,160 # ultimate	Large
6	Fuel Inlet Tube (228166)	A-286	35	131.8 ksi ultimate bursting pressure	140 ksi ultimate	+0.06
		A-286	35	397 # ult. shear preload & pressure thread shear	1800 # ultimate	Large
		A-286	35	130.0 ksi ultimate preload & pressure	140 ksi ultimate	+0.07
7	Insert (SP234E192L) Eng. Mnt. Attach	A-286	RT	18.1 ksi ultimate boost mount loads	85 ksi ultimate	Large
8	Insulator (228171)	Phenolic	RT	73.6 ksi ultimate boost & interfer.	96 ksi	+0.22

CHAPTER 8

MATERIAL SELECTION

BY

E. E. RITCHIE

TABLE OF CONTENTS

	<u>Page</u>
I INTRODUCTION	8-1
A. Description of the Engine	8-1
B. Reasons Considered for Material Selection	8-1
II DISCUSSION OF COMPONENTS	8-4
A. Injector	8-4
B. Solenoid Valves	8-14
C. Combustion Chamber	8-20
D. Seals and Attach Hardware	8-29
III SPECIAL EVALUATION	8-32
A. Coating Development	8-32
B. Compatibility	8-32
C. Alternate Combustion Chamber Materials Evaluation	8-34

LIST OF ILLUSTRATIONS

<u>Figure Number</u>	<u>Title</u>	<u>Page</u>
1	Exploded View of MA-109XAA Rocket Engine	8-2
2	Exploded View of the R-4D Engine	8-3
3	Injector Configurations Tested	8-6
4	Seal Configuration	8-7
5	Oxidizer Stand Off	8-9
6	Head and Valve Assembly-Model R-4D Rocket Engine	8-11
7	Solenoid Valve Assembly	8-15
8	Valve Seat Designs	8-18
9	Chamber Wall Temperature	8-23
10	Flo-Turn Manufacturing Process	8-24
11	Photomicrograph of Coated Chamber	8-25
12	Engine With One Piece Ribbed Combustor	8-27
13	Chamber Life Molybdenum Disilicide Coating	8-33
14	Columbium Bend Test Results	8-36

## MATERIAL SELECTION

### I. INTRODUCTION

#### A. Description of the Engine

The 100-pound thrust reaction control engines developed and manufactured by The Marquardt Company for the Apollo Service Module and the Lunar Module are pressure-fed, bipropellant thrust generators capable of either steady state (continuous) or pulse-modulated operation. These engines attain their rated 100-pounds of thrust utilizing a very low pressure, moderate temperatures and a radiation cooled combustion chamber. The engine assembly is 13-1/2 inches long and weighs 5 pounds and operates by injecting hypergolic propellants consisting of nitrogen tetroxide ( $N_2O_4$ ) as the oxidizer and Aerozine-50, a 50-50 blend of unsymmetrical dimethyl hydrazine (UDMH) and hydrazine ( $N_2H_4$ ), or monomethylhydrazine as the fuel.

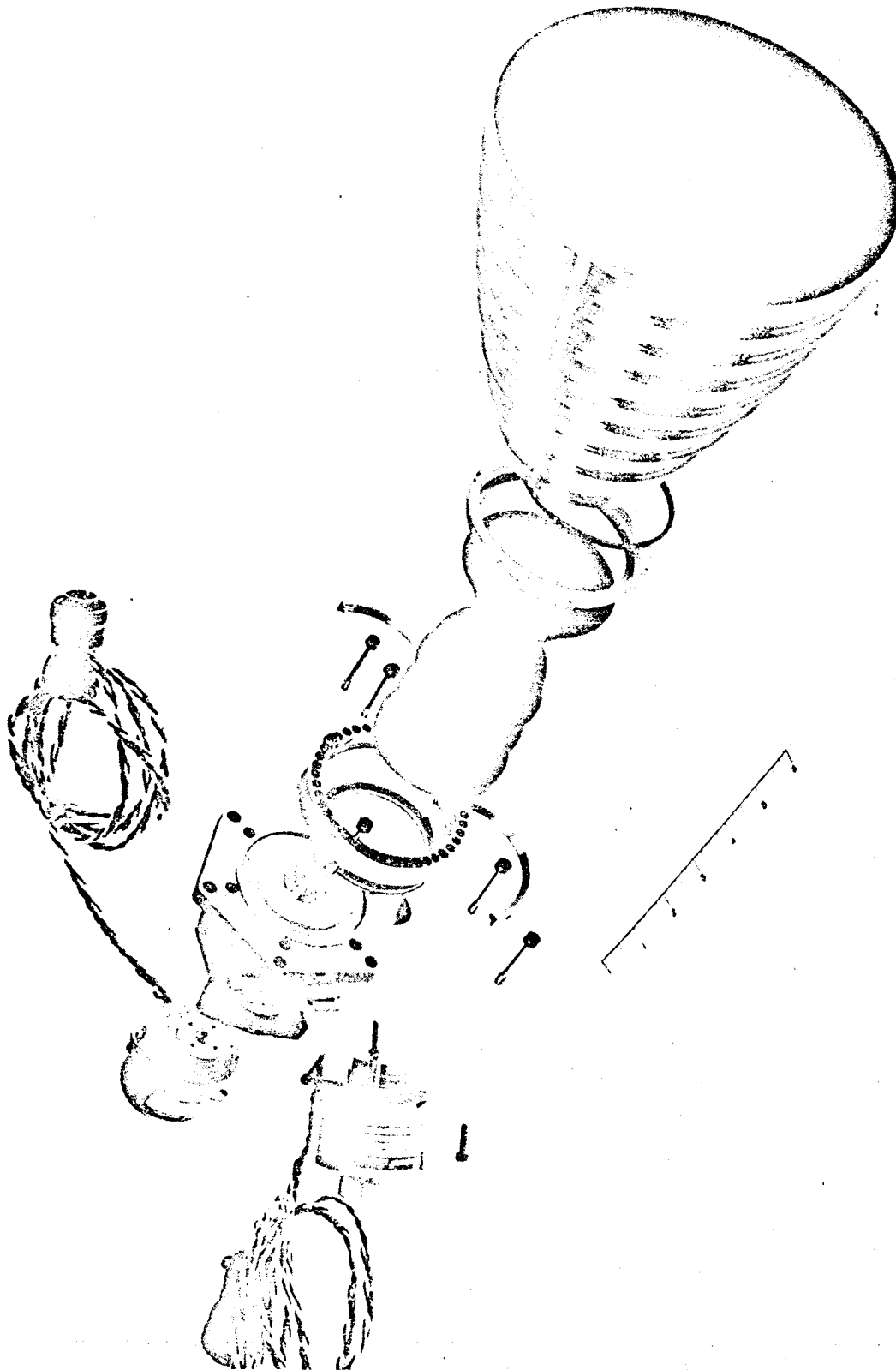
The basic components of this engine are the injector head assembly, the fuel and oxidizer solenoid valves, the combustion chamber and the various seals and attach hardware necessary for assembly and operation of the engine. Figure 1 shows a cutaway view of an early 100-pound thrust engine which was initially tested on 14 August 1962 and Figure 2 shows the R-4D engine currently being supplied for space exploration. A detailed description of the components and their function will be discussed later in this chapter.

#### B. Reasons Considered for Material Selection

The Marquardt 100-pound thrust engine (Figure 2) appears to be an extremely simple piece of hardware. The engine was designed with only four moving parts, the combined armature-seat pintle in each of the two valves and the spring for returning the armature to the fail safe closed position. However, operation of the engine in the realm of outerspace imposes several extremely severe and stringent requirements on the components and ultimately on the material selected for each application. The engine converts chemical energy stored in the propellants into thrust by combustion in the combustion chamber and subsequent acceleration of the combustion products in a convergent-divergent nozzle. The combustor is a pressure vessel for containment and direction of the combustion pressure which is normally 96.7 psi with ignition pressures as high as 1500 psi and combustion temperatures of approximately 5200°F. The current chamber operates with a throat temperature in excess of 2000°F and a maximum forward flange temperature, less than three inches away, of less than 600°F to prevent vaporation of the propellant in the injector head. Early models of the engine operated with throat temperatures in excess of 3000°F. In







NEG. 6449-5

Exploded View of the R-4D Engine

addition to the temperature and mechanical property requirements the valves and injector must be compatible with the liquid propellants and the injector face and combustion chamber must be compatible with the products of combustion. The strength-to-weight properties of the various materials at temperature are extremely important due to the cost of orbiting a pound of payload. The close tolerances of the valve components and the repeated cyclic type operation require the use of highly wear resistant materials with antigalling characteristics. The extreme temperature profile experienced by the engine during operation necessitates a thorough knowledge of the thermal expansion and thermal conduction characteristics of the various materials utilized to prevent relaxation of some attach hardware pre-stresses or the overstressing of other parts of the engine. Space operation itself presents several materials problems associated with vacuum exposure. Materials with high vapor pressures tend to sublime, the normally occurring oxides of some metals sublime resulting in the cold welding of the unprotected substrates as well as the evaporation of seals and lubricants.

## II. DISCUSSION OF COMPONENTS

### A. Injector

#### 1. Function

The injector head is the focal point of the engine. The fuel and oxidizer solenoid valves are mounted on the forward side and the combustion chamber on the aft side. The engine is attached to the service module through the injector housing and must transmit the rocket engine thrust to the vehicle. During launch the air drag on the engine and vibration during launch and boost are transmitted to the vehicle through the injector housing. However, the main function of the injector is to introduce and mix the propellants in the combustion chamber in such a manner that good performance results.

#### 2. Current Injector Design

The current 100 pound thrust injector assembly design is a multiple doublet (8 on 8) injector with an integral preigniter to reduce the instantaneous pressure surge from propellant ignition to an acceptable level. A doublet consists of one fuel port and one oxidizer port, drilled and aligned such that when propellants flow through them, the fuel stream impinges on the oxidizer stream. The assembly is composed of seven basic parts. The injector housing, discussed above, and the injector insert ring, which form the fuel annulus for distribution of fuel to the doublets, are both 6061 aluminum in the T-6 condition procured in accordance with QQ-A-325. The remaining five parts which comprise the components of the preigniter and the injector-valve interface are A-286 steel in the heat treat condition in accordance with AMS 5737.

Materials selected for the injector head assembly were required to have two basic characteristics: (1) propellant compatibility and (2) high heat conductivity. Compatibility with the propellants was essential to insure that no reaction with the

propellants or slow erosion because of prolonged exposure would occur. Both materials have a class A rating<sup>(1)</sup>, less than 1 mpy attack, with Aerozine-50 and  $N_2O_4$ . Heat transfer to the injector during an engine firing required a material that could conduct heat away from the injector face rapidly to prevent melting of the material and boiling of the propellants in the injector head.

### 3. Injector Development

#### a. Initial Concept

The injector development program is discussed in detail in Chapter 10 therefore, only the significant design changes which affect the overall performance or mode of operation of the engine and resulted in material changes will be discussed in this chapter.

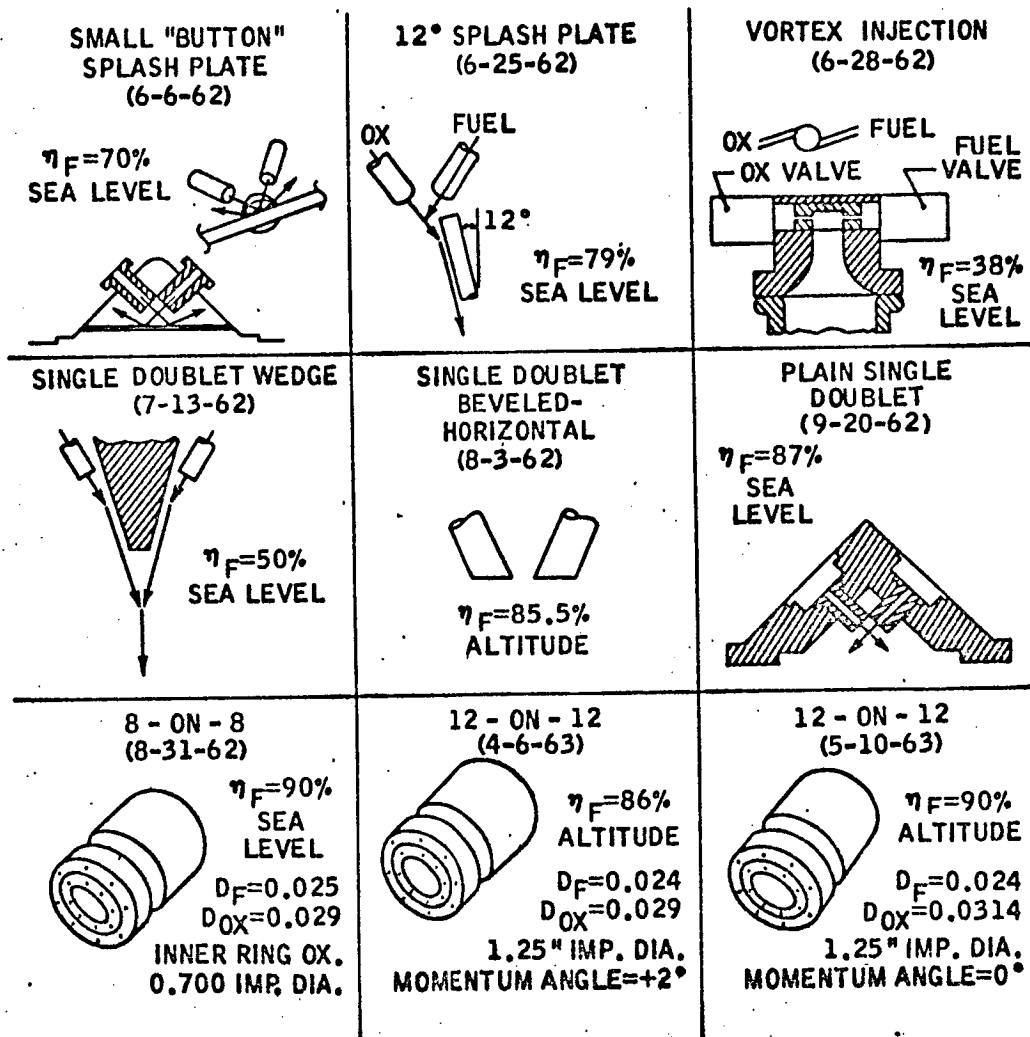
The initial injector concepts (Figure 3) were of the single doublet type and a 90 degree impingement angle. Several different splash plate configurations inserted into the propellant streams were tested in an attempt to obtain better mixing of the propellants and ultimately more uniform combustion. Extremely high combustion chamber wall temperatures, in excess of 3000°F, were experienced which resulted in high head temperatures from thermal conduction at the combustor-injector interface.

Refinement of the single doublet injector included the insertion of a wedge between the fuel and oxidizer injection ports to break up the hypergolic propellants into a finer spray before contact could take place. Steady state performance with these injectors was poor and the injector head assemblies became extremely hot. The splash plates and wedges did not improve the efficiency of the engine and burned away very rapidly.

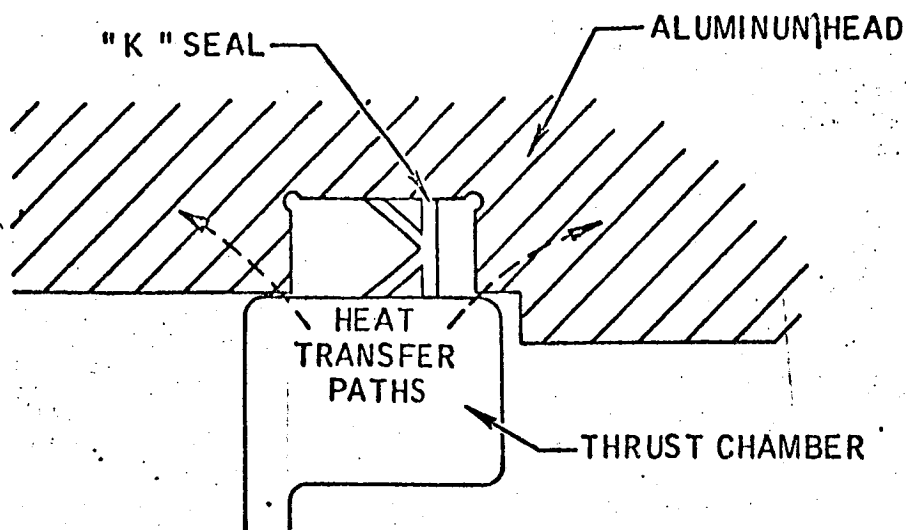
#### b. Multiple Doublet Concept

The first major breakthrough in the injector design was the incorporation of the multiple doublet injector concept. Several designs including a, 4-on-4 (four oxidizer jets impinging on four fuel jets), 6-on-6, 8-on-8, 12-on-12 and 24-on-24 were evaluated with a substantial increase in engine efficiency being experienced as the number of doublets were increased to the 8-on-8 design. The 12-on-12 injector design was selected for one of the early prototype engines because of its better specific impulse, satisfactory temperature levels and a history of no chamber failures. The advantage of the multiple doublet injector concept over the single doublet was division of the propellants into finer jets before impingement and a smaller reaction zone at each doublet resulting in better control of the oxidizer to fuel O/F ratio and a greater thrust efficiency. Fuel to the multiple doublets was delivered through a fuel annulus with a diameter slightly less than that of the combustor seal, thereby providing a liquid cooled heat sink. Thus a great deal of heat conducted to the head by the combustion chamber was carried away from the system by the fuel. The combustor-injector seal was also modified in an attempt to lower the head temperature further by eliminating the bearing contact of the combustion chamber on the aluminum head in order to reduce conduction from the chamber to the head as shown by Figure 4.

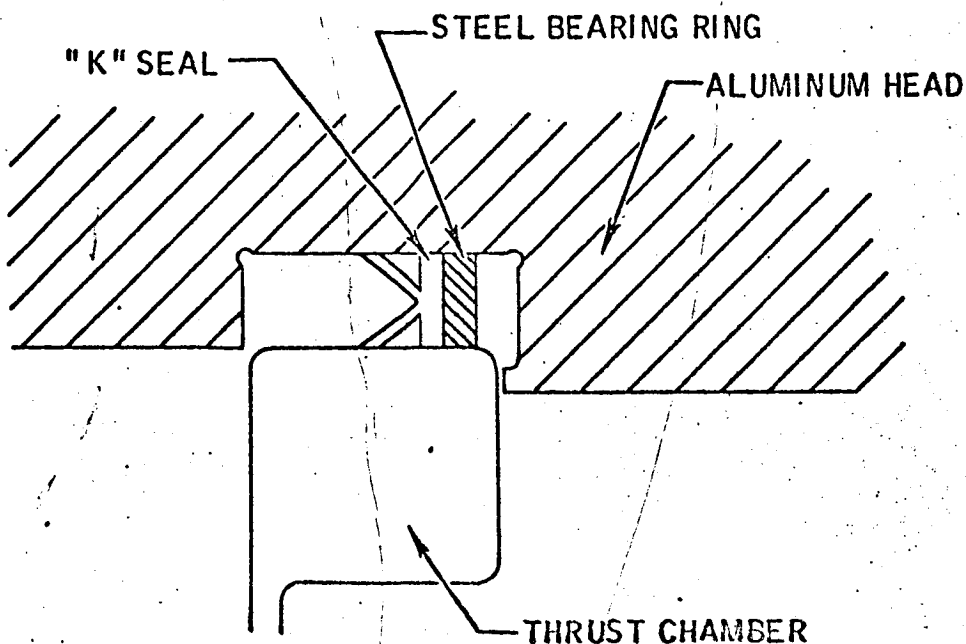
## INJECTOR CONFIGURATIONS TESTED



# SEAL CONFIGURATION



SEAL CONFIGURATION WITH THE THRUST CHAMBER  
BEARING ON THE ALUMINUM HEAD



c. Oxidizer Valve Stand-Off

During the latter part of 1963 several injector configurations were evaluated in an attempt to prevent vaporation of the propellants in the valves during soak-back and in the injector head during subsequent firing. A stand-off section between the oxidizer solenoid valve and the injector head was incorporated in the design to transport the oxidizer from the valve to the head assembly and isolate the valve from the high head temperatures. Type 303 CRES stainless steel was selected as the material for the stand-off because of its "A" rated compatibility (less than 1 mpy attack) with the oxidizer and its resistance to heat conductance. This high resistance plus the thin-walled cross-section (Figure 5) of the stand-off adapter provided a good thermal barrier between the oxidizer valve and the injector head assembly. The insulating characteristics of the stand-off injector design was enhanced by the use of a phenolic spacer to insulate the upper part of the stand-off adjacent to the valve. MIL-F-9084 (181 glass cloth fabric) bonded with MIL-R-9299 Type II, Class 2 resin was selected as the spacer material because of its good thermal insulation properties. Thermal conduction between the head assembly and the stand-off adapter will be further retarded in space by venting the annulus around the stand-off to the vacuum of space. The stand-off adapter concept proved effective in reducing the temperature in the oxidizer valve to an acceptable level, a later much improved version of the stand-off adapter has been incorporated in both the oxidizer and fuel valves of the current injector. Redundant "omniseals" were used to prevent oxidizer leakage between the stainless steel stand-off adapter and the aluminum injector insert and between the oxidizer valve and the stand-off adapter. Current design eliminated the stand-off injector seals by using a shrink fit; however, the same type seals have been used to seal both valves to the stand-off adapter. The seals consist of TFE Teflon with a horseshoe shaped cross section with a PH 15-7 Mo coil spring to keep the legs of the horseshoe seal spread apart. Both materials have an "A" compatibility rating in contact with the propellants. No compatibility problems have been encountered with the seals.

d. Propellant Vaporization

The stand-off adapter concept was successful in lowering the temperature of the oxidizer valve to a satisfactory level where the oxidizer would not vaporize in the valve itself during maximum soakback conditions. However, the liquid oxidizer had to be transferred from the valve through the stand-off adapter with its thermal gradient into the passages of the individual doublets in the hot injector. Initial contact of the oxidizer with the hot injector at pressures lower than maintained in the closed valve by the pressurized propellant system resulting in boiling of the oxidizer and the injection of hot vapors into the combustion chamber. Injection of vaporized oxidizer into the combustor produces a high heat transfer burning phase which resulted in burnthrough of the throat section of combustion chamber walls. Several injector designs were evaluated in an attempt to prevent the vaporization of the oxidizer in the head assembly. Among these designs was the insertion of aluminum tube liners into the oxidizer cross passages in an unsuccessful attempt to insulate the oxidizer flow from the high injector head temperature.

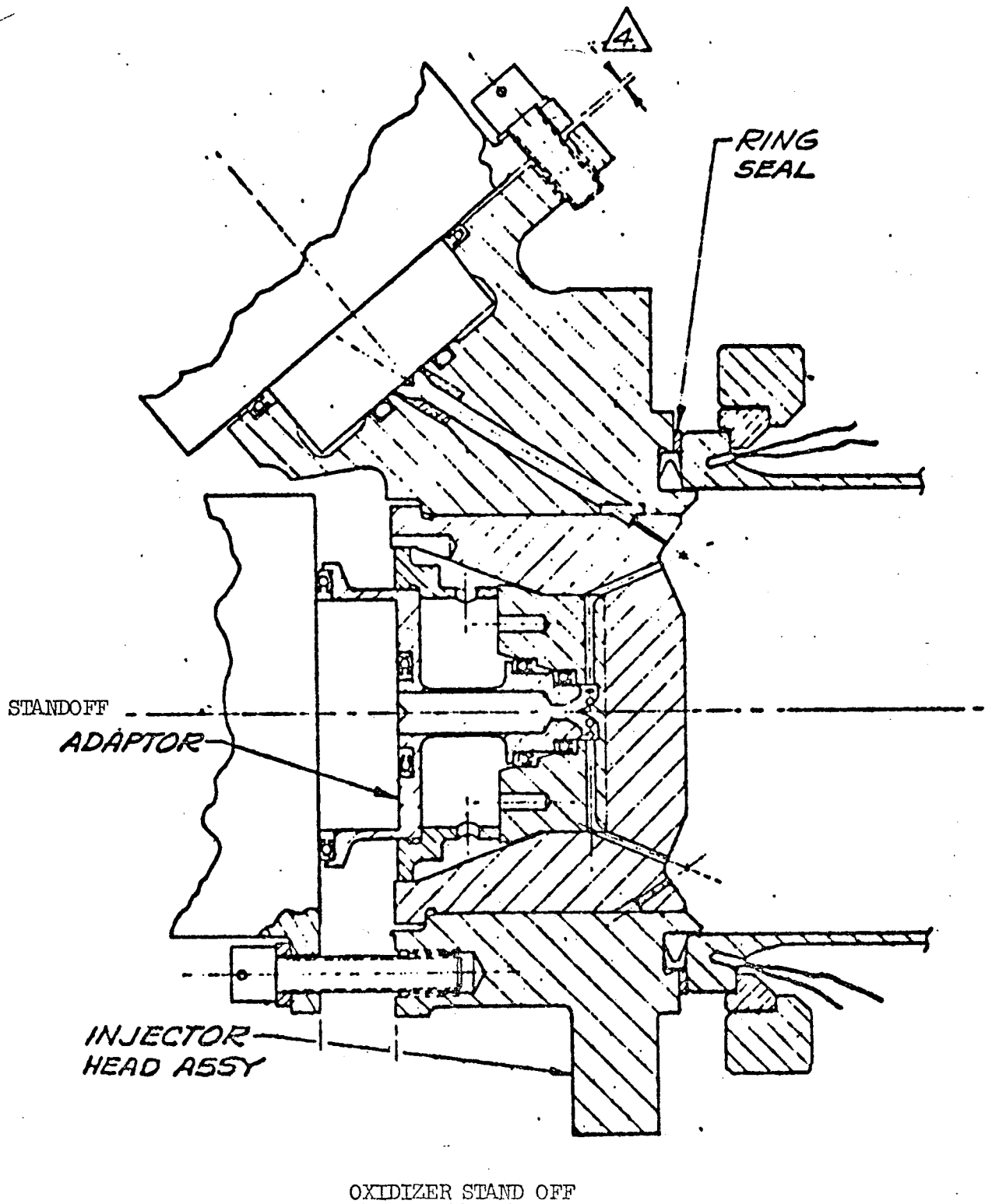


Figure 5



e. Emittance Improvement

The steady state operating temperature of the combustion chamber was lowered significantly by grit blasting the outside diameter of the combustor wall and throat section prior to coating. The roughened surface resulted in a higher emittance value for the chamber thus providing an increased heat rejection rate. Lowering of the combustor temperature also lowers the injector assembly temperature due to less heat transfer through the combustor-injector seal thus reducing the tendency to vaporize the propellants. Details of the grit blasting and emittance evaluation are discussed in Section II-C-3-e.

f. Fuel Film Cooling

Movies of a combustion chamber being test fired with an 8-on-8 injector indicated that cool streaks appeared on the chamber in between the doublets because of the cooling effect of the doublet fanning action overlapping at the cool streaks. It was thus decided that substantial cooling of the engine could be obtained by injecting a fuel bleed stream onto the hottest portion of the chamber wall. Eight fuel bleed holes radially in line with the eight existing doublets were added to inject 11 percent of the fuel flow onto the wall 0.500 inch downstream from the injector face. The effect of the fuel bleeds on engine performance was very small and the wall temperature was only 2500°F with a forward flange temperature of approximately 500°F.

The fuel film cooling concept was thoroughly investigated during the injector development program. Variables such as oxidizer film cooling, variation in the percent flow to the fuel bleed holes, angle of fuel impingement on the chamber wall, location of the impingement area with respect to the forward flange. Optimization of these variables has led to the selection of an injector incorporating a fuel bleed of 24 percent at an impingement angle of 40° and resulted in a steady state forward flange temperature of approximately 350°F and a maximum soakback temperature of approximately 400°F. This temperature decrease has eliminated several of the material problems in the injector design.

g. Preigniter Concept

The preigniter can be described as a small rocket engine located inside of the main thrust chamber. The oxidizer stand-off adapter has been made an integral part of the preigniter. The injector was also modified by the addition of a fuel stand-off adapter which is similar to the oxidizer stand-off portion of the preigniter. Propellant lead to the preigniter is assured by the use of a preigniter tube with a direct passage from the valve to the preigniter doublet. Propellant to the remaining doublets is delayed because of the flow path through the injector. The propellant must pass through lateral holes in the preigniter tube into an annulus before it enters the injector passages to the doublets and fuel bleed ports. The preigniter injector is shown in Figure 6.

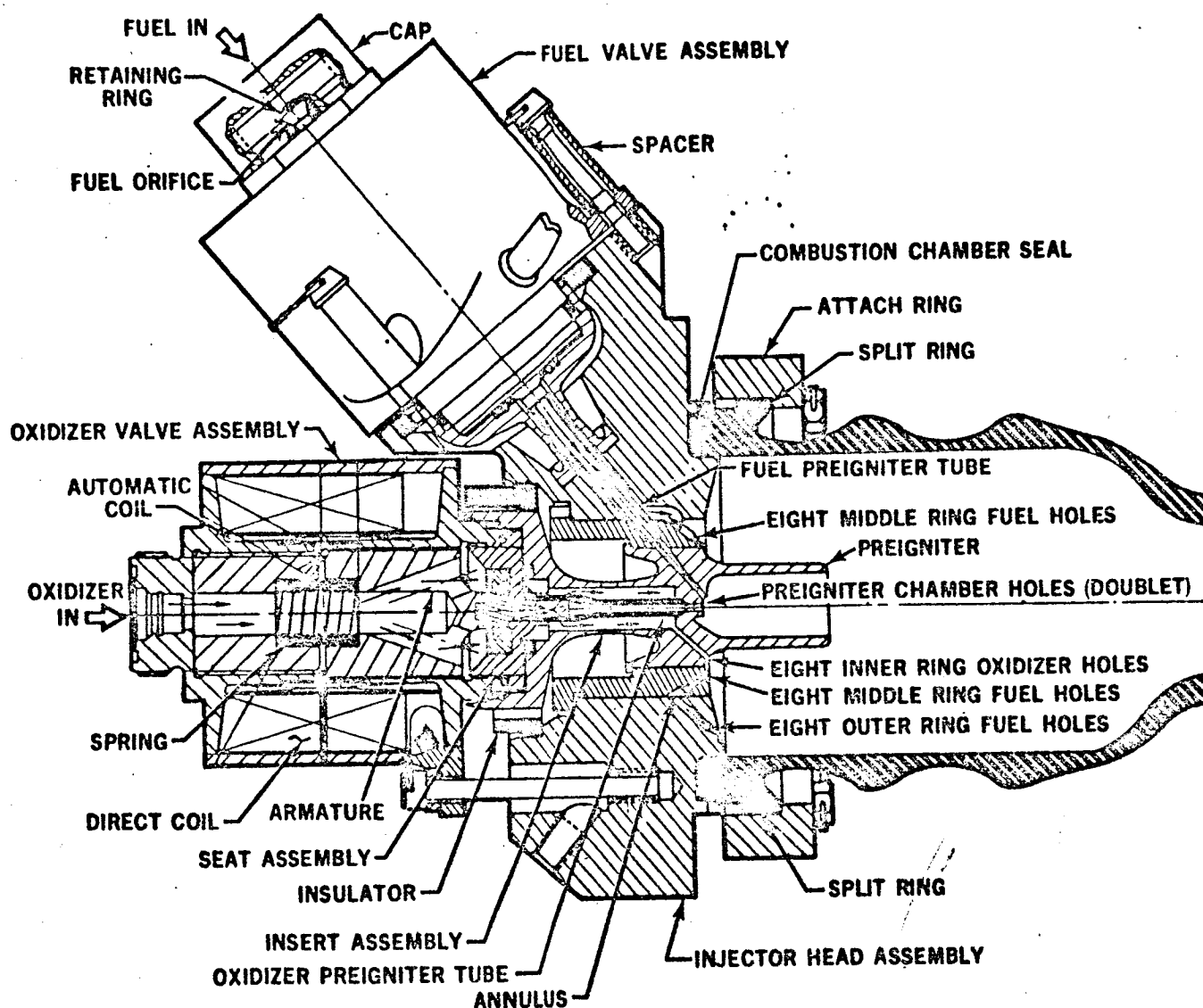


FIGURE 6. HEAD AND VALVE ASSEMBLY - MODEL R-4D ROCKET ENGINE

Type A-286 austenitic precipitation hardening stainless steel was selected as the material for the preigniter components and the fuel stand-off adapter, replacing the type 303 stainless steel originally used for the oxidizer stand-off adapter. This material change was made to accommodate the increased strength and oxidization resistant requirements imposed on the preigniter having to contain the initial combustion and the fact that the preigniter was now exposed to and protruded into the environment of the combustion chamber. A-286 has an "A" compatibility rating (less than 1 mpy attack) in contact with the propellants and has good machining characteristics, an essential for this application and was readily available. The 6061-T6 aluminum originally selected for the injector housing was still adequate, therefore no material change was required.

#### 4. Fabrication and Assembly

The 6061-T6 aluminum for the injector housing and the preigniter ring insert are procured in accordance with QQ-A-325 in the T-6 condition. The housing assembly is reheat treated to the T-6 condition after rough machining as a stress relieving operation because of the complex shape and extensive machining required to produce the part. The A-286 stainless steel for the preigniter components and the fuel stand-off adapter are procured in accordance with AMS 5737 in the heat treated condition. The preigniter and the fuel stand-off adapter are stress relieved at 1250°F for four hours after rough machining. The remaining components are machined to final configuration without an intermediate stress relief.

The aluminum components are chromic acid anodized all over, except for critical mating surfaces for corrosion protection. The mating surfaces are alodined which provides a softer surface than anodizing thereby enhancing the necessary intercomponent seal. Assembly of the injector requires four shrink fitting operations which are extremely critical because of the accurate alignment of mating parts and the propellant tight seal necessary to prevent leakage and mixing of the propellants in the head assembly. The components are matched and final machined to produce an interference fit between mating surfaces. The amount of interference is varied to accommodate the different diameters of the mating surfaces. A temperature differential is required to assemble the parts with a maximum temperature of 450°F permitted for a maximum of 10 minutes to prevent over aging of the aluminum. The temperature differential is successively decreased during the assembly to avoid any undue disturbance of the previous joints.

#### 5. Special Investigations

The majority of the problems encountered in the development of the injector have been discussed above; however, a few significant isolated or intermittent problems which have been omitted are discussed below with the corrective action employed.

a. Discrepant Propellant Passages

During the early development phase of the program, several injectors had to be rejected because of discrepancies in the propellant passages resulting in non-uniform propellant streams. Corrective action required hand rework of the passages which could not be performed without disassembly of the injector. A technique has been developed whereby the injector inserts are shrink-fitted into plastic housings which are hydraulically similar to the actual aluminum injector housings. Water flow testing of the inserts prior to installation in the head assembly permits rework of any discrepancies and additional testing.

b. Insert Leak Repair

Several injector housings had to be rejected after final assembly because of inadequate sealing between the shrink fitted joints. The joints are pressurized for five minutes at 460 psig with dry filtered nitrogen with no leaks allowed. A thermal shock cycle was initiated where the leaky injectors could be repaired by redistribution of the joint stresses. The injector assemblies are heated to the precipitation aging treatment of the 6061-T6 aluminum, approximately 340°F for 30 minutes, and quenched in an alcohol bath maintained at a temperature of -90°F or lower. This cycle may be repeated up to a total of three times before the assembly is rejected.

c. Excessive Cleaning

Several injector parts had to be rejected because of discoloration and variation in the anodic coating of both the aluminum insert ring and the aluminum injector housing. An extensive investigation revealed the following conclusions:

- (1) The cause of discoloration and variation on the anodized 6061-T6 parts resulted from attack of the coating by repeated cleaning in the ultrasonic cleaner. The color of the coating variation varied from light gray to black as a result of contamination of the cleaner with metal salts (copper, lead and tin).
- (2) The condition of discoloration was not found to be detrimental to the life, function, interchangeability or service of the engine. This problem has been eliminated by reducing the number of ultrasonic cleaning cycles to a minimum and imposing stringent controls on the cleaning solutions.

## B. Solenoid Valves (Fuel and Oxidizer)

### 1. Function

The functions of the injector solenoid valves are: (1) to respond rapidly to an electrical signal, thus supplying the proper ratio of fuel and oxidizer to the injector, and (2) provide a positive propellant shut-off to prevent leakage during periods of time when the engine is not operating.

### 2. Operation

An electro-magnet actuating mechanism is used to open the propellant valves. The valves are normally closed and fail closed upon loss of electrical power. Application of current to the coil in the valve body draws the armature, which is also the moving component of the seal, away from the seat assembly allowing propellant to flow through the valve into the injector head assembly. Removal of the electrical current permits the spring and propellant pressure to seat the armature thus stopping the flow of propellants.

### 3. Design Criteria

The solenoid valves, being the only engine components with moving parts, impose several unique factors on the valve design which are not applicable to the rest of the engine. Only the requirements which are related to material selection will be discussed in this section, the remainder are presented in Chapter 9, "Propellant Valve Design". Some of the more important requirements are compatibility with the propellants, wear and galling characteristics, electrical and magnetic properties, and seat leakage.

The basic components of the electro-magnet portion of the solenoid valve (Figure 7) are: (a) the electrical coil, (b) the valve cover which forms the outer leg of the iron circuit, (c) the valve body which is magnetically insulated at the mid-plane, forms the ends of the iron circuit, (d) the valve body plug which forms half of the inner leg of the circuit, and (e) the movable armature which forms the remainder of the inner leg when the coil is energized. The various solenoid valve components were designed to meet the above criteria while utilizing readily available materials.

### 4. Material Selection and Component Fabrication

Two materials, No. 5 relay steel and type 446 CRES, were considered for the electro-magnetic components of the solenoid. The No. 5 relay steel was considered because of its optimum magnetic properties; however, it had to be plated for corrosion resistance. Annealed Type 446 CRES was selected as the prime material for the electro-magnetic components of the valve although it does not have optimum magnetic properties. Type 446 CRES has an "A" compatibility rating in contact with the propellants. The 446 CRES is procured in annealed bar stock form in accordance with QQ-S-763.

## SOLENOID VALVE ASSEMBLY

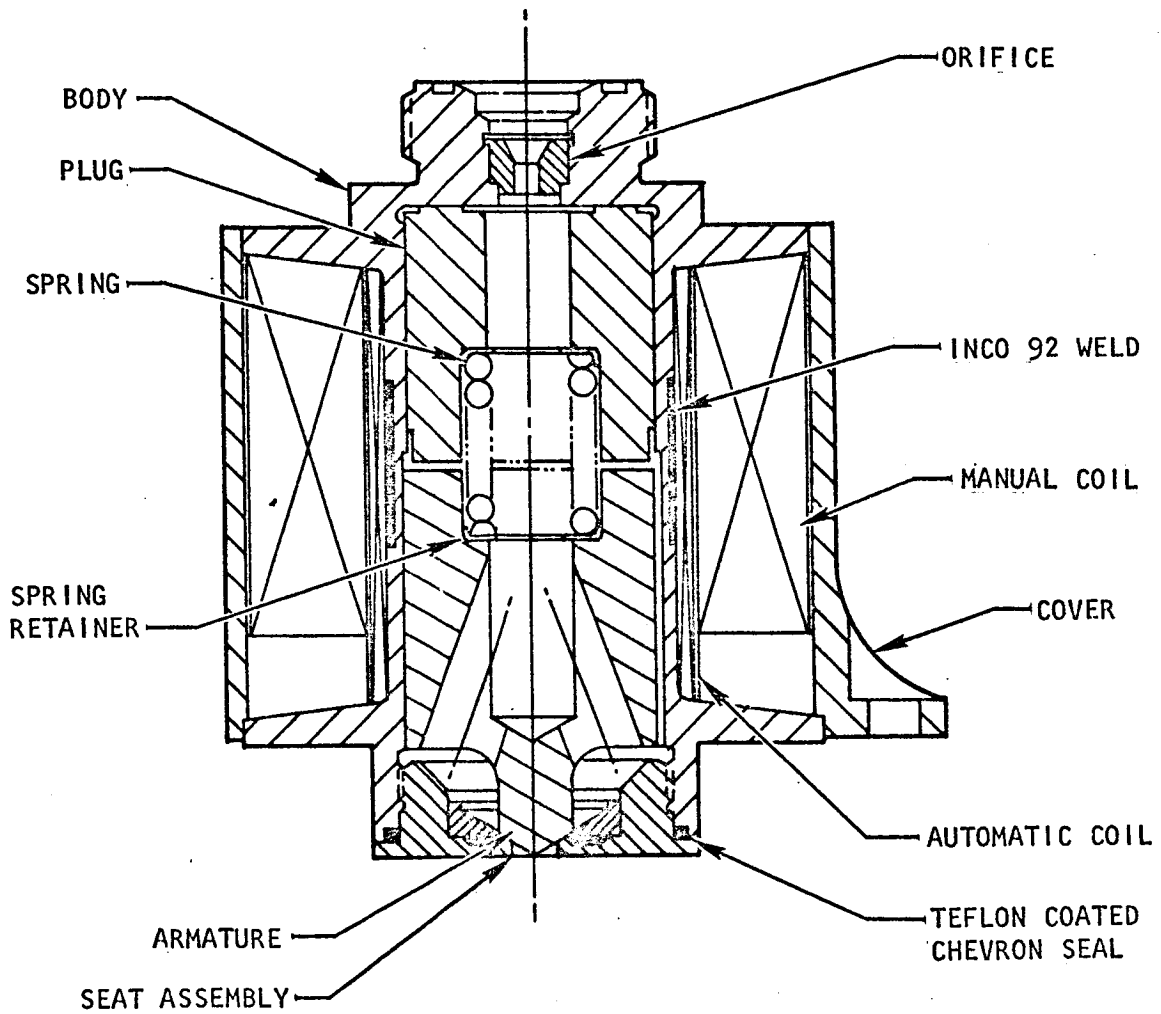


Figure 7

a. Solenoid Valve Cover

The cover for the solenoid valve is machined to final configuration in the form of a cylinder. The outlet end of the cover has three equally spaced integral lugs for attaching the valve assembly to the injector head.

b. Solenoid Valve Body

The body is the main structural component of the valve assembly and is machined in the configuration of a spool. The magnetic coils are wound directly onto the valve body. The inlet end of the spool has a threaded fitting for attachment of the propellant lines with an internal recess for the propellant flow control orifice and strainer. The outlet end of the spool has female threads to accept the valve seat assembly. The valve body forms the ends of the iron circuit of the electro-magnet as discussed above; however, the one piece construction formed a short circuit for the magnetic field and would not actuate the valve. Originally the spool assembly was made in two parts and welded at the mid-plane using Inco 92 weld rod, a non-magnetic material. Several problems were encountered with this design because of defective welds allowing propellant seepage into the windings of the coils. The current design has eliminated this problem by rough machining the spool as a one piece item with a 0.5 inch wide groove around the outside diameter of the spool at the mid-plane where the original two piece unit was joined. The groove is machined to within approximately 0.015 inch of the final inside diameter of the spool. The groove is back filled by automatic welding using Inco 92 weld rod to form a non-magnetic gap. After final machining, the valve body is Electrolyzed (a proprietary hard chromium plating) to enhance the wear characteristics of the 446 CRES in sliding contact with the moving armature.

c. Solenoid Valve Body Plug

The valve body plug or pole piece forms the stationary pole of the electro-magnet. The plug is cylindrical in shape with propellant flow passage through the center. The downstream end of the plug has a larger concentric recessed hole to position the armature closing spring and retainer without restricting the propellant flow. The valve body plug is shrink-fit with the plug seated against the inlet end of the solenoid valve body. The plug and valve body are machined to have a 0.0002 to 0.0006 inch diametrical interference fit. An upper limit of 500°F is placed on the valve body temperature during the shrink-fit operation.

d. Solenoid Valve Armature

The solenoid valve armature is machined with an integral poppet tip and forms the moving component of the valve seat. Stellite 6-B hardfacing alloy is weld deposited to the end of the poppet tip to resist wear from repeated contact with the valve seat. The armature is completely surrounded by the propellants; however, the primary propellant flow path to the injector head assembly is through a single hole at the upstream

end which also position the armature closing spring and spring retainer. This passage narrows below the retainer ending in blind hole near the downstream end of the armature. Four equally spaced propellant passages drilled at an angle through the downstream face of the armature intercept the above passage just above the poppet tip. Propellant flow through the four passages surround the valve seat and tend to center the armature in the valve body during operation. The outside diameter of the armature has three narrow close tolerance lands running the length of the armature to minimize drag against the valve body and help align the poppet with the valve seat. The armature is Electrolyzed for better wear resistant characteristics.

e. Solenoid Valve Seat Assembly

The valve seat assembly currently being used for both propellant valves consists of a three piece assembly. The valve seat and the valve seat insert are machined from AM 355 bar stock procured in accordance with AMS 5743. The valve seat seal is machined from TFE Teflon procured in accordance with a Marquardt Corporation specification. Both TFE Teflon and AM 355 have an "A" compatibility rating in contact with propellants. The valve seat is the largest component of the assembly and has male threads to mate with the downstream side of the valve body. A chevron type seal of TFE Teflon coated 17-4 PH stainless steel provides the seal between the seat assembly and the valve body. The armature poppet tip strikes and seats against the conical AM 355 seat; however, the poppet tip seals against the Teflon insert in the seat assembly. The Teflon seal is held in position in a recess in the valve seat insert by shrink-fitting the insert into the valve seat using a 300°F temperature difference with a maximum temperature of 100°F for the seat. After assembly and before final machining of the Teflon seat, the valve seat assembly is stabilized at 200°F for 8 to 10 hours and a subsequent room temperature hold for a minimum of 12 hours. This treatment reduces the tendency for the Teflon to creep and deform after final machining.

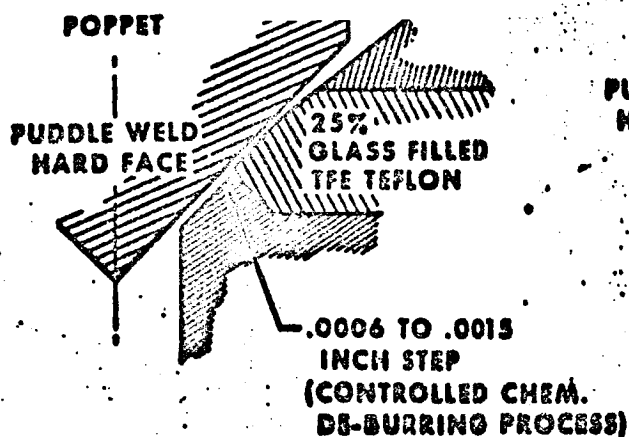
Early vintage valve seat assemblies were fabricated from Type 303 CRES and glass fiber filled TFE Teflon. Galling of the 303 CRES was a problem both in the attach threads and from impacting of the armature poppet tip. Shredding and cold flow of the glass filled Teflon resulted in changing the seal material to pure TFE Teflon.

Other than the above material changes, the valve seat design has remained essentially unchanged. The double angle Teflon seal (Figure 8) was changed to a single angle seal to provide a better seal surface and reduce the tendency to cold flow the Teflon. The inside diameter of the insert was changed to provide a void for the Teflon to cold flow upward rather than being extruded over the lower lip of the seat assembly and being shredded into the injector head.

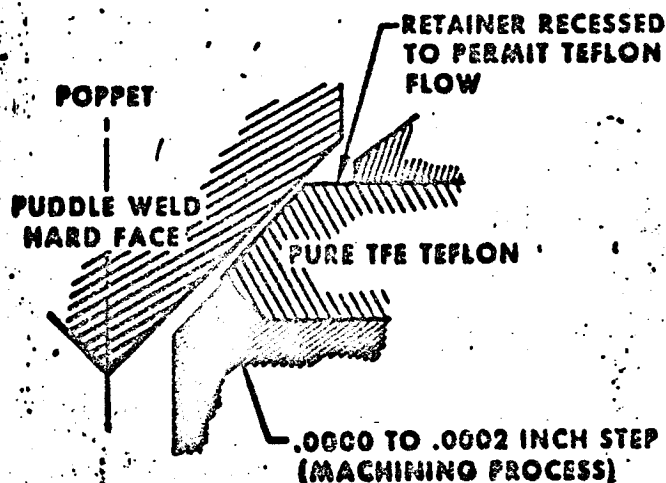


## VALVE SEAT DESIGNS

### DOUBLE ANGLE SEAT



### SINGLE ANGLE SEAT



f. Solenoid Valve Spring and Spring Retainers

The valve spring is made from Inconel X wire procured in accordance with AMS 5698. The function of the spring is to assure the necessary pressure for the valve to seal properly and provide the force required to rapidly close the valve. The spring has a working rate of 250 pounds per inch and maintains a pre-load on the sea armature of 2.75 pounds. Abrasion of the armature and the valve body plug is prevented by two 17-7 PH stainless steel spring retainers. The 17-7 PH stainless steel bar stock is procured in accordance with AMS 5644 in the TH-950 condition. Both materials have an "A" compatibility rating in contact with the propellants.

g. Flow Control Orifice

Propellant flow rate is regulated by a properly sized flow control orifice inserted in the inlet side of the valves. The orifices are machined from Type 304 stainless steel held in position by PH 15-7 Mo retainer rings.

h. Sediment Strainer

A type 304 L stainless steel strainer is located downstream of the flow control orifice in the valve body plug. The sediment strainer consists of a cylindrical shaped element rolled and seam welded from 20 mesh, 0.010 inch diameter wire. An inverted spherical shaped bottom formed from the same material as the cylinder is fusion welded to the downstream side of the strainer. The upstream side of the cylinder is resistance seam welded to a 304L ring which positions the strainer element in the valve below the flow orifice.

i. Solenoid Valve Coils

The electrical coils for actuation of the solenoid valve has an automatic coil for normal operation of the valve and a direct coil for manual or emergency operation. The coaxially wound coils are insulated from the valve body by two layers of MIL-I-15126 Type MFT 2.5 tape and from each other by MIL-Y-1140 grade ECC-B glass tape. The automatic coil consists of 685 turns of No. 30 AWG copper wire procured in accordance with MIL-W-583C, Class 220 Type M2 and extends the entire length of the valve body. The outer direct coil has 1,020 turns of No. 26 AWG copper wire procured in accordance with MIL-W-583C Class 220, Type M. The direct coil is wrapped with an insert located at the downstream end of the valve to provide a void for later attachment of the power cable. After wrapping, the coils are vacuum impregnated with 3M electrical insulating epoxy No. 250 and cured at 260°F for three hours. The insert at the end of the direct coil is removed and the four conductor electrical power cable consisting of 19 strand nickel coated copper wire is soldered to the automatic and direct coils. SN 60W Type K RA condition P3 solder procured in accordance with QQ-A-571d is used for this joint. The individual conductor of the power cable is insulated with color coded TFE Teflon sheathing. The Teflon is cleaned with Tetra-Etch to enhance the adhesion of the 3M electrical insulating epoxy No. 248 potting compound applied over each of the solder joints. After curing of the potted joints at 260°F for three hours the direct coil is wrapped with two layers of 3M polyester electrical insulation tape

No. 74 and the void around the power cable connection and the outside of the direct coil are covered with the 3M electrical insulating epoxy No. 248. The assembly is press fitted into the cover and the final potting compound is cured at 260°F for three hours. Abrasion of the power cable Teflon jacket where it enters the solenoid valve through the valve cover is prevented by a Teflon grommet.

The early version of the solenoid valve coil utilized a three coil system: (1) an opening coil, (2) a holding coil, and (3) an emergency coil which was separated from the other coils by a fire wall. This arrangement was later changed to the coaxially wound automatic and direct coil system without the fire wall. Burn out tests of the automatic coils at approximately 750°F resulted in a temperature of less than 270°F (maximum allowable 300°F) in the direct coil. Aluminum windings were used in the original coils to reduce the overall weight of the engine. However, several problems were encountered in joining the aluminum windings and the copper leads of the power cable. The major problem was associated with the incomplete removal of the highly corrosive flux necessary to solder the aluminum. The flux problem was eliminated by using an ultrasonic soldering technique but the aluminum windings were replaced with the current copper winding to improve the reliability of the rocket engine system.

## 5. Special Investigations

### a. Literature Survey

A literature survey indicated that solenoid valves with Teflon seats would perform satisfactorily in the hard vacuum of space. Static and dynamic tests were conducted at  $10^{-6}$  mm Hg with no adverse affect on seat leakage, coil dielectric strength, coil resistance, activation amperage and voltage or response characteristics. The dissimilar metals, Stellite 6 and AM 355, used in the valve seat and the poppet tip will preclude the tendency for materials to cold weld in space.

### b. Endurance Testing

A prototype solenoid valve was subjected to an endurance test with the accumulation of over one million cycles. Response time, flow, stroke and leakage tests were conducted at several points during the test. No change was observed in either response time or pressure drop. Zero leakage was noted at each point. The stroke increased from 0.0310 inch to 0.0315 inch over the total accumulated cycles. Visual and microscopic inspection of the valve components indicated that, due to permanent set in the downstream portion of the seat assembly, the sealing point of the poppet on the Teflon seal had relocated from the downstream to the upstream side. The poppet seats on the AM 355 metal portion of the seat assembly but seals on the Teflon.

## C. Combustion Chamber

### 1. Function

The combustion chamber must perform two essential functions in the operation of the engine. These functions occur in two distinct areas of the combustor; (1) the chamber portion must present a boundary for the liquid propellant mixing and combustion, and (2) the exit nozzle including the necked down throat section must direct, accelerate and eject the combustion gas in an efficient manner. Liquid propellants are sprayed into the chamber region by the injector where they are mixed and burned resulting in rapid expansion of the hot gaseous combustion products. Ejection of the hot gas from the combustor and acceleration in the throat nozzle to supersonic velocities produce the forward thrust of the engine. These simple functions are compounded considerably by the fact that the combustion temperatures are extremely high, approximately 5200°F.

## 2. Material Selection

Materials capable of operation at this temperature and environment were not and are still not available, however, fuel film radiation cooling of the combustion chamber to the infinite heat sink of space and a partial gas cooling boundary film lowered the temperature to a level that could be tolerated by existing materials. The initial criteria for selection of the combustion chamber material was a material with the capability to withstand an inner wall temperature of approximately 3000°F and 3000 psi induced stress for 10 minutes with less than 2 percent creep. In addition, the material was required to have a low specific heat and low density for rapid cooling of the chamber wall after engine shutdown to prevent high injector head temperatures. The operating environment consists of space vacuum on the outside diameter and oxidizing combustion products, mostly water vapor and short term exposure to raw propellants on the inner wall. The radiation cooled design made it desirable to use a high emittance material for better heat rejection. These design conditions dictated the use of a refractory metal alloy. Since the potential for oxidation would always be present because of the combustion products, the material selected had to be oxidation resistant itself or have an oxidation resistant coating available. A literature search led to the choice of investigating: (1) molybdenum alloys because of their known successful application at Marquardt under similar conditions, or (2) columbium alloys for their ease of fabrication, ductility and limited application experience at Marquardt, or (3) the 90 percent tantalum-10 percent tungsten alloy for its higher temperature capabilities and good fabrication characteristics. Tungsten was not considered because of its high density, fabrication problems and the lack of an oxidation protection system.

Since no single refractory alloy exhibited all of the desirable properties, a compromise was made based on previous experience and coating availability. Unalloyed molybdenum with a silicide coating applied by the pack cementation process was selected.

## 3. Fabrication and Operating Condition Improvement

### a. Combustion Chamber Fabrication

Operation of the combustion chamber with a wall temperature of approximately 3000°F results in a temperature in excess of 1600°F at the aft end of the expansion nozzle. A typical temperature profile taken from one of the early

engines is shown by Figure 9. Because of these temperature requirements the combustion chamber and expansion nozzle were fabricated as a single unit from an unalloyed molybdenum forging. The steps in the manufacturing process are shown by Figure 10. As indicated the forgings were machined to the approximate configuration of the combustor and to the flow-turn preform shape. The expansion nozzle portion of the preform was flow-turned to final shape in a two step process with an intermediate anneal. Final machining of the combustion chamber section and trimming of the aft end of the expansion nozzle completed the shaping of the combustor. Flow-turning of the expansion nozzle resulted in a refined grain structure and imparted a greater strength without significant loss of ductility in the thin section.

#### b. Silicide Coating

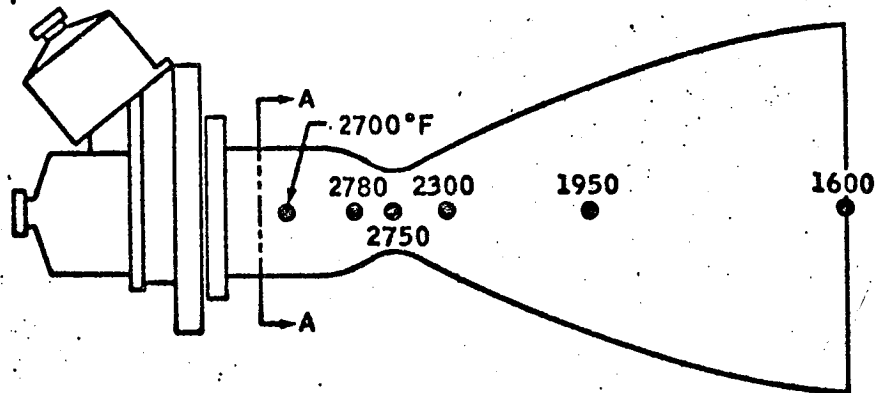
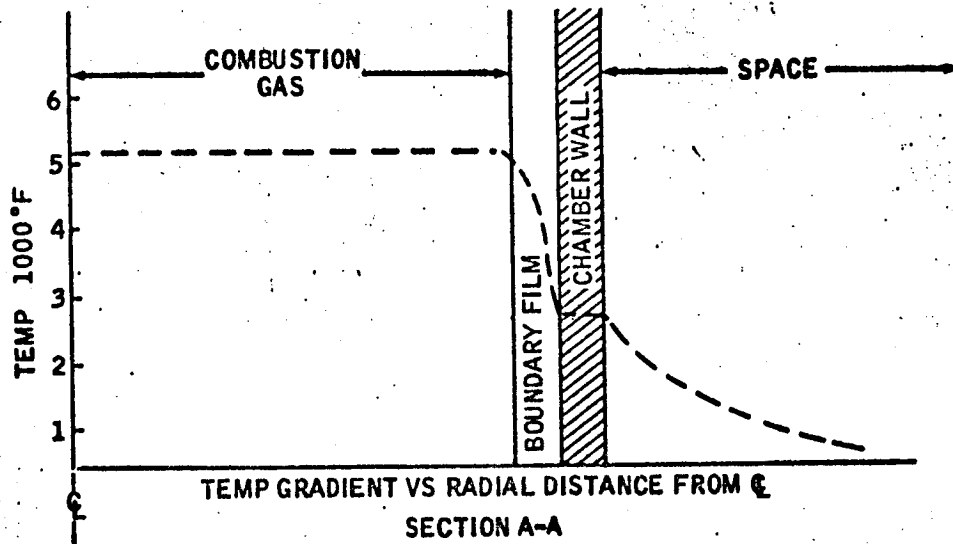
Since refractory metals exhibit high oxidation rate, they require an oxidation protective coating for satisfactory operation in a high temperature oxidizing atmosphere. The chambers are coated with molybdenum disilicide ( $\text{MoSi}_2$ ) by the Chromizing Corporation Durak "B" pack cementation process. The chambers are sealed into a retort containing silicon metal and other proprietary chemicals and held at approximately  $1800^\circ\text{F}$  for several hours to accomplish the coating process. The resulting coating has the capability of withstanding the conditions and environment of the combustion chamber for periods in excess of 90 minutes.

The integrity of the coating was initially evaluated by a "smoke test" consisting of placing the completed combustion chamber in a  $2500^\circ\text{F}$  furnace for 5 minutes with a visual examination every minute by raising the furnace door. The open door insures ample access of air to the parts which accelerates oxidation at any defect in the coating. Defects can be readily observed by the formation of  $\text{MoO}_3$ , which appears as a white smoke. The coating consists of a multiple layered structure with varying compositions of molybdenum and silicon as shown by Figure 11.

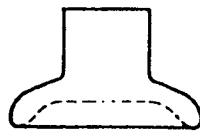
#### c. Operating Temperature Reduction

The operating temperature of the combustion chamber has been reduced significantly during the development of the current 100-pound thrust engine. The temperature of the combustor wall which was originally in excess of  $3000^\circ\text{F}$  has now been lowered to a maximum localized temperature of less than  $2400^\circ\text{F}$ . Several factors are responsible for this improvement in operating conditions. The most significant was the development and incorporation of fuel film cooling (see Section II-A for details) where fuel from ports in the injector head are sprayed directly on the previously hot spots of the combustor wall without being reacted with oxidizer. The hot spots are located between the fuel oxidizer doublets. Another important improvement in the operating conditions of the combustor was accomplished by increasing the emittance of the chamber. The outside diameter of the chamber was roughened by grit blasting the wall with silicon carbide. The rough surface increased the total hemispherical emittance from approximately 0.45 to approximately 0.64 and reduced the wall temperature by approximately  $200^\circ\text{F}$ . because of the higher heat rejection rate. Utilization of these design changes and the resultant lower wall temperature reduced the operating temperature of the expansion nozzle section of the thrust chamber sufficiently enough to allow the use of a more ductile oxidation resistant uncoated high temperature alloy. L-605, a cobalt base alloy was

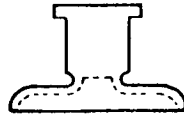
## CHAMBER WALL TEMPERATURE



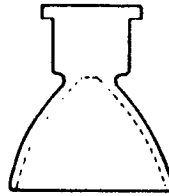
## FLO-TURN MANUFACTURING PROCESS



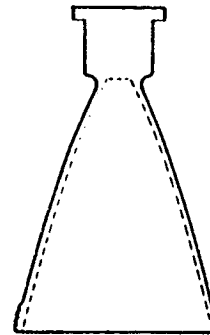
FLO-TURN  
FORGING



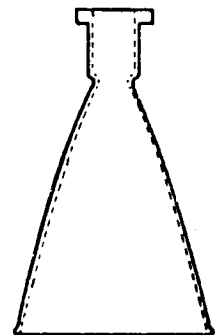
MACHINED  
PREFORM



FIRST  
FLO-TURN



SECOND  
FLO-TURN



FINISH  
MACHINED

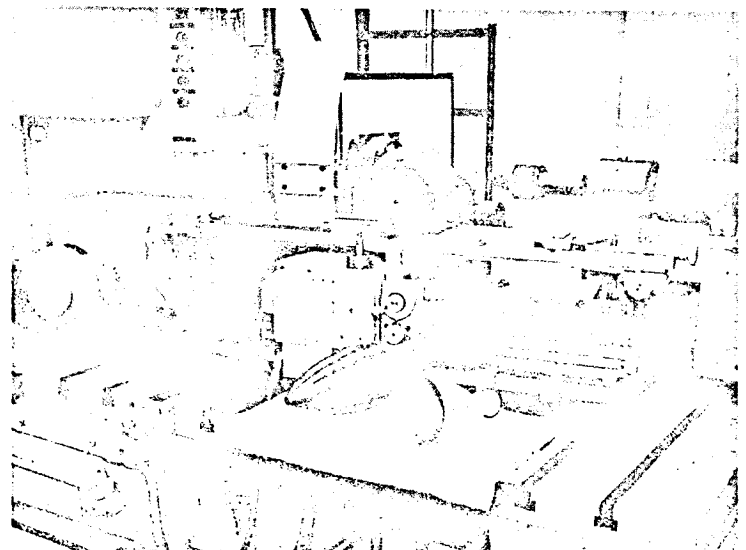
### FIRST STEP OF THE FLO-TURNING OPERATION



NEG. 4703-3



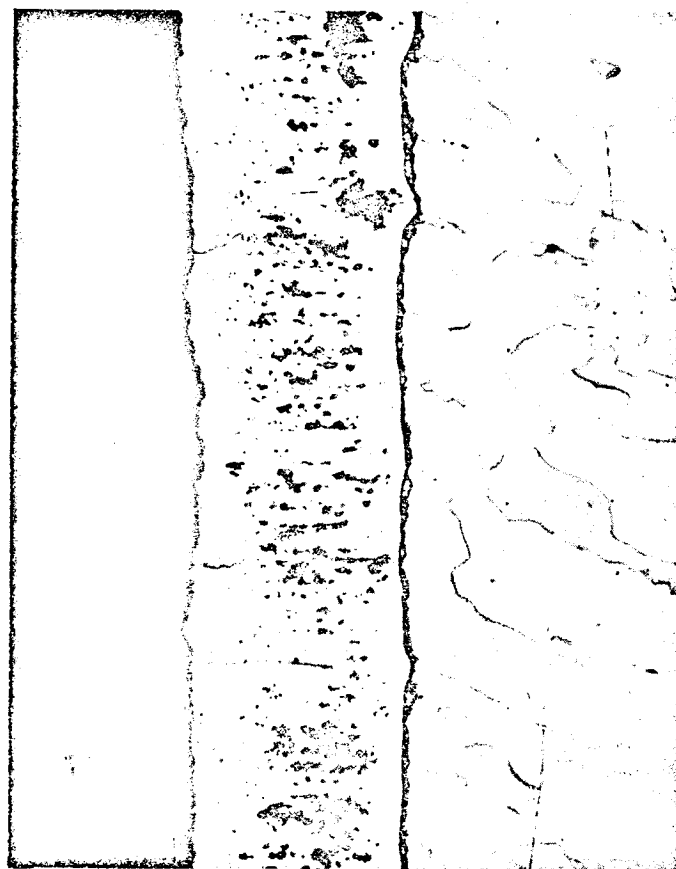
NEG. 4703-4



NEG. 4703-5

### SECOND (FINAL) STEP OF FLO-TURNING

NEG. C9654-1



Photomicrograph of Unalloyed Molybdenum  
Coated with Molybdenum Disilicide (X500)



selected for replacement of the expansion nozzle section starting approximately 1.4 inches aft of the divergent section of the combustor throat. The temperature at the attach point of the L-605 expansion bell is approximately 1600°F during steady state operation.

d. Ribbed Chamber Configuration

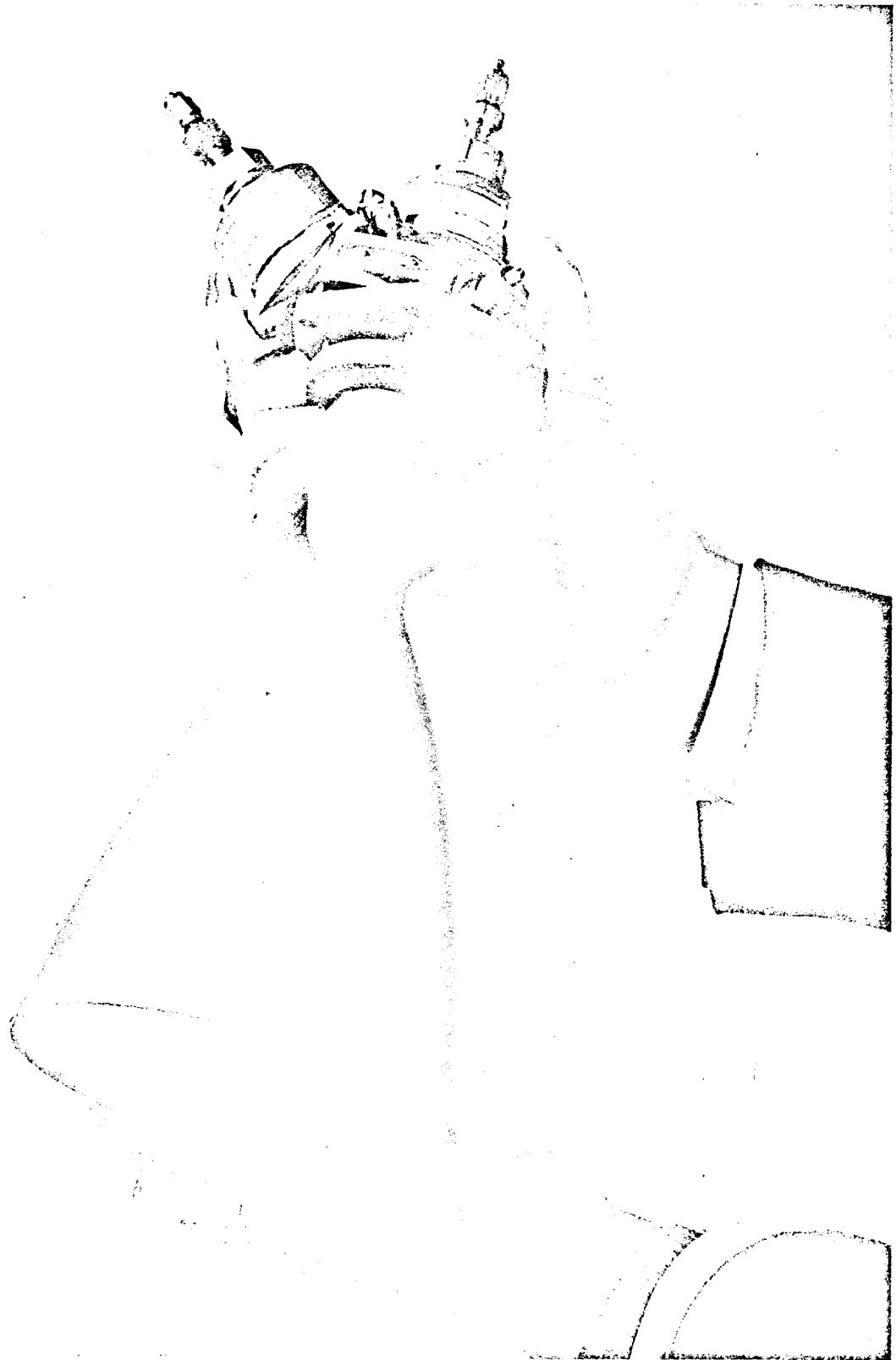
Evaluation of the initial straight walled combustion chamber configuration instrumented with strain gages indicated that bending of the combustor wall was occurring during the combustion process. In order to reduce the degree of bending possible a contoured chamber with stiffening ribs was designed and evaluated. The internal size and shape of the chamber was unchanged; however, two external ribs running circumferentially around the chamber (Figure 12) were added to increase the hoop strength of the chamber and reduce the tendency to bend during firing of the engine. The thin section of the wall above and between the contoured ribs remained the same as the initial wall thickness (0.064 inches).

e. Current Combustion Chamber

The current combustion chamber design for the Marquardt 100-pound thrust rocket engine consists of a two component unit. The combustor is machined from the same type unalloyed molybdenum forging discussed above except the skirt section of the forging originally required for the expansion nozzle is not used. The combustor is machined to final configuration and vacuum stress relieved at 1850°F for one hour prior to silicon carbide grit blasting to increase the emittance of the hotter portions of the chamber. The exterior surface, extending from the thickest section of the rib nearest the forward flange to within 0.020 inch of the downstream side of the aft flange, is roughened to a surface finish in excess of 100 RMS. The chamber is silicide coated with Durak "B" by the Chromizing Corporation's pack cementation process to a nominal thickness of 0.0026 inch. The coating thickness is evaluated by metallographic evaluation of a ring machined from the skirt sections of the unalloyed molybdenum forging and coated in the same retort as the representative combustion chamber. After acceptance, the coated chamber is subjected to a 2000°F five minute duration smoke test for evaluation of the coating integrity. The smoke test temperature was reduced from 2500°F to permit better observation of the chamber in the furnace and to avoid excessive grain growth of the recrystallized material at the higher temperature. One part from each furnace run is submitted for x-ray diffraction of the coating to determine the coating composition.

f. Combustion Chamber Seals

The mating surfaces of the forward and after combustor flanges are lapped to a flatness of less than three light bands to provide a seal between the injector head seal and the L-605 expansion bell. A minimum of 0.0008 inch of coating must remain on the lapped surface to provide oxidation protection for the molybdenum substrate. The amount of coating remaining on the lapped flanges is measured with a Dermitron instrument which operates on eddy current principles using calibration standards with the coating thickness established metallographically. After lapping, the chamber is subjected to a second 2000°F five minute duration smoke



NEG. 6029-1

Engine with One Piece Ribbed Combustor

test to evaluate the adequacy of the coating remaining on the lapped flanges. The minimum coating thickness requirement was established by oxidation exposure (smoke testing) of lapped samples with varying coating thickness. Several samples having less than a 0.0004 inch coating failed with catastrophic oxidation of the molybdenum substrate. No failures were observed on samples with coatings greater than 0.0006 inch thick. The second smoke test is a check on the Dermitron evaluation of the lapped surfaces and also isolates local defects in the coating.

#### g. Expansion Nozzle Fabrication

As previously discussed, L-605 a cobalt base alloy was selected as the material for the expansion nozzle section of the two piece combustion chamber configuration. L-605 is a high strength elevated temperature alloy with excellent oxidation resistance and has been used for several rocket applications at Marquardt. The material is procured as vacuum arc remelted bar stock by the forging vendor. The bar stock is hot upset forged into a shear spinning blank and solution annealed. The blank is machined into a shear spinning preform and flo-turned at Marquardt to the final internal configuration. The wall section of the bell is reduced to a final thickness of 0.010 to 0.014 inch by machining the external surface. Eight circumferential ribs 0.110 inch high with varying thicknesses are left around the outside diameter of the bell to provide a light weight rigid structure. The wall at the forward end of the expansion bell is increased in thickness from the first strengthening rib forward. A recessed flange is machined into this thicker portion of the bell to mate with the lapped after end of the combustion chamber. The outside diameter of the bell flange is threaded to mate with a Waspaloy attach nut. The combustion chamber and the expansion bell are assembled into a unit by placing a L-605 washer machined to fit the inside diameter of the expansion bell recessed flange in contact with the upstream side of the after flange of the combustor. Torquing the attach nut onto the expansion bell flange forms a compression type seal between the two components. The attach nut is prevented from working loose by a L-605 lock ring which is crimped over the nut and held in position by a L-605 pin spotwelded to the external surface of the heavy portion of the expansion bell.

#### 4. Special Investigations

##### a. Combustion Chamber Life

The useful life of the silicide coated unalloyed molybdenum combustion chamber is dependent on degradation of the coating resulting from oxidation of the molybdenum substrate. The predicted life of the chamber (Figure 13) was obtained from analytical studies and test data. Degradation of the coating is negligible during pulse type operation in a hard vacuum. The largest coating loss would occur during steady state operation. The coating life at 2350°F is more than 2500 minutes in a hard vacuum on the outside of the chamber and 7500 minutes on the inside wall. Since the loss of coating from the outside wall will not result in engine failure, the actual life of the engine is 7500 minutes at 2350°F. The minimum life of a silicide coated combustion chamber during steady state operation at 2700°F and 3000°F is 500 and 50 minutes, respectively.

b. Defective Coating Evaluation

Mishandling of coated combustion chambers during fabrication and inspection can result in chipping of the coating edge radii of some parts. The coating in this area is structurally weak because of the crazing cracks inherent in the coating. An engine test, to support this investigation, was conducted using a chamber with a coating chip on the inside diameter of the aft flange. The combustor was subjected to 1620 seconds of burn time without adverse effect on the engine.

D. Seals and Attach Hardware

1. Valves - Injector Head

The injector head components are assembled using metal to metal seals formed by an interference press and shrink fitting operation. The details of the assembly procedure are discussed in Section II-A. The valves are sealed to the injector head assembly by redundant omniseals consisting of a Teflon seal with a "U" shaped configuration. The legs of the "U" are separated by a PH 15-7 Mo coil spring. One seal is located around the preigniter tube and seals against the preigniter insert and the downstream side of the valve seat. This seal stops the flow of propellants leaking past the metal to metal spherical seat. A chevron type seal, consisting of Teflon coated 17-4 PH stainless steel, located between the valve seat assembly and the valve body prevents propellant leakage from the valve itself. A second omniseal located between the valve body and preigniter insert provides a back-up seal for the two primary seals. The seals are procured as finished items.

The valves are attached to the injector head by three equally spaced screws installed through the downstream flange of the valve body cover and torqued into an A-286 insert in the injector head. A-286 screws are used to attach the oxidizer valves and titanium 6Al-4V screws are used for the fuel valve attachment. The two different fastener materials were selected because of mechanical property requirements and the necessity for the materials thermal expansion characteristics to be compatible with that of the injector, preigniter and valve configuration. The design was based on the high operating temperatures of the early engines. The A-286 oxidizer valve screw material is procured in accordance with AMS 5735 or AMS 5737 and the Titanium 6Al-4V fuel valve screw material is procured in accordance with NAS 621. Both screws are hot headed, centerless ground to size and threaded by a thread rolling operation. The threaded portion of the screws are coated with Lubu-Bond "A" to prevent galling during assembly.

The screws are torqued to 3 inch-pounds above the free running torque in the lock nut. Stainless steel lock wire is threaded through the three screw heads of each valve to prevent the screws from working loose during service. The seals are checked by pressurizing the downstream side of the injector head with 350 psig dry filtered nitrogen for 10 minutes. No leakage is permissible.

## 2. Combustion Chamber - Expansion Nozzle

The combustion chamber to the expansion seal is obtained by lapping the rough surface of the as-coated aft flange of the combustor, where it mates with the expansion nozzle, to a three light band flatness requirement. The expansion nozzle flange is machined to a 32 rms surface finish with a flatness requirement of 0.0005 inch. A Waspaloy nut, machined from bar stock procured in accordance with AMS 5706, threaded to the expansion nozzle is used to attach the components. Abrasion of the coating by the nut during torquing is prevented by a L-605 compression washer located between the nut and the forward side of the aft flange of the chamber. The washer is procured in accordance with AMS-5706 and used in the solution annealed condition. The Waspaloy attach nut is torqued to 1,000 inch-pounds and is prevented from working loose during service by a L-605 lock ring. The lock ring is pinned to the expansion nozzle and is crimped to the nut wrenching lugs at four locations.

## 3. Combustion Chamber - Injector Head

The combustion chamber to the injector head seal consists of compressing a L-605 seal ring between the forward flange of the combustor and the injector head. The temperature requirements imposed on this seal have been downgraded considerably during the development of the engine. Initially the forward flange of the combustor operated at approximately 1800°F and in addition to providing a seal, the seal ring had to provide a thermal barrier between the combustor and the injector head. Utilization of the fuel film cooling concept and increasing the emittance of the chamber by grit blasting has reduced the normal steady state operating temperature of the flange to approximately 300°F. Therefore, the complex seal designs originally required has been replaced by a flat L-605 washer. The seal groove in the injector head has a flatness requirement of 0.0005 inch with a 16 rms surface finish. The rough as-coated surface of the mating forward flange of the combustion chamber is lapped to a three light band flatness. The L-605 seal ring is machined to a 6 rms surface finish with a flatness requirement of 0.0001 inch.

The combustion chamber is attached to the injector head with Rene' 41 hardware. This high temperature alloy was initially required because of the strength requirements at elevated temperatures necessary to maintain the proper seal pressure. The attach hardware consists of a split ring which contacts the downstream side and the outside diameter of the forward flange of the combustor and an attach ring which clamps the split ring in position and provides a uniform distribution of the attach bolts compressive loads. The split ring and the attach ring are machined from Rene' 41 bar stock procured in accordance with Marquardt Specification MMS-2212. The compressive load on the seal is maintained by six Rene' 41 attach bolts threaded into A-286 clinch nuts mounted in the injector head. The stock for the attach bolts is procured in an annealed condition in accordance with AMS-5712. The bolts are hot headed, centerless ground and the shanks cold reduced approximately 2 percent by flat rolling prior to the precipitation heat treatment. The cold work increases the yield strength from a 130,000 psi to over 150,000 psi. The attach ring has a total of 42 holes drilled through the cylindrical portion, six for the combustor attach bolts and the remainder to reduce the weight of the unit. The extra holes also increase the surface area of the ring

providing an increase in the heat rejection rate to space. The components are assembled and the attach bolts tightened in sequence to 18 inch-pounds torque above the free running torque in the clinch nuts. The installation criteria is based on a uniform 0.0027 to 0.0034 inch elongation of the bolt rather than to a given torque value. However, a maximum torque of 28 inch-pounds may be used to obtain the desired elongation. The combustion chamber to the injector head seal is pressure checked with dry filtered nitrogen at 175 psig for five minutes with a maximum pressure decay of less than 15 psig during the five minute test.

### III. SPECIAL EVALUATION

#### A. Coating Development

The initial operating conditions of the combustion chamber required a material capable of withstanding an inner wall temperature of approximately 3000°F and a 3000 psi induced stress for 10 minutes with less than 2 percent creep. The refractory alloys capable of meeting the strength requirements had to be protected from oxidation by the application of a suitable coating material. Several coatings were evaluated by oxyacetylene torch test exposure at temperatures in excess of 2800°F. The evaluation included such coatings as: (1) titanium nitride, (2) zirconium diboride-chromium, (3) zirconia-chromium, (4) silicide applied over plasma sprayed tungsten, (5) electro-phenolic deposition of a chromium-cermet, and (6) Durak MGF. The most promising coatings evaluated were: (1) Chromizing Durak B, (2) Chromizing Durak B modified with boron, (3) Marquardt silicide, and (4) General Telephone and Electronics Laboratories aluminide. Some of the coatings which were evaluated early in the program failed during the five minute duration 2500°F furnace oxidation exposure prior to torch testing and others in less than 30 seconds at 3000°F. The aluminide (tin-aluminum) coating performed exceptionally well with torch test life determined at 3400°F, 3200°F, and 3000°F of approximately 15 minutes, 3 hours and in excess of 3 hours, respectively. However, the aluminide coating deteriorates extremely rapidly when subjected to an elevated temperature vacuum environment. The Marquardt developed silicide coating and the Chromizing Durak B exhibited approximately equivalent torch test endurance; however, the Durak B coating modified with boron provided an increase in the coating life. The expected life of boron modified Durak B coated molybdenum combustion chambers as a function of time at temperature is shown by Figure 13.

#### B. Compatibility

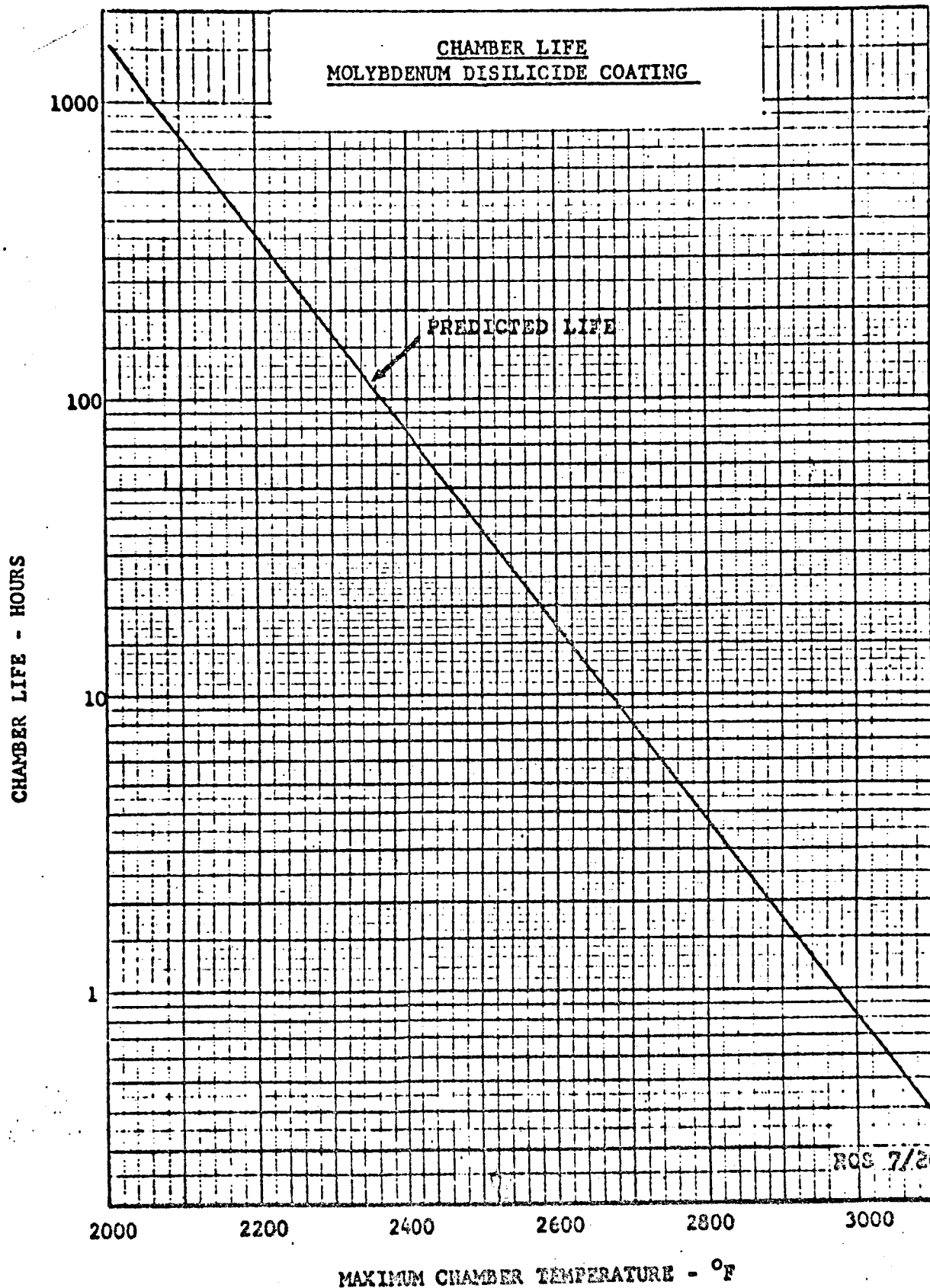
The various materials used in the Marquardt 100-pound thrust engine were selected with propellant compatibility as one of the major criteria. The compatibility rating of the various materials in contact with the propellants have been discussed in Section II. The materials also had to meet the compatibility requirements discussed below.

##### 1. Humidity Test

One of the 100-pound thrust engines was placed in a humidity environmental chamber for 10 days after acceptance testing. The purpose of the test was to determine the extent of any changes in the functional or performance characteristics of the engine or components resulting from the humidity exposure. The environmental chamber was maintained at a relative humidity of  $95 \pm 5$  percent at  $125 \pm 5^\circ\text{F}$ . No corrosion or other deterioration of the engine components or operation was observed.

##### 2. Salt Spray Tests

A 100-pound thrust engine was subjected to a salt spray environmental test in accordance with MIL-STD-810. The test consisted of a 48-hour exposure to a five percent sodium chloride fog at 95°F. The purpose of this investigation was to determine the sensitivity of the engine to corrosion and possible contamination when exposed to a salt atmosphere on the launch pad. After 24 hours the salt solution





was checked for conformance to MIL-STD-810, the engine was also given a cursory inspection. Corrosion was observed around the lock nut fittings of the injector head bolts and on the fuel valve cap. The same conditions were observed after completion of the scheduled 48 hour exposure. There was no indication of coating deterioration or corrosion on any part of the combustion chamber. Examination of the interior of the injector head showed no evidence of salt deposits or corrosion.

A test program was conducted to investigate the effect of corrosion on the lock nuts and attach screws. An injector head with the A-286, Ti-6AL-4V and Rene' 41 attach screws in place was subjected to a 48 hour salt spray test in accordance with MIL-STD-810. The same type of general corrosion, as discussed above, was observed around the lock nuts. The screws were removed from the injector head, visually examined and tensile tested to the 0.2 percent yield strength using standard tensile grips to obtain a stress-strain curve. The screws were then replaced in the injector head and tested to failure using the injector head and lock nuts as part of the test fixture. All of the screws failed in the shank portion, typical of parts tested to failure in the standard test fixture. The salt spray exposure did not reduce the holding power of the lock nut below the ultimate strength of the screws. The ultimate tensile strengths of the exposed screws were slightly below the average values obtained on similar parts without the salt spray exposure; however, this decrease was attributed to misalignment of the screw in the test setup.

#### C. Alternate Combustion Chamber Materials Evaluation

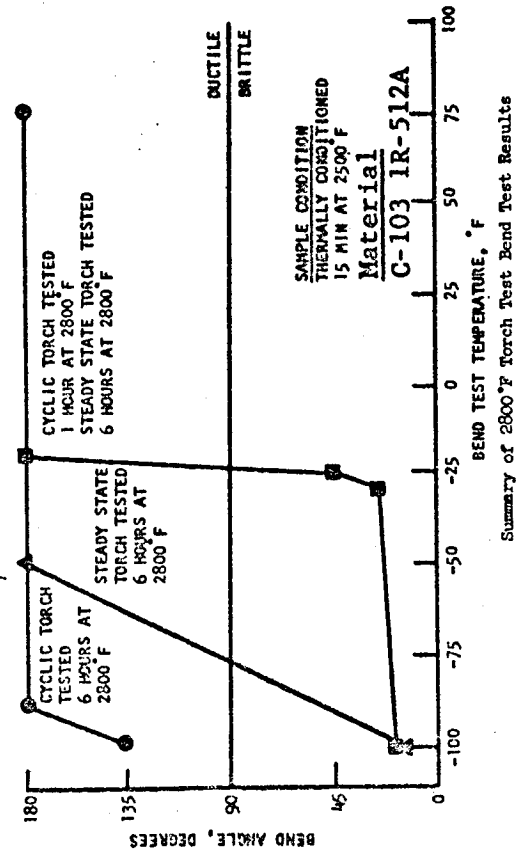
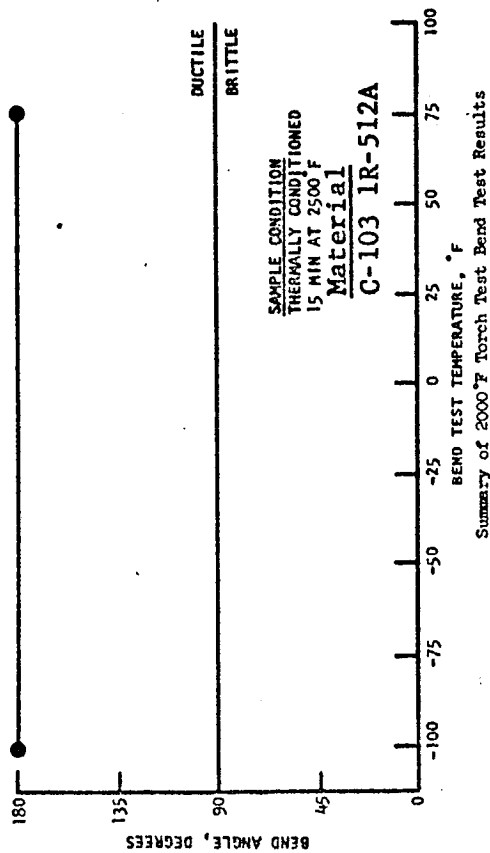
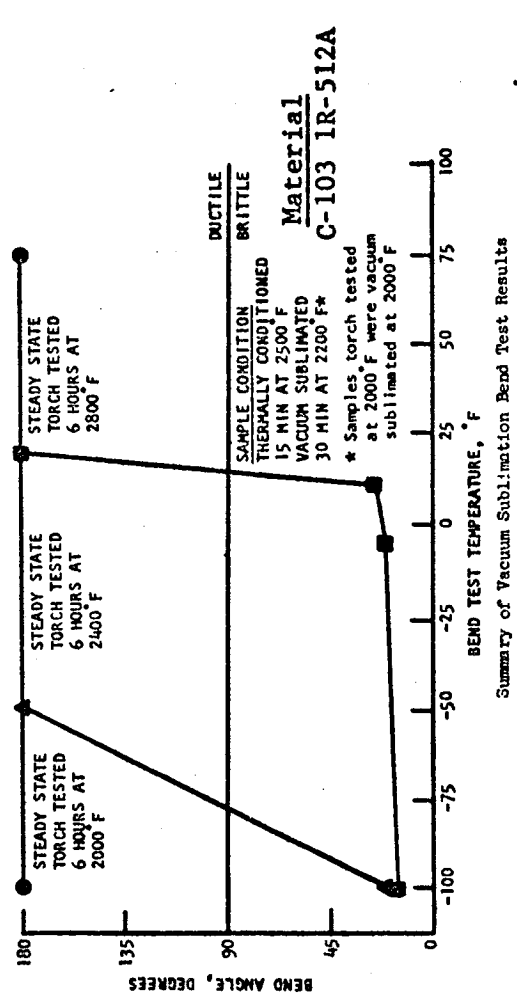
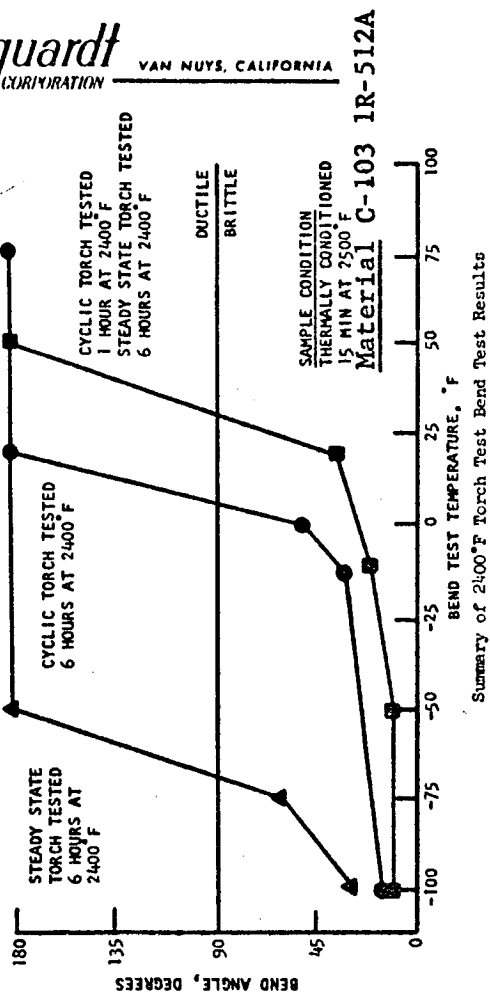
Marquardt has been actively pursuing the development of a ductile refractory alloy for rocket engine combustion chamber applications for several years through comprehensive material testing programs and rocket engine firing. An extensive survey of refractory alloys and oxidation protective coatings conducted in 1962 resulted in the selection of several columbium base alloys for evaluation with both silicide and aluminide coatings. One of the major problems encountered in the early development program was associated with embrittlement of the substrate because of interstitial gas (primarily hydrogen) absorbed during the pack cementation coating process. However, the loss of ductility could be restored to the substrate by subjecting the embrittled combustor material to a thermal outgassing cycle at temperatures in excess of 2000°F.

Extensive testing during the early development of the Apollo Service Module Reaction Control System engine with the unalloyed molybdenum combustion chamber resulted in high, almost instantaneous, pressure transients. The pressures encountered when the engine was started during simulated high altitude conditions resulted in plastic deformation and strain rates large enough to damage the combustion chamber. The NASA Manned Spacecraft Center, Houston, Texas awarded a contract to Marquardt in 1965 for the "investigation of High Strain Behavior of Refractory Alloys and Coatings". The objective of the program was the evaluation of coated and uncoated refractory alloys under rocket engine environmental and loading conditions resulting from ignition pressure spikes.

The high strain rate evaluation consisted of testing coated and uncoated tensile specimens at normal strain rates at  $-100^{\circ}\text{F}$ , room temperature and  $2500^{\circ}\text{F}$  and at high strain rates (100 to 250 inches/inch/second) at  $-100^{\circ}\text{F}$  and room temperature. The high strain rates were equivalent to those experienced by the combustion chamber during maximum combustion ignition pressure conditions. Full size combustion chambers of the Apollo configuration were also evaluated on a Marquardt designed hydraulic rig with a capacity equivalent to or exceeding those experienced in actual engine firing. The ultimate strength performance of the coated and uncoated ductile materials (C-103, C-129Y and 90 Ta-10W) tested at high strain rates, were found to be 50 to 100 percent higher than the strength values obtained at standard strain rate conditions. The material ductility was generally not affected. The unalloyed molybdenum control material confirmed the engine test experience, exhibiting a brittle nature.

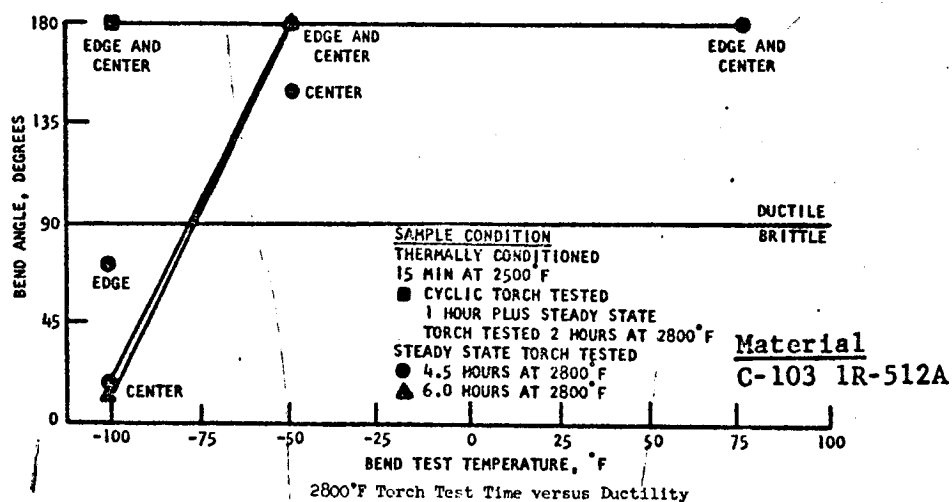
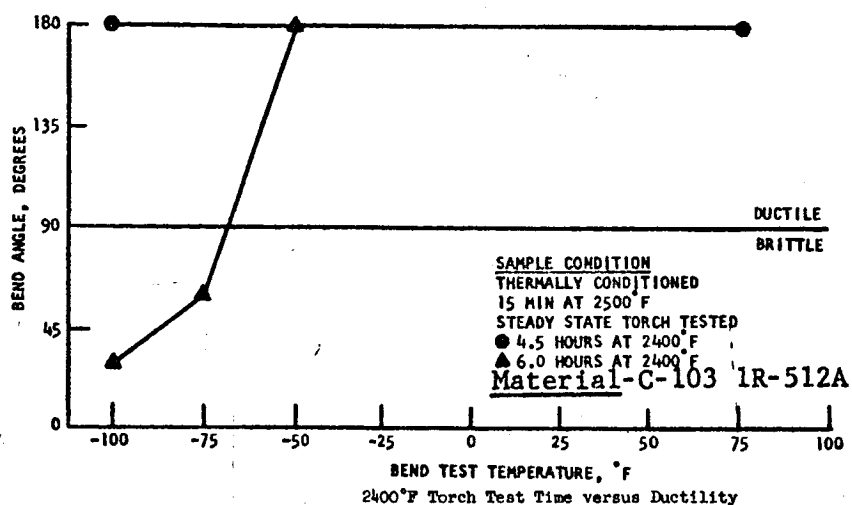
In 1965, a very extensive program was conducted for the purpose of selecting a ductile material-coating system as an alternate for the unalloyed molybdenum radiation cooled combustion chamber of the 100-pound thrust engine. This company funded program included various combinations of three columbium base alloys (C-103, SCb-291 and C-129Y) and three silicide coating systems (Sylvania R-512A, Chromizing Durak KA, and the TRW Si-Ti-Cr) and one aluminide (VacHyd Lunite). The coating selection was based on the results of test samples exposed to: (a) furnace oxidation at  $2800^{\circ}\text{F}$ , (b) cyclic and steady state oxy-propane torch testing at  $2800^{\circ}\text{F}$ , (c) vacuum sublimation in a  $10^{-4}$  torr vacuum at  $2600^{\circ}\text{F}$  plus cyclic and steady state torch testing, (d) hydrogen exposure (30%  $\text{H}_2$ , 70% A) at  $1400^{\circ}\text{F}$  and (e) rocket engine testing of combustion chambers. Evaluation of the test samples and combustion chambers included: (a) visual examination, (b) weight change, (c) bend testing, (d) metallography, (e) x-ray diffraction, (f) chemical analysis and electron beam microprobe analysis. Columbium alloy C-103 coated with Sylvania R-512A was selected as the most promising material/coating system evaluated.

The suitability of the C-103/R-512A material/coating system was confirmed by additional sample evaluation and rocket engine testing conducted on a NASA Manned Spacecraft Center contract, "Development of a Ductile Columbium Alloy Rocket Engine Combustion Chamber". The life of the R-512A silicide coating during oxy-propane torch testing at temperatures of  $2000^{\circ}\text{F}$ ,  $2400^{\circ}\text{F}$  and  $2800^{\circ}\text{F}$  was shown to be in excess of seven hours, which was chosen as an arbitrary limit for the duration of testing. Some loss of cryogenic ductility was observed as a result of interstitial gas absorption during the longer duration, higher temperature oxy-propane torch testing. A limited amount of work indicated that outgassing of the absorbed interstitial elements would occur in a space vacuum, and thus the cryogenic ductility would be maintained during the life of the coating. Figure 14, summarize the results of the bend tests as a function of oxypropane test temperature with and without vacuum sublimation.



COLUMBIUM BEND TEST RESULTS

Figure 14



COLUMBIUM BEND TEST RESULTS

Figure 14 (continued)

CHAPTER 9

PROPELLANT VALVE DESIGN

BY

H. H. DE BOI

TABLE OF CONTENTS

		<u>Page</u>
I	INTRODUCTION	9-1
II	CHRONOLOGY OF VALVE DEVELOPMENT	9-7
	A. Evolution of Valve Configuration	9-7
	B. Valve Test History	9-11
III	VALVE DESIGN CRITERIA	9-47
	A. Leakage	9-47
	B. Response Repeatability	9-50
	C. Propellant Compatibility	9-55
	D. Design Requirements	9-55

LIST OF ILLUSTRATIONS

<u>Figure Number</u>	<u>Title</u>	<u>Page</u>
1	R-4D Engine	9-2
2	Valve Materials	9-3
3	Valve Development History	9-8
4	Valve Seat Design	9-9
5	Launch Vibration Envelope - Random	9-16
6	Launch Vibration Envelope - Sinusoidal	9-17
7	Conducted Transient Pulse Shapes	9-19
8	Conducted Transient Susceptibility Pulse Circuit	9-20
9	LM Random Vibration Spectrum Input to Primary Structure Overstress Test	9-29
10	Mean Coil Temperature vs. Time	9-36
11	Electrical ON Limitation - Qualification Valve	9-37
12	Double Angle Glass Filled Teflon Valve Seat Use in Hot Propellant Test	9-39
13	Armature From Test Engine After 103,000 Actuations in Hydrazine Mix Propellants	9-40
14	Valve Seat Test Engine After 103,000 Actuations in Hydrazine Mix Propellants	9-41
15	N <sub>2</sub> H <sub>4</sub> /Apollo Valve Compatibility Test Internal Pressure vs. Time - 49 Days	9-44
16	N <sub>2</sub> H <sub>4</sub> /Apollo Valve Compatibility Test Internal Pressure vs. Time - 45 Days	9-45
17	Driver Schematic for High Power Opening/Low Power Holding Circuit	9-51
18	VoltageCurrent Curves for Special Driver Circuits	9-52
19	Effect of Zener Cut Off Voltage on Valve Closing Response	9-53

LIST OF TABLES

<u>Table Number</u>	<u>Title</u>	<u>Page</u>
1	Valve Particulars	9-4
2	Fuel Valve Test Data	9-5
3	Oxidizer Valve Test Data	9-6



## I. INTRODUCTION

Two valves, one fuel and one oxidizer, control the flow of the propellant to the R-4D engine. Because the engine is required to fire for 10-15 milliseconds, these valves must open and close quickly. These valves are shown on the engine in Figure 1. A cutaway drawing of the present valve is shown in Figure 2, while Tables I through III summarize the valve characteristics and test response data of the valve.

The two valves are electrically operated solenoid valves with two coils called the automatic coil and direct coil. The automatic coil provides quick response (opens in 7 ms and closes in 6 ms) while the direct coil is a backup coil with slower response. The direct coil may be also used by the astronaut to fire the engine. The coils of the valves are wired such that the fuel valve opens 2 milliseconds before the oxidizer valve, since engine test experience showed that more reliable starts were obtained with a small fuel lead.

A soft teflon valve seat and a hard stellite armature tip or pintle provide a leak tight seal. This valve seating arrangement has remained leak free after more than 100,000 cycles during engine ground tests and 338 days of propellant exposure in space during Lunar Orbiter flight II.

The valve must also withstand the conditions of launch and space.

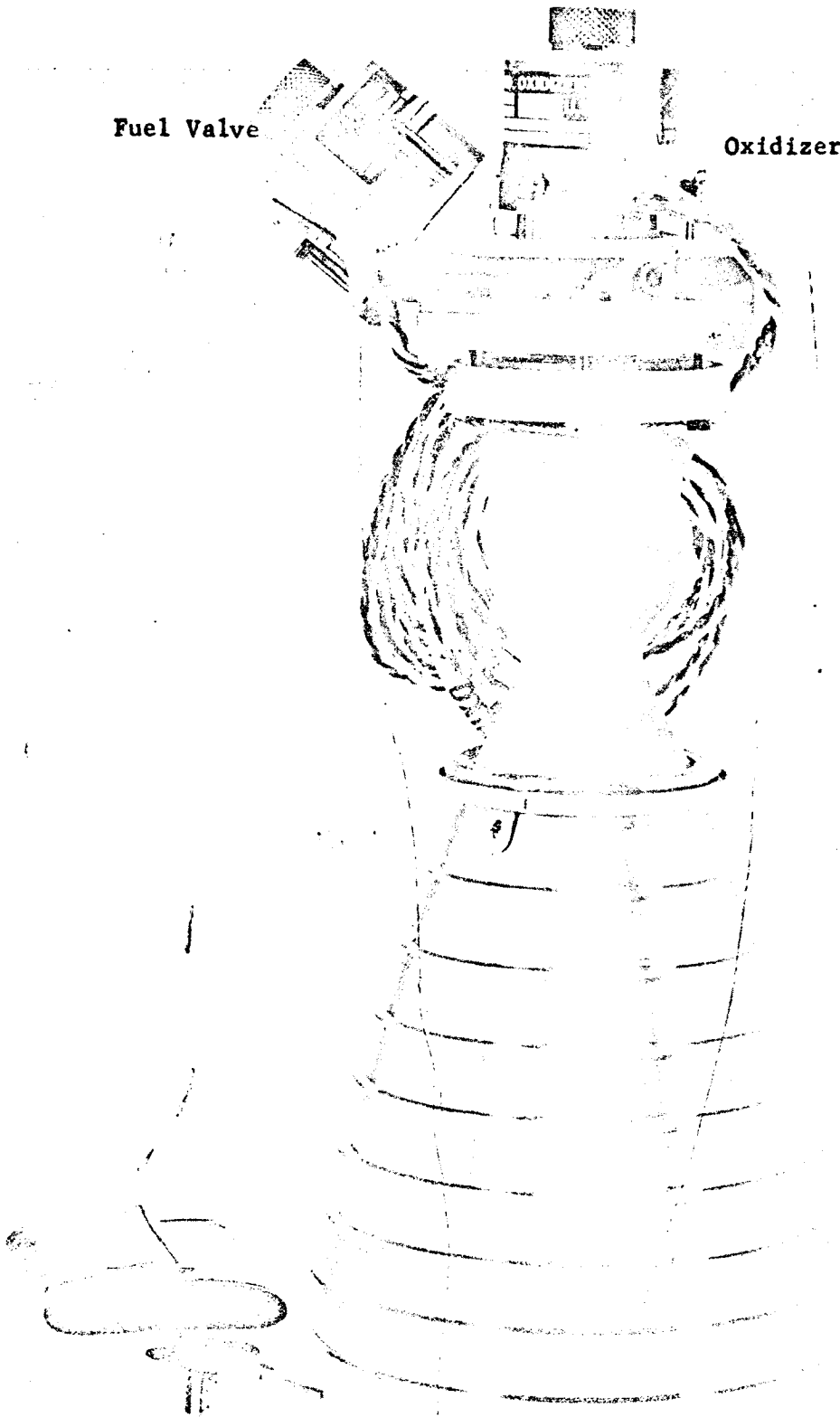
### Brief History of Valve Development

The first valve constructed at TMC for the Apollo Mission, was a 3 coil brazed body design. Use of the 3 coil configuration imposed added complexity on the valve driver since the driver was required to switch from a high amperage power circuit to a low amperage holding circuit each time it signaled the valve to open. (The third coil was a manually controlled low amperage, low response design.) Tests were conducted to determine if an amperage - response tradeoff could be found and culminated in a single high performance nominal 2 amp coil for both opening and holding.

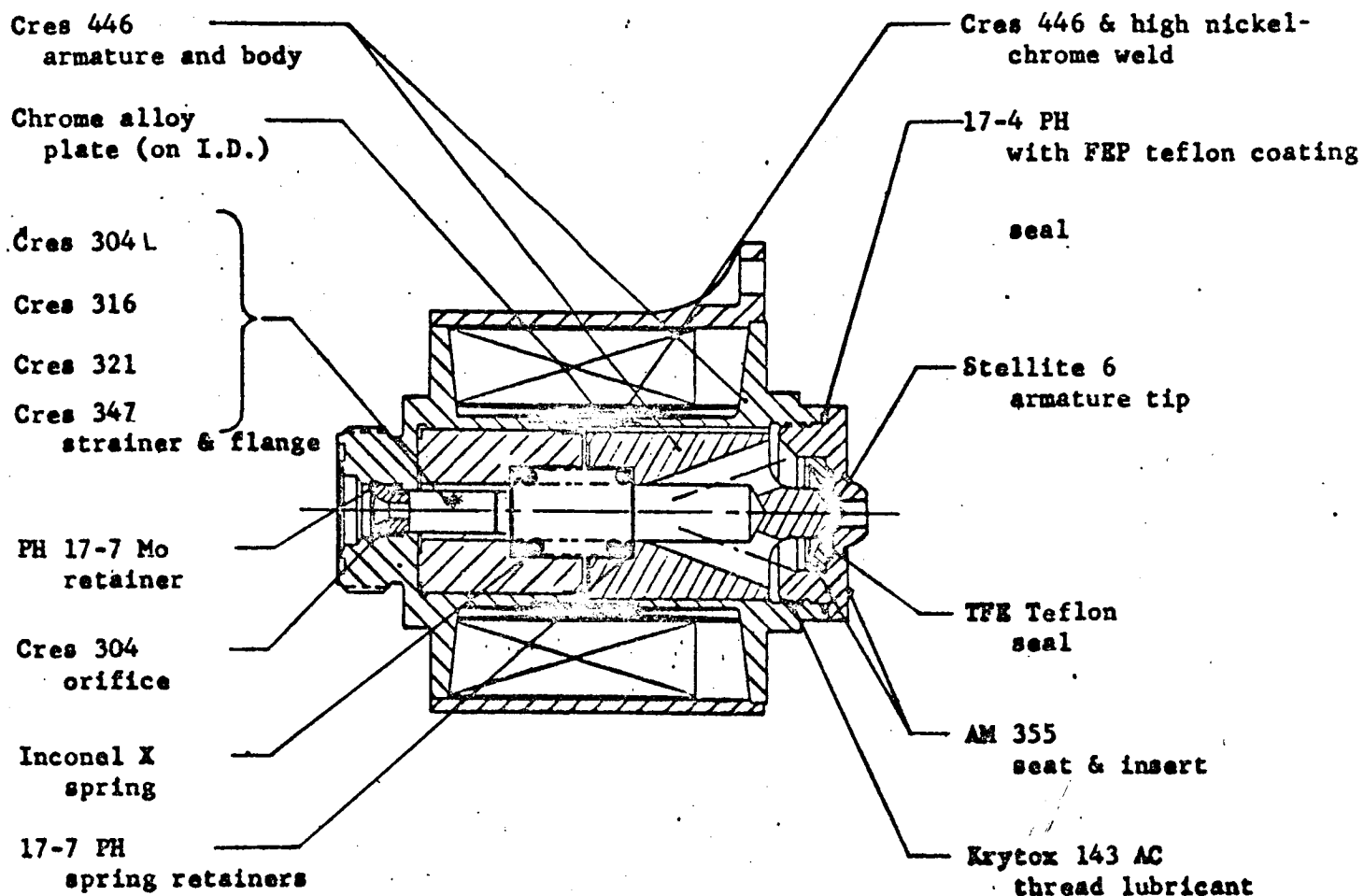
Two coils have been used throughout the balance of the program. The only change, since that time, was one to affect a fuel lead. This and other changes to valve detail parts, which grew out of manufacturing and valve performance improvements, are described in the section on valve configuration.

Fuel Valve

Oxidizer Valve



R-4D Engine



VALVE MATERIALS

TABLE I

VALVE PARTICULARS

Valve Type	Poppet, coaxial flow, normally closed, spring actuated to close	
Part Number	228683	228684
Operating Fluid	Aerazine 50 (50% N <sub>2</sub> He - 50% UDMH)	Nitrogen Tetroxide
Nominal Operating Voltage	27vdc	27 vdc
Pressure*		
Operating	250 psig	250 psig
Proof	490 psig	490 psig
Burst (design)	700 psig	700 psig
Stroke (inch)	0.018 - 0.020	0.020 - 0.021
Weight (lbs)	0.97	0.98
Resistance (ohms)		
Auto Coil	12.40 $\pm$ 0.4	17.2 $\pm$ 0.4
Direct Coil	14.40 $\pm$ 0.4	14.0 $\pm$ 0.4
Number of Turns		
Auto Coil	505	685
Direct Coil	1080	1020
Inductance at 400 cps (mh)		
With Valve Closed		
Auto Coil	57.2	103.4
Direct Coil	237.2	217.5
Inductance at 1000 cps (mh)		
With Valve Closed		
Auto Coil	19.7	37.2
Direct Coil	93.8	85.9
With Valve Open		
Auto Coil	18.	34
Direct Coil	88.	81.
Coupling Coefficient at 50 cps		
1.0 Volt Signal To:		
Auto Coil	0.69	0.77
Direct Coil	0.82	0.89

\*Pressures shown are required for Apollo mission. Valve may be operated at more than 750 psig working pressure with suitable stress margin, and has actually been operated at greater than 900 psig with automatic and direct coils energized simultaneously.

TABLE II  
FUEL VALVE TEST DATA  
531 Valve Samples (P/N 228682)

Test Parameter	Test Conditions				Results (2)		
	Coil	Pressure (1) (psig)	Voltage (vdc)	Other	Mean -3	Mean	Mean +3
Flow Rate	HA	170. flowing	NA	P = 17.0 psid (3)	438.031	500.889	563.747
Response - On to fully closed	A	181.	27	EPW = 10 msec W = 440.	13.8	15.5	17.2
Response - On to fully open	A	181.	27		6.3	6.8	7.4
Response - Off to fully closed	A	NA	27	EPW = 1000 ms W = 440	4.7	6.1	7.5
Response - On to fully open	A	181.	24		7.1	7.7	8.3
Response - On to fully open	A	250.	21		9.7	10.6	11.5
Response - On to fully open	D	250.	11		31.5	35.0	38.5
Current - Pull-in	A	250.	NA		0.886	0.972	1.057
Current - Dropout	A	NA	NA	W 590 pph	0.042	0.095	0.147
Current - Pull-in	D	250.	NA		0.415	0.458	0.501
Current - Dropout	D	NA	NA	W 590 pph	0.019	0.045	0.072

(1) All pressures are non-flowing except as noted.

(2) Units are: flow in pph water, response in msec and current in amps.

(3) EPW = electrical pulse width.

TABLE III  
OXIDIZER VALVE TEST DATA  
527 Valve Samples (P/N 228684)

Test Parameter	Test Conditions			Results (2)		
	Coil	Pressure (1) (psig)	Voltage (vdc)	Other	Mean -3	Mean +3
Flow Rate	NA	170. flowing	NA	P = 38 psid (3) EPW = 10 msec W = 700	666.866	839.772
Response - On to fully closed	A	181	27		13.9	17.0
Response - On to fully open	A	181	27		8.2	9.4
Response - Off to fully closed	A	NA	27	EPW = 1000 msec W = 700	5.3	7.4
Response - On to fully open	A	181	24		9.4	10.7
Response - On to fully open	A	250	21		12.9	15.3
Response - On to fully open	D	250	11		32.3	39.8
Current - Pull-in	A	250	NA		0.696	0.822
Current - Dropout	A	NA	NA	968 pph	0.050	0.140
Current - Pull-in	D	250	NA		0.468	0.558
Current - Dropout	D	NA	NA	968 pph	0.034	0.093

(1) All pressure are non-flowing except as noted.

(2) Units are flow in pph water, response in msec and current in amps.

(3) EPW = electrical pulse width.

## II. CHRONOLOGY OF VALVE DEVELOPMENT

### A. Evolution of Valve Configuration

Figure 3 depicts the major steps in the evolution of the various valve details dating from the prototype configuration through the final design.

#### 1. Seat Assembly - Body Seal

An FEP coated metal "V" seal was adopted after difficulty was experienced to effect a seal, and simultaneously positioning the valve seat assembly with respect to the valve body with a solid Teflon gasket. The latter is required to precisely set the valve stroke. The coated metal "V" seal permits the seat assembly to bottom against the body while the sealing surfaces flex to maintain appropriate sealing pressure. This seal must be replaced each time the seat assembly is removed because a thin stringer of Teflon may be displaced from the I.D. of the seal, which reduces its sealing possibility integrity.

#### 2. Seat Assembly Seal

Use of a glass filled teflon seal to effect a closure with the poppet was aimed at achieving dimensional stability at elevated temperatures. However, in propellant exposure tests conducted at 250°F, the filled teflon lost some glass fibers. These fibers lie across the metal stop surface of the seat assembly and prevent the poppet from closing. Tests with unfilled TFE, which were conducted concurrently, proved this material to be completely satisfactory, particularly with regard to dimensional stability at temperature.

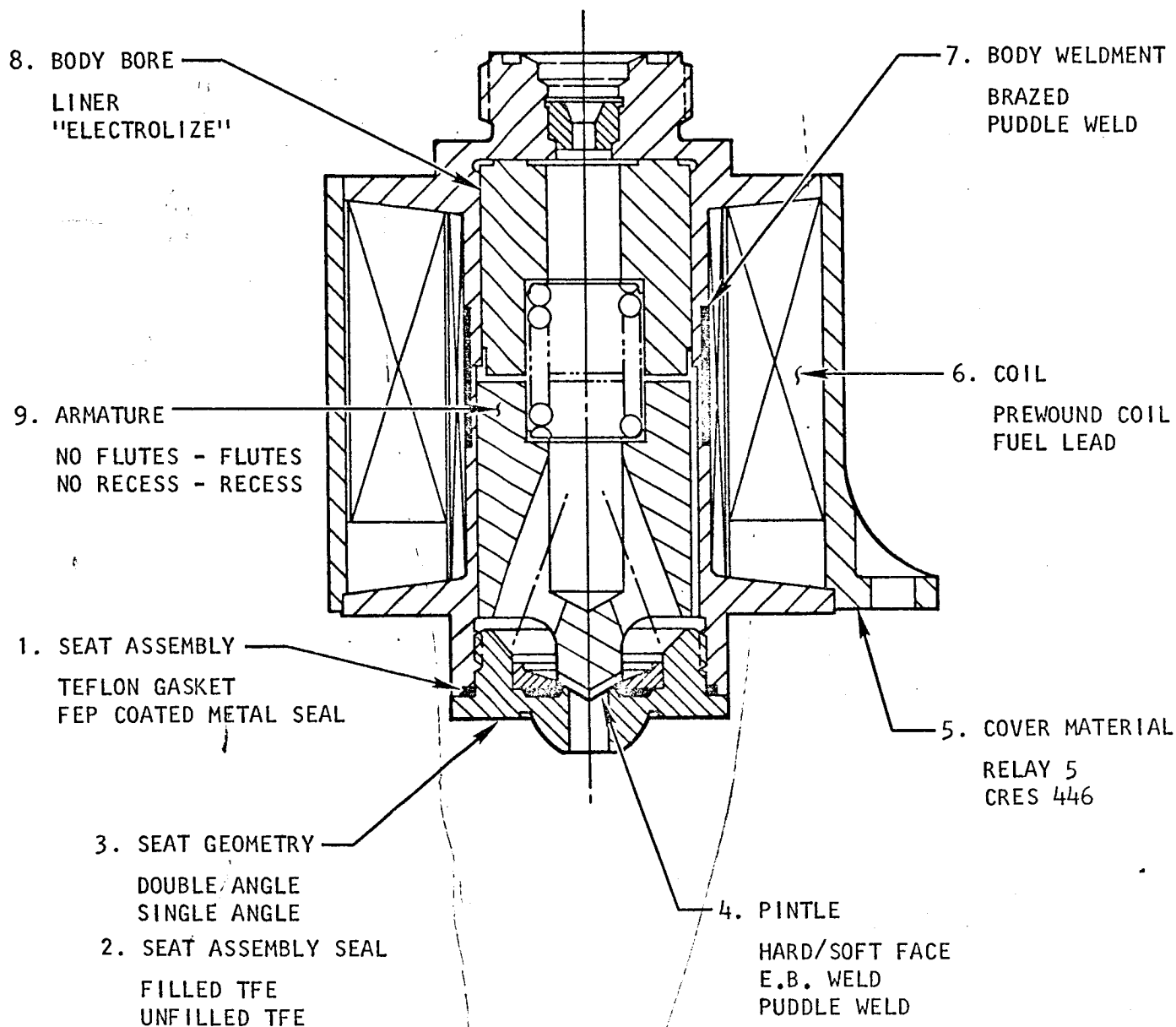
#### 3. Seat Assembly and Geometry

It was found with the double angle seat design (Figure 4), that under impact the teflon seal becomes distorted and flows into the path of the pintle. This condition can result in loss of teflon from the seal and valve leakage. By redesigning the seal as shown in the single angle drawing of Figure 4, the location of the teflon, under the load of the pintle, is positioned in such a way as to avoid wear.

#### 4. Pintle

Actuation tests established the need for a difference in the hardnesses of the pintle and contact area of the seat assembly to improve the wear characteristics. Two fabricating methods were investigated to achieve this feature, both dealing with the pintle. The first, was to electron beam weld a separate hard pintle tip to the armature. The alternate method was to puddle weld material on the pintle and finish grind the weldment. The latter technique proved the most trouble free at the manufacturing level and was incorporated in the final design.

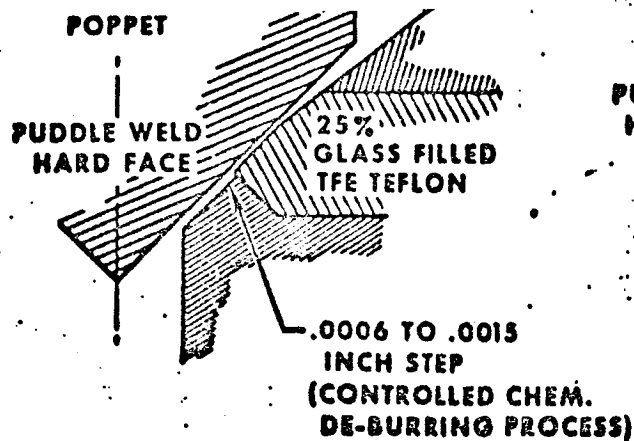
## VALVE DEVELOPMENT HISTORY



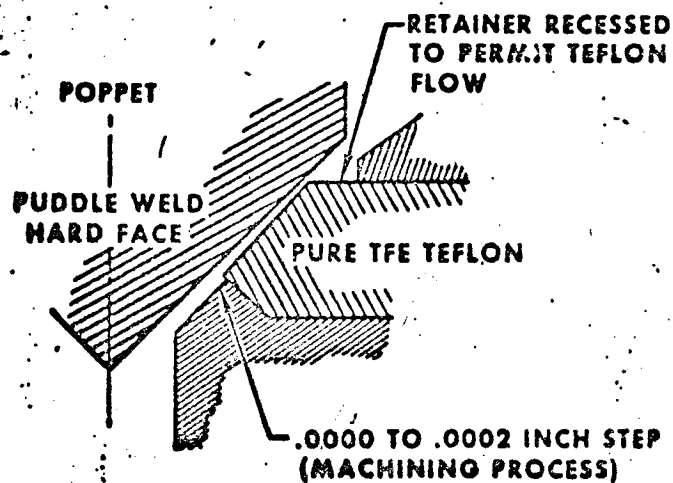


## VALVE SEAT DESIGNS

### DOUBLE ANGLE SEAT



### SINGLE ANGLE SEAT



## 5. Cover Material

Cres 446 was selected for the cover when it was found that the plating used to protect the original Relay 5 materials was peeling off following exposure to engine test conditions.

Response tests confirmed that the change of material did not affect the opening and closing response times of the valve.

## 6. Coil

A separate spool, which permitted winding the coil prior to assembly on the valve body, was used initially. It was later concluded that manufacturing procedures were simplified if the coil were wound and potted directly on the valve body.

The second major coil change grew out of an engine operating requirement that fuel always flow first to the injector. Originally no attempt was made to get a fuel or oxidizer valve lead and the coils of both valves were the same. As a result, one valve or the other opened a few milliseconds before the other from one engine to the next. Engine tests established that safe initiation of combustion under all conditions required that the fuel reach the injector first. This is now accomplished in two different ways for the automatic and direct coils.

The automatic coils are wound such that the fuel coil has fewer turns than the oxidizer valve. The result is a lower inductance, lower resistance coil with consequently shorter current rise time and higher steady state current for the fuel valve. When the two valve coils are subsequently wired in parallel, these parameters provide a fuel valve opening lead. A statistical study based on acceptance test results for 166 valves indicated a nominal 1.9 ms fuel lead with a  $3\sigma$  range of 1.4 to 2.4 ms. The most adverse accumulative effects of pressure, voltage, and temperature, as calculated from the test results of a small number of test valves, is 1.2 ms with a  $3\sigma$  minimum of 0.7 ms. The effects of wear were found to be zero.

The fuel lead for the direct coils is accomplished in a different manner. The operation of the automatic coils dictated fast response and a total of 4 amperes per engine is available. Operation of the direct coils is intended for situations allowing a long opening response and only one ampere per engine is budgeted. By using series hookup, sequential valve response is dependent on the relative number of ampere turns, and no longer on the relative inductances. Fuel lead is accomplished by winding the fuel valve direct coil with more turns than the oxidizer valve. Further assurance of maintaining fuel lead against the adverse effects of different inlet pressures is accomplished by selecting the fuel valve so that the direct coil pull-in current is less than the oxidizer valve by 0.01 amperes. The nominal pull-in current for the fuel valve is .972 amps.

## 7. Body Weldment

Three major approaches were investigated to provide a non-magnetic barrier (necessary to route the flux across the armature working gap) in the valve body, and culminated in a puddle weldment design. The location of the barrier zone is presented in Figure 3 and is seen to be symmetrical with the armature working gap.

The initial design was a brazed configuration in which the magnetic barrier was a separate piece of cres 304L. To improve the integrity of the interface joints, electron beam welding was investigated concurrently with fill or puddle welding. The puddle welding technique was the first to meet the requirements for the valve body and is the design now in use. This weldment is produced by locally reducing the thickness of body wall and then filling the area with weld material containing 46% nickel. The magnetic barrier then consists of a zone of high nickel material which is comparable to cres 300 series in composition. The manufacturing sequence includes radiographic, fluorescent dye penetrant inspections and helium leakage tests at  $2.0 \cdot 10^{-5}$  torr (Veeco) and internal pressure of 490 psig to insure the weld is sound.

## 8. Body Bore

A chrome alloy is vapor deposited to a thickness of .00005 to .00015 inch on the bore of the valve to provide a hard (Rockwell C-70), corrosion resistant low friction surface. The deposit is accomplished by a proprietary process identified as "Electrolize" by the Electrolize Co. and eliminates the need for a separate liner for wear resistance.

## 9. Armature

The small armature to bore clearances (.0032 to .0052) are necessary to minimize lateral misalignment between the poppet and the seat assembly when the valve closes. At the same time, such clearances are conducive to the entrapment of hard particles with the resulting possibility of seizure of the armature in the bore. Use of flutes on the armature provides clearance for the passage of these particles.

The counterbore in the upstream surface of the armature serves the function of shortening the valve closing time with only a small increase in opening time. For the common engine valve a counterbore depth of .003 to .004 inch resulted in an opening time increase of 0.1 ms and a shorter closing time of 2.0 ms, producing an overall decrease in full open time of 1.9 ms for a fixed pulse width.

## B. Valve Test History

The valve test history may be considered in three separate groups as follows:

1. Formal tests conducted on the valve only; viz, the prototype development test.
2. Formal engine tests:
  - a. PFRT
  - b. Qual
  - c. Supplemental Qual
  - d. Off Limits
  - e. LM Production System
  - f. LM Environmental
3. Special tests performed on the valve only and intended to answer specific questions regarding a particular operating mode or design feature. These tests include:
  - a. Dry Cycling and Continuous "On" Time
  - b. High and Low Temperature Propellant Exposure
  - c. NASA/Houston Vacuum
  - d. Cycle Test
  - e. Long Duration Liquid Leakage
  - f. Monopropellant Engine Test and Exposure
  - g. Martin/Marietta (Denver) Sterilization

The particulars of these tests follow.

1. Formal Valve Test (Prototype Development)

The major part of this test program was performed in the period from May to September of 1963, with some additional testing in September of 1964. This was the only formal valve test on the Apollo valve.

The prototype test matrix appeared as follows:

Order of Prototype Valve Testing

Test Description	Valve Number									
	1	2	3	4	5	6	7	8	9	10
Leakage, Flow, Response	1	1	1	1	1	1	1	1	1	1
	4	4	3	3	3	3	3	3	3	3
	6	6	5	5	5	5	5	5	6	6
Electrical					7		8	8		
	3	3	6	6			6	6	4	4
					2	2	4	4	2	2
Endurance										
Burst Pressure			7	7						
Temperature	5	5					2	2		
Vibration	2	2	2	2						
Propellant Exposure			4	4					5	5
Electromagnetic Interference							7	7		
Contamination					6					
High Temperature Vacuum					4	4				

A total of 10 valves consisting of 3 different valve designs were tested in this program.

225974

Brazed body assembly - 6 valves (prototype)

225975

225995

First welded body design - 2 valves

225996

225920

Pre-qual configuration - 2 valves

225930

A brief description of these tests follows:

a. Leakage, flow, response

These tests were performed on all valves at regular intervals throughout the program to determine if any degradation had occurred.

Leakage tests were conducted at an inlet pressure of 100 psig and then at an outlet (reverse) pressure of 20 psig gaseous nitrogen.

Flow tests were conducted, using distilled water at several flow rates for all valves. The inlet pressure was maintained at 170  $\pm$  5 psig under flowing conditions and the pressure drops recorded.

Response tests were conducted using the non-actuated coil induced voltage as an indicator of armature motion. Distilled water was the test fluid for these tests.

b. Electrical

These tests were performed on all valves to assess degradation of the valve coils.

The insulation resistance was determined at a potential of 500 vdc applied for a period of one minute between the following components:

- (1) Manual coil to automatic coil.
- (2) Manual coil to valve body.
- (3) Manual coil to lead shield.
- (4) Automatic coil to valve body.
- (5) Automatic coil to lead shield.

(The lead shield was eliminated following prototype valve tests.)

c. Endurance

The valve was cycled a total of 100,000 times by the automatic coil under the following conditions:

Static/dynamic pressure	181/170 psig
Steady state distilled water flow:	
Oxidizer valve	.18 PPS
Fuel valve	.11 PPS
Valve voltage	28 vdc
Pulse frequency	10 cps
Pulse width	.050 sec

The valve was then cycled 10,000 times by the manual coil under the following conditions:

Static/dynamic pressure	250/237 psig
Steady state water flow:	.
Oxidizer valve	.18 PPS
Fuel valve	.11 PPS
Valve voltage	32 vdc
Pulse frequency	4 cps
Pulse width	.050 sec

Upon reaching 10,000, 40,000, 70,000, and 100,000 cycles of operation, leakage, flow, and response tests were performed.

d. Burst Pressure

The valve was disassembled and the internal valve dimensions measured.

A pressure of 700 psig (distilled water) was applied to the inlet and the valve heated to a temperature of 140°F for a period of 15 minutes.

The valve was then depressurized, purged of water, and subjected to an internal pressure of 150 psig GN<sub>2</sub> for a period of 15 minutes. All joints were checked for leakage.

The valve was disassembled and the internal dimensions remeasured.

e. Temperature

The valve was heated by mounting it on a heater block and wrapping with insulation.

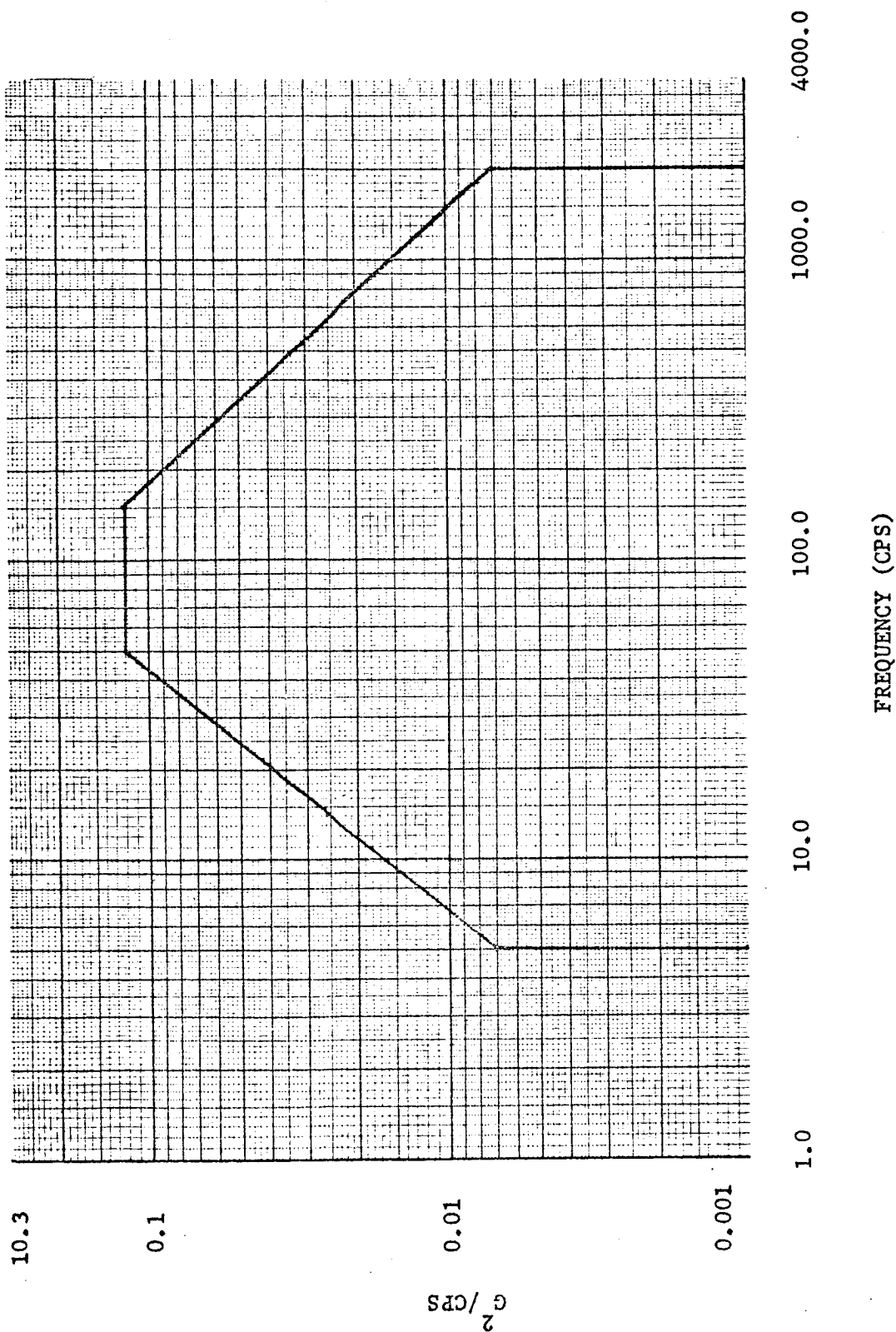
A water pressure of 181  $\pm$  5 psi was maintained at the valve inlet and a series of one hour exposure periods conducted at temperatures of 200°F, 225°F, and 250°F.

Following each exposure period, leakage, flow, and response tests were performed.

f. Vibration

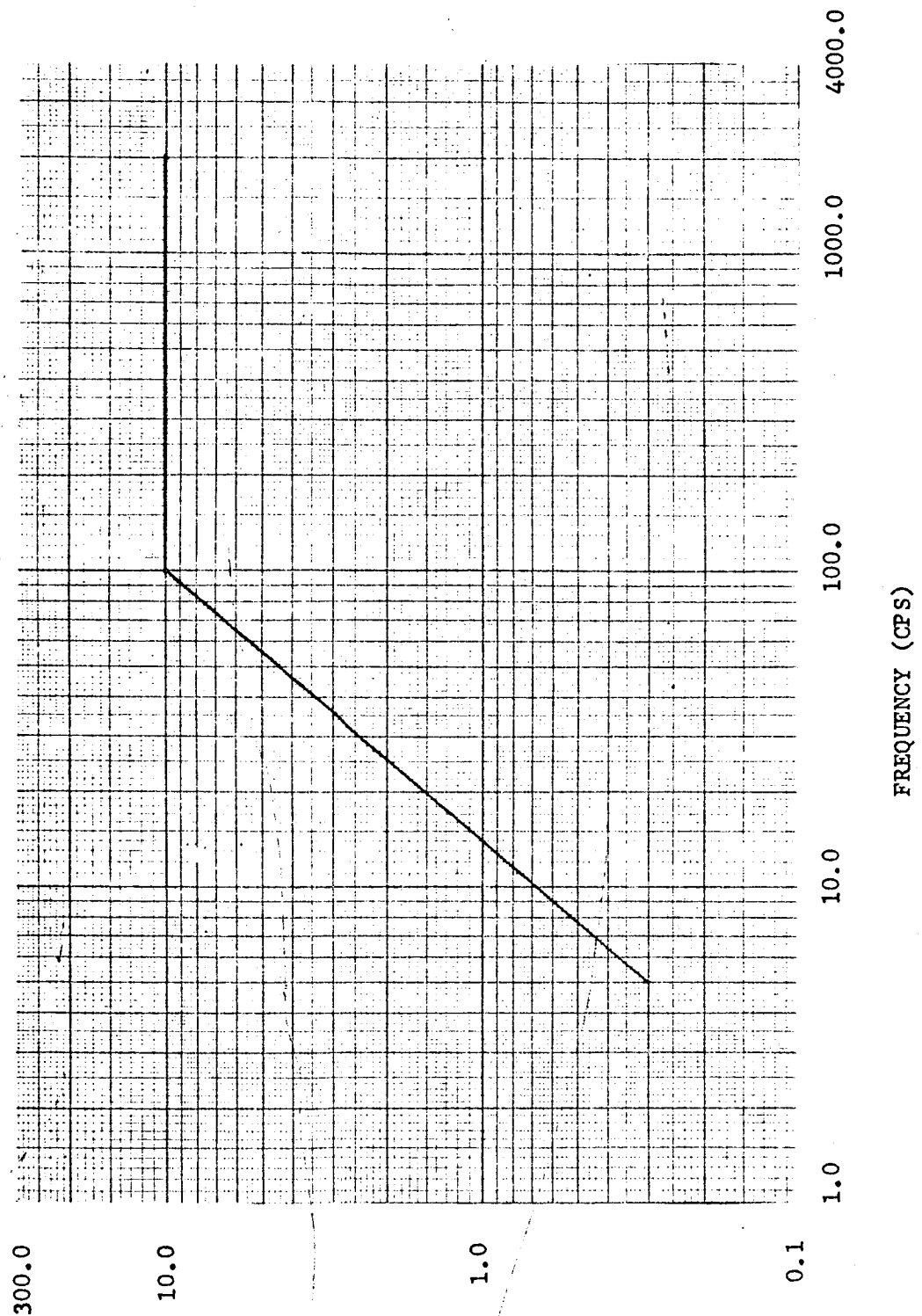
Two vibration modes were used for launch vibration tests. One 15 minute random mode per Figure 5 was performed and one 5 minute sweep of the sinusoidal mode per Figure 6 was superimposed during the random vibration.

LAUNCH VIBRATION ENVELOPE-RANDOM





LAUNCH VIBRATION ENVELOPE-SINUSOIDAL



Vibration testing was conducted in each of two separate orthogonal mounting planes identified as transverse and longitudinal. The longitudinal plane was defined as the plane in which shaker excitation is parallel to the longitudinal axis of the injector valve.

The valve was filled with distilled water and pressurized to 181 psig during all vibration testing.

Valve seat leakage was documented during all vibration testing.

g. Propellant exposure

The valves were exposed to propellant for a period of 21 days during which the actuations noted in the table below were performed on each working day.

Cycles	Coil	Valve Voltage ±2.0 vdc	Static Tank Pressure ±3.0 psig	Pulse Width ±.005 sec	Pulse Frequency ---
1000 ±20	Automatic	28 vdc	181 psig	.015 sec	2.0-4.0 cps
350 ±10	Manual	28 vdc	250 psig	.030 sec	2.0-4.0 cps

The dynamic response of the valve was recorded and the pressure drop across the valve checked at the beginning and end of each day.

h. Electromagnetic interference

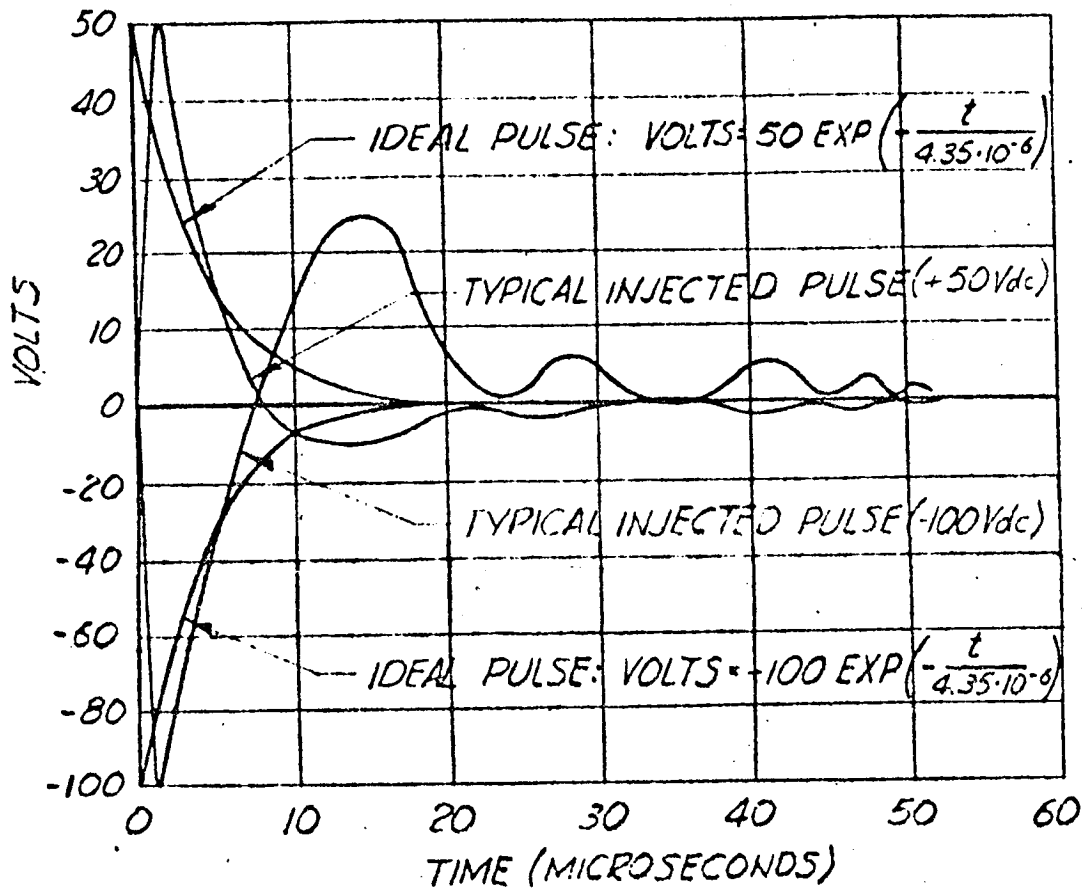
These tests were performed to insure that no degradation would occur in valve performance when a transient conducted signal was applied to the valve leads.

Two transient signals were used. The first was a 50 volt positive pulse with a time width of 10 microseconds and a repetition rate of 10 pulses per second. The second was a 100 volt negative signal with the same pulse width and rate. The transient wave shape and the circuit for the generation of the pulses are shown in Figures 7 and 8.

The transient conducted signal was applied to the automatic coil for a period of not less than 1.0 minute at each at the following times:

- (1) When the valve was closed.
- (2) When the valve was opened.
- (3) While the valve was in cyclic operation at 28 vdc, a rate of 10 cps and pulse width of .020 seconds. The transient

CONDUCTED TRANSIENT PULSE SHAPES



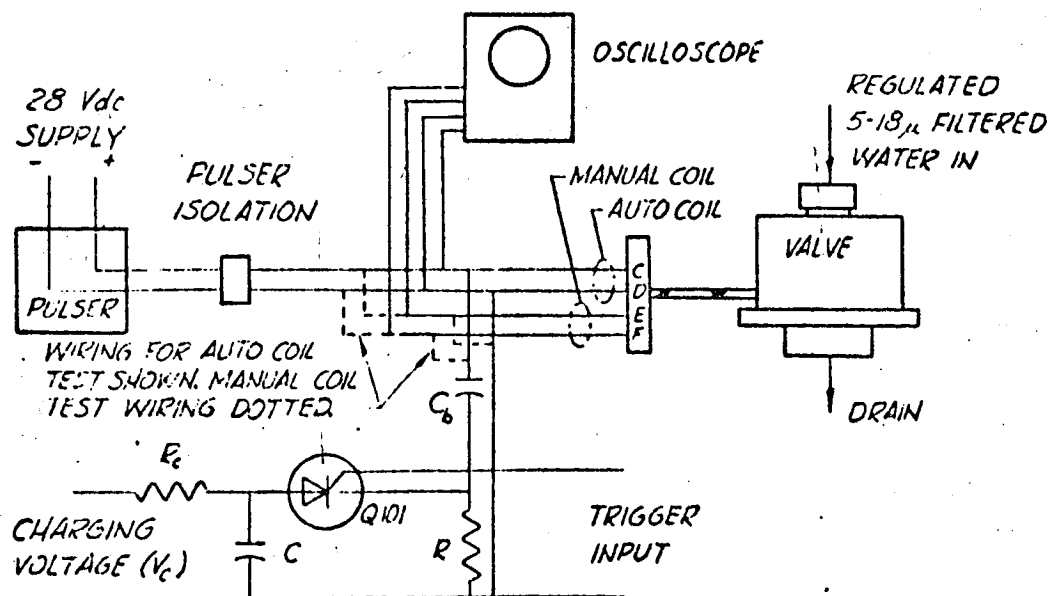
**INJECTED PULSE TOLERANCES:**

AMPLITUDE =  $50 \pm 2$  VOLTS

RISE TIME =  $1 \mu\text{SEC}$  MAX FROM 5 VOLTS TO 45 VOLTS

PULSE WIDTH =  $10 \pm 4 \mu\text{SEC}$  AT 5 VOLT LEVEL

CONDUCTED TRANSIENT SUSCEPTIBILITY PULSE CIRCUIT



LEGEND

$R$  (STABILIZING) = 5  $\Omega$  NOMINAL  
CARBON,  $\frac{1}{2}$  W.

$C$  = 1.0  $\mu$ fd NOM, PAPER, 600 WVDC.

$R_c$  = 10K  $\Omega$  NOM, CARBON 1 W.

$C_b$  = 10  $\mu$ fd, PAPER, 200 WVDC.

$Q_{101}$  = SILICON CONTROLLED RECTIFIER.  
MIN RATINGS: 10 AMPS, 200 VOLTS.  
(G.E. ZJ39L OR EQUIV.).

$V_c$  = DC SOURCE, 100 TO 150 VOLTS (100  
VOLTS NOM), 15 ma.

TRIGGER SPECIFICATIONS

DURATION: LESS THAN 20  
MICROSECONDS.

RATE: 10 PULSES PER SEC.

AMPLITUDE: 50 TO 85 ma INTO  
ZERO RESISTANCE LOAD.

RISE TIME: 0.5  $\mu$ SECS OR LESS.

conducted signal was made to slowly traverse the time interval between electrical "on" and valve fully opened.

- (4) While the valve is operating as above. The transient conducted signal was made to slowly traverse the time interval between electrical "off" and valve fully closed.

i. Contamination

The valve was cycled 60,000 times while flowing water containing aluminum oxide particles with a size distribution as follows:

Particle size in microns	25-50	50-75	75-100
Number of Particles	1960	110	12

The inlet pressure was 40 psig. The valve was operated at a voltage of 28 vdc to the automatic coil at a pulse width of 10 milliseconds and a frequency of 25 cps.

Leakage across the valve seat was detected by pressurizing to 181 psig upstream of the test valve, "locking off" the upstream pressure, and observing any pressure decrease. The valve operating and leak check sequence was as shown below:

Operation	Duration of Operation (Minutes)						
	0	1/2	1	2	3	4	5
Valve cycled	_____						
Supply manifold pressurized to 181 psig	_____						
Leakage check performed by observing pressure decay	_____						

j. High temperature vacuum

The valves were installed in a test chamber, the chamber evacuated to a pressure of  $7.5 \times 10^{-6}$  and the valve heated to a case temperature of 145°F.

After the valve temperature stabilized, the following measurements were made:

- (1) A continuity and resistance check.
- (2) An insulation check.
- (3) A five minute leakage check by pressurizing the valve to 100,  $\pm 5$  psia GN<sub>2</sub>, isolating the valve and observing any pressure decay on the upstream pressure gage.

These steps were repeated one week after initiation of test and immediately before returning test chamber to sea level conditions.

### Prototype Valve Test Conclusions

During the propellant exposure part of the prototype tests, the brazed body valves developed an armature sticking problem which was apparently due to a reaction between the braze alloy and the propellants. It was at this time that the change to a welded body design was made. This was the only significant change which was made as a result of these tests. All other tests were passed satisfactorily although only one valve was tested in aluminum oxide contaminated water, because of difficulties in maintaining control of the contamination level.

## 2. Formal Engine Tests

The following section summarizes the usage history and physical condition of the valves after engine test programs. A list of the tests comprising these programs is repeated here for convenience.

### a. PFRT (Apollo Program) September 1965

The test sequence and engine operational summary were as follows:

Parameter	Engine No. I	Engine No. II	Engine No. III
Total Burn Time (sec.)	1297.6	823.7	1207.3
Total Number of Firings	8548	6111	9699
Total Propellant Exposure (hrs.)-(min.)	150 hr.-43 min.	102 hr.-25 min.	134 hr.-47 min.
Total Oxidizer Valve * Actuations	8665	6284	9973
Total Fuel Valve * Actuations	8648	6397	10014

Actuation totals are exclusive of acceptance test.

\*Oxidizer and fuel valve cycles are different due to purging, bench testing or valve checkouts.

Upon conclusion of tests, all valves had zero leakage and were suitable for additional operation.

b. Qualification (Apollo Program) January 1966

The following summarizes the tests comprising the Apollo Qualification Test Program.

APOLLO S/M RCS  
QUALIFICATION TEST PROGRAM

Test Number	Test Name	Engine No.					
		1	2	2	3	4	5
1	Calibration Test (Ambient)	X	X	X	X	X	X
2	Shock (Transportation)	X					
3	Vibration (Transportation)	X					
4	Humidity	X					
5	Salt Fog	X					
6	Static Load	X					
7	Boost Vibration		X	X		X	
8	Boost and Space Vibration	X			X		X
9	Electrical and Structural Integrity	X	X	X	X	X	X
10	Calibration Test (Hot)	X					
11	Calibration Test (Cold)		X	X			
12	Mission Simulation (Hot)	X					
13	Mission Simulation (Cold)		X	X			
14	Pulse Operation Survey	X			X	X	X
15	Calibration Test (Ambient)				X		
16	Mission Simulation (Ambient)				X		
17	Orbit Retrograde			X		X	
18	Direct Coil Duty Cycle	X		X	X	X	X
19	Calibration (Ambient)	X		X	X	X	X
20	Electrical and Structural Integrity	X		X	X	X	X

Engine valve firing time and actuation summary incurred during these tests is as follows:

SUMMARY OF ACCUMULATED FIRING TIME AND VALVE ACTUATIONS

	Firing Time - seconds		Valve Actuations	
	Planned	Actual	Planned	Actual
Engine No. 1	1446	1490.37	17,220	18,491
Engine No. 2'	1562	1758.38	13,147	15,057
Engine No. 3	1399	1467.22	17,173	17,507
Engine No. 4	1360	1393.05	10,538	11,463
Engine No. 5	1374	1404.50	15,673	16,100

Valve inspection and leakage tests performed after these tests indicated no significant degradation and several valves were used in a supplemental qualification program which followed.

c. Off-Limits (Apollo Program) May 1966

These tests were performed with the same engines as were used in the qualification tests and were intended to determine the effect of additional operating time and over spec. vibration levels on the engine.

The test sequence was as shown below:

Test Sequence Number	Test	Appendix	Remarks	Engine Number				
				1	2	3	4	5
1	Pulse Operation Survey	B	To be conducted 2 times	X	X			
2	Hot Oxidizer	G					X	
3	2100-second Run	F		X	X			
4	Boost Vibration (Destruct)	D				X		
5	Post Check	J		X	X	X		
6	Valve Leakage	L						X
7	Post Examination	M		X	X	X	X	X



were: and the accumulative valve actuations and engine firing time

SUMMARY OF ACCUMULATED VALVE ACTUATIONS

Engine Identification	Qualification Program	Off-Limit Program	Cumulative Total
Engine No. 1	18,491	8,062	26,553
Engine No. 2	15,057	8,042	23,099
Engine No. 3	17,507	29	17,536
Engine No. 4	11 463	25	11,488
Engine No. 5	16,100	0	16,100

SUMMARY OF ACCUMULATED ENGINE FIRING TIME

Engine Identification	Qualification Program	Off-Limit Program	Cumulative Total
Engine No. 1	1490.37 sec.	3042.00 sec.	4532.37
Engine No. 2	1758.38 sec.	3061.50 sec.	4819.88
Engine No. 3	1467.22 sec.	0.0 sec.	1467.22
Engine No. 4	1393.05 sec.	135.0 sec.	1528.05
Engine No. 5	1404.50 sec.	0.0 sec.	1404.50

Upon conclusion of these tests, the valve leakages were zero and all hardware was suitable for additional use.

d. Supplemental Qualification (SM RCS) November 1966.

This program utilized three engine assemblies to verify satisfactory operation with helium saturated propellants and used a valve pulser circuit with a new arc suppression design.

The test matrix was as follows:

SM RCS SUPPLEMENTAL QUALIFICATION

Test Sequence No.	Test	Engine No.		
		1	2	3
1	Calibration - Ambient (Non-saturated propellants)	X	X	X
2	Calibration - Hot (Nonsaturated propellants)	X		X
3	Calibration - Cold (Nonsaturated propellants)	X	X	
4	Calibration - Ambient	X		X
5	Mission Simulation (Cold) Part 1	X		
6	Mission Simulation (Cold) Part 2		X	
7	Mission Simulation (Cold) Part 3	X		
8	Mission Simulation (Cold) Part 4		X	
9	Mission Simulation (Ambient)			X
10	Mission Simulation (Hot)			X
11	Pulse Temperature Survey			
12	Direct Coil Duty Cycle			X
13	Orbit Retrograde			X
14	Calibration - Ambient (Non-saturated propellants)	X	X	X
15	Electrical and Structural Integrity	X	X	X

A summary of valve exposure and actuations is as follows:

ENGINE NO.	ACTUAL BURN TIME (Sec.)	*RELIABLE BURN TIME (Sec.)	ACTUAL NO. OF PULSES	*RELIABLE NO. OF PULSES
1	492.367	282.95	8225	4575
2	290.346	85.89	5977	2066
3	1320.69	1016.99	13175	8031

NOTE: \*The reliable burn time and reliable number of pulses refers to the total actual burn time less those burn seconds and number of pulses accrued during the ambient calibration test with A-50, the first ambient calibration test with MMH, and the final ambient calibration test with MMH. This definition of reliable burn time and reliable number of pulses applies to the Supplemental Qualification Program only by mutual agreement between TMC and NAA/S&ID.

program. All valve leakage was zero in tests performed at the end of the

e. Cluster Test (LM) February 1967

Two four-engine clusters were tested in the following order:

CLUSTER TEST SEQUENCE

CLUSTER NO. 1

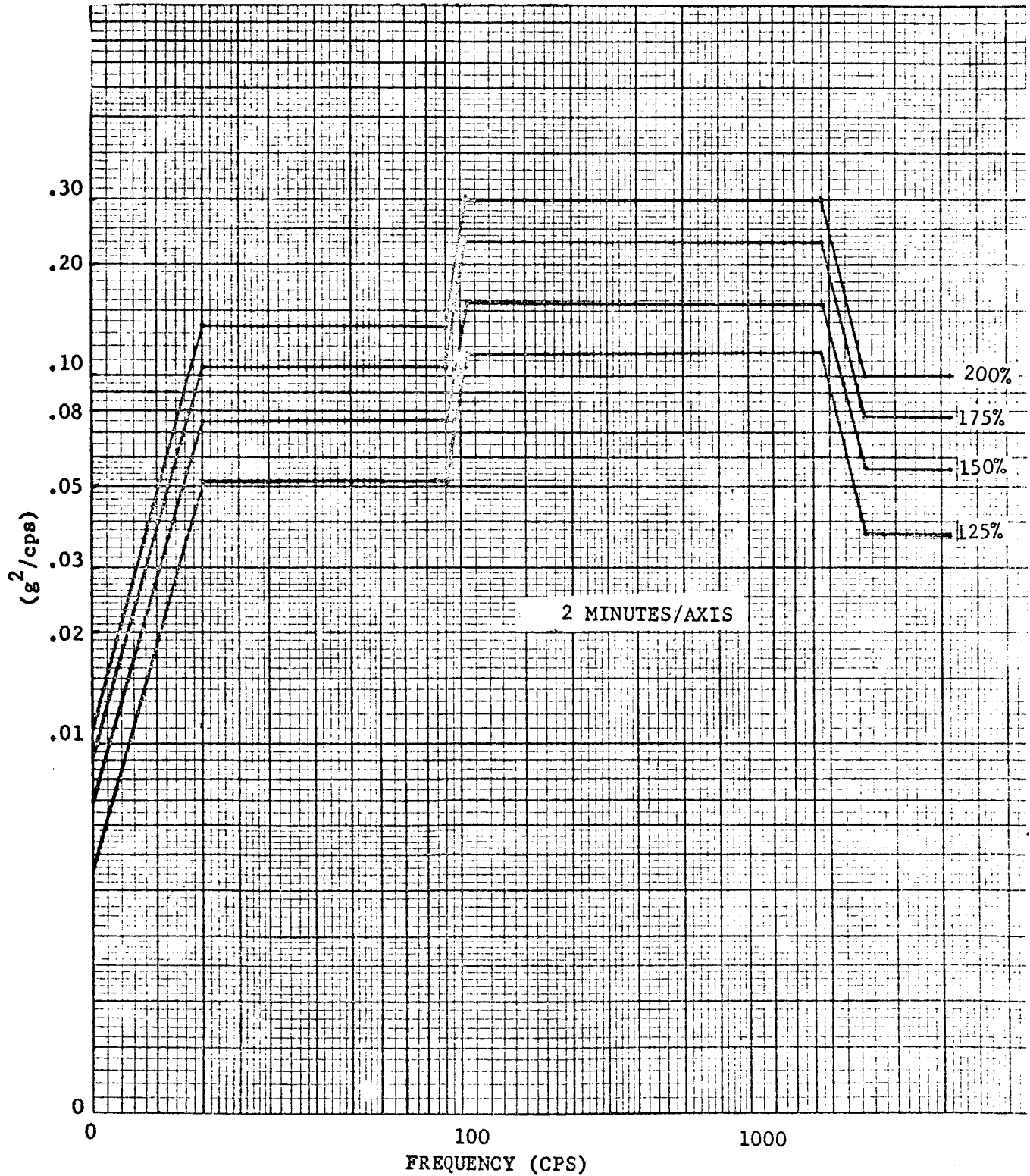
- (1) Vibration Test
- (2) Cluster Leak Checks
- (3) Shock Test
- (4) Cluster Leak Checks
- (5) Baseline Performance Test
- (6) Mission Duty Cycle
- (7) Baseline Performance Test
- (8) Cluster Leak Checks
- (9) Passive Overstress Testing
- (10) Cluster Leak Checks

CLUSTER NO. 2

- (1) Baseline Performance Test
- (2) Maximum Soakback
- (3) Baseline Performance Test
- (4) Cold Mission Duty Cycle
- (5) Baseline Performance Test
- (6) Multi-Engine Firing
- (7) Baseline Performance Test
- (8) Cluster Leak Checks

Vibration was performed to the "over-test" levels shown on Figure 9.

LM RANDOM VIBRATION SPECTRUM  
INPUT TO PRIMARY STRUCTURE  
OVERSTRESS TEST



These tests, performed at zero GN<sub>2</sub> inlet pressure, resulted in leakage for several valves when teflon flakes were deposited on the pintle and preventing seating.

When the flakes were removed, all leakage rates became zero. The source of the teflon for the flakes was a thread lubricant used in assembling the seat to the valve. The amount of lubricant used at this time was not closely controlled. Since these tests, the procedure for the application has been very carefully spelled out, reducing the lubricant to only the amount necessary for the assembly of the seat assembly.

Two other valves developed leakage following vibration tests, but the cause was traced to system contamination.

f. Production test (LM) February 1967

These tests included the following:

- Appendix A System Checkout Procedures
- Appendix B System Operating Procedures -
  - Helium system fill and vent procedures
  - Propellant tank fill and drain procedures
  - Propellant system priming
  - System securing procedure
  - Engine performance referee tests
- Appendix C System Activation -
  - Engine performance baseline tests
- Appendix D Control Event Tests
- Appendix E Duty Cycle Operation
- Appendix F High Temperature and Low Temperature Test
- Appendix G Off-Design Operation
- Appendix H Cross Feed and Ascent Interconnect Tests
- Appendix I Failure Mode Operation
- Appendix J Duty Cycle Performance
- Appendix K Decontamination and Disassembly

The burn time and number of actuations accumulated in the duty cycle operation and performance tests were:

Cluster No.	Engine Orientation	Burn Time (Sec.s)	Actuations
I	Forward	303.3	1469
II	Down	560.0	6303
III	Side	192.0	1507
IV	Side	27.7	19
IV	Down	305.8	4271
I	Side	21.2	19
I	Down	656.3	8870
II	Side	253.5	1793
III	Down	256.2	1897
IV	Forward	142.3	730

and the valve leakage tests performed at the end of the tests were:

Engine P/N	Engine S/N	Post Fire Test Number	Valve Leakage Rate at 100 psig GN <sub>2</sub>	
			Oxidizer (scc/hr)	Fuel (scc/hr)
227895	1002	1	0	0
		2	1200 (1)	0
227895	1004	1	0.25	0
		2	0.75	0.25
227895	1009	1	0	0
		2	0.25	0
227895	1013	1	0.75	0.25
		2	0	1.00
227895	1038	1	0.25	0
		2	0	0
227895		1	1.0	1.0
		2	1.0	0
227895	1042	1	0	0.25
		2	0	0.50

(Continued)

(Table Continued)

Engine P/N	Engine S/N	Post Fire Test Number	Valve Leakage Rate at 100 psig GN <sub>2</sub>	
			Oxidizer (scc/hr)	Fuel (scc/hr)
227895	1043	1	0	0
		2	0	0.50
227895	1012	1	0.50	0.50
		2	2400 (2)	0.50
227895	1035	1	0	2.0
		2	0.75	2.0
227895	1037	1	0.75	0.75
		2	0.50	0
227895	1036	1	0	0.50
		2	0	0.50
228745	1001	1	3.25	0
228745	1004	1	0.75	0
228745	1003	1	0	0
228745	1002	1	4.00	0.75

- NOTES: (1) FMR investigation concluded leakage was due to contamination which resulted from inadequate procedures then used for system decontamination.
- (2) FMR investigation concluded excess thread lubricant produced teflon flakes during vibration, which were deposited on the pintle and prevented it from seating properly. (See note in preceding test summary.)

The engine assemblies previously used in the Production System Test Program were used in the DVT tests so that the following totals were accumulated.



ENGINE STARTS AND BURN TIME

Engine			DVT System		Production System		Total	
P/N	S/N	Location	Starts	Time	Starts	Time	Starts	Time
227895	1035	IU	0	0	14590	1275.728	14590	1275.728
227895	1044	ID	5324	607.366	-	-	5324	607.366
227895	1045	IS	338	103.668	-	-	338	103.668
227895	1013	IF	1802	414.098	645	230.190	2447	644.288
228745	1004	II U	0	0	0	0	0	0
227895	1046	II D	4704	563.909	0	0	4704	563.909
227895	1043	II S	1803	379.163	3500	749.267	5303	1128.430
227895	1037	II F	655	227.041	0	0	655	227.041
228745	1003	III U	0	0	0	0	0	0
227895	1038	III D	1675	309.780	0	0	1675	309.780
227895	1042	III S	1788	283.995	4429	664.384	6217	948.379
227895	1039	III F	630	193.427	4184	886.090	4814	1079.517
228745	1002	IV U	0	0	0	0	0	0
227895	1009	IV D	3134	325.487	2008	527.918	5142	8534.0
227895	1004	IV S	447	137.698	8948	856.756	9395	994.454
227895	1036	IV F	876	218.542	1481	467.024	2357	685.566

Valve leakage rates measured at the end of the test were:

Engine Location	Oxidizer Valve		Fuel Valve	
	Leakage (ml)	Time (min)	Leakage (ml)	Time (min)
Quad I				
Up, S/N 1035	1.1	12	0 <sup>1</sup>	6
Forward, S/N 1013	1.6	12	*10.0	31 sec.
Down, S/N 1044	1.3	12	0	6
Side, S/N 1045	0.9	12	0.7	12
Quad II				
Up, S/N 1004	0.6	12	0.9	12
Forward, S/N 1037	0.4	12	0	6
Down, S/N 1046	0	6	0	6
Side, S/N 1043	0.3	12	1.4	12
Quad III				
Up, S/N 1003	0.8	12	0.5	12
Forward, S/N 1039	1.0	12	0.3	12
Down, S/N 1038	0.7	12	0	6
Side, S/N 1042	0.7	12	0	6
Quad IV				
Up, S/N 0324	0.6	12	0.5	12
Forward, S/N 1036	0.4	12	0.7	12
Down, S/N 1009	0.4	12	0.5 <sup>2</sup>	12
Side, S/N 1004	0	6	*10.0	4.5

\*Values exceeding the maximum allowable rate of 15 cc/hr allowed at this test level.

NOTES: (1) Inadequate purge procedure resulted in a low level detonation in the valve and damage to the valve seat assembly.

(2) System contamination deposit across the seat seal.

### 3. Special Tests

#### a. Dry Cycling and Continuous "on" time

These tests were conducted to determine the effect of long time operation of a dry valve in both the pulsed or cycling mode and the non-pulsed or continuous mode. Pulsing operation of the valve causes degradation by generating particles of contamination which can accumulate on the Teflon seal. Continuous operation overheats the coil and reduces the insulation resistance.

The dry cycle tests were performed in 1963 with prototype Apollo solenoid valves (225974 and 225975). These tests indicated that although no leakage resulted from an accumulated 10,000 cycles, the Teflon seal could become heavily contaminated with metallic particles, presumably generated by the sliding action between the armature and body bore. The number of particles was considered excessive and it was concluded that 10,000 cycles far exceeded the maximum number to which the valve could be subjected. The test was very significant from the standpoint that it was possible, although not consistently probable, for the seal to absorb a large number of particles and still not leak.

The first continuously "on" tests were performed at the same time. The upper temperature limit for the valve was based on the maximum allowable temperature of 311°F for the coil wire insulation. Because the coil temperature in the tests was measured as a function of change in resistance, the upper allowable limit for the coil was set at 250°F. This allows for local spots which could be slightly hotter than indicated by the overall change in coil resistance. The coil temperature-time data from these tests are plotted in Figure 10 and show that with no fluid in the valve the automatic coil can reach 250°F in two and one-half minutes at 32 vdc, or six and one-half minutes at 24 vdc.

In a final dry-continuous "on" test to destruction with the prototype valve, the automatic coil temperature reached 530°F in 90 minutes. Damage to the valve resulting from this high temperature included:

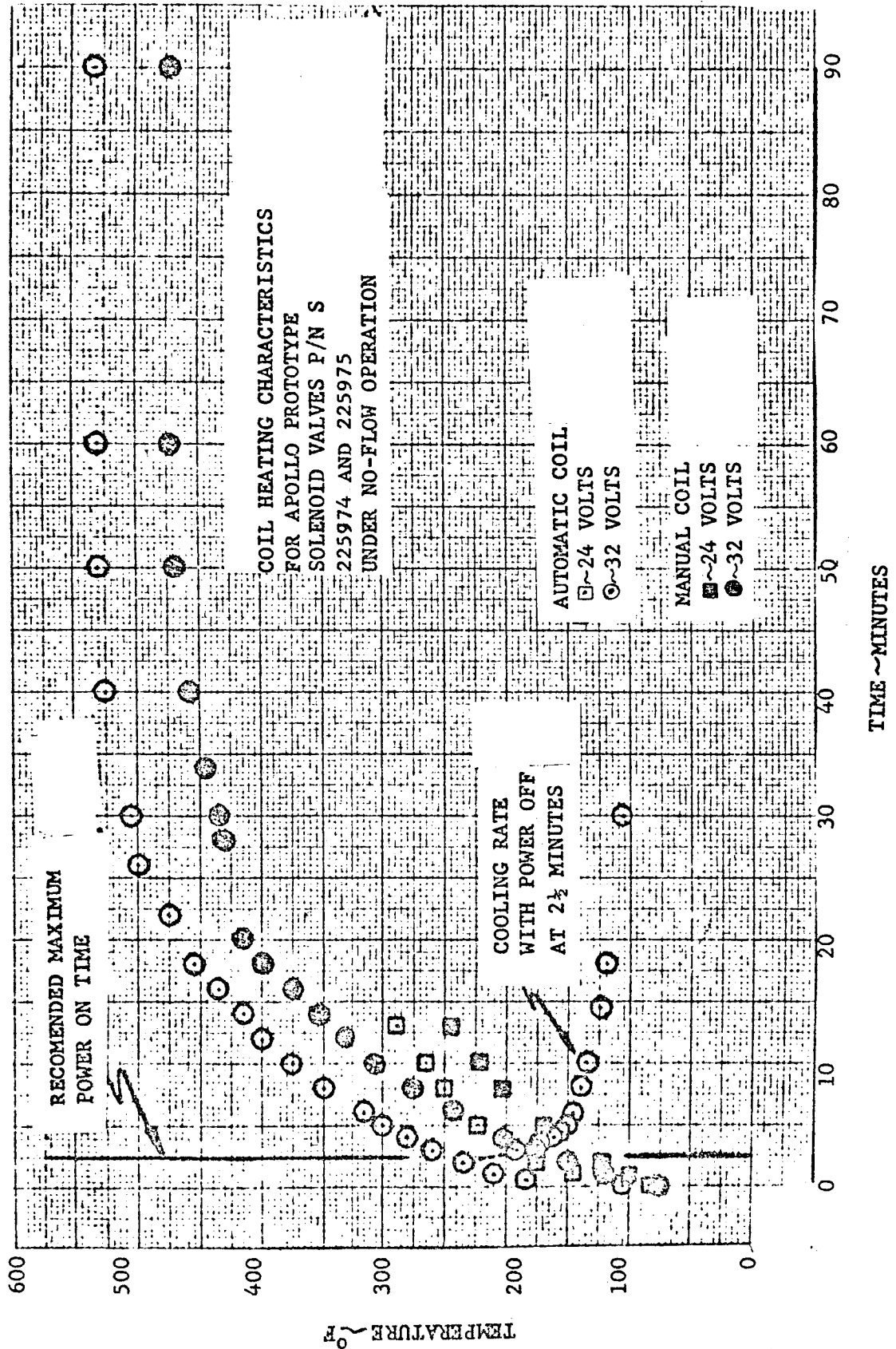
- 1) Extrusion of the Teflon seat seal which shortened the stroke from 0.022 inch to 0.012 inch, and increased the valve pressure drop from 16.1 psi to 28.3 psi.

- 2) Shortening of the automatic coil to the valve case.

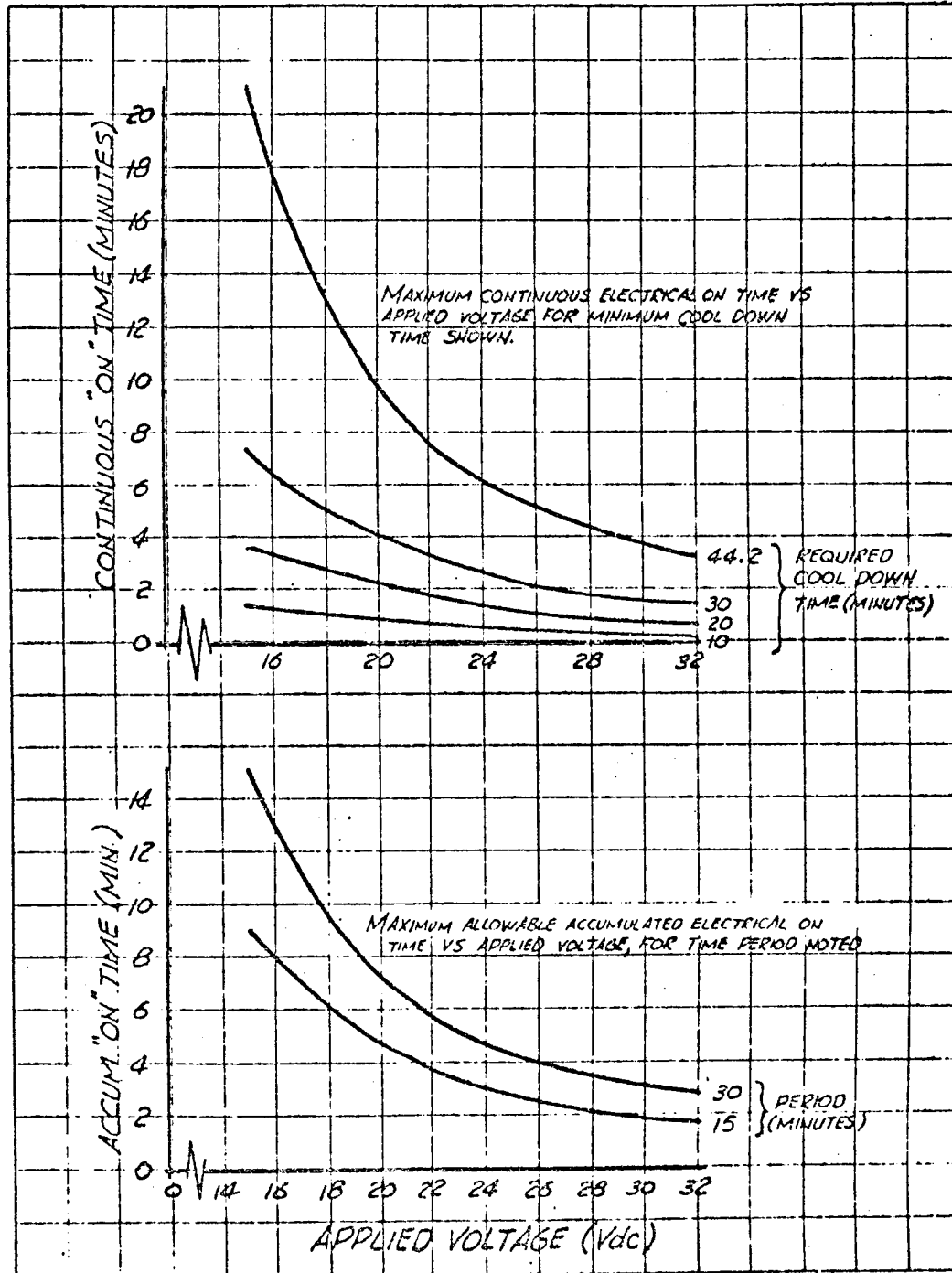
- 3) Expansion of the potting compound and insulation inside the cover to push the cover one-eighth inch off to its fully seated position on the body. Had the valve been mounted on an engine head, this may have broken off the mounting ears.

Recent results measured in tests with the qual valve were used to construct the curves of Figure 11.

MEAN COIL TEMPERATURE vs. TIME



ELECTRICAL ON LIMITATION - QUALIFICATION VALVE



b. High and low temperature propellant exposure

As a result of these tests, performed in July 1965, the seal in the seat assembly was changed from a 20% glass-filled Teflon, double angle configuration, to an unfilled, pure TFE Teflon with a single angle design. A comparison of these seal configurations is shown in Figure 4. A double angle glass-filled Teflon seat assembly used in the hot propellant test is shown in Figure 12 and illustrates the effect of poppet impact on a design in which the Teflon flow is restricted.

c. NASA Houston hard vacuum test

These tests were performed by NASA Houston during the latter part of 1965 to determine if any sticking or cold welding of the poppet to the seat assembly would occur. The tests were conducted on two valves at a pressure of  $10^{-12}$  torr, a valve temperature of 100°F, and for a period of 36 hours. During this time, one of the valves was actuated hourly during the working day. No cold welding or other form of degradation occurred during these tests.

d. Cycle test

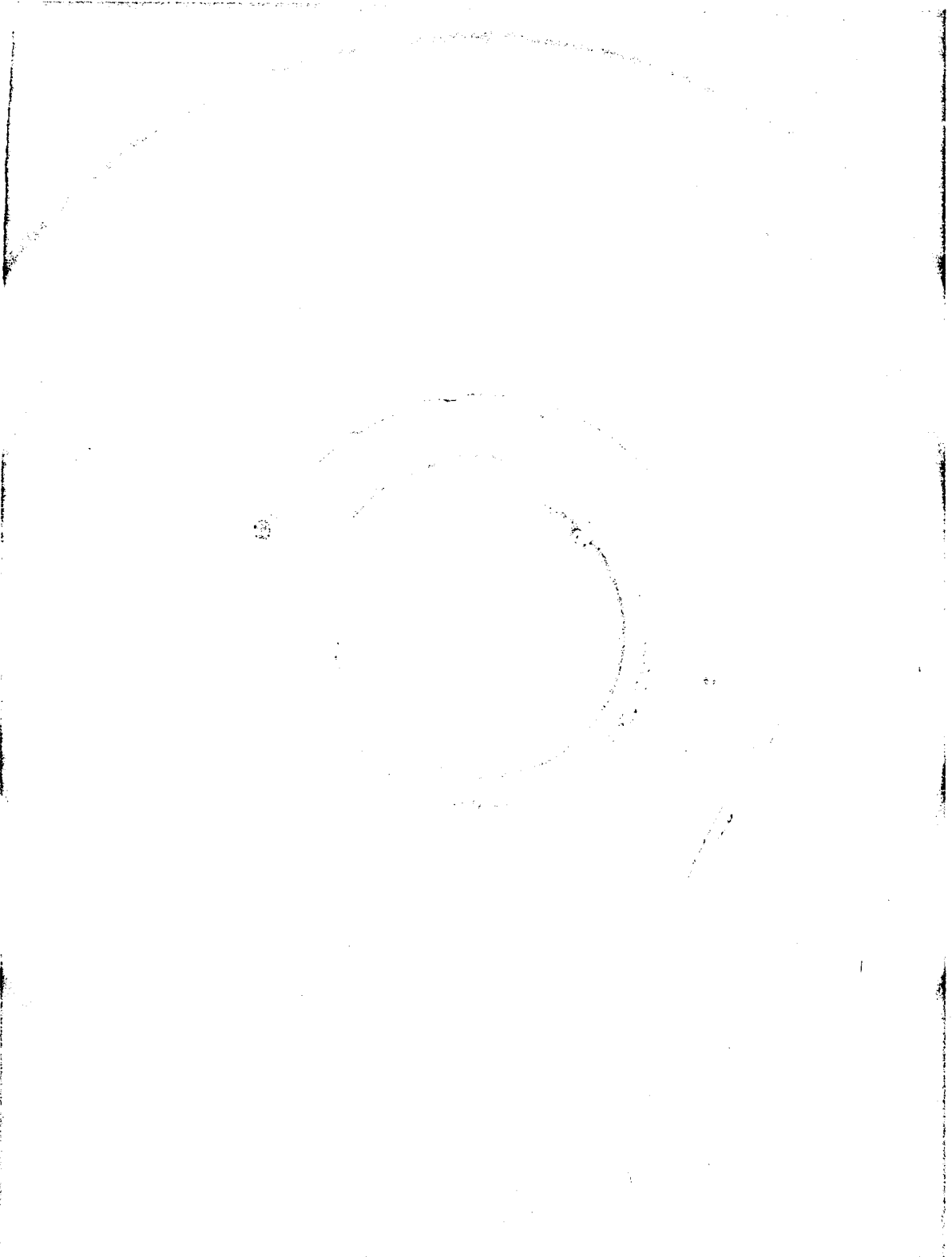
This test, conducted in December of 1965, was performed with a complete engine assembly and subjected to two valves to a total of 103,548 actuations each in NTO and hydrazine mix propellants. (Previously, valve actuation tests had been performed on the water flow bench to one million cycles with several different valves.)

The operational summary for the engine was as follows:

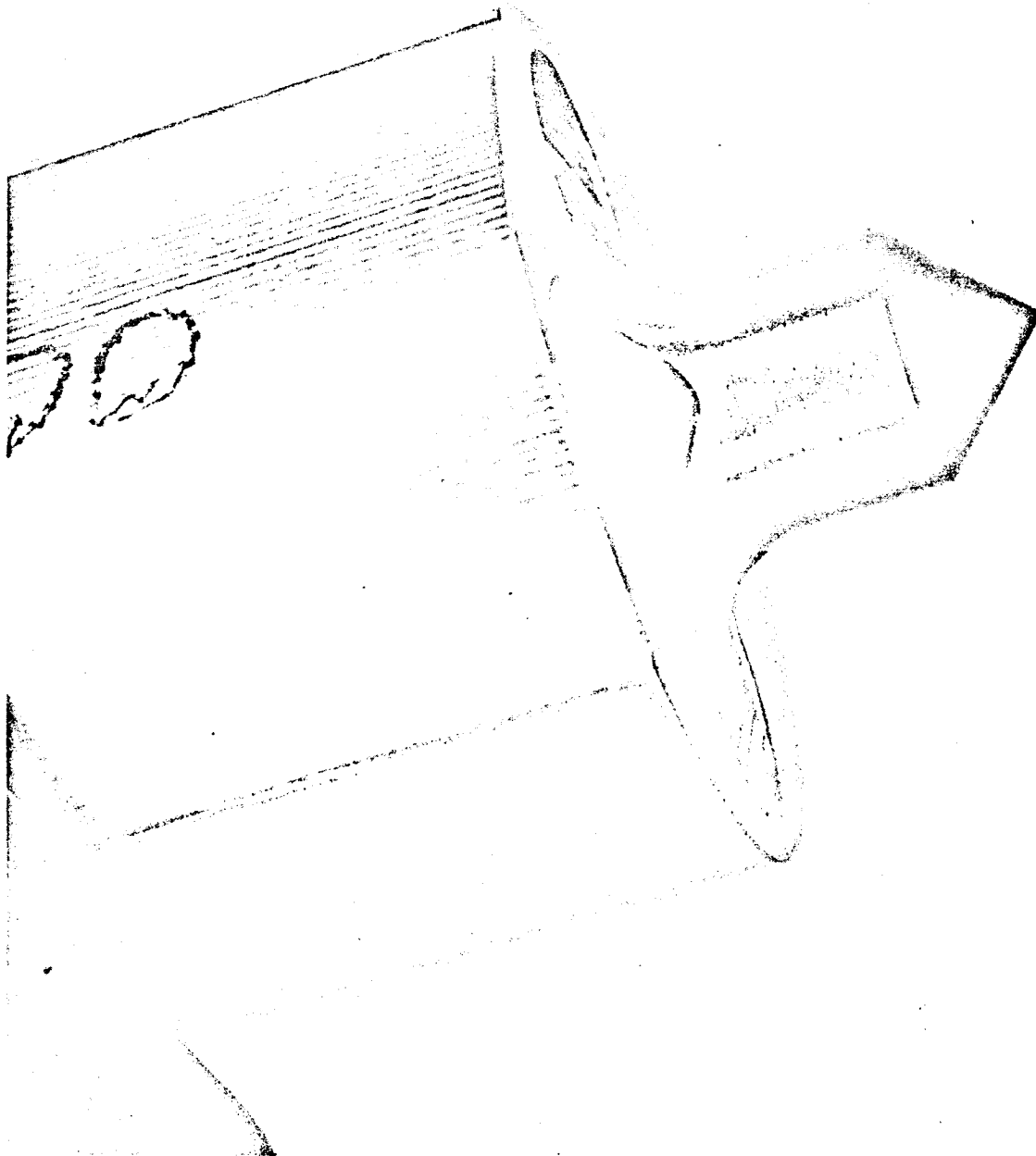
Total accumulated burn time	10,536 seconds
Total number of starts	103,548
Maximum single run time	1,020 seconds
Minimum pulse width	0.008 second
Pulse frequency range	2 to 50 cps
O/F range tested	1.2 to 2.2
Pulse widths tested	8, 8.5, 9, 10, and 50 ms
Propellant utilized	N <sub>2</sub> O <sub>4</sub> /Aerozine 50 N <sub>2</sub> O <sub>4</sub> /MMH

No performance degradation was experienced in the operation of the engine. Valve pre and post test responses were relatively unchanged, and valve wear was confined mainly to the impact zones on the pintle and seat assemblies. The pre and post test valve data are tabulated below and the wear patterns on the pintle and seat assembly is shown in Figures 13 and 14.

DOUBLE ANGLE GLASS FILLED TEFLON VALVE SEAT  
USED IN HOT PROPELLANT TEST



NEG. 6775-5CN



NEG. 6992-2

Armature from Test Engine after 103,000 Actuations in Hydrazine  
Mix Propellants

9-40

Figure 13





NEG. 6992-1

Valve Seat Test Engine After 103,000 Actuations in Hydrazine Mix  
Propellants

PRE & POST TEST DATA FROM VALVES  
WITH 103,536 ACTUATIONS

Parameter	Acceptance Limits	Pre-Test	Post-Test
Forward Leakage			
Oxidizer Valve	$\leq 10$ scc/hr	0 scc/hr	0 scc/hr
Fuel Valve	$\leq 10$ scc/hr	0.75 scc/hr	0 scc/hr
Fuel Valve Response			
Auto Coil - Opening at 27 vdc	5.7 - 7.4 ms	6.9 ms	6.9 ms
Auto Coil - Closing at 27 vdc	4.0 - 7.5 ms	5.0 ms	5.6 ms
Direct Coil - Opening at 11 vdc	$35 \pm 10$ ms	37.0 ms	36.0 ms
Direct Coil - Closing at 11 vdc	4.0 - 20.0 ms	not chk'd	6.6 ms
Oxidizer Valve Response			
Auto Coil - Opening at 27 vdc	7.8 - 9.5 ms	8.3 ms	8.5 ms
Auto Coil - Closing at 27 vdc	4.5 - 8.0 ms	6.2 ms	5.9 ms
Direct Coil - Opening at 11 vdc	$35 \pm 15$ ms	36.0 ms	36.0 ms
Direct Coil - Closing at 11 vdc	4.0 - 20.0 ms	not chk'd	6.1 ms
Water Flow Check			
1. Oxidizer Section at 72 psi	within 2% of pre-test	435 pph	431 pph (-0.9%)
2. Fuel Section at 72 psi		694 pph	683 pph (-1.6%)

e. Long duration liquid leakage

This test was performed with two valves in April and May of 1967 over a test period of 36 days. The fluid was water, at an inlet pressure of 250 psig. The data taken before, during, and following the test may be summarized as follows:

SUMMARY OF LONG DURATION LEAK RATES

Valve	Leak Rate with GN <sub>2</sub> at		Veeco Leak Rate with GHe at 250 psig (cc/sec)	Leak Rate in water based on total accumulated Leakage over 36-day net test period (lb/yr)	Veeco Leak Rate with GHe at 250 psig (cc/sec)	Leak Rate with GN <sub>2</sub> at 100 psig (bubbles/min)
	100 psig	250 psig				
Oxidizer	0	0	$289 \times 10^{-8}$	$5.88 \times 10^{-3}$	$90 \times 10^{-8}$	
Fuel	0	0	$289 \times 10^{-8}$	$5.02 \times 10^{-3}$	$58 \times 10^{-8}$	
Extra valve (not used in long duration leak check)					$90 \times 10^{-8}$	0

f. Hydrazine exposure

Two separate tests have been performed using anhydrous hydrazine. The first, in December 1967, was a storage compatibility test with valves only at various temperatures. The second, in April 1968, was with a complete engine assembly.

1) Valve compatibility test

Four Apollo fuel valves were exposed to hydrazine at 400 psig pressure and at the temperatures and durations shown below.

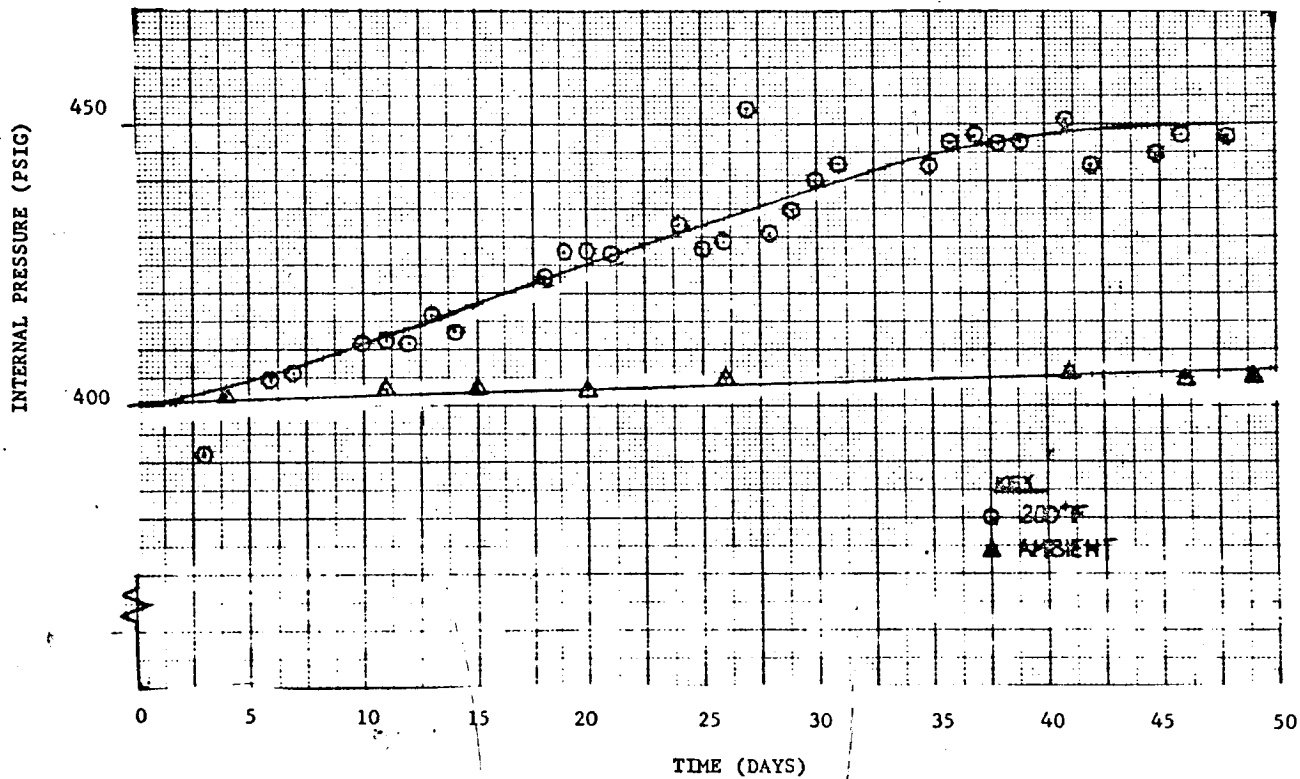
Test Valve	Test Temperature	Test Duration
1	150°F	49 days
2	200°F	94 days
3	105°F	49 days
4	Room temp.	94 days

Data from this program indicate that the Apollo valve assembly does catalyze the decomposition of hydrazine, but only to a limited extent. Calculations based on valve internal pressure rise indicate that at 200°F a maximum of 0.016 gm of hydrazine was decomposed in 49 days. At 70°F, the decomposition was 0.002 gm of hydrazine in 49 days.

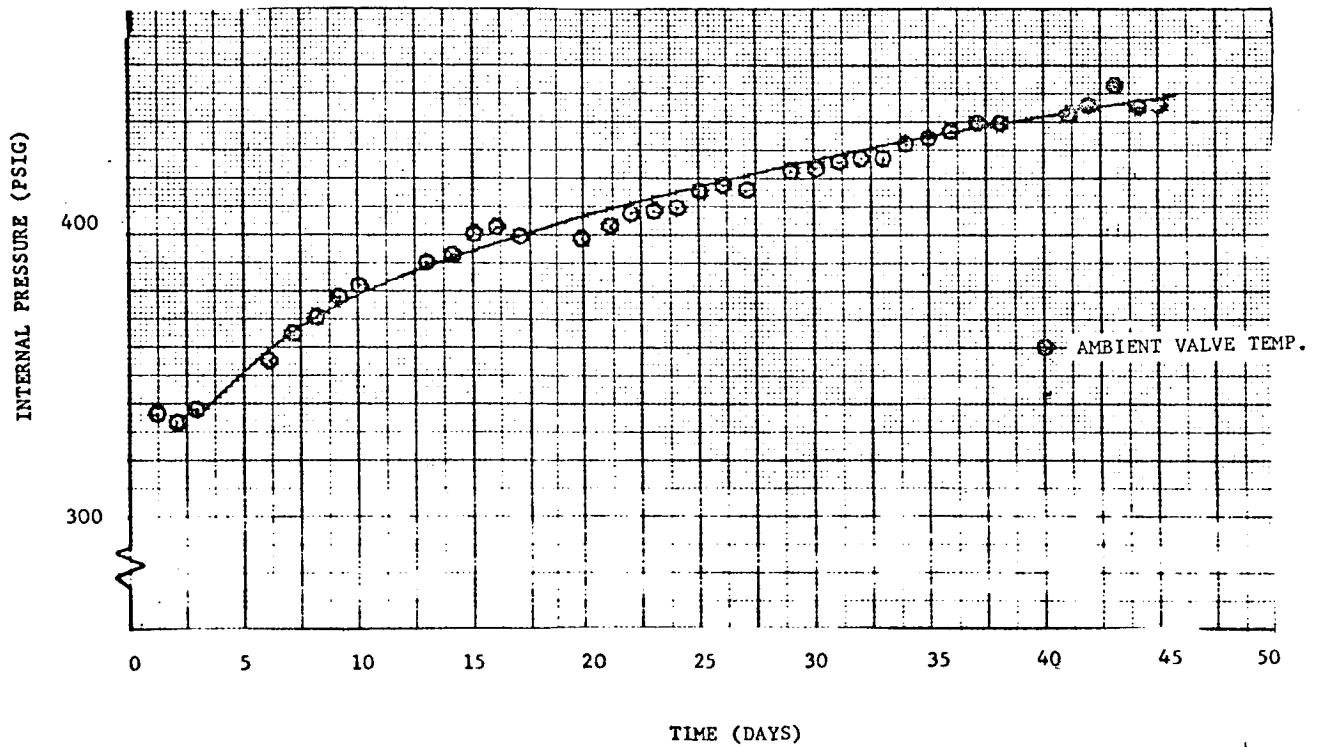
Visual examination of three valves revealed no corrosion. The fourth valve, which had been exposed a total of 94 days at 200°F, showed some evidence of attack on the 17-7 PH spring retainers. The pressure vs. time data are presented in Figures 15 and 16.

$N_2H_4$ /APOLLO VALVE COMPATIBILITY TEST  
INTERNAL PRESSURE vs. TIME

(FIRST PORTION-49 DAYS)



$N_2H_4$ /APOLLO VALVE COMPATIBILITY TEST  
INTERNAL PRESSURE vs TIME  
(SECOND PORTION-45 DAYS)



2) Monopropellant engine test

In these tests, the valves were cycled a total of 1,150,000 times in an 11-hour period. No leakage was measured in eight leak checks performed during and following the test.

g. Engine sterilization test

This program, conducted by the Martin Marietta Company, Denver Division, subjected an engine assembly to six 29-hour wash cycles in 120° F ethylene oxide vapor, then temperature-cycled the assembly six times between room temperature and 275° F over a 432-hour period. Upon completion of these tests, the valves had zero leakage and the engine was successfully fired.

### III. VALVE DESIGN CRITERIA

The following section outlines special criteria for the design of small thruster, small impulse propellant control valves. It is drawn from the experience gained at The Marquardt Corporation on the Apollo S/M RCS engine valve and similar designs.

#### A. Leakage

Leakage is the service parameter of first importance in valve design. Internal leak rates are necessarily higher than external rates since the first is the path containing the pintle-seat interface while the second usually lends itself to redundant static-sealing designs and weldments.

##### 1. Internal Leakage

After the allowable internal gaseous or liquid propellant leakage rates have been established, inert gas is most often used to perform the measurement. The use of gas, with the advantages of convenience and sensitivity, outweighs the uncertainty of knowing the exact liquid propellant equivalent when the valve is intended for this type of service. This uncertainty, however, must be accounted for when the allowable gas rate is defined, by using a conservative gas-to-liquid leakage ratio. Tests conducted at Marquardt indicated that the minimum gas-to-liquid  $N_2H_4$  volumetric ratio was approximately 50 with a helium gas  $\Delta P = 100$  psi, and  $N_2H_4 \Delta P = 181$  psi. The corresponding ratio for Aerozine 50 was 37.5.

Some difficulty was experienced in these tests in maintaining consistent liquid leakage over a 5-minute period of time through a soft seat valve which had a 15.0 cc/hr leak rate at 100 psig  $GN_2$  inlet pressure. Liquid leakage tended to decrease with time. Tests by other investigators indicate that valves with gaseous leak rates in the range of 5.0 cc/hr often completely seal themselves. The geometry of the leak path, which may consist of several flow regimes, can change in the test period needed to complete the measurement.

For the Apollo requirement, zero leakage across the valve poppet/seat interface is defined as a  $GN_2$  leak rate of  $\leq 5.0$  cc/hr at an inlet pressure of 100 psig for a new valve, and  $\leq 10$  cc/hr following completion of in-house engine testing.

##### (a) Seat Seal Material

A comparison of soft and hard seats can be summarized as follows:

Use/Fabrication Parameter	Seat Material	
	Hard	Soft
Easiest to fabricate		X
Least susceptible to dirt		X
Least likely to leak under vibration		X
Usable in "exotic" propellants	X	
Best for nuclear survivability	X	
Dimensionally most stable for long-term use and storage	X	
Usable at high temperature	X	
Ability to self-clean	X	

Until recently, hard seal valves with leakage rates of 5 scc/hr helium were not available because of the difficulties in fabrication and inspection of the surfaces. Valves designed for a large number of life cycles cannot use high, "brute force" seating stresses because of the resulting pitting and fretting. The need for low stresses places emphasis on smooth, flat surfaces, approximately 1.0 AA and 1 helium light band.

An advantage of the soft seal is its ability to accept dirt. However, while some valve assemblies have maintained zero leakage after 20 or 25 foreign particles of .005 inch diameter have collected on the seal, leakage can readily occur if one long fiber .005 inch in diameter scores the seal in the appropriate manner. The conclusion is that while a soft seal material will effectively accept dirt and not leak, its use does not preclude the use of a propellant filter in the supply system.

Fillers, including metal powders, asbestos and glass fibers, may be added to the soft seal material for dimensional stability and improved properties at elevated temperature. These fillers must not be a source of potential contamination or surface discontinuity. Under certain conditions of wear and high temperature, glass fiber filler used in TFE Teflon, for example, can become exposed and dislodged. This condition will occur particularly when the valve design permits scuffing action to take place between the poppet and the seat seal.

The use of soft seals permits the relaxation of close tolerances since the seal will comply with small discontinuities in the pintle. When the poppet strikes the soft seal, compression and distortion result. Provisions must be made to keep this distortion from moving into the path of the pintle, particularly at temperatures of 250°F and above where cold flow occurs more easily, since extrusion and wear will result.



b) Seat Seal - Configuration

To perform the very critical fabrication and inspection operations on metal sealing surfaces, poppets and seats are usually designed flat. This permits ready access to the critical surfaces with lapping equipment, optical flat and surface finish measuring devices. Flat surfaces complicate the overall pintle-seat design, however, in that centering of the two sealing surfaces is no longer inherent in the geometry. Alignment, if desired, must be accomplished with added valve components.

c) Sliding Fits

Possible effects of sliding fits on internal leakage are, first, to produce contamination, and; second, wear. In short life usage and with lubricating propellants, the small particles which may be generated by sliding surfaces are flushed through the valve and no problem is encountered. However, if dry cycling with no gas flow or similar purging media is a requirement, particles may accumulate on the sealing surface of the poppet-seat interface and ultimately result in leakage. The use of sliding fits in the valve must, therefore consider the related effects of surface hardness, fluid flow (or the lack of it), and the required number of actuations. The Apollo SM/RCS valve is an example of a design which incorporates the necessary features to successfully use sliding fits; hard surfaces between the components in contact, and flutes to minimize contact area.

The second possible effect of sliding fits, wear, causes degradation of parts, in addition to producing contamination at an increasing rate. Designs which have eliminated sliding fits in the propellant cavity usually resort to the use of bellows or flexure tubes. These thin wall pressure vessels are highly stressed and introduce a new potential failure mode, namely, fatigue due to cycling or vibration. This failure mode has in the past been found to be more severe than the disadvantages of sliding fits.

2. External Leakage

Allowable external leak rates must necessarily be zero, as detected by proof pressure tests or sophisticated leakage detection devices, because today's applications are in long duration missions and most often use highly toxic or corrosive propellants. Zero leakage for a small valve body weldment is defined at Marquardt as no detectable leakage on an instrument with a sensitivity of  $2.0 \times 10^{-9}$  scc/hr at an internal pressure of 490 psig helium. When weldments cannot be used because of manufacturing limitations, or inspection requirements which necessitate disassembly, redundant static seals should be used.

## B. Response Repeatability

This characteristic will be considered from two standpoints,

1. Single valve repeatability when operated under different conditions.
2. Valve-to-valve repeatability when operated under the same conditions.

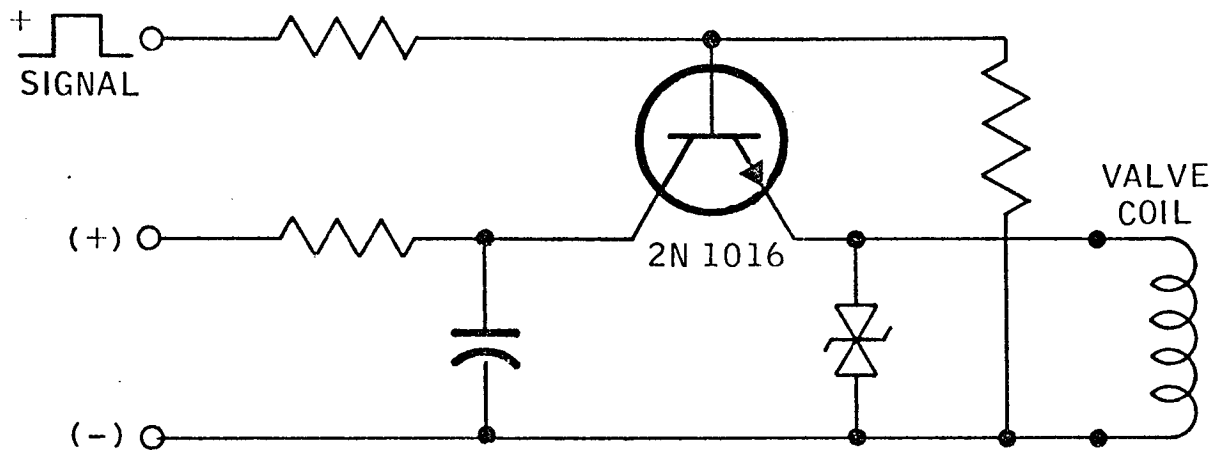
### 1. Single Valve Repeatability

Single valve repeatability is particularly important for small thruster engines, so that impulse bits will be the same for a given electrical pulse width. That is, valve opening and closing response should be relatively insensitive to variations in inlet pressure, environmental temperature, and operating voltage. This characteristic is also important for bipropellant engines using two valves, when one of the valves may be required to consistently open before the other, and the pressure, temperature and voltage conditions may be different for each. One direct technique for obtaining single valve repeatability is by the use of devices to provide high pull in force margins.

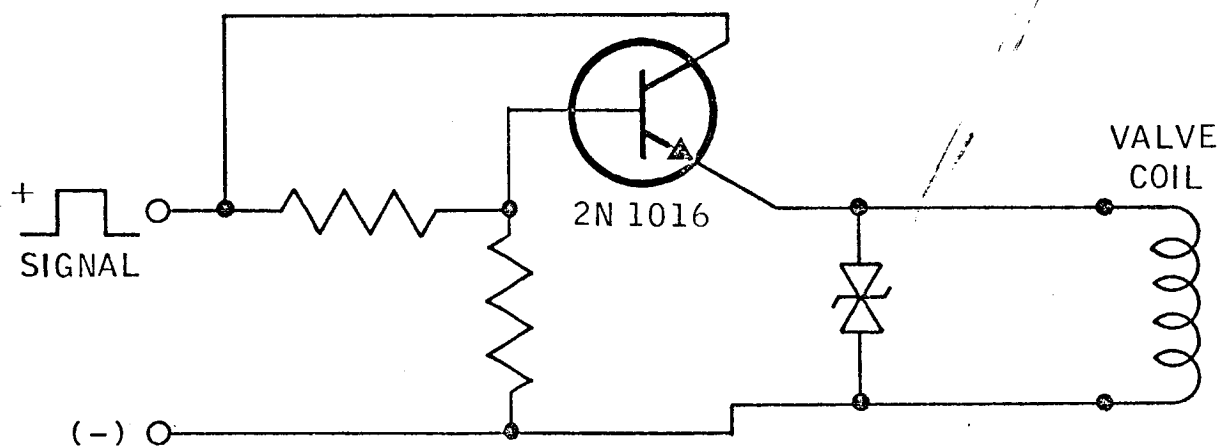
Since more power is required to open a valve than to keep it open, drivers can be designed with circuits to momentarily provide higher than normal voltages during the opening transient. Such circuits include switching, "kicker," and current-limiting designs. The switching circuit can be one which simply switches from a high to a low voltage level after a predetermined interval of time. The "kicker" and current-limiting designs may utilize components such as are shown in Figure 17. These circuits produce the voltage-current curves shown in Figure 18, which also shows the effect these high current rise rates have on both the valve opening response and opening response spread as a function of high and low operating voltage. All circuit modifications require additional driver components, and therefore represent some added complexity. In addition, the "kicker" circuit can be used only when sufficient time can be allowed between pulses, for the capacitor to recharge.

Driver circuits used for response testing of SM/RCS type valves often contain a Zener diode to protect the driver against the high voltage generated by the valve when it closes. A typical driver circuit, shown in Figure 17 does not affect the opening response, but the Zener cutoff voltage significantly affects closing time, as shown in the curve of Figure 19. This effect on closing time is of concern when small impulse bits are a requirement, but does not affect valve repeatability except in a system sense where the tolerance of the zener may be different from one pulser to the next.

## DRIVER SCHEMATIC FOR HIGH POWER OPENING/LOW POWER HOLDING CIRCUIT

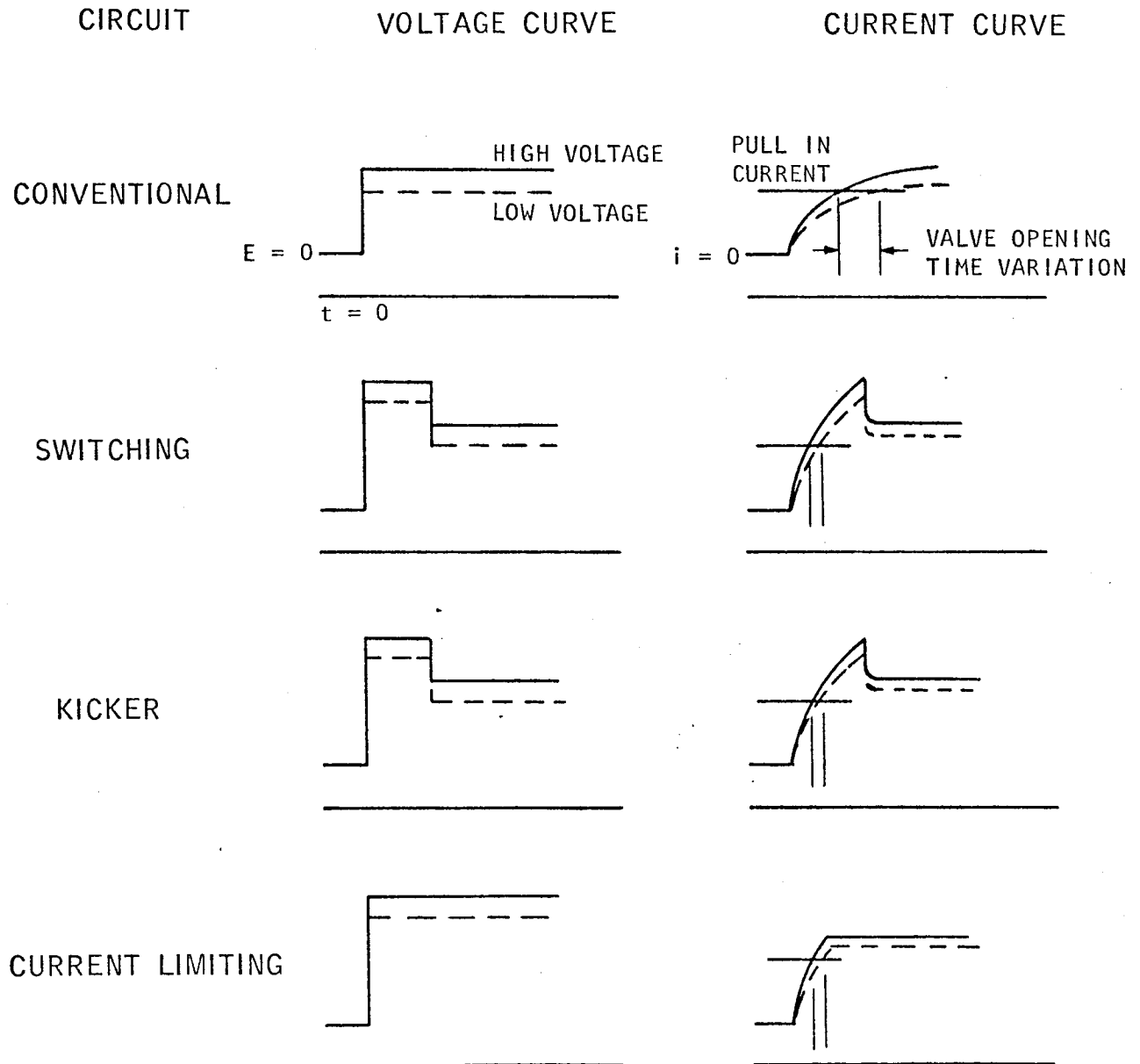


KICKER CIRCUIT

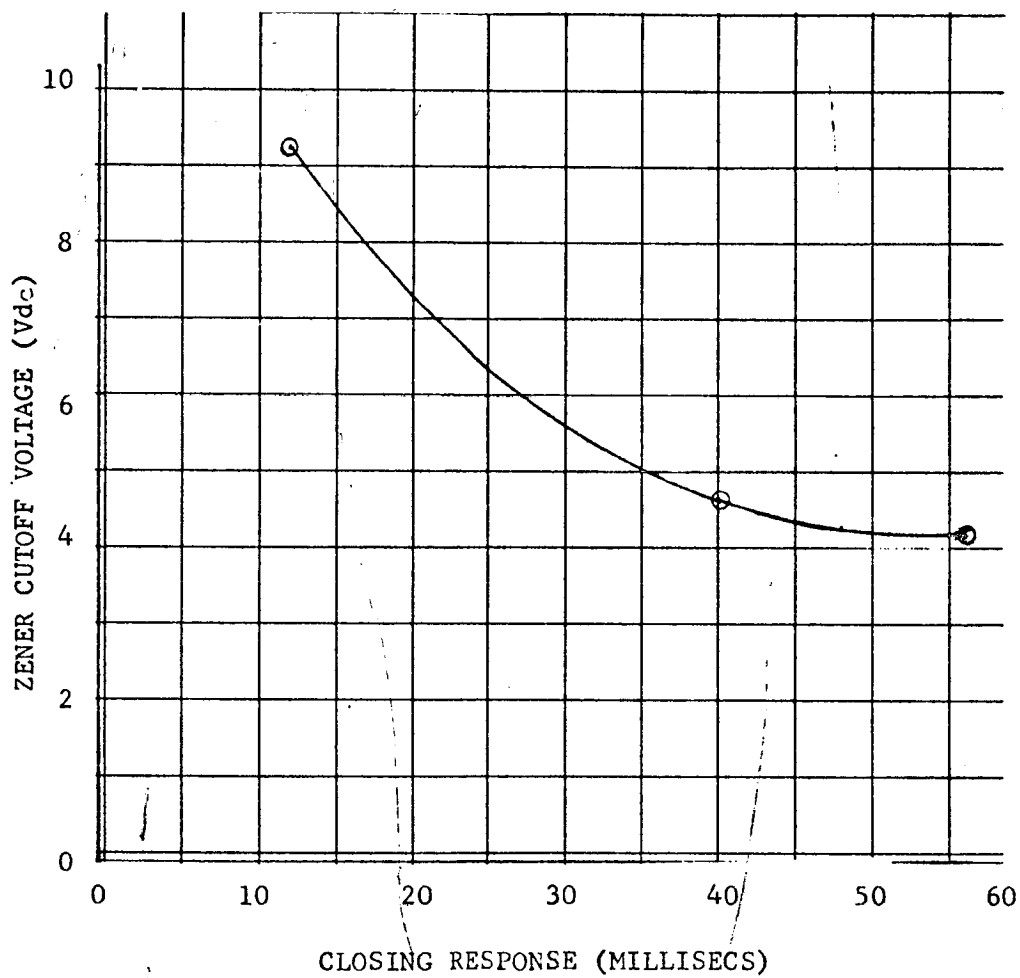


CURRENT LIMITING CIRCUIT

## VOLTAGE-CURRENT CURVES FOR SPECIAL DRIVER CIRCUITS



EFFECT OF ZENER CUTOFF VOLTAGE  
ON VALVE CLOSING RESPONSE



Another consideration of importance in single valve repeatability is the effect of usage. Valve components susceptible to dimensional change as a function of exposure or operating life must be avoided so that the opening force margin does not change. The soft seal in the seat assembly of the Apollo valve design extends less than .001 inch (measured perpendicular to the center line of the valve) into the envelope of the pintle in its fully closed position. The design includes provisions to relieve the compressive stresses that occur when the pintle is fully seated so that the sealing diameter won't change as a result of temperature or wear. In this way, the seating force, which is a function of seating diameter and inlet pressure, is maintained within acceptable limits throughout the operating life of the valve.

When the valve is to be exposed to high temperatures and pulser modifications are not desirable, other techniques to reduce the slowdown effect on valve response include, 1) routing the propellant through passages near the coil, 2) using coil wire with a low thermal coefficient of resistance, such as one of the copper nickel alloys, or 3) placing a thermometer in the temperature-affected zone of the coil.

## 2. Valve-to-Valve Repeatability

Valve-to-valve repeatability insures that all valves of a given design perform within a suitably narrow band, and engine performance remains relatively unchanged throughout its operating life. These characteristics are attained by maintaining tight manufacturing tolerances and minimizing those parts of the valve which, as a result of wear, would cause a change in response time.

### a. Manufacturing Tolerances

The response times are an example of the narrow data scatter obtained by holding valve manufacturing dimensions and tolerances as follows:

1. Stroke =	.019 $\pm$ .001 in.
2. Coil turns =	505. $\pm$ .00
3. Coil resistance =	12.40 $\pm$ 0.4 ohms
4. Seat load =	2.7 $\pm$ 0.1 lb.
5. Spring length: at 2.75 lb. =	.442 $\pm$ .005 in.
at 7.75 lb. =	.422 $\pm$ .010 in.
6. Armature to bore diametral clearance =	.0042 $\pm$ .0010 in.

The poppet and soft seat is dimensioned so that a tolerance of  $\pm$  .0037 is held on a nominal diameter sealing diameter of .218 in.

The non-magnetic barrier in the valve body is located axially on the body to within  $\pm .015$  in., has a length tolerance of  $\pm .03$  in., and a preweld diameter tolerance of  $\pm .002$  in. The barrier is welded automatically, and includes the following setup tolerances:

- |                        |                          |
|------------------------|--------------------------|
| 1. Amperage =          | $121 \pm 10$ amps        |
| 2. Voltage =           | $10.0 \pm 1.0$ vdc       |
| 3. Rotational speed =  | $3.75 \pm 0.25$ rpm      |
| 4. Wire feed rate =    | $18.75 \pm 1.0$ in./min. |
| 5. Torch travel rate = | $2.68 \pm .44$ in./min.  |

### C. Propellant Compatibility

Literature searches for material compatibility in propellant are good only for preliminary design. Information on all materials used in the valve is usually incomplete, particularly above temperatures of  $175^{\circ}\text{F}$ . Storage tests with a complete valve at the appropriate temperature must be performed to insure getting correct exposure information. Corrosion or other signs of incompatibility can occur during exposure to normal engine operating procedures or during in-house handling. It has been TMC's experience that water flush and drying procedures, if not carefully carried out, can produce nitric acid in a valve previously exposed to NTO. Handling procedures must be written, and material selection made in recognition of such conditions.

Another type of problem, while not propellant compatibility per se, relates to the valve-propellant interface and has been previously referred to as a pressure decay phenomenon and rheopexy by investigators. While this last condition has occurred only in systems flowing NTO, it points up the need to maintain a constant surveillance of the valve under all operating and handling conditions.

### D. Special Design Requirements

Special system or mission requirements which have been considered in the Apollo program include exposure to high vibration levels, and ignition transients.

#### 1. Vibration

Valve design for application in high random vibration fields must consider means for reducing or eliminating poppet-to-seat movement by providing high seat loads, or appropriately orienting the valve to reduce or eliminate this motion. Also, the valve must not contain materials which can become worn or displaced. For example, leakage in valves tested at very high vibration levels was caused by Teflon flakes which were generated by the vibratory motion of the pintle on the seat.

## 2. Ignition Transients

Valves designed for high pressure ignition transients must survive those originating in the thrust chamber, as well as detonations in the manifold passages downstream of the valve. Results of tests in which a detonation was deliberately made to occur in a test section just downstream of the valve exit orifice, showed that short duration pressures of 25,000 psig could be withstood by the Apollo valve without leakage or damage. When higher pressures were generated in the downstream tube, the resulting damage was loss of the Teflon seal. The test was performed in such a way that the valve was open at the time of the detonation. The survivability of the seal at such high pressures was due to the fact that it did not project into the path of the reverse flow pressure wave.



CHAPTER 10

INJECTOR DESIGN

BY

J. F. FOOTE

TABLE OF CONTENTS

	<u>Page</u>
I INTRODUCTION	10-1
II CHRONOLOGY OF INJECTOR DEVELOPMENT	10-3
Phase I - Early Development	10-3
Phase II - Multiple Doublet Development	10-3
Phase III - Multiple Doublet - Film Cooled Chamber	10-17
Phase IV - Preigniter Development	10-48
III INJECTOR DESIGN CRITERIA	10-60
Unlike Doublets	10-60
Steady State Performance	10-61
Thermal Performance	10-67

# LIST OF ILLUSTRATIONS

<u>Figure Number</u>	<u>Title</u>	<u>Page</u>
1	Preigniter Injector	10-2
2	Injector Chronology	10-4
3	Injectors Tested	10-5
4	Single Doublet X18297	10-7
5	X18299 Vortex Injector & X18333-501 Vortex Insert	10-8
6	4x4 Insert for Vortex Housing	10-9
7	6x6 Insert for Vortex Housing	10-10
8	First Multiple Doublet Injector	10-12
9	Typical T6910 & T7305 Injector	10-13
10	Extra Fuel Cooling Loop X19790	10-14
11	12x12 Injector X19900	10-15
12	Typical X20560 Injector	10-18
13	T9290 Injector - Steel Oxidizer Tubes	10-33
14	O/F 1.6 8x8 Injector T9669	10-34
15	O/F 1.6 12x12 Injector T9659	10-35
16	O/F 1.3 8x8 Injector T9689	10-36
17	Splash Plate Injector T9665	10-37
18	First Fuel Cooled Injectors	10-39
19	T10040 for % Film Cooling Variation Tests	10-40
20	One Piece Oxidizer Standoff T10050	10-41
21	T10060 Injector	10-42
22	Equal Hole Diameter 8x8 T10479	10-45
23	Equal Hole Diameter 8x8 T10467	10-46
24	Constant Momentum Angle Injector Ass'y - T9930	10-47
25	Experimental Preigniter on 20560-511 Injector	10-49
26	Four Valve Preighiter Test Rig	10-50
27	Preigniter Heat Transfer Injector	10-51
28	Preigniter Injector Schematic	10-52
29	First Preigniter Injector T10650	10-55
30	Range of O/F's and Total Propellant Flows Tested	10-56
31	Replaceable Fuel Tube Injector	10-58
32	Specific Impulse vs. Number of Doublets	10-62
33	Non-Film Cooled-Non Preigniter Specific Impulse vs. Rupe Factor	10-63
34	Specific Impulse vs. Rupe Criteria Fuel Film Cooled - Non Preigniter Injectors	10-64
35	I <sub>sp</sub> Efficiency vs. Rupe Criteria Preigniter Engines	10-65
36	Preigniter Injector Doublet Mixture, Ratio Rupe Criteria and Momentum Angles	10-66

LIST OF FIGURES (continued)

<u>Figure Number</u>	<u>Title</u>	<u>Page</u>
37	Specific Impulse vs. Percent Fuel Cooling	10-68
38	Non-film Cooled - Nonpreigniter Flange and Throat Temperature vs. Momentum Angle - 8 Doublet Injectors	10-70
39	Throat Temperature vs. Specific Impulse	10-71
40	Flange Temperature vs. Mixture Ratio	10-73
41	Effect of Bleed Angle and Throat Temperature Upon The Transition From Nucleate to Film Boiling of Cooling Fluid	10-74
42	Throat Temperature vs. Percent Fuel Cooling	10-75

LIST OF TABLES

<u>Table Number</u>	<u>Title</u>	<u>Page</u>
I	X20560 Injectors	10-19
II	Engine Dribble Volumes & Fuel Bleed Percents	10-43
III	First Preigniter Hydraulics	10-54
IV	Preigniter Test Summary	10-57
V	Early Preigniter Engines	10-59

## I. INTRODUCTION

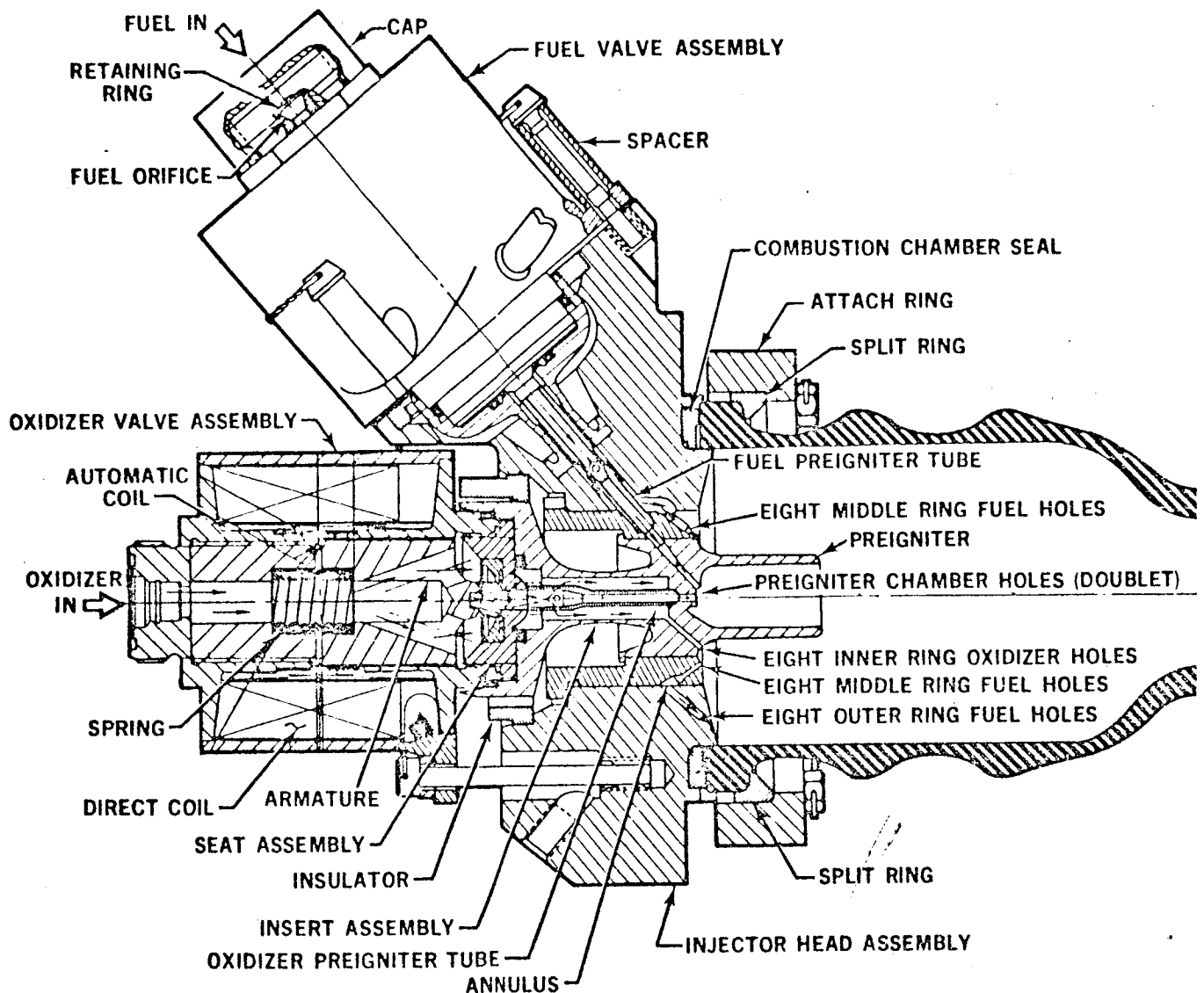
The injector is perhaps the heart of a successful rocket engine. It is responsible for performance, both steady state and pulse, for the thermal characteristics of the engine and it is also somewhat responsible for the structural integrity of the engine. The injector is responsible for the mixing of the two propellants which is the most significant event in achieving good performance. It is also responsible for the thermal characteristics of the engine. It must isolate the propellant and propellant valves from the hot chamber and it must also distribute the propellant so as to avoid chamber overheating. The injector is also responsible for low ignition pressure so that the structural limits of the engine are not exceeded.

The present injector is the result of approximately 2 1/2 years of evolutionary development. The first tests in 1962 indicated that the multiple doublet injector would give the best performance so that the bulk of the injector development has been with multiple doublet unlike injectors. Fuel film cooling holes were added to the injector in February 1964 to cool the chamber and chamber flange area. A preigniter was added to the injector in June 1964 to eliminate ignition overpressures. These break-throughs solved two of the most serious problems that occurred during the development of the engine. Prior to the fuel film cooling there was very little control available over the thermal characteristics of the engine. But with the addition of fuel film cooling the thermal characteristics, flange temperature, throat temperature, injector temperature, for example, could be controlled. The flange temperature before film cooling was too high, 2000°F, so that the injector head was also too hot (300°-500°) and the chamber to injector seal would not stand this temperature.

Prior to the addition of the preigniter, ignition overpressures would sometimes exceed the structural limit of the combustor. The preigniter eliminated this problem for single pulse operation. The injector is designed so the propellants enter the preigniter first and ignition takes place there. This pressurizes the main chamber with hot gas to 10-20 psia. The propellants then reach the main doublets and ignite smoothly.

The present injector features (Figure 1) a center unlike doublet enclosed in a preigniter cup, 8 unlike doublets arranged in a circle around the preigniter, 8 fuel cooling holes for the main chamber and 8 for the preigniter cup. The fuel and oxidizer valves are thermally isolated by stainless steel stand-offs. The oxidizer passages are in stainless steel and the fuel in aluminum. The stainless steel surfaces of the oxidizer passages cool down quickly when the injector is hot so that the oxidizer does not boil. The aluminum helps the fuel remove the heat from the injector head.

PREIGNITER INJECTOR



## II. CHRONOLOGY OF INJECTOR DEVELOPMENT

The evolution of the Apollo R-4D injector can be broken down into four periods or phases as shown graphically in Figure 2. The first phase was the period when many different types of injectors were tested and it was realized that the multiple doublet configuration held the most hope of reaching the specific impulse goal of 300 seconds. The next phase was testing with many different multiple doublet configurations in an effort to reach the specific impulse goal. During the third phase, injectors were tested to optimize fuel cooled engine performance and evaluate engine starting overpressures. This phase ended with the introduction of the preigniter to eliminate the ignition overpressures. The fourth phase was testing with the preigniter engine that led to the basic configuration existing today.

### Phase I - Early Injector Development

Between the receipt of the contract in February 1962 and October 1962, many different types of injector concepts were tested before the multiple doublet was selected as having the best promise for future development. These early injectors shown in Figure 3 can be categorized into essentially four groups.

1. Single doublet
2. Single doublet with splash plates and premix chambers
3. Vortex
4. Multiple doublet.

Shown on the sketches are the best specific impulse obtained with each configuration. The best single doublet specific impulse was 285 seconds at an O/F of 2.0 while several multiple doublet configurations had specific impulses from 290 to 300 seconds. Figures 4 and 5 are drawings of the basic single doublet and vortex injectors.

### Phase II - Multiple Doublet Development

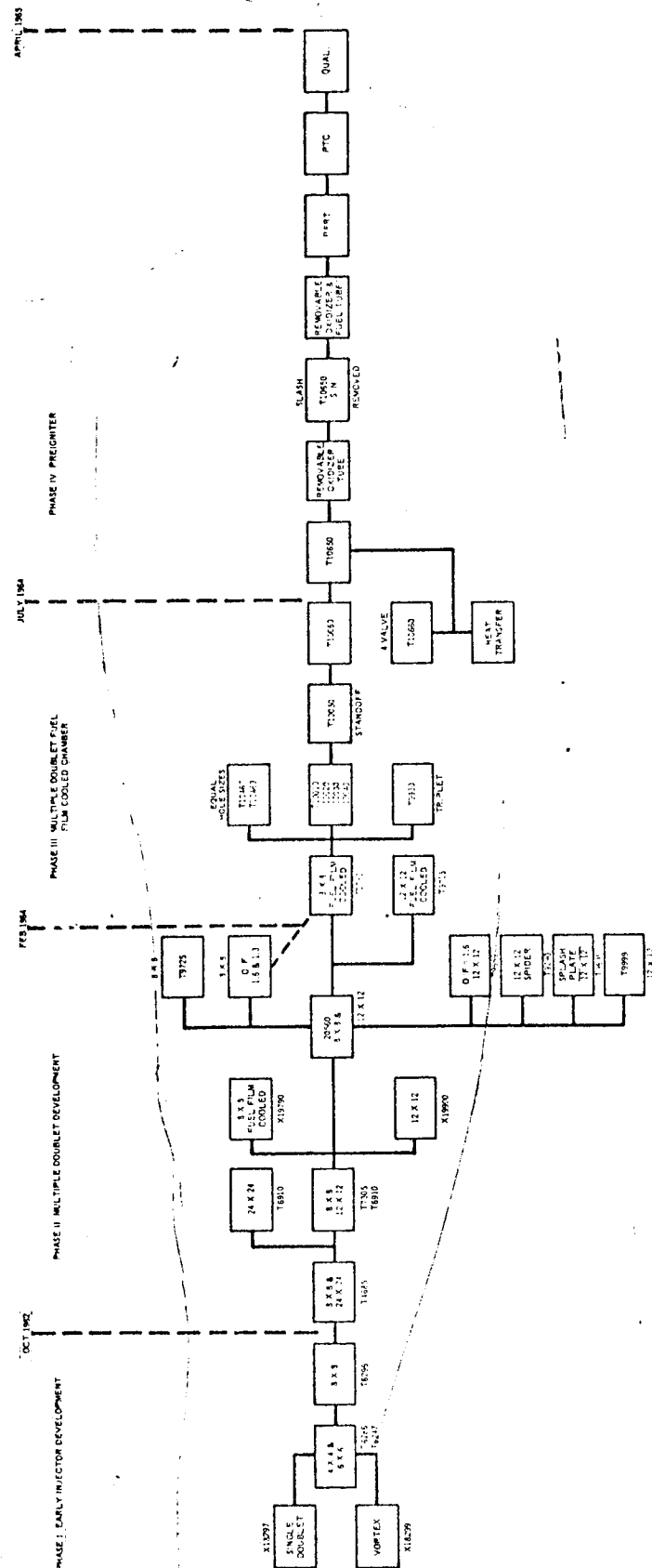
Because the early injector testing indicated that the multiple doublet injector had the best possibility of reaching the performance goal of 300 seconds, all development effort was spent on the multiple doublet injector.

The first multiple unlike doublet injector was a  $4 \times 4$ . The injector used the vortex housing and a special insert in place of the vortex insert. Figure 6 is a detailed drawing of this injector. The specific impulse of this injector was 271 seconds. The number of doublets of this injector was increased to 6 by using the insert shown in Figure 7. The specific impulse increased to 285 seconds.


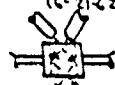



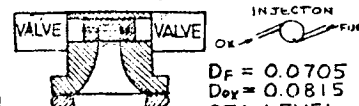

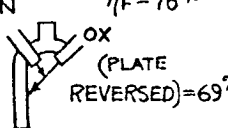

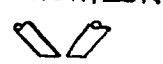
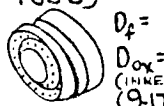
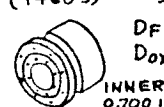
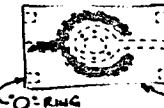

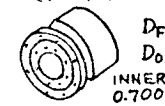
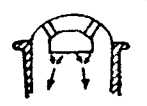


The next injector was an  $8 \times 8$  that used the single doublet housing. The specific impulse for this engine was 294 seconds.



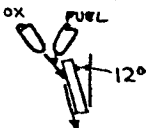
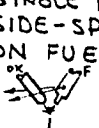
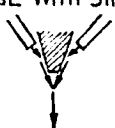

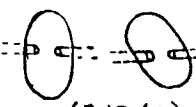

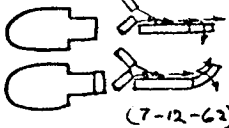
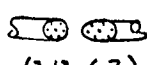
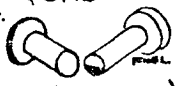
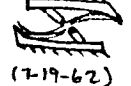
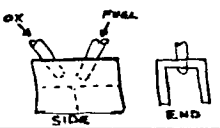
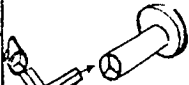

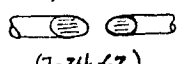

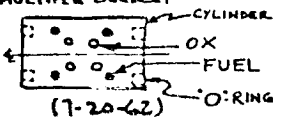

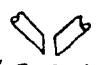
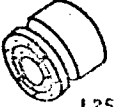
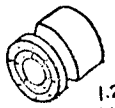
## INJECTOR CHRONOLOGY

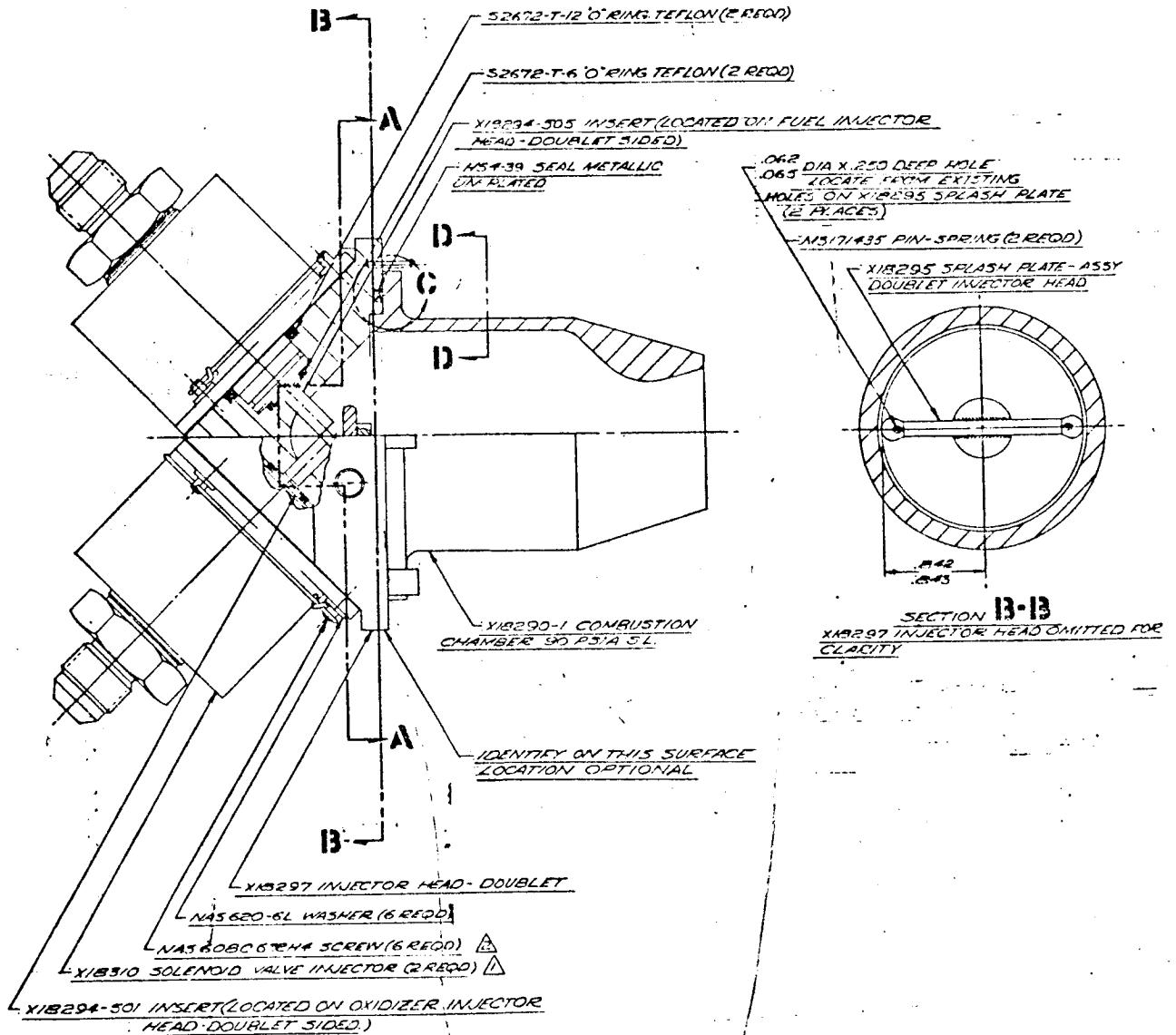


## INJECTORS TESTED

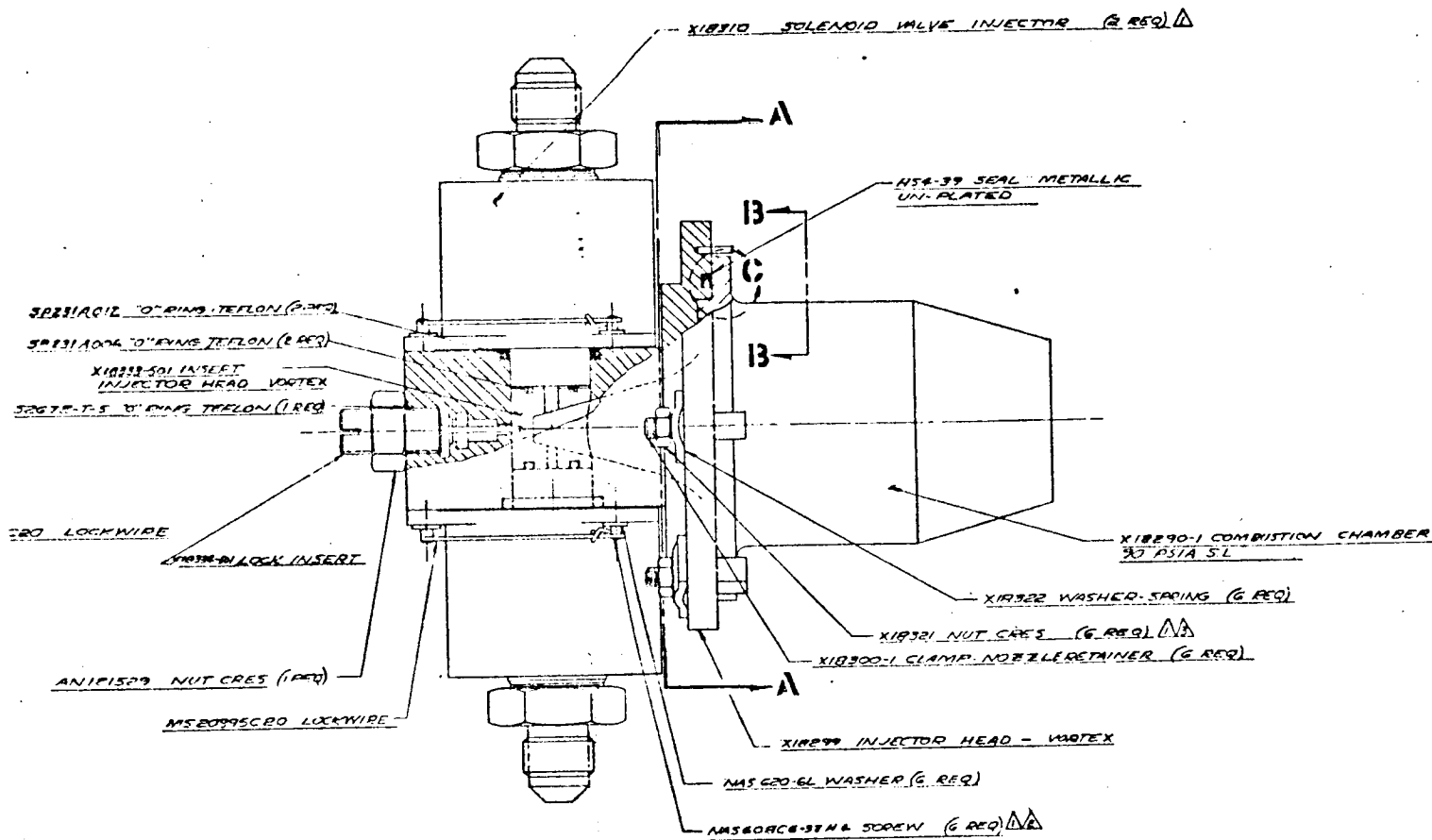
<p>PLAIN SINGLE DOUBLET (X18297)</p> <p><math>D_F = 0.0705</math> <math>D_{OX} = 0.0815</math> 9-20-62 <math>\eta_F = 87\%</math> SEA LEVEL</p> 	<p>SMALL PREMIX CYLINDER (6-21-62)</p> <p><math>\eta_F = 80\%</math> SEA LEVEL</p> 	<p>MUSTACHE PLATE (7-5-62)</p> <p><math>\eta_F = 80\%</math> SEA LEVEL</p> 
<p>SMALL "BUTTON" SPLASH PLATE (6-6-62)</p> <p><math>\eta_F = 70\%</math> SEA LEVEL</p> 	<p>LARGE PREMIX CYLINDER (6-22-62)</p> <p><math>\eta_F = 80\%</math> SEA LEVEL</p> 	<p>VORTEX (6-28-62)</p> <p><math>\eta_F = 38\%</math></p> <p><math>D_F = 0.0705</math> <math>D_{OX} = 0.0815</math> SEA LEVEL</p> 
<p>LARGE "BUTTON" SPLASH PLATE (6-12-62)</p> <p><math>\eta_F = 70\%</math> SEA LEVEL</p> 	<p>DUST PAN (PLATE REVERSED) = 69%</p> <p><math>\eta_F = 76\%</math> SEA LEVEL</p> 	<p>VORTEX (WITH BAFFLE WASHER) (6-28-62)</p> <p><math>\eta_F = 46\%</math> SEA LEVEL</p> 
<p>SINGLE DOUBLET BEVELED-HORIZONTAL (8-3-62)</p> <p><math>\eta_F = 85.5\%</math> ALTITUDE</p> 	<p>24-ON-24 (T4685)</p> <p><math>\eta_F = 90\%</math> SEA LEVEL</p> <p><math>D_F = 0.018</math> <math>D_{OX} = 0.018</math> (INNER RING OX) (9-17-62)</p> 	<p>8-ON-8 (T4685)</p> <p><math>\eta_F = 90\%</math> SEA LEVEL</p> <p><math>D_F = 0.025</math> <math>D_{OX} = 0.029</math> INNER RING OX. 0.700 IMP. DIA. (8-31-62)</p> 
<p>6-ON-6 VORTEX HEAD MULTIPLE DOUBLET (8-10-62)</p> <p><math>\eta_F = 87.5\%</math> SEA LEVEL</p> <p><math>D_F = D_{OX} = 0.038</math> (INNER RING OX) (8-10-62)</p> 	<p>CONE FAN CONCENTRIC ANNULAR IMPINGEMENT NOT BURNED</p> <p>WATER TESTED LOOKED POOR</p> 	<p>8-ON-8 (T6910)</p> <p><math>\eta_F = 88.8\%</math> ALTITUDE</p> <p><math>D_F = 0.029</math> <math>D_{OX} = 0.037</math> INNER RING OX. 0.700 IMP. DIA. (11-19-62)</p> 
<p>SINGLE DOUBLET 8-ON-8 ATTACHMENT (T6246)</p> <p><math>\eta_F = 90\%</math> SEA LEVEL</p> <p><math>D_F = .029</math> <math>D_{OX} = .029</math> (8-14-62)</p> 	<p>2-ON-2 (LIKE-ON-LIKE) FOR VORTEX HEAD NOT BURNED</p> <p>WATER TESTED HIGH <math>\Delta P</math></p> 	<p>12-ON-12</p> <p><math>\eta_F = 86\%</math> ALTITUDE</p> <p><math>D_F = 0.024</math> <math>D_{OX} = 0.029</math> 1.25" IMP. DIA. MOMENTUM ANGLE = +2° (4-6-63)</p> 

## INJECTORS TESTED

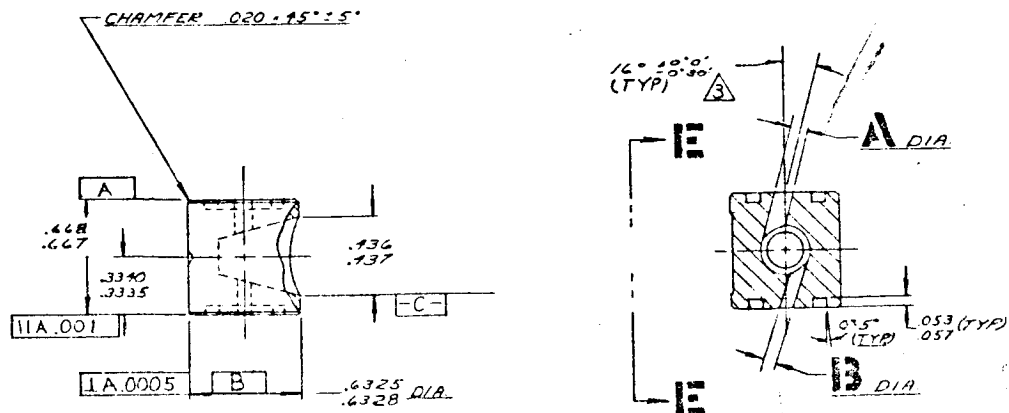
<p>12° SPLASH PLATE    <math>\eta_F = 79\%</math>  SEA LEVEL  (6-25-62)</p>	<p>SINGLE DOUBLET SIDE-SPRAY PORTS ON FUEL INSERT.    <math>\eta_F = 70\%</math>  SEA LEVEL  (7-5-62)</p>	<p>WEDGE WITH SINGLE DOUBLET    <math>\eta_F = 50\%</math>  SEA LEVEL  (7-13-62)</p>
<p>SINGLE DOUBLET SLOTTED ATTACHMENT    <math>\eta_F = 75\%</math>  SEA LEVEL  (7-12-62)</p>	<p>SINGLE DOUBLET ELLIPTICAL PREMIX CHAMBER    <math>\eta_F = 78\%</math>  SEA LEVEL  (7-12-62)</p>	<p>SINGLE DOUBLET WITH TWIN ORIFICES    <math>\eta_F = 65\%</math>  SEA LEVEL  (7-19-62)</p>
<p>SPLASH PLATE ATTACHMENTS -SINGLE DOUBLET    <math>\eta_F = 80\%</math>  SEA LEVEL  (7-12-62)</p>	<p>SINGLE DOUBLET 7 HOLES IN EACH TUBE    <math>\eta_F = 69\%</math>  SEA LEVEL  (7-13-62)</p>	<p>HALF MOON (FUEL) EQUAL STREAM O.D.    <math>\eta_F = 80\%</math>  SEA LEVEL  (7-19-62)</p>
<p>DOUBLE LAYER IMPINGEMENT PLATE FOR SWIRL    <math>\eta_F = 81\%</math>  SEA LEVEL  (7-19-62)</p>	<p>SINGLE DOUBLET WITH SHROUD    <math>\eta_F = 62.5\%</math>  SEA LEVEL  (7-20-62)</p>	<p>SINGLE DOUBLET SPLIT JET    <math>\eta_F = 77\%</math>  SEA LEVEL  (7-26-62)</p>
<p>60° INCLUDED ANGLE DOUBLET    WATER FLOW ONLY-ATTACHMENT LEAKED  7-25-62</p>	<p>SINGLE DOUBLET WITH SLOTS    <math>\eta_F = 74\%</math>  <math>\eta_F = 68\%</math> (ROTATED)  (7-24-62)</p>	<p>SINGLE DOUBLET    <math>\eta_F = 84\%</math>  (8-1-62)</p>
<p>4-ON-4 VORTEX HEAD MULTIPLE DOUBLET    <math>\eta_F = 83\%</math>  SEA LEVEL  (7-20-62)</p>	<p>SINGLE DOUBLET CENTER PLATE MAX. DIA. CONTACT    <math>\eta_F = 43\%</math>  SEA LEVEL  (KNIFE EDGE)  (7-24-62)</p>	<p>SINGLE DOUBLET BEVELED. VERTICAL    <math>\eta_F = 83\%</math>  SEA LEVEL  (8-2-62)</p>
<p>12-ON-12    <math>\eta_F = 90\%</math>  ALTITUDE  <math>D_F = 0.024</math>  <math>D_{OX} = 0.0314</math>  1.25" IMP. DIA. MOMENTUM ANGLE = 0°  (5-10-63)</p>	<p>12-ON-12    <math>\eta_F = 87\%</math>  ALTITUDE  <math>D_F = 0.024</math>  <math>D_{OX} = 0.033</math>  1.25" IMP. DIA. MOMENTUM ANGLE = -2°  (6-19-63)</p>	



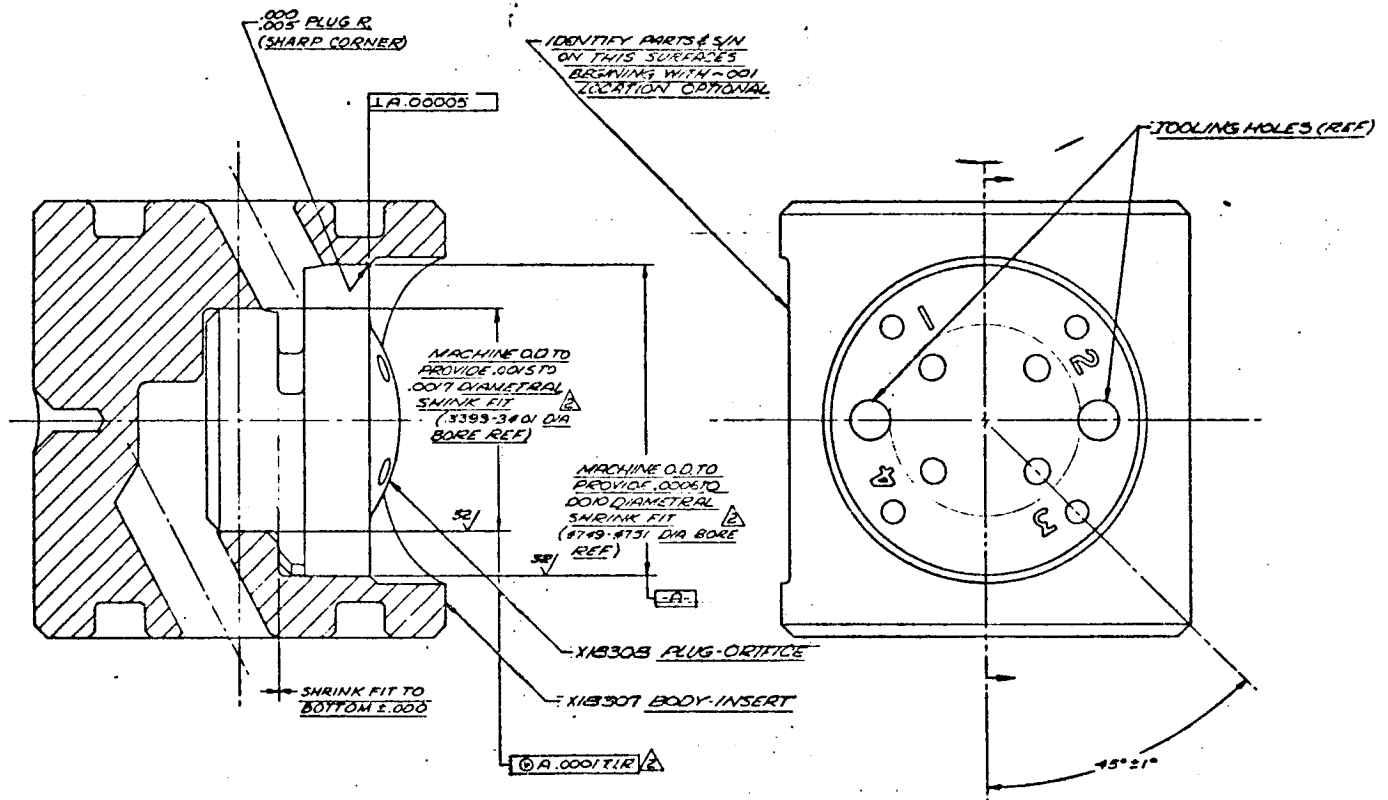
SINGLE DOUBLET X18297



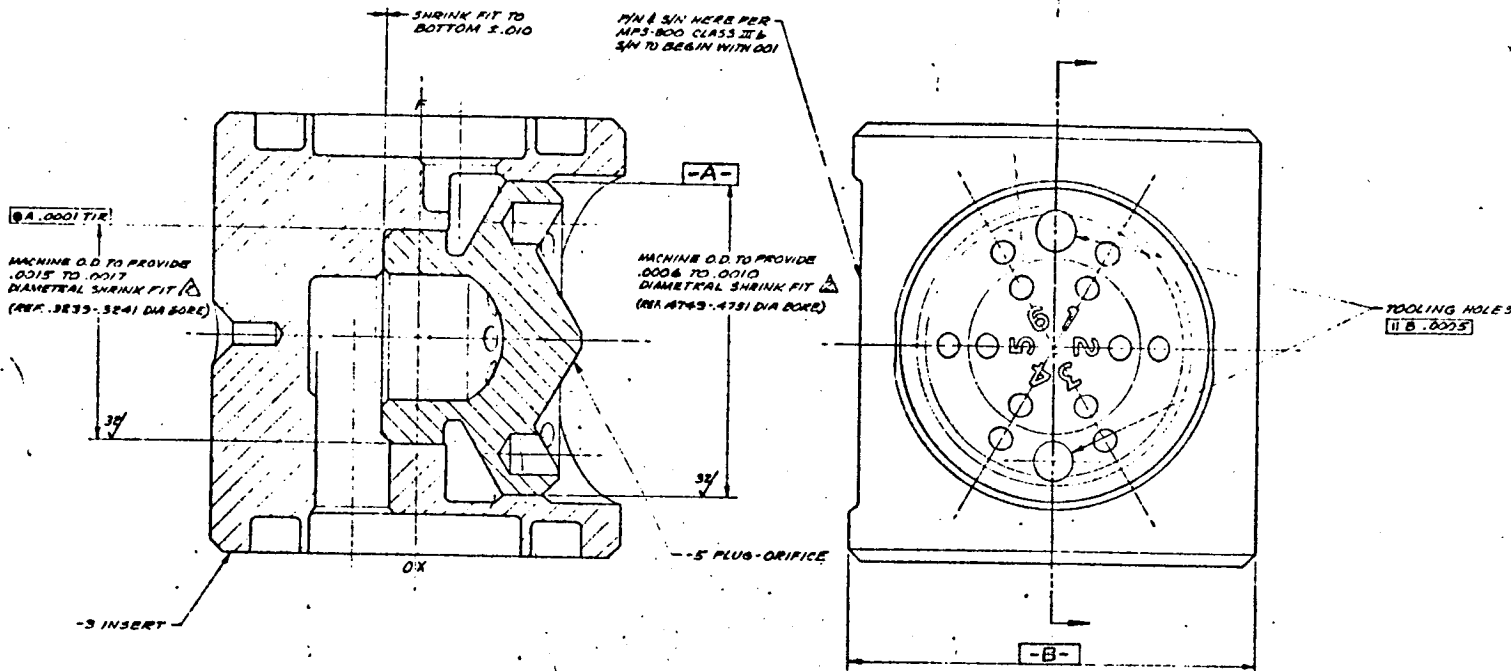
X18299  
VORTEX INJECTOR



X18333-501  
VORTEX INSERT



4x4 INSERT FOR VORTEX HOUSING



6x6 INSERT FOR VORTEX HOUSING

After the tests with the vortex and single doublet housing had shown that the multiple doublet injector was a good concept, a development engine was built to test the effect and the number of doublets, doublet diameter, impingement diameter and included angle on performance. Figure 8 is a detailed drawing of this injector. Note that the insert slipped in so that the doublet configuration could be changed easily. The engine was tested with 8 and 24 doublets. The specific impulse was 294 seconds for eight and 283 for twenty four doublets.

This injector was not tested as often as originally planned because the valves and injector head soakback temperatures were much too high, and it was realized that the premix was not necessary or important in improving the performance.

The next two injectors were identified as T6910 and T7305. They were tested from October 1962 to June 1963 with the objective of reaching the performance goal of 300 seconds. Many different minor modifications were made to these injectors. The drawing for the first T6910 injector is shown in Figure 9. All the injectors were similar in nature. The number of doublets tested were 8, 12, 24; the doublet diameters were varied to improve the performance and the impingement diameter was also varied. In general these injectors came close to the performance goal of 300 seconds at an O/F of 2.0 (295-300 seconds). However, the 8 doublet injector head steady state and soakback temperatures were too high (approximately 400°F running and 500° soakback).

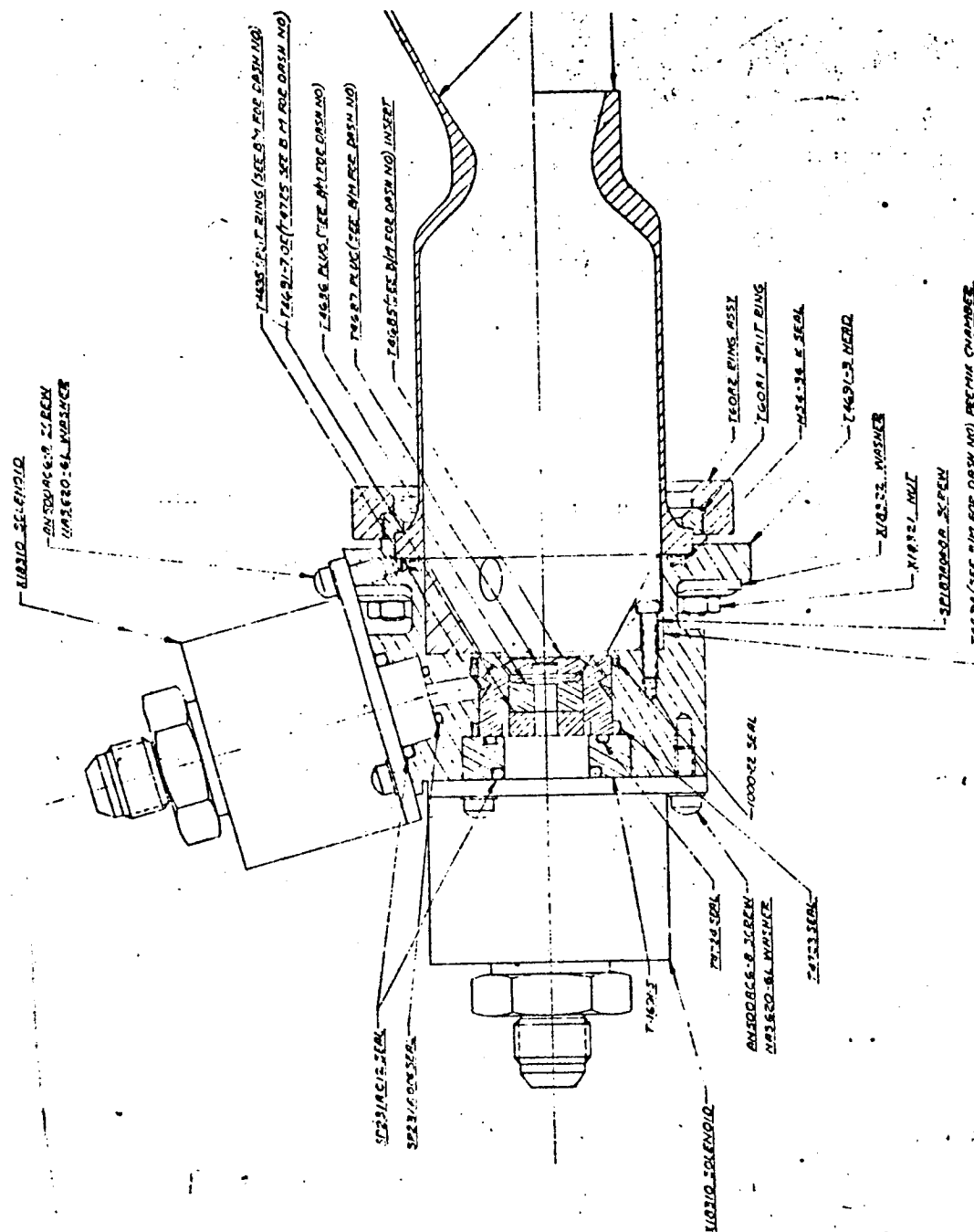
To lower the injector head temperature the next injector had an extra fuel cooling loop added. Figure 10 is a detailed drawing of this injector. The fuel cooling loop did succeed in lowering the steady state head temperature to 250° but the head still soakbacked to 400°F. This engine had a fuel dribble volume of 140% and an oxidizer dribble volume of 40%. Two structural chamber failures occurred with this injector. Both can be attributed to the test conditions, cold chamber, oxidizer lead due to the large fuel dribble volume and also the accumulation of fuel residue from the previous pulse when the fuel dribble volume empties. Because of the chamber failures, this injector concept was dropped.

The next injector (XL9900) was a 12 doublet injector similar to the 12 doublet T7305. Figure 11 is a detailed drawing of this injector. The specific impulse for this injector was 300 seconds. The injector head running temperature was 250°. The larger diameter fuel annulus, compared to the 8 x 8 injector, cooled the injector better. This injector came from the T7305, 12 x 12 injector.

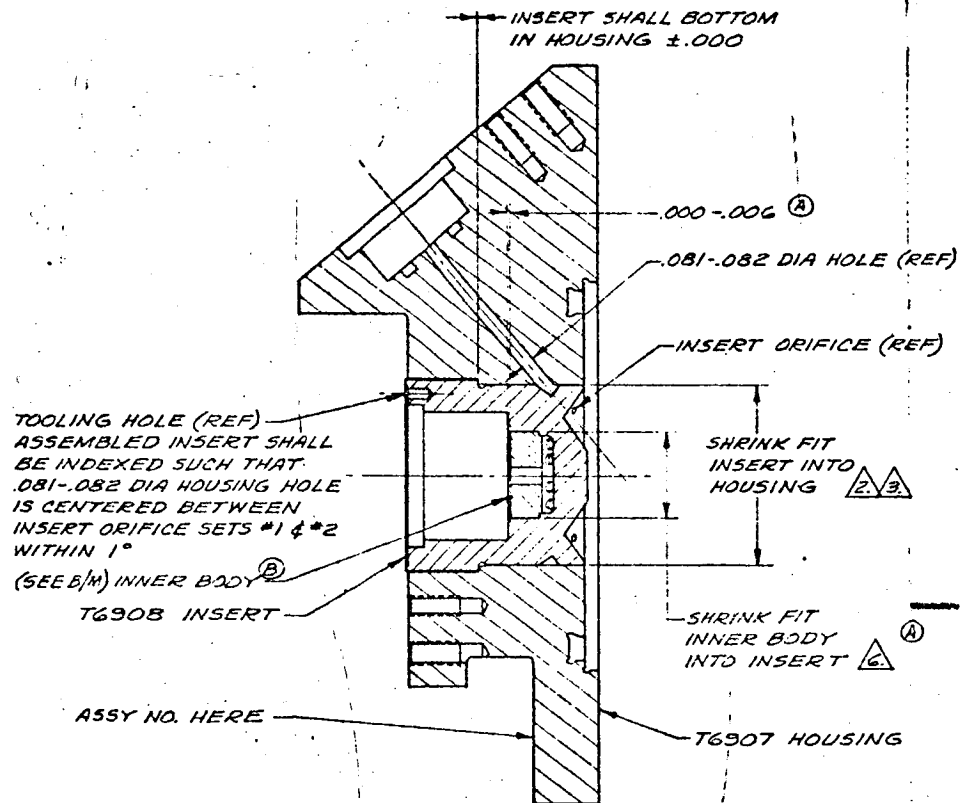
The XL9900 injector proceeded into what was called a prequal since the performance goal of 300 seconds at an O/F of 2.0 was met and no other problems were envisioned. During this prequal testing two new problems were discovered; hot phase and ignition overpressures or spikes.

During the last run of what was called a maneuver, number 1 (10 ON, 30 Off-3 ON, 360 Off, 20 ON) the combustion chamber would become too hot and sometimes

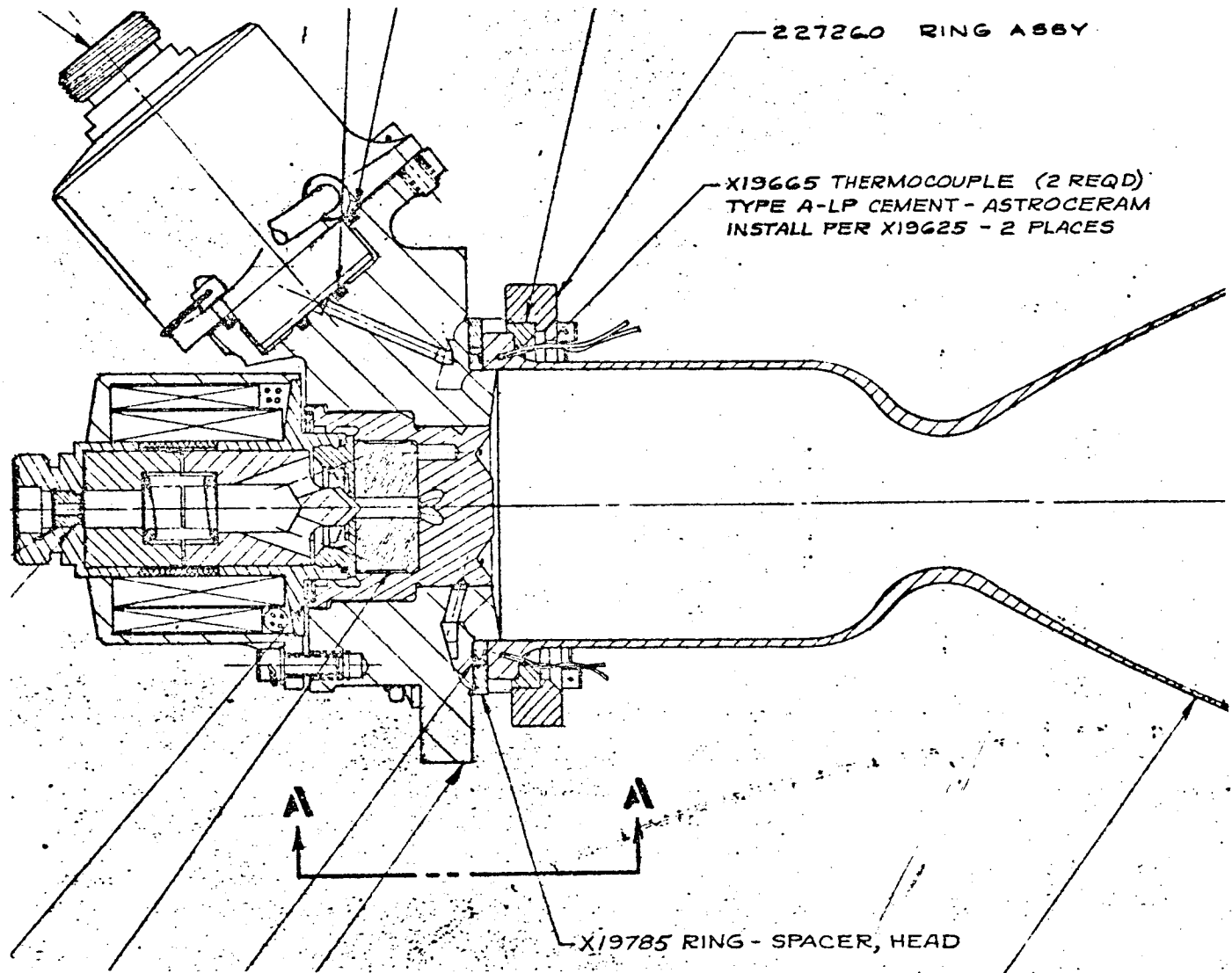




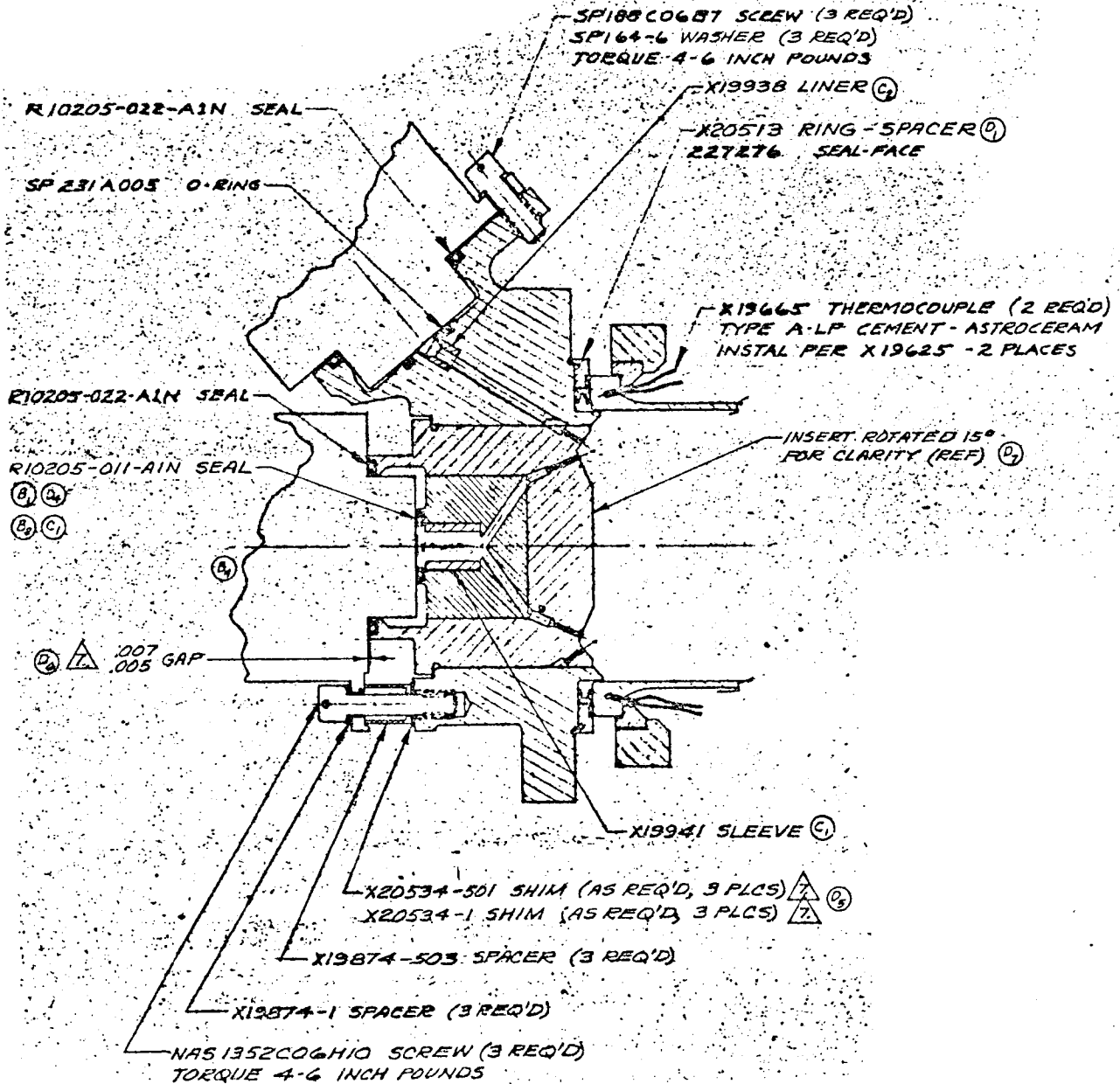
FIRST MULTIPLE DOUBLET INJECTOR



TYPICAL T6910 and T7305 INJECTOR



EXTRA FUEL COOLING LOOP X19790



12 x 12 INJECTOR X19900

fail. The other characteristics of Hot phase or High Heat Transfer Burning (HHTB) are tabulated below.

COMPARISON OF ENGINE PARAMETERS FOR NORMAL AND HIGH HEAT TRANSFER BURNING

Parameter	HHTB	Normal
	(Approximate Values)	
Thrust	91 lb.	97.1 lb.
Chamber Pressure	84.1 psia	94.7 psia
Fuel Flow	0.118 lb/sec.	0.117 lb/sec.
Oxidizer Flow	0.217 lb/sec.	0.234 lb/sec.
Visual Observation	Incandescent	Cherry Red
Temperature Rise Rate at 2000°R	1000°F/sec.	330°F/sec.
Accelerometer Trace	Peaks at 12000 cps	Peaks at 19000 cps
	High overall acceleration level (42.3 g's)	Normal acceleration level (4.2 g's)

After several seconds the engine would usually return to normal operation but if the HHTB mode continued for very long the chamber would burnout. HHTB correlated well with elevated injector head temperatures caused by heat soaking back from the combustion chamber into the injector head following engine shutdown. An analysis was conducted along with the engine testing that showed that HHTB was due to the oxidizer two phasing as it passes through the injector head. Consequently, the rest of the injector designs attempted to eliminate two phase oxidizer flow by thermally isolating the oxidizer in the injector or cooling the chamber so the head would also be cooler.

The second problem during the prequal testing was the failure of a chamber during a pulsing duty cycle. As a consequence of the two chamber failures with the fuel cooled head engine, ignition tests were made with the prequal engine, X19900. During one of these ignition tests a chamber failure occurred.

Because of the HHTB and ignition overpressures prequal was stopped and a program was undertaken to eliminate high heat transfer burning and ignition overpressures using engine X20560.

The X20560 engines were 12 on 12 doublets with 1.25 impingement diameter except for one 8 doublet configuration. The orifice diameter, doublet angles, and oxidizer valve standoffs were varied in an effort to eliminate the problems. A sketch of the typical injector is shown in Figure 12. Table I describes the injectors, reason for design, and test results.

The best configuration, engine X20560-511 had a specific impulse of 295-300 seconds and an O/F of 2.0 and High Heat Transfer Burning was reduced to an acceptable level. It still occurred but the engine stepped out before the chamber got too hot. It was thought that the fuel lead characteristics of the engine also reduced the ignition pressures to an acceptable level.

In order to eliminate hot phase entirely, injector T9290 was built and tested. This injector incorporated steel oxidizer tubes to feed the doublets (Figure 13). This configuration did eliminate hot phase but the manufacturing problems were very severe and it was never really considered as a solution.

Two injectors were also designed and tested for O/F of 1.6. One was an 8 doublet and the other a 12 doublet. Figures 14 and 15 are sketches of both. The 8 x 8 injector had specific impulse of 310 seconds at an O/F of 1.6 but the engine temperatures were excessive. The 12 x 12 also had good performance but the temperatures were also high.

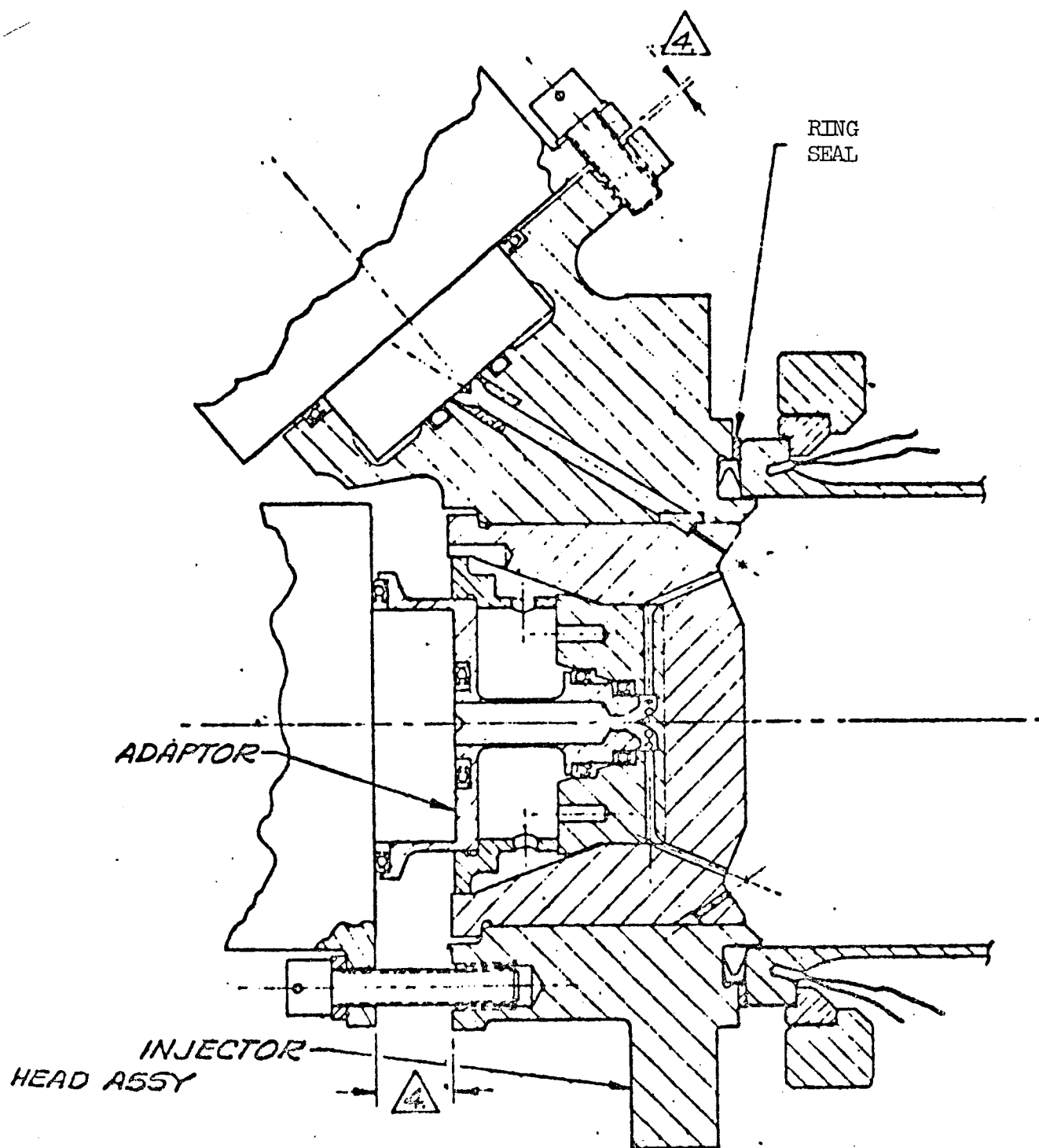
An injector was designed and tested at an O/F of 1.3. This injector was an 8 doublet injector (Figure 16). The chamber temperatures exceeded 3100° and the specific impulse was 299 seconds.

A splash plate 12 x 12 injector was also built. In this injector (Figure 17) the resultant momentum angle after the doublets had impinged hit the flange area of a special chamber. The performance of this injector was poor (270 seconds), the chamber was cool, 2240°, at the throat, but still quite hot at the flange, 2170°F.

Two more "T" engines were built during this time, T9725, an 8 x 8 and T9999 a 12 x 12, to see if different hole sizes would improve the performance. The engines both had Isp's below 290.

### Phase III - Multiple Doublet - Film Cooled Chamber

Eight fuel film cooling holes were added to the O/F 1.6, 8 x 8 injector and it was tested on February 6, 1964 with tremendous success. Both the chamber and the injector head temperatures were significantly cooler. High heat transfer burning did not occur. The specific impulse was 295 seconds at an O/F of 2.0 which was below the goal of 300 seconds but close enough to continue development of this concept.



TYPICAL X20560 INJECTOR

TABLE I  
X20560 INJECTORS

Configuration Number	Configuration Description	Design Purpose	Test Results				
20560-1	<p>(a) The -1 configuration was the first to incorporate a steel standoff between the oxidizer solenoid and injector head. Standoff diameter was .171 in. The injector head assembly consisted of a prototype (X19900) housing, 0.043 drilled oxidizer passages &amp; 0.171 in. diameter standoff (ox.).</p> <table><tr><td>Fuel dribble volume</td><td>74%</td></tr><tr><td>Oxid.dribble volume</td><td>81%</td></tr></table> <p>The insert was a 12 on 12 normal orientation insert with a "vee" cut between doublets. <math>D_{fuel} = 0.024</math>, <math>D_{ox} = 0.0314</math>, <math>\alpha_{fuel} = 35^\circ</math>, <math>\alpha_{ox} = 23^\circ</math>, Dimping = 1.25.</p>	Fuel dribble volume	74%	Oxid.dribble volume	81%	<p>(a) The standoff was designed to reduce the maximum heat soakback of the ox valve to 150°F to eliminate high heat transfer burning.</p>	<p>(a) High Heat transfer operating condition was improved in that the engine stepped out of the condition after ~4.5 seconds of the third 10 second run of maneuver No. 1 (Prop. temperatures 100°F - maximum wall temp. 3200°F). The engine successfully completed maneuver No. 1 with propellant temps. at 75°F. Testing confirmed the criticality of the ox. condition.</p> <p>Other designs were initiated to further improve the operating condition.</p>
Fuel dribble volume	74%						
Oxid.dribble volume	81%						
20560-501	<p>The -501 configuration was identical to the -1 assembly except that the ox. standoff diameter was reduced to 0.090 in. to match the oxidizer valve vena contracta.</p> <table><tr><td>Fuel dribble volume</td><td>74%</td></tr><tr><td>Oxid.dribble volume</td><td>55%</td></tr></table>	Fuel dribble volume	74%	Oxid.dribble volume	55%	<p>The reduced standoff diameter was designed to prevent sudden expansion of the oxidizer (liquid to gas) during engine operation at maximum heat soakback conditions.</p>	<p>The 0.090 I.D. standoff flow passage apparently aggravated the high heat transfer problem. Once started in high heat transfer operation, the engine would not recover and step out.</p>
Fuel dribble volume	74%						
Oxid.dribble volume	55%						



TABLE I (Cont'd.)

X20560 INJECTORS

Configuration Number	Configuration Description	Design Purpose	Test Results
20560-503	<p>The -503 assembly was identical to the -1 configuration except that in this configuration aluminum tube liners were inserted in the ox. crossfeed passages.</p> <p>Fuel dribble volume 74% Oxid.dribble volume 77.6%</p>	<p>The design was an attempt to insulate the oxid. flow as much as possible from injector head temperature conditions to prevent boiling of the oxidizer, a condition known to contribute significantly to high heat transfer burning.</p>	<p>No significant improvement in high heat transfer burning operating conditions was seen and the configuration was dropped. Heat transfer performance was very similar to -1 configuration.</p>
20560-505	<p>The configuration was identical to the -1 configuration except for the following:</p> <p>(a) The diameter of the crossfeed passages for the ox. was reduced from .043 to 0.031 inches diameter.</p> <p>(b) The injector insert was rotated 15° so that one of the fuel holes was in line with the injector head fuel inlet passage. This No. 1 hole diameter was reduced to flow same as the others.</p> <p>(c) The cross sectional area of the fuel annulus was reduced and made of a constant cross-sectional area.</p> <p>(d) Fuel dribble vol. 64% Oxid.dribble vol. 67%</p>	<p>(a) The diameter reduction of the ox. cross feed passages was a design change to investigate an analysis which indicated that a reduction in the tube diameter would be effective in preventing ox. boiling by reducing the wetted area.</p> <p>(b) Rotation of the fuel hole in line with fuel inlet allowed the hole to "see" a dynamic pressure, thus reducing the time required for fuel to enter the combustion chamber. The diameter of this No.1 fuel hole was reduced to flow the same as the others.</p> <p>(c) The change in fuel annulus cross-section further lowered time to fuel entry into the combustion chamber from valve open.</p>	<p>(a) The .031 diameter cross-feed passages showed no apparent improvement over the .043 passages with regard to high heat transfer burning.</p> <p>(b) Reorientation of the fuel hole provided some improvement in ignition pressure spike level but not enough improvement was seen to consider the problem solved.</p> <p>(c) No effect on performance of the reduced dribble volumes was noted.</p>

TABLE I (Cont'd.)

## X20560 INJECTORS

Configuration Number	Configuration Description	Design Purpose	Test Results
20560-507	The -507 configuration used .031 diameter oxidizer crossfeed passages and an eccentric annulus. In addition, a flat faced 13th doublet was added in the center of the injector face, in other respects it was the same as the -1 configuration. Fuel dribble volume ~ 64% Oxid. dribble volume ~ 67%	The .031 diameter ox. crossfeed passages were incorporated to try to reduce ox. boiling effects by reduction of the wetted tube area.  The 13th doublet design incorporated short, low volume flow paths from the injector valves to the doublets. Previous engine tests had indicated that no damaging pressure peaks would be encountered if initial chamber pressure levels were above 4 psi. 13th doublet design was to start a localized reaction which would raise chamber pressure level prior to main propellant entry into the chamber.	No heat transfer tests were performed with this configuration because of the probable similarity of internal ox. passage configuration with the -505.  The 13th doublet apparently made significant improvement in the ignition pressure spike level, but the absolute level was still too high for acceptance.
20560-511	The -511 configuration incorporated the following:  (a) .031 diameter oxidizer crossfeed passages rather than .043 passages.  (b) A flat injector face.  (c) The injector insert was rotated 15° to align one of the injector fuel holes with the fuel inlet and this No.1 fuel hole diameter was reduced to 0.018 to flow the same as the other 11 holes.	(a) As in the -505 configuration the 0.031 diameter ox. crossfeed passages were incorporated to reduce oxidizer boiling & effects by reduction of the wetted tube area.  (b) The flat injector face design provided near minimum obtainable free stream travel to impingement to (1) promote liquid phase mixing for good ignition characteristics, and (2) prevent expansion of the propellants to the gaseous state and subsequent freezing of the ox. on the	Two of the -511 configuration engines were tested. S/N 0001 was tested to determine both heat transfer and ignition pressure spike characteristics and S/N 0002 was tested to determine its heat transfer characteristics.  S/N 0001 - The engine was tested with both hot and cold propellants. Both maneuver No. 1's and 60 second runs, followed by runs at maximum soakback. High heat transfer in this engine was apparently

TABLE I (Cont'd.)

## X20560 INJECTORS

Configuration Number	Configuration Description	Design Purpose	Test Results
20560-511 (continued)	<p>(d) Reduced fuel volume was as a result of tapering the fuel annulus.</p> <p>Fuel dribble volume 58% Oxid. dribble volume 68%</p>	<p>chamber wall, a condition contributing to ignition delay.</p> <p>(c) Reduction of the fuel annulus volume and rotation of the injector insert ensured a fuel lead into the combustion chamber.</p>	<p>reduced to an acceptable level.</p> <p>S/N 0002 - The engine was tested with two chambers; one grit blasted, and one a standard chamber. Steady state wall (chamber) temperatures were comparable with S/N0001 but in maximum soakback firing conditions, excessive wall temperature from high heat transfer burning was experienced. The injector insert was found to be faulty in that the ox. crossfeed tubes were misaligned with the final transport tubes. Testing after rebuilding of S/N 0002 indicated that the anomaly in heat transfer characteristics still existed. The ignition pressure spike characteristics of this configuration were quite encouraging probably due to the short propellant free-stream length. Pressure spike levels in the S/N 0001 increased in later tests with strain gaged chambers because of injector face deterioration as a result of cavitation at the doublet entrance to the chamber.</p>

TABLE I (Cont'd.)

X20560 INJECTORS

Configuration Number	Configuration Description	Design Purpose	Test Results
20560-515	<p>The -515 configuration was identical to the -505 configuration except that the ox. valve standoff had a diameter of 0.201" rather than 0.171" and incorporated a fixed area restrictor at its downstream end.</p> <p>Fuel dribble volume ~ 64% Oxid.dribble volume ~ 76%</p>	<p>It was hypothesized that as temperatures increased, <math>N_2O_4</math> would tend to vaporize upon exiting from the valve into a relatively large cavity. Calculations indicated that the downstream restrictor designed would cause the vaporized ox. flow to choke at the restrictor. Thus, standoff passage pressure would rise and further vaporization of the ox. would be prevented. In addition, the downstream restrictor would tend to delay ox. arrival into the combustion chamber and thus further assure a fuel lead.</p>	<p>The downstream restrictor provided no significant improvement in ignition pressure spike tests so no further testing was conducted with this configuration.</p> <p>No heat transfer data was taken on this configuration.</p>
20560-517	<p>The -517 injector was identical to the -511 flat face, rotated insert configuration except for the substitution of the 0.201" I.D. oxidizer standoff, with downstream fixed restrictor.</p> <p>Fuel dribble volume ~ 58% Oxid.dribble volume ~ 77%</p>	<p>As in the -515 configuration listed above, the design was to do two things: (a) reduce or eliminate possible vaporization of the oxidizer in the oxidizer standoff area, and (b) by rotation of the insert ensure a fuel lead into the combustion chamber.</p>	<p>Test data indicated that the ignition pressure spike levels recorded for this engine were equivalent to those recorded for the -511 configuration.</p> <p>No high heat transfer data was obtained for this configuration.</p>

TABLE I (Cont'd.)

## X20560 INJECTORS

Configuration Number	Configuration Description	Design Purpose	Test Results
20560-519	<p>The -519, 12 on 12 configuration utilized the 0.171 standoff, and a fuel inlet passage diameter of 0.073 inches. It was a flat-faced injector with a normal orientation insert (fuel inlet between #1 and #12 doublets) and utilized an eccentric fuel annulus. The fuel hole diameter was unchanged at 0.024" but the oxidizer hole size was reduced from 0.031 on previous injectors to 0.026". The momentum angle at an O/F = 2.0 was +5°. The fuel dribble volume was 58% and the ox. dribble volume was 80%.</p>	<p>A flat-face was utilized in the -519 configuration to provide good ignition characteristics. The insert was installed in the normal orientation to provide uniform steady-state wall heating. The eccentric fuel annulus was utilized to minimize the fuel dribble volume while providing equal fuel hole flows. The oxidizer hole size was reduced to test the effect of higher velocity ox. injection on ignition peak pressure levels and on steady state wall heating. The momentum angle of +5° at O/F = 2.0 was to provide increased wall cooling which appears necessary since previous high injection velocity engines tended to have hot walls.</p>	<p>The -519 configuration did not receive extensive high heat transfer testing. Only one 4 second run was made in Cell 6, chamber wall temperature exceeded 3100°F at this time and the test was discontinued.</p>

TABLE I (Cont'd.)

## X20560 INJECTORS

Configuration Number	Configuration Description	Design Purpose	Test Results
20560-521	The -521 injector was an 8 on 8 flat-face insert. (Normal orientation) $D_{ox} = 0.29$ , $D_f = 0.29$ , $D_{imp} = 700$ , $M.A. = +16^\circ$ , $D.V._{ox} = 60\%$ and a .171 ox. standoff. The chamber was a standard moly non-grit blasted chamber with a standard K-seal with Rene heat barrier spacer.	The -521 engine was designed to verify previous performance results with 8 on 8 injectors using the same hole sizes and included stream angles, but incorporating the new oxidizer valve "standoff" concept to prevent high heat soakback temperatures to the oxidizer solenoid valve. All previous similar engines had run cool but had not been tested for high heat transfer burning operation. It was reasoned that the low engine temperature would not bring the propellants to a temperature that would promote high heat transfer burning. A flat face was incorporated in the injector to aid the ignition process.	High heat transfer phase burning was greatly improved, but not eliminated. The chamber wall temperature was extremely low (2000-2245) as well as the moly flange temperatures (1227-1430) for 60 sec. steady-state runs at $O/F = 2.0$ and $W_p \approx 333$ pps. steady-state Isp was 280 sec. for an $O/F = 2.0$ and $W_p \approx 333$ pps.
20560-521 Test of 1-10-64	The configuration was the same as above but with a standard moly grit blasted chamber and a wide flange K-seal.	This variation was conceived to increase thermal resistance between the chamber and head thereby reducing heat transfer back to the head to eliminate high heat transfer phase burning. It was also designated to decrease chamber wall temperature and thus reduce heat transfer to the head assembly.	No detrimental high heat transfer burning was experienced at $O/F = 2.0$ and $W_p \approx 333$ pps. At propellant temperatures from 100-118°F the chamber wall temperature was extremely low (1990-2235) as well as the moly flange temperature (1447-1489). The steady-state Isp was 276 sec. for an $O/F = 2.0$ and $W_p \approx 333$ pps. The pulse Isp was within specification requirements up to 50 ms pulse widths.

TABLE I (Cont'd.)

X20560 INJECTORS

Configuration Number	Configuration Description	Design Purpose	Test Results
20560-521 (continued) Test of 1-25-64	The configuration is the same as the first -521 but with a standard moly grit blasted chamber and a lucalox (ceramic) seal between the injector head and the combustion chamber.	This change was made to increase thermal resistance between the chamber and head to decrease the heat transfer back to the head and therefore eliminate high heat transfer burning. It was also run to evaluate the lucalox seal and to decrease chamber wall temperatures and thus reduce heat transfer to the head assembly.	The injector head was approximately 500F higher than previous tests as the lucalox seal did not conform to thermal resistance predictions. High heat transfer phase burning was experienced during extended Maneuver #1 because of higher head temperatures caused by the lucalox seal. The chamber wall temperatures were low (1900-2100F) as well as moly flange temperatures (1135F) for 60 seconds steady state runs at $O/F = 2.0$ and $W_p = 335$ pps. The steady-state Isp was 280 sec. for an $O/F = 2.0$ and a $W_p \approx 355$ pps.
20560-521 Test of 2-4-64	The configuration is the same as the first -521 except for a ribbed moly sleeve with strain gages which replaced the standard combustion chamber. It was instrumented with 140 kc kistler transducers.	This test was run on this configuration to document ignition characteristics.	The maximum pressure recorded (from strain gages) was 1720 psi. This is an improvement of $\approx 27\%$ over the 12 on 12 engine, 2490 psi.

TABLE I (Cont'd.)

X20560 INJECTORS

Configuration Number	Configuration Description	Design Purpose	Test Results
20560-523	<p>Free stream travel of the injected streams was minimized and the injector face was "vee" cut to inhibit fuel to oxidizer interpassage flow, resulting in the "knobby" face configuration.</p> <p>The configuration used a normally orientated injector insert. An eccentric (tapered) fuel annulus was incorporated. The injector hole sizes and angles were the same as the -1.</p>	<p>Short free stream length was to capitalize on the flat-faced (-511) type of injectors lower ignition peak pressures, while the incorporation of the "knobby" face design prevented the interpassage flow of the propellants. The eccentric fuel annulus further reduced the fuel dribble volume to ensure a fuel lead into the chamber to further minimize ignition pressure peaks. The normally orientated injector insert was designed to minimize steady state wall temperature variations.</p>	<p>The anticipated steady state performance would have been identical to the -1 configuration because of the basic injection similarities. Consequently, no high heat transfer tests were performed on this configuration. Ignition peak pressure tests indicated peak ignition pressure levels comparable to those measured with the -511 configuration.</p>



TABLE I (Cont'd.)

X20560 INJECTORS

Configuration Number	Configuration Description	Design Purpose	Test Results
20560-525	<p>The -525 as did the -523 configuration, incorporated the "knobby" face and minimum free stream length design. The No. 1 fuel orifice of the injector insert was rotated 15° to line up with the fuel inlet. The angle of the No. 1 oxidizer hole was increased and its inlet location changed to provide it with a total pressure source. The fuel hole sizes were the same as for the -511 configuration. The No. 1 ox. hole diameter was .0352 inches and the other 11 were .0314 diameter.</p>	<p>The knobby face, designed for minimum free stream length prevented explosions due to propellant flow from one hole to another. Rotation of the injector insert, and increased angle of the No. 1 oxidizer hole were design changes to assure early propellant arrival at the No. 1 doublet, thus raising chamber pressure prior to flow from the remainder of the doublets and thereby lowering the ignition peak pressure.</p> <p>In addition, increased angle and total pressure source for the No. 1 oxidizer hole were designed to counteract the high momentum of the No. 1 fuel stream providing a more uniform spray pattern than the similar -511 configuration.</p>	<p>Ignition peak pressures measured on the -525 were comparable to those of the similar free stream to impingement length -511 configuration. The -525 injector insert face also was better than the -511 in that no deterioration of the injector hole exits was noted. The configuration was subjected to a limited heat transfer test series in Cell 1 and showed only slight evidences of high heat transfer burning at <math>O/F = 2.0</math>.</p>

TABLE I (Cont'd.)

## X20560 INJECTORS

Configuration Number	Configuration Description	Design Purpose	Test Results
20560-527	<p>The -527 injector configuration is identical to the -519 configuration with the exceptions that the injection hole diameters are smaller. <math>D_{fuel} = 0.021</math> and <math>D_{ox} = 0.024</math>, and the ox. cross passages are 0.043 instead of 0.031. These diameters create a momentum angle of <math>+3.8</math> at an <math>O/F=2.0</math> with an ox. hole angle of <math>23^\circ</math> and a fuel hole angle of <math>35^\circ</math>.</p> <p>Fuel dribble volume is 57% Oxid. dribble volume is 80%</p>	<p>The fuel and oxidizer holes were made smaller in the -527 injector to promote better propellant mixing for "softer" engine ignition by providing higher stream velocities, and to inhibit high heat transfer burning. That is propagated through boiling the oxidizer by keeping the propellants at a higher pressure level in the injector. The oxidizer and fuel hole diameters were changed to provide a <math>3.8^\circ</math> (outward) momentum angle to provide a reasonable chamber wall temperature since previous experience with high velocity injection indicated high wall temperatures. The injector insert was used in the normal orientation of provide uniform wall temperatures.</p>	<p>No ignition peak pressure tests were run on this configuration.</p> <p>Two heat transfer test series were attempted but in both cases the engine suffered combustion chamber bell breakage (flow turned chamber) which stopped the testing. In the limited amount of heat transfer data which was obtained, the engine indicated high heat transfer burning when fired at maximum soakback conditions and showed no tendency to step out of the condition. As with the other flat-faced injectors, such as -511, the injector hole exits exhibited erosion after approximately 627 seconds of burn time. Exit erosion appears to be worse on the smaller holes.</p>

TABLE I (Cont'd.)

X20560 INJECTORS

Configuration Number	Configuration Description	Design Purpose	Test Results
20560-529	<p>The -529 injector was made the same as the -511 configuration with the exceptions:</p> <p>(a) A concentric fuel annulus providing 64% fuel dribble volume was used.</p> <p>(b) An insulating air gap was left between the insert inner body and the insert main body. A small bleed hole was drilled connecting the air gap to the combustion chamber.</p> <p>(c) The fuel dribble volume is 64% and the ox. dribble volume is 67%.</p>	<p>The -529 configuration was made with a concentric fuel annulus because it provides more nearly equal flow out of the fuel holes. The "air gap" was provided between the bottom of the inner body, which contains the oxidizer cross passages, and the insert main body. To minimize the heat transfer to the oxidizer and prevent it from boiling in the cross passages, which appears to cause high heat transfer burning. The small bleed hole was provided at the combustion chamber to prevent any gas formed from oxidizer trapped in the air gap from being forced into the oxidizer streams. A flat face was incorporated to minimize peak ignition pressures.</p>	<p>Limited heat transfer tests were performed on the -529 configuration in Cell 6. Combustion chamber wall temperatures from cold head starts were over 3100°F on two 60 second run attempts. On succeeding runs, wall temperatures were approximately 2900-3000°F. The engine showed no improvement over the -511 configuration during the high heat transfer burning. The combustion chamber was blistered during the test series due to excessive wall temperatures. No ignition pressure tests were performed on this configuration.</p>

TABLE I (Cont'd.)

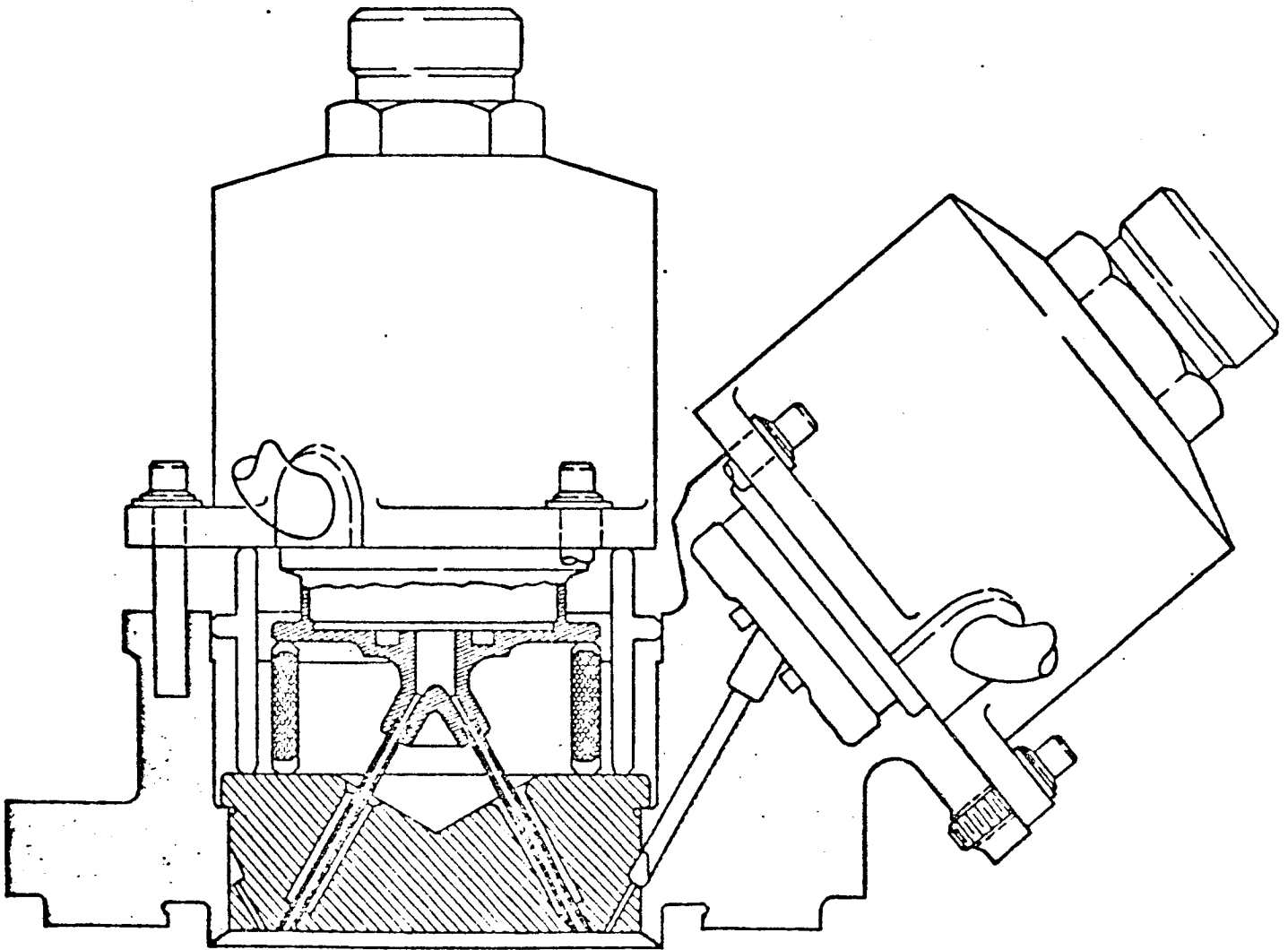
X20560 INJECTORS

Configuration Number	Configuration Description	Design Purpose	Test Results
20560-531	<p>The -531 engine was 0.5" longer than the other engines since it had straight, drilled ox. injection passages. The ox. passages were counterbored 0.044 diameter but the ox. and fuel injection hole diameters were the same as the -1 configuration. The ox. hole angle was increased from 23° to 31.5° which increased the momentum angle at an O/F - 2.0 from 0° to +5°.</p> <p>The fuel dribble volume is 58% and the ox. dribble volume is 80%.</p>	<p>Straight ox. passages were used in the -531 configuration because it was reasoned that the sharp turns in the oxidizer passages in the previous injectors were inducing cavitation in the oxidizer streams, causing bubbles to form which in turn caused two phase (gas plus liquid) flow from the injector, thereby propagating the instable combustion, manifested in the high heat transfer burning phase. The ox. stream angle was changed from 23° to 31.5° to provide a +5° (outward) momentum angle to help cool the chamber wall with propellant spray. The injector had the flat face for good ignition characteristics.</p>	<p>The -531 configuration showed no significant improvement in high heat transfer burning. Steady state wall temperatures were approximately 2800°F on the only long steady state run performed on the engine. Tests were stopped because the combustion chamber had started to melt during an 8 second run following a 60 second soakback run. No ignition pressure tests were conducted on this configuration.</p>

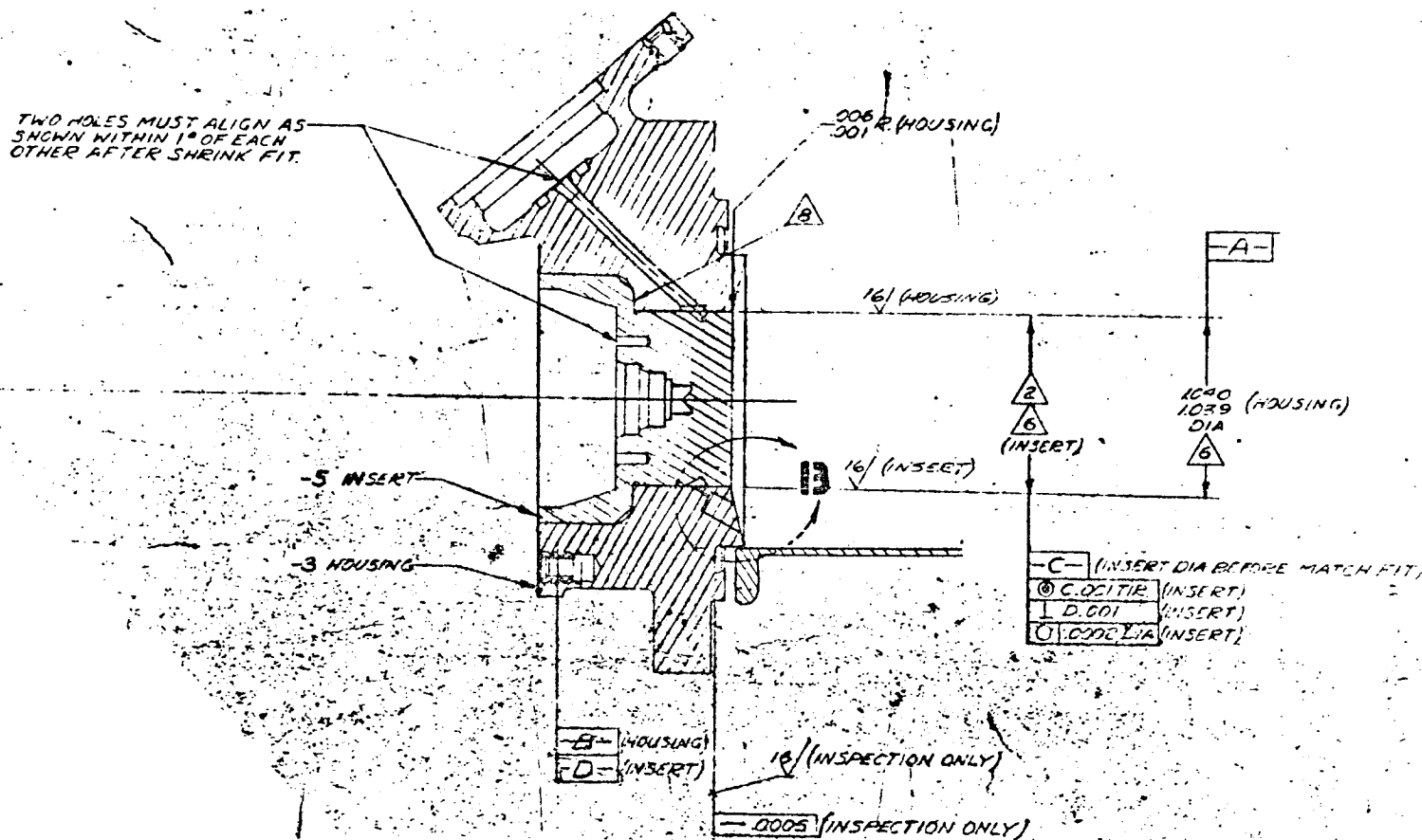
TABLE I (Cont'd.)

## X20560 INJECTORS

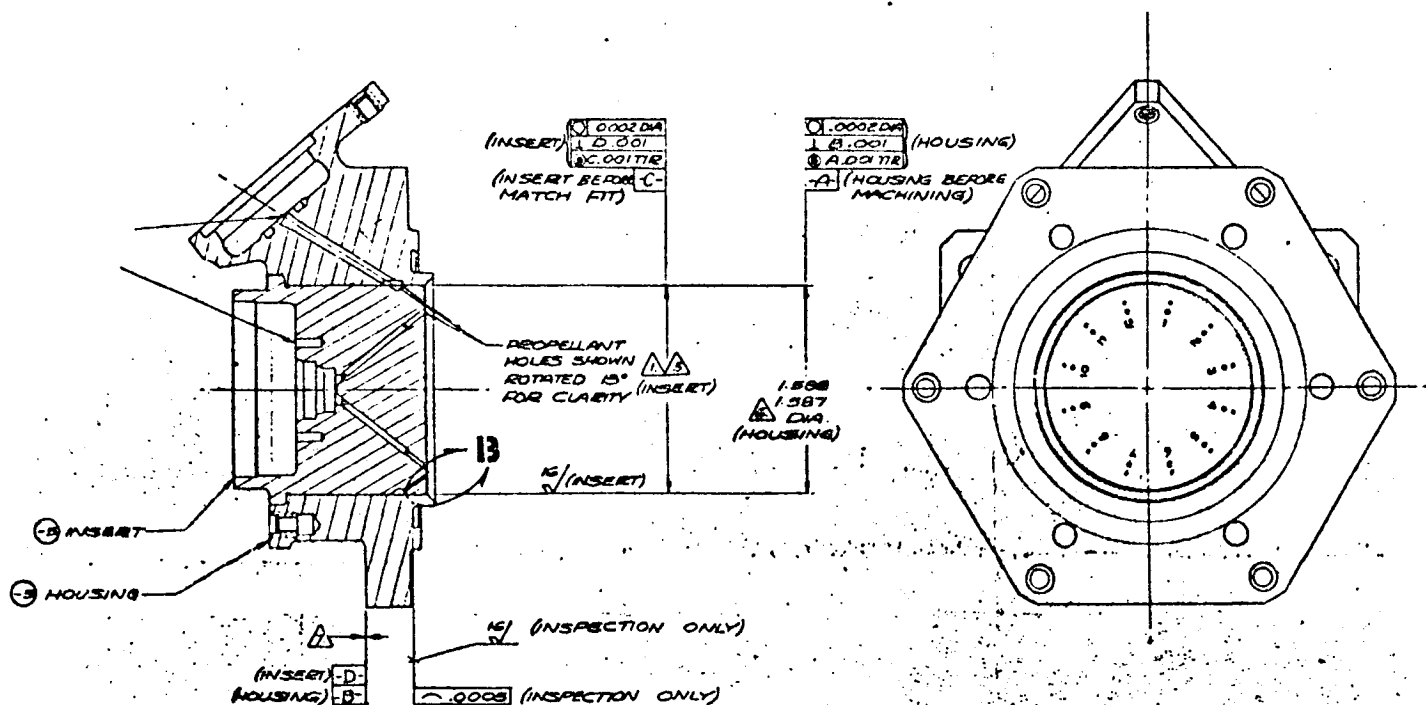
Configuration Number	Configuration Description	Design Purpose	Test Results
20560-533	<p>The -533 configuration is the same as the -531 configuration with the exceptions:</p> <p>(a) Steel insulating tubes with the same I.D. as the previous drilled injector holes were driven into the oxidizer passages.</p> <p>(b) The steel tubes eliminated the oxidizer hole counterbores.</p> <p>(c) The oxidizer dribble volume is 78%.</p>	<p>The -533 configuration oxidizer passages (straight) were insulated by driving steel tubes into the passages which were supported at both ends, because the X20560-531 which was of the same design in all other respects, went into the high heat transfer burning phase due to overheating and boiling the oxidizer in the injector passages. It was anticipated that this configuration would prevent the high heat transfer burning phase and make unnecessary the impending next step of building an injector with individual independent oxidizer injection tubes. The flat face was incorporated in the -533 configuration to provide good ignition characteristics.</p>	<p>The -533 configuration high heat transfer performance was not significantly better than the -531 or -511 configurations. The steady state chamber wall temperatures were somewhat lower, however. During a steady state run of 37 minutes to evaluate chamber life, chamber wall temperatures were approximately 2800°F and chamber flange temperatures stabilized at 1800-1850°F while the engine maintained a mean Isp of 300 seconds. The test was concluded when the facility propellant supply was exhausted.</p> <p>No ignition pressure level tests were performed with this engine.</p>



T9290 INJECTOR STEEL OXIDIZER TUBES



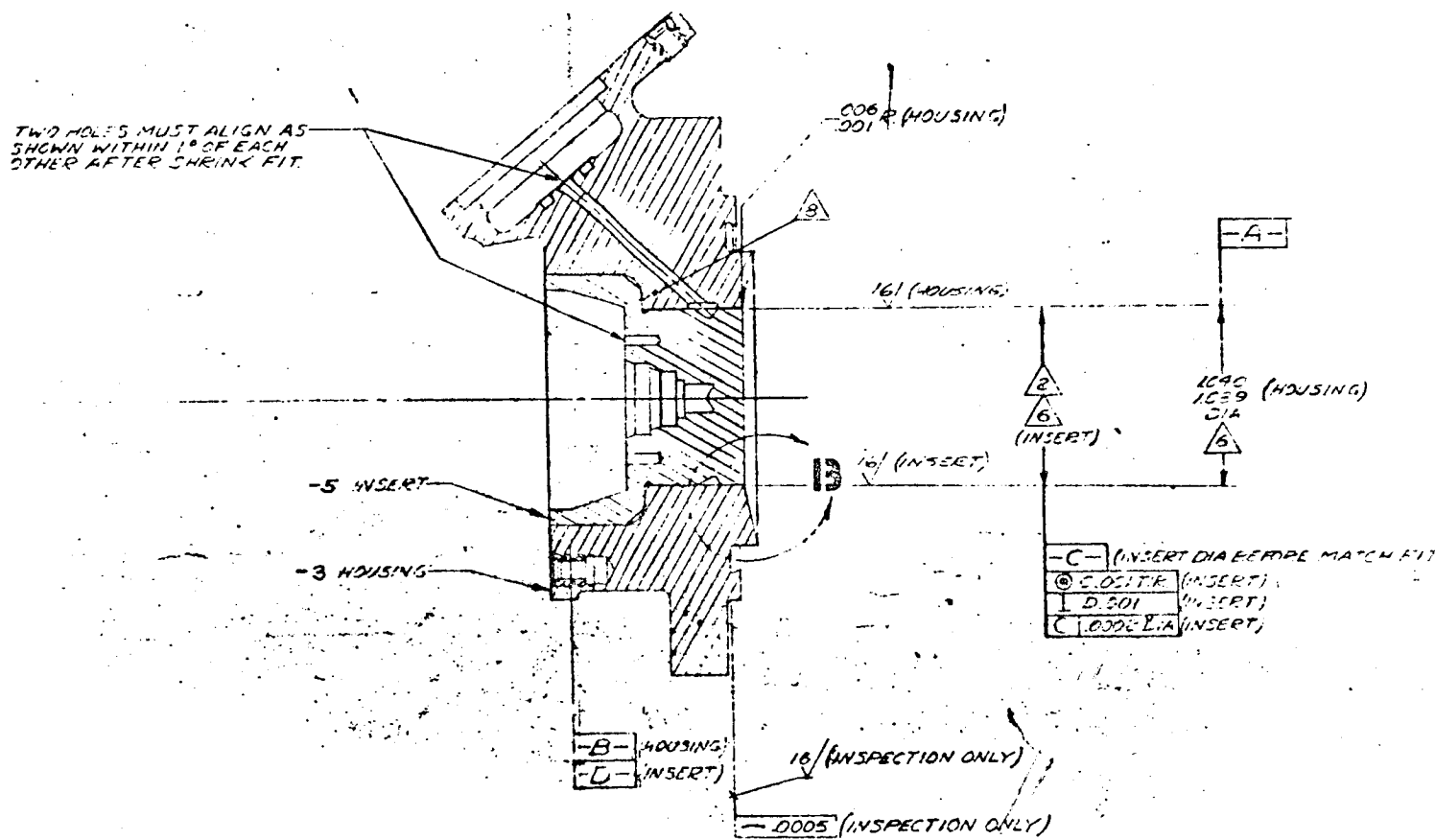
O/F 1.6 8x8 INJECTOR T9669



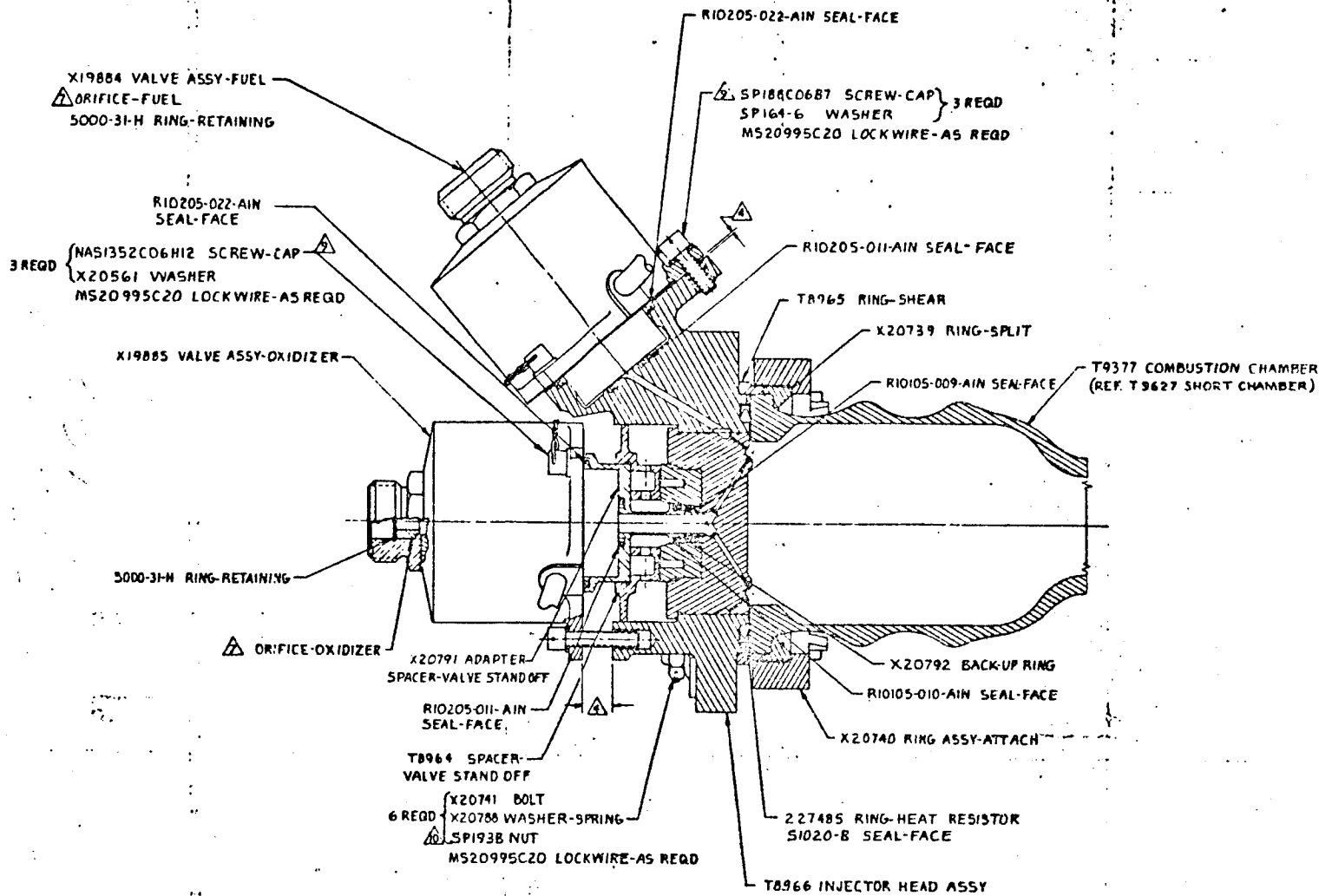
O/F 1.6 12x12 INJECTOR

T9659





O/F 1.3 8x8 INJECTOR T9689



SPLASH PLATE INJECTOR T9665

Twelve fuel film cooling holes were also added to 20560-511 injector ( $12 \times 12$ ). The specific impulse was 285 seconds at an O/F of 2.0.

Because the  $8 \times 8$  specific impulse was better than the  $12 \times 12$ , development during this phase consisted of improving the  $8 \times 8$  fuel cooled performance. Ignition tests were also made to understand or select a configuration that significantly reduced the ignition overpressures.

Figure 18 is a drawing of the first  $8 \times 8$  fuel cooled injector. This injector was a modified T9662, which was an injector designed for an O/F of 1.6. Because the performance of this injector with 11% of the fuel used as coolant was 295 seconds, the doublet sizes were kept the same on all other injectors and the film cooling parameters varied to optimize the thermal characteristics of the engine.

The percentage of fuel used as a coolant, the angle that the fuel impinged on the chamber, and the impingement point were varied in the engines identified as T10010, T10020, T10030, T10040, T10050, T10060, and T10100. Figures 18-21 and Table II show the significant features of these injectors.

Engine T10050 is noteworthy because it was the first injector that had a one piece integral stainless steel oxidizer standoff and an aluminum sleeve. This injector concept successfully isolated the oxidizer valve from the soakback temperatures. Also, the surfaces of the oxidizer holes in the stainless steel cooled much quicker than in the aluminum used previously giving added insurance against two phase flow and high heat transfer burning. All injectors now have a one piece stainless steel oxidizer and fuel standoff.

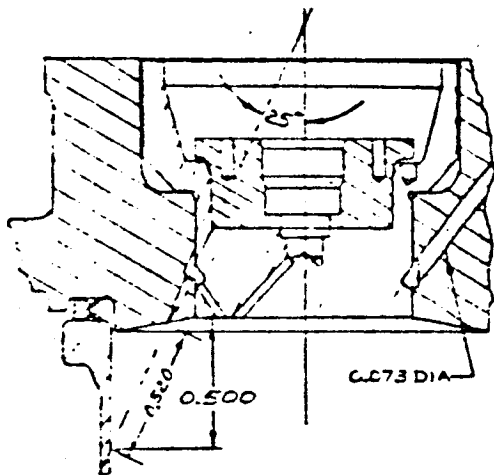
Engine T10060 incorporated all the best characteristics of the fuel cooled engines up to this time, including the stainless steel standoff and a "V" groove between the doublets on the injector face to prevent hole exit erosion from doublet splashback. This engine had an Isp of 295 seconds and a maximum throat temperature of  $2800^{\circ}$  and a flange temperature of  $300^{\circ}\text{F}$ .

Two other fuel cooled injector concepts were tested during this time. One was an  $8 \times 8$  doublet injector with equal fuel and oxidizer orifice sizes. The other was a triplet injector. Both concepts were built to test the effect of not having oxidizer hit the chamber wall on ignition overpressures. Figures 22 and 23 are drawings of the equal hole size injectors. The specific impulse of T10467 was 282 seconds at an O/F of 2.0. Engine T10469 was ignition tested. A chamber failure occurred with the manifold set pressures set for an equivalent O/F of 6.0.

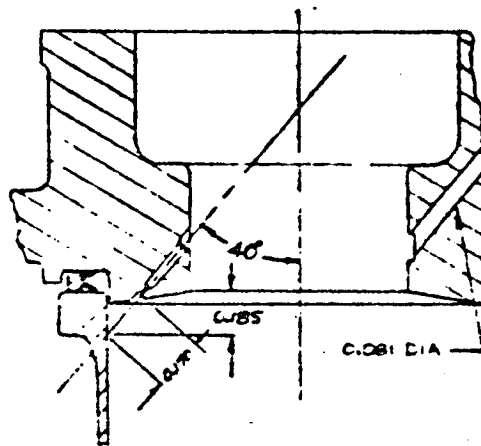
The triplet injector, T9930, is shown in Figure 24. The specific impulse was 270 seconds at an O/F of 2.0. Because the performance was low this engine was not ignition tested.

ORIGINAL FUEL COOLED  
INJECTOR

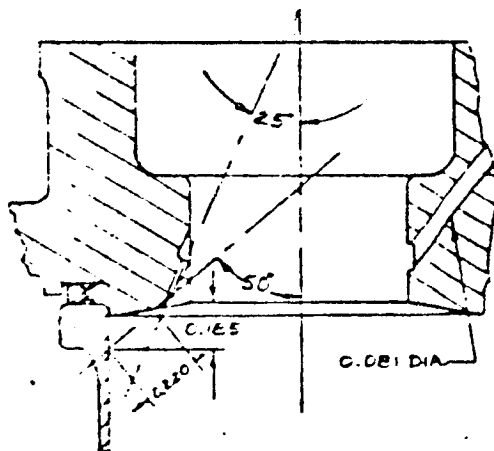
T-9730



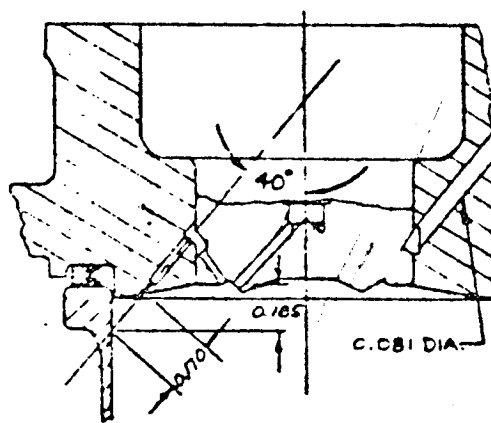
T-10020



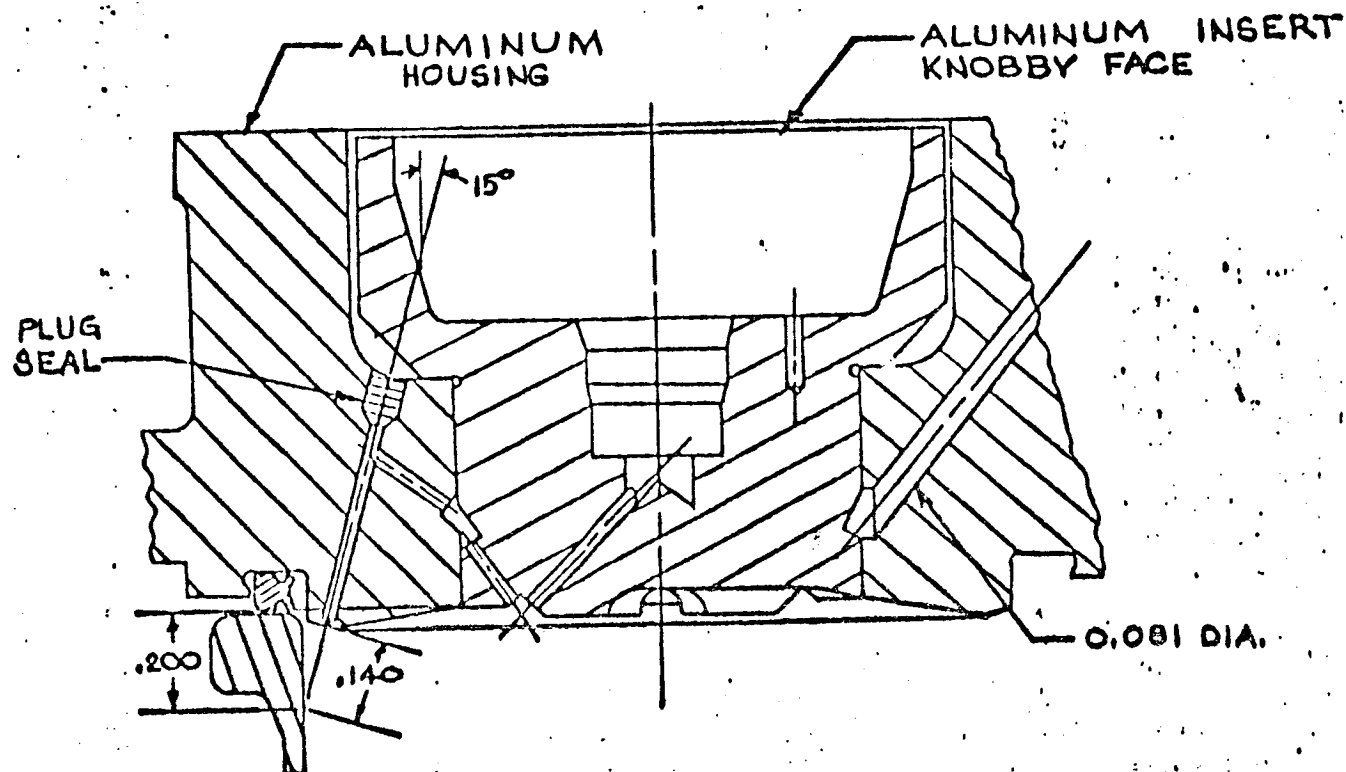
T-10010



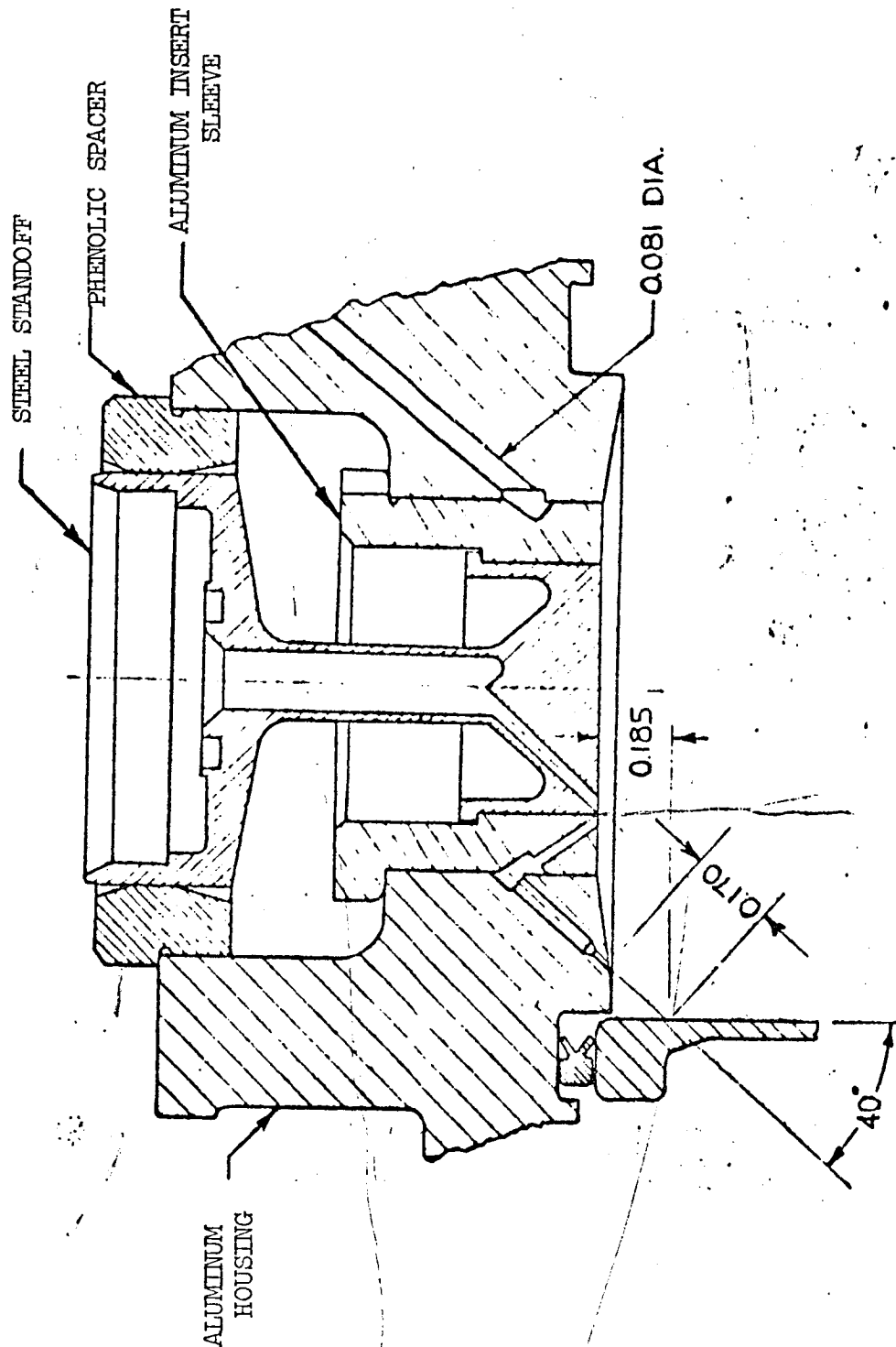
T-10030



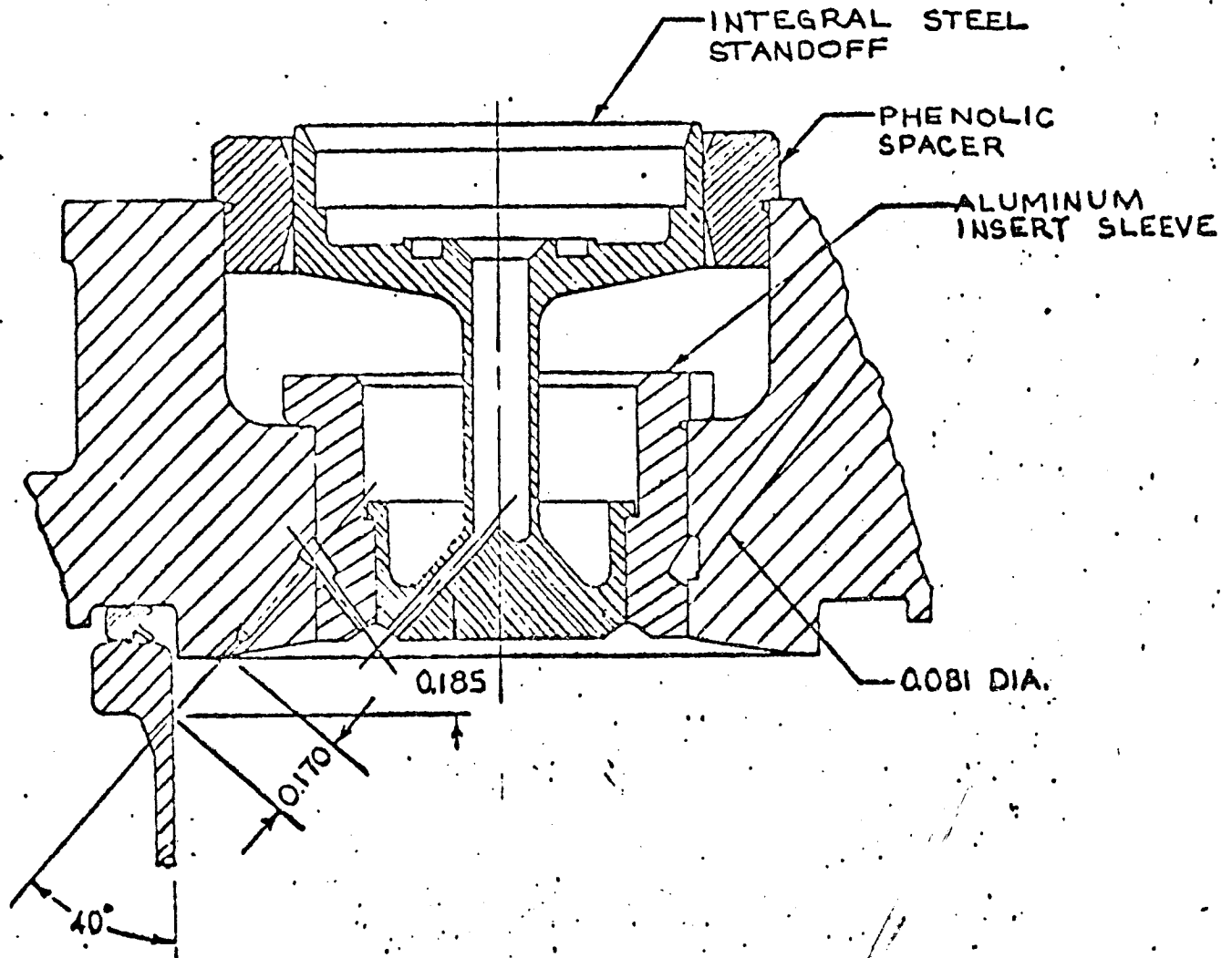
FIRST FUEL COOLED INJECTORS



T10040  
FOR % FILM COOLING VARIATION TESTS



ONE PIECE OXIDIZER STANDOFF T10050



T-10060 INJECTOR

TABLE II  
ENGINE DRIBBLE VOLUMES & FUEL BLEED PERCENTS  
Non-Preigniter

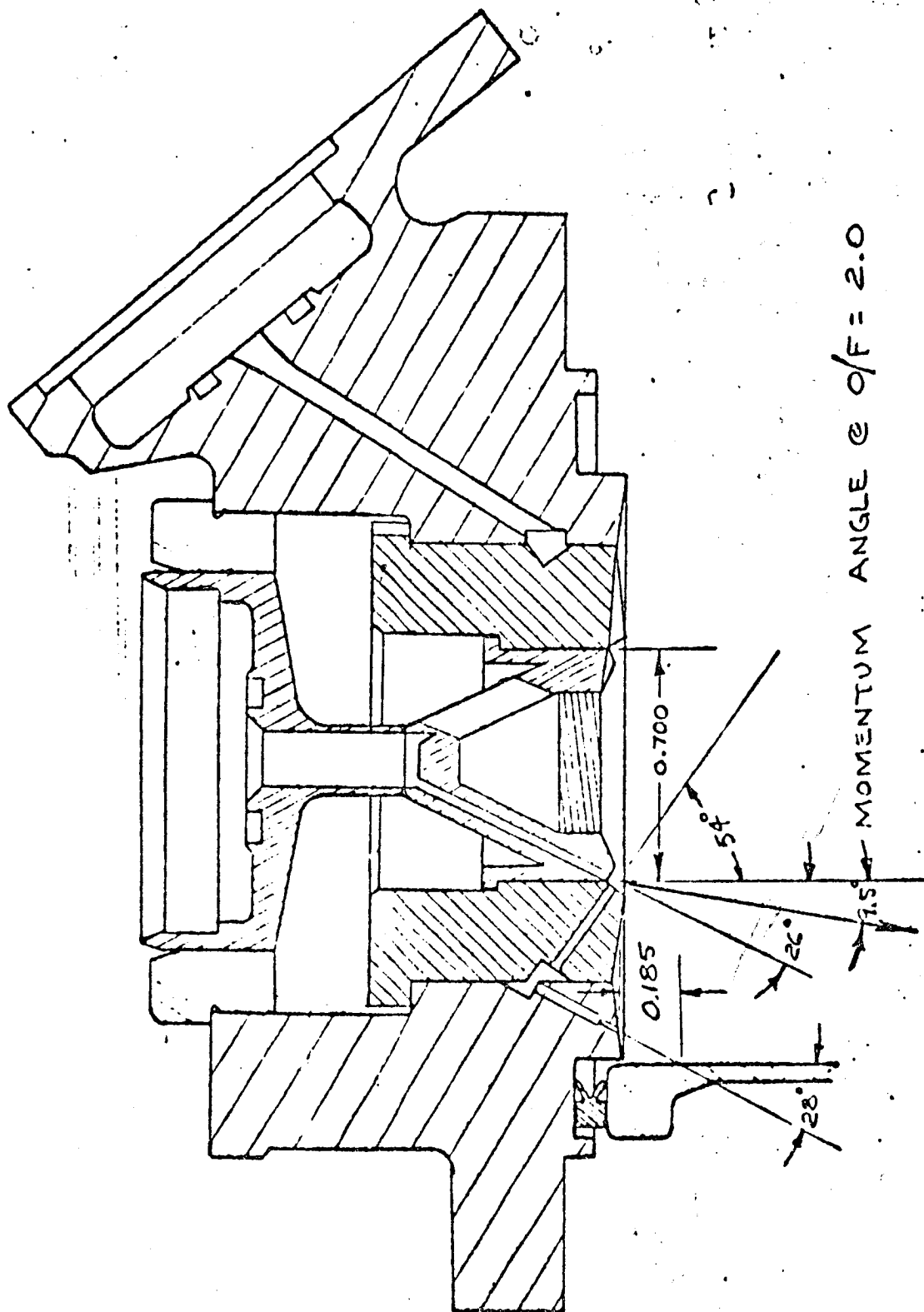
ENGINE PART NO.	ENGINE SERIAL NO.	DRIBBLE VOLUME FUEL-%	OXIDIZER-%	BLEED HOLE DIA.-IN.	ACTUAL FUEL BLEED-%	REMARKS
T-10050	0001-1	70	68.4	.0118	12.02	INTEGRAL STEEL STANDOFF (.171" ID); 40° BLEED HOLE ANGLE; FLAT FACE @ 0.0/F = 2.0 IS 22.0°
T-10050	0001-2	70	68.4	.0118	12.98	NO REASON FOUND FOR FUEL BLEED DIFFERENCE; SAME AS ABOVE @ 0.0/F = 2.0 IS 22.4°
T-10050	0002	70	68.4	.0118	12.9	
T-10050	0003	70	68.4	.0118	12.03	S.S. ALT. CHAMBER; @ 0.0/F = 2.0 IS 22.0°
T-10050	0004	70	68.4	.0118	12.4	L-605 CHAMBER; @ 0.0/F = 2.0 IS 22.2°
T-10060	0001-1	70	68.4	.0118	13	GROOVED INJECTOR FACE FROM T-10050 S/N 0001-1; L-605 CHAMBER @ 0.0/F = 2.0 IS 22.4°
T-10060	0002-1	70	68.4	.0118	10.35	321 S.S. SHORT CHAMBER; GROOVED INJECTOR FACE; @ 0.0/F = 2.0 IS 21.4°; NO REASON FOUND FOR FUEL BLEED DIFFERENCE
T-10060	0003-1	70	68.4	.0118	12.92	90° TA/10° W CHAMBER; @ 0.0/F = 2.0 IS 22.4°; MOLY DISCILLICIDE COATING
T-10040	0001-1	85	68	.0078	5.91	KNOBLY FACE INSERT; 15° FUEL BLEED ANGLE; @ 0.0/F = 2.0 IS 19.7°
T-10040	0001-2	85	68	.010	11.6	SAME AS T-10040 S/N 0001-1; @ 0.0/F = 2.0 IS 21.9°
T-10040	0001-3	85	68	.0126	14.45	SAME AS T-10040 S/N 0001-1; @ 0.0/F = 2.0
T-10060	0001-2	70	68.4	.0118	13	SAME AS T-10060 S/N 0001-1 BUT WITH CONICAL L-605 CHAMBER
T-10060	0001-3	70	68.4	.0118	13	SAME AS T-10060 S/N 0001-1 BUT WITH CHAMBER $f^* = 5.95$ IN.
T-10060	0004-1	70	68.4	.0118	12.45	90/10 CHAMBER WITH TIN ALUMINIDE COATING; @ 0.0/F = 2.0
T-10060	0001	70	68.4	.0105	10.6	@ 0.0/F = 1.6; @ 0.0/F = 2.0; HOUSING PASSAGE DIA. = 0.081"; SAME AS T-10060 S/N 0001-1
T-10060	0004-2	70	68.4	.0118	12.45	90/10 CHAMBER WITH DISCILLICIDE COATING; @ 0.0/F = 2.0
T-10060	0004-3	70	68.4	.0118	13.2	90/10 CHAMBER WITH TIN ALUMINIDE COATING; @ 0.0/F = 2.0
T-10060	0004-4	70	68.4	.0118	13.2	L-605 CHAMBER WITH BLACK OXIDE COATING; @ 0.0/F = 2.0
T-10060	0004-5	70	68.4	.0118	13.2	SEA LEVEL 90/10 CHAMBER WITH DISCILLICIDE COATING



TABLE II (Cont'd.)  
ENGINE DRIBBLE VOLUMES & FUEL BLEED PERCENTS  
Non-Preigniter

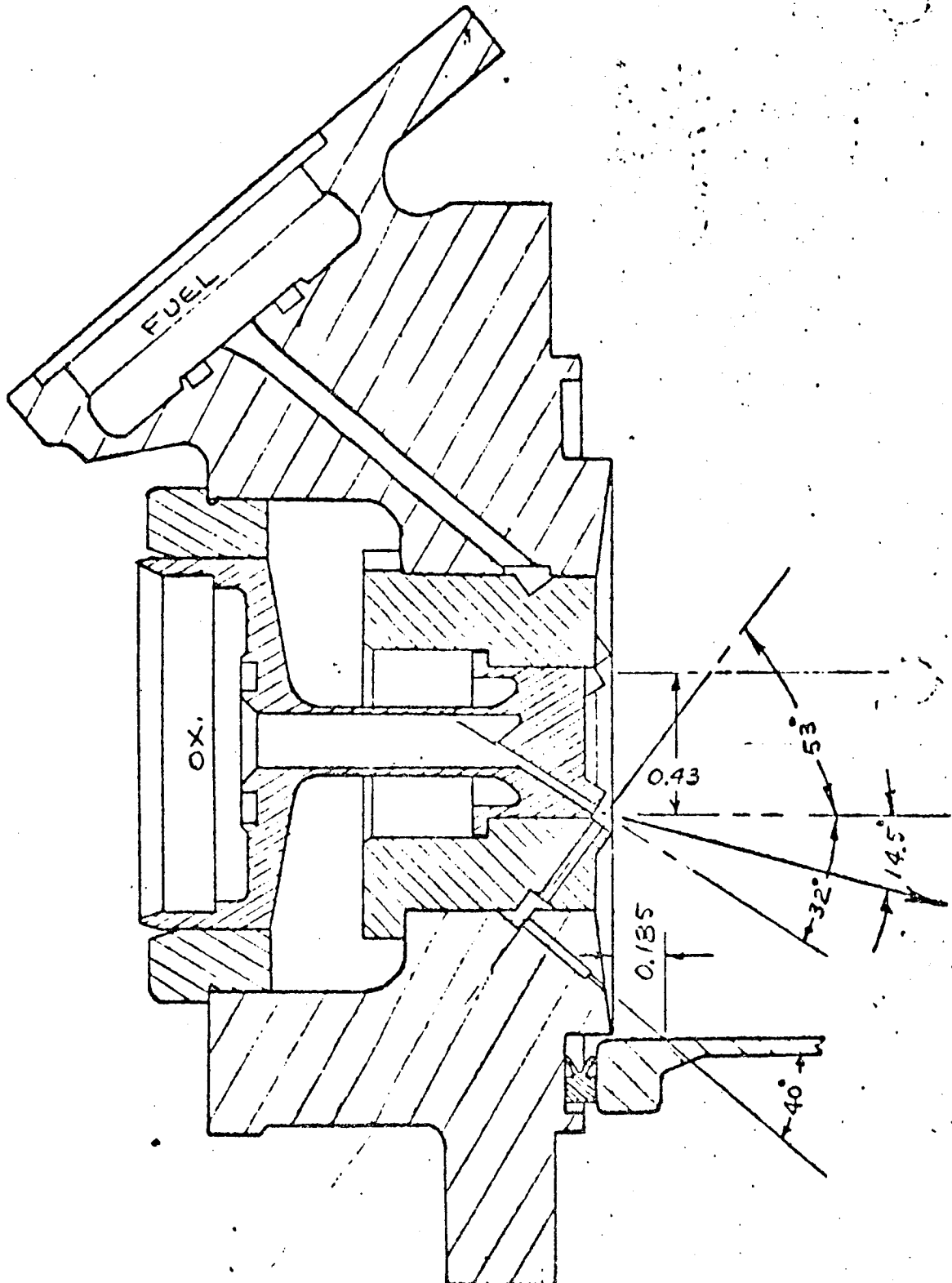
ENGINE PART NO.	ENGINE SERIAL NO.	DRIBBLE FUEL-%	VOLUME OXIDIZER-%	BLEED HOLE DIA.-IN.	ACTUAL FUEL BLEED-%	REMARKS
T10467	0001-1	*	*	.0118	11.6	D <sub>1</sub> D <sub>2</sub> 0.029, 430 IMP. DIA., 85° INCLUDED $\angle$ , $\theta = 14.5^\circ$ @ O/F=2.0, KNOBBY FACE
T10479	0001-1	*	*	.0118	11.6	D <sub>1</sub> D <sub>2</sub> 0.029, $\theta = 80^\circ$ , $\theta = 9.5^\circ$ @ O/F=2.0, RAISED DOUBLET, 40° BLEED HOLE $\angle$
T10477	0001-1	*	*	.0118	*	D <sub>1</sub> D <sub>2</sub> 0.029, $\theta = 85^\circ$ , OX BLEED HOLE DIA. = 0.0124, OX BLEED = 18.9%, 40° FUEL BLEED HOLE $\angle$ , 65° OX BLEED HOLE $\angle$ , $\theta = 8.3^\circ$ @ O/F=2.0
T10060	0007-2	70	68.4	.0118	10.4	RIBBED MOLY CHAMBER L* = 11.2; GROOVED INJECTOR; $\theta = 21.4^\circ$ @ O/F=2.0
T10060	0002-3	70	68.4	.0118	10.4	321 S.S. CHAMBER L* = 11.2; GROOVED INJECTOR FACE; $\theta = 21.4^\circ$ @ O/F=2.0
T10060	0002-4	70	68.4	.0118	10.4	L-605 CHAMBER L* = 5.95; GROOVED INJECTOR FACE; $\theta = 21.4^\circ$ @ O/F=2.0
T10060	0002-5	70	68.4	.0118	10.4	L-605 CHAMBER L* = 8.6; CAVITATING VENTURIS IN VALVES; $\theta = 21.4^\circ$ @ O/F=2.0
T10060	0002-6	70	68.4	.0118	10.4	RIBBED MOLY CHAMBER L* = 11.2; CAVITATING VENTURIS IN VALVES
T10060	0002-7	70	68.4	.0118	10.4	TM, L-605 2 PIECE CHAMBER LIFE TESTED; $\theta = 21.4^\circ$ @ O/F=2.0
T10060	0002-8	70	68.4	.0118	10.4	RIBBED MOLY CHAMBER; SERIES M-VALVES; $\theta = 21.4^\circ$ @ O/F=2.0
T10060	0003-2	70	68.4	.0118	11.2	CONICAL L-605 CHAMBER; GROOVED INJECTOR FACE; $\theta = 22.4^\circ$ @ O/F=2.0
T10060	0003-3	70	68.4	.0118	11.2	RIBBED MOLY CHAMBER; GROOVED INJECTOR FACE; $\theta = 22.4^\circ$ @ O/F=2.0
T10060	0003-4	70	68.4	.0118	11.2	TM, L-605 2 PIECE CHAMBER; GROOVED INJECTOR FACE; $\theta = 22.4^\circ$ @ O/F=2.0 <i>(L-605 3 PC. BLEEDING TIME (4.8 sec) <math>\theta = 8.6</math>)</i>
T10060	0003-5	70	68.4	.0118	11.2	LIFE TEST ON 2 PIECE MOLY, L-605 CHAMBER; $\theta = 22.4^\circ$ @ O/F=2.0
T10060	0005-1	75	54	.0118	10.9	TM, L-605 2 PIECE CHAMBER FAILURE, L* = 8.6; $\theta = 22.4^\circ$ @ O/F=2.0
T10060	0005-2	75	54	.0118	10.9	321 S.S. CHAMBER L* = 11.2; $\theta = 22.4^\circ$ @ O/F=2.0
T10060	0005-3	75	54	.0118	10.9	321 S.S. CHAMBER L* = 8.2; $\theta = 22.4^\circ$ @ O/F=2.0
T10060	0001-4	85	68	.0124	14.45	ALT. MOLY CHAMBER; KNOBBY FACE INJECTOR; $\theta = 23.0^\circ$ @ O/F=2.0
T9930	0001-1	N.A.	N.A.	.0118	10.4	TRIPLET INJECTOR; $\theta = 0^\circ$ @ ALL O/F RATIOS; $\theta = 0.024$ , $\theta = 0.034$ ; IMPINGEMENT DIA. = 1.000; 2.7° FUEL BLEED ANGLE; 8 BLEED HOLES BETWEEN TRIPLETS; RIBBED MOLY CHAMBER
T10060	0005-4	75	54	.0118	10.9	

T-10479 ENGINE



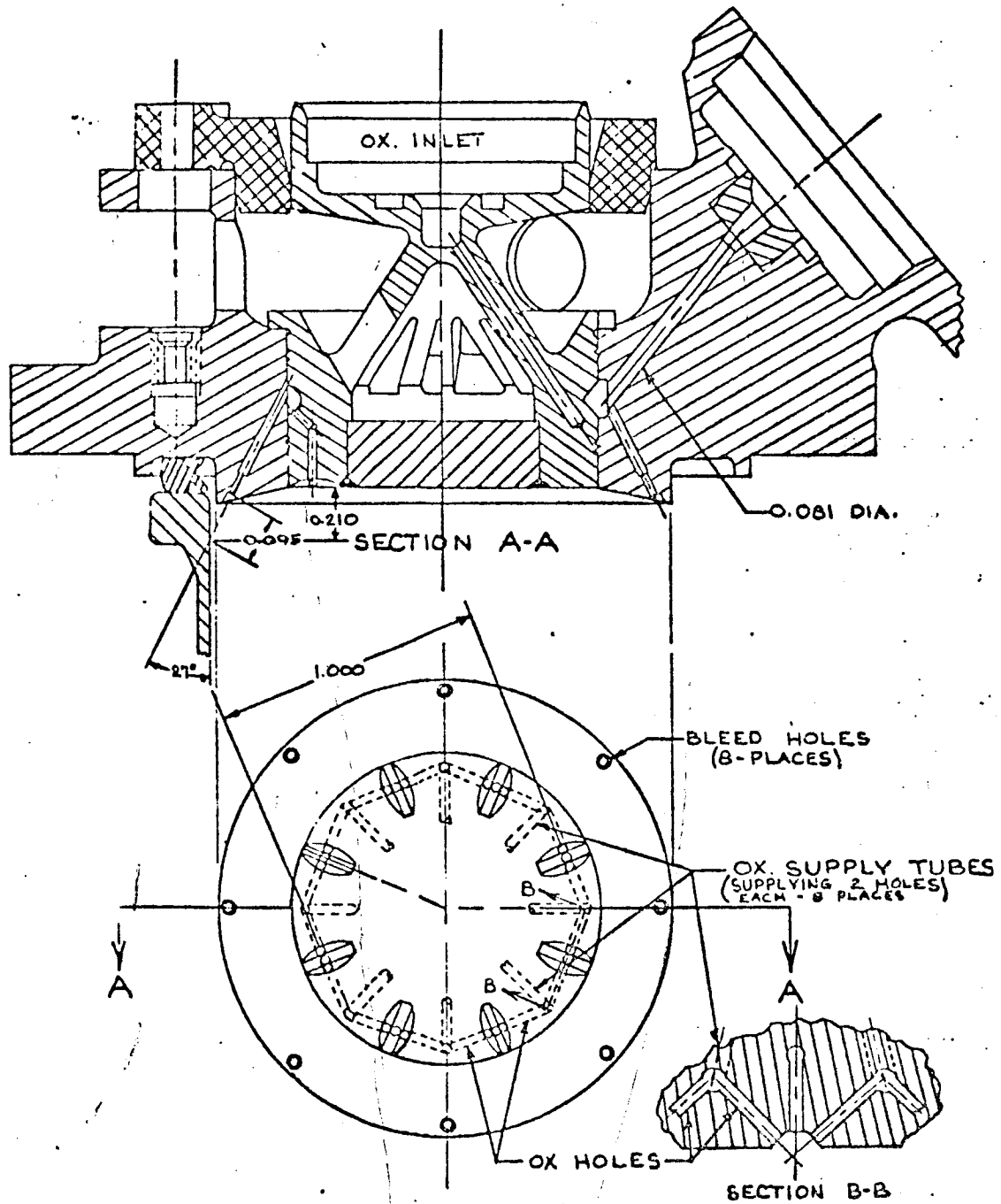
EQUAL HOLE DIAMETER 8-ON-8

T-10467 ENGINE



EQUAL HOLE DIAMETER 8X8 WITH FUEL COOLING

Figure 23



CONSTANT MOMENTUM ANGLE INJECTOR ASS'Y

T9930

#### Phase IV - Preigniter Development

In May, 1964, Marquardt proceeded with the development of a preigniter engine that would completely eliminate ignition overpressures. Prior to this Marquardt had done some preliminary preigniter tests.

Engine T9640 was a modified X20560-511 injector that included a preignition cup over the number one doublet (Figure 25). The engine was damaged by a facility error before any preignitor tests could be made. The engine was later tested but it did not completely eliminate ignition spikes.

The next engine was built to investigate whether a preignitor would successfully eliminate ignition overpressures. It was a four valve injector (Figure 26) that had two valves that controlled the propellant to the main doublet, which were the same configuration as the fuel bleed injectors, and two other valves that controlled the propellant to a center doublet around which different preigniter cups could be held. This engine successfully demonstrated that the preigniter cup could eliminate ignition overpressures. The results of this test were used to help design the first preigniter engine.

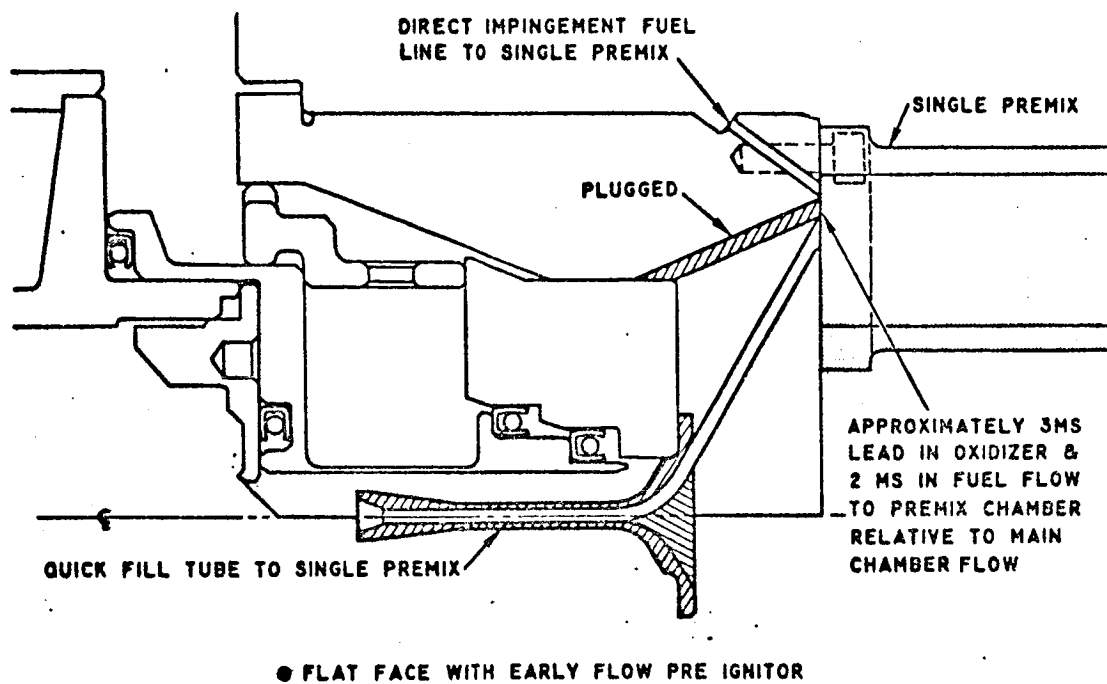
A special heat transfer injector was also built to determine whether the preigniter would be able to withstand the thermal environment during steady state operation. Figure 27 is a drawing of this injector. These tests showed that the preigniter would withstand the thermal environment.

The four (4) valve injector test and the heat transfer injector test showed that a preigniter engine would eliminate ignition overpressures and withstand the thermal environment. The results of these two tests plus a hydraulic analysis, discussed below, were used to design the first preigniter engine.

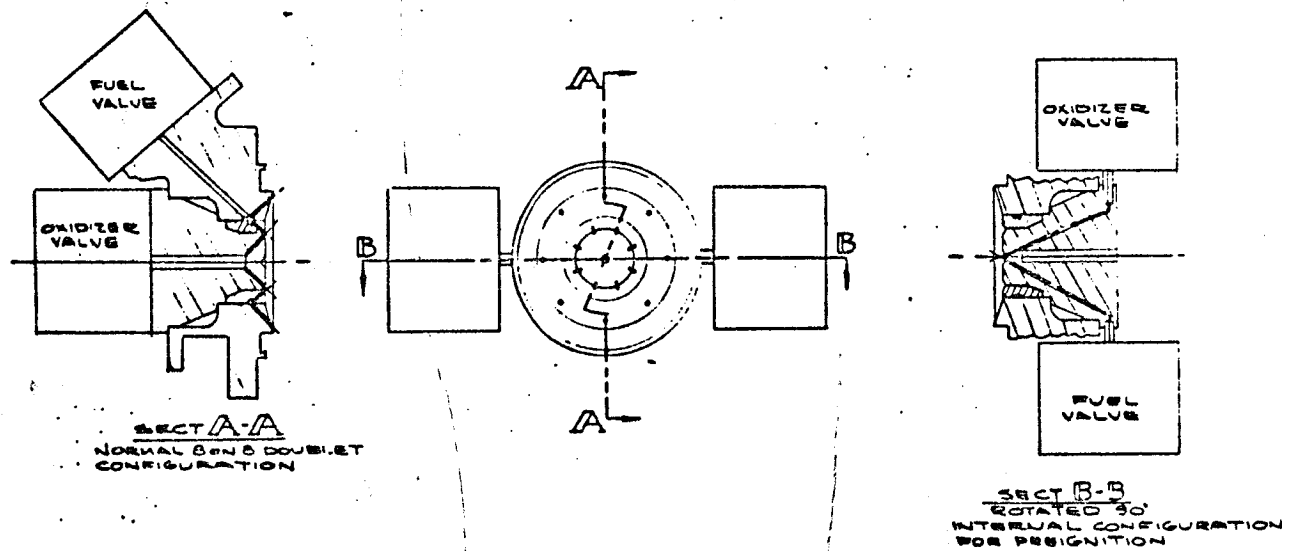
The preigniter injector hydraulics are a little more complicated than the non-preigniter injector. A schematic of the injector is shown in Figure 28. The restrictor between the valve and the dribble volume (Kwf & Kwo) is there to control the flow to the preigniter and dribble volume and to keep the preigniter from chugging while the dribble volume is filling. If that restrictor was not there, the propellant flow would decrease to the preigniter after it had lit and might even increase into the dribble volume. The preigniter pressure would drop and go out at which time the flow would again go to the preigniter and it would light again.

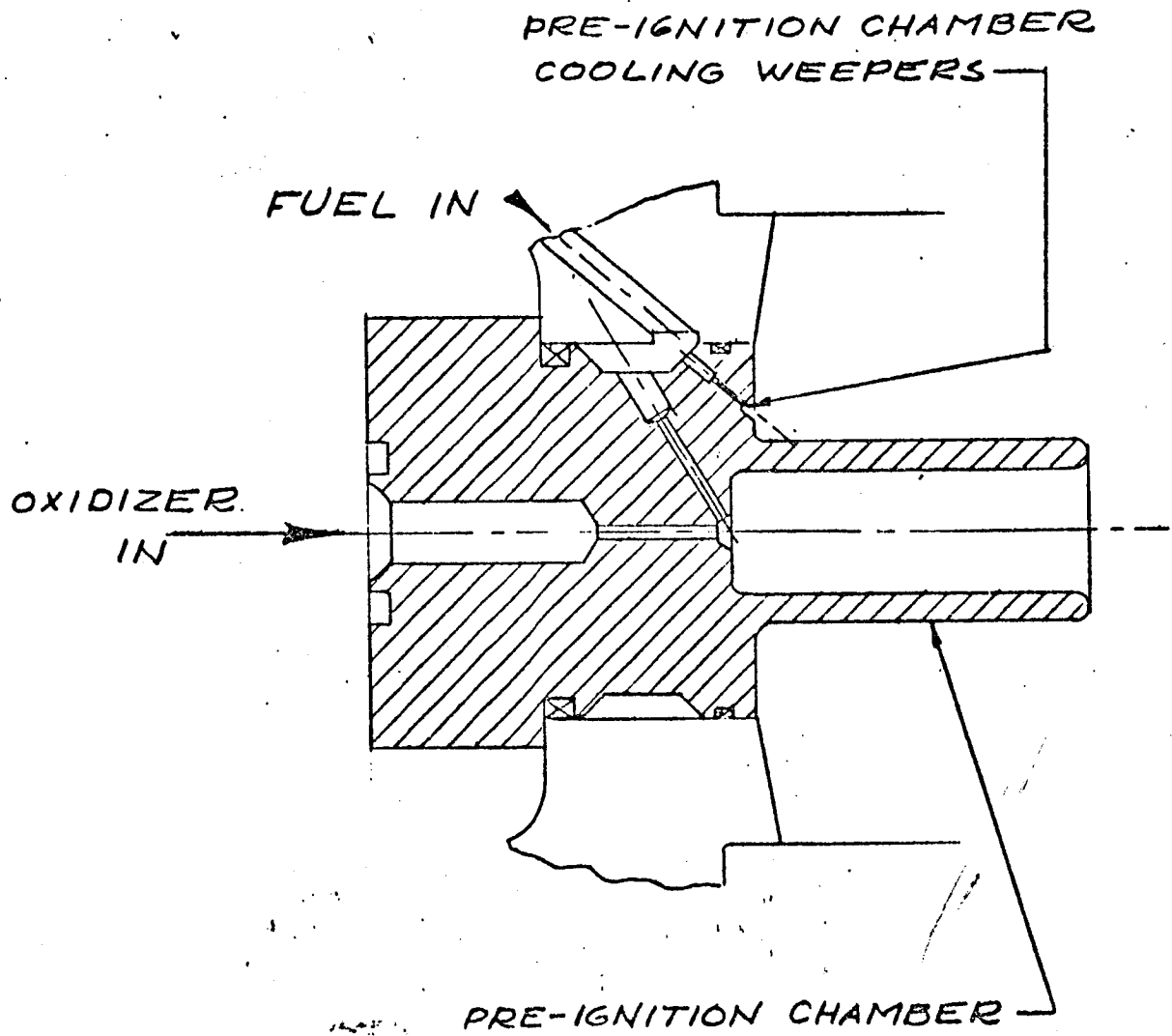
The first preigniter engine was successfully ignition tested on June 29th, 1964. The injector used a throatless preigniter cut off at 45° angle because this seemed to give the best results during the four valve test. The preigniter was cooled by eight fuel cooling holes, providing it with the same amount of cooling as was provided the main thrust chamber (11%). The flow rates to the various main elements of this engine along with the pressures at significant points are

EXPERIMENTAL PREIGNITER ON 20560-511 INJECTOR



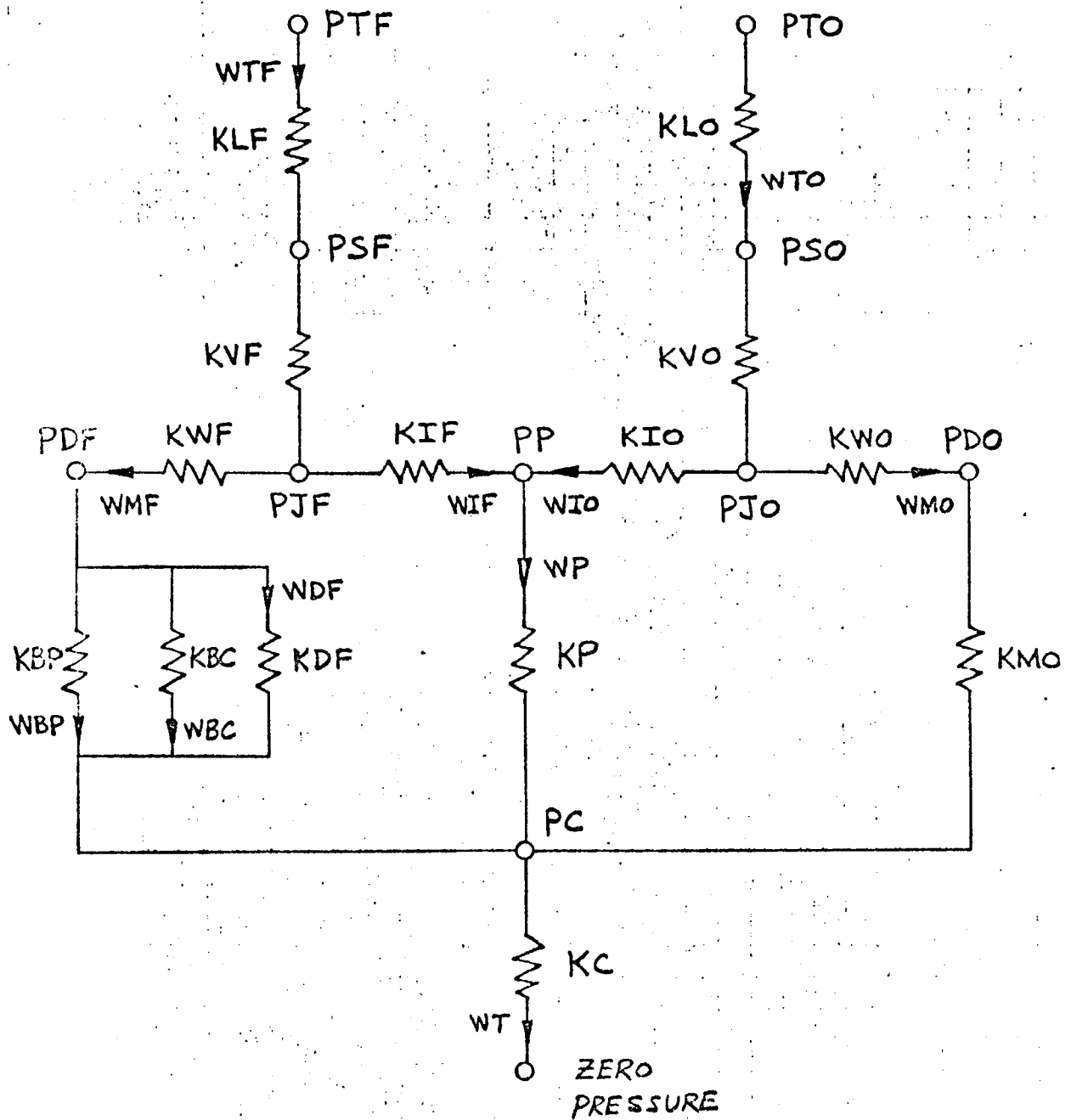
FOUR VALVE PRE-IGNITER TEST RIG





PREIGNITER HEAT TRANSFER INJECTOR





PREIGNITER INJECTOR SCHEMATIC

shown in Table III. This table was the result of a calculation which takes into account the interaction between the preigniter and the injector manifold. Figure 29 is a drawing of this injector.

The early preigniter injector tests were divided into two groups, ignition tests and performance tests.

For the ignition tests, the preigniter mixture ratio and total flow rates were varied to optimize preigniter ignition, chugging characteristics, and the ability to eliminate ignition overpressures when the main doublets lit. The propellant flow rates to the preigniter were controlled by varying the preigniter tube window area and the preigniter tube diameter. Figure 30 shows the range of O/F's and total preigniter flows tested for Case 1, preigniter ignition, and Case 3, preigniter burning. The ignition, chugging and spiking characteristics are shown in Table IV.

For the performance test the main doublet diameters, the main chamber coolant hole diameters, and the main chamber coolant angles were varied to achieve a good compromise between performance and thermal characteristics. The three critical engine temperatures were the chamber flange, the chamber throat and the chamber bell nut temperature. It was necessary to reach a compromise between these temperatures and steady state specific impulse. Several engines had specific impulses greater than 290 seconds but the engine temperatures were too hot.

The original preigniter engine had a throatless preigniter cutoff at 45° angle. This angle was removed on engine T10650, S/N 002, and the preigniter end was made square after the slashed cup eroded on another engine sometime during two steady state runs of 85 and 80 seconds duration. The squared end preigniter was as effective in eliminating ignition overpressures as the slashed preigniter.

The original preigniter engines also had replaceable oxidizer preigniter tubes where the oxidizer flow to the preigniter and doublets could be varied by changing the windows on the side of the tube and the preigniter doublet size. To control both the oxidizer and fuel flow split to the preigniter an engine was designed that had a replaceable fuel preigniter tube as well as a replaceable oxidizer tube. This engine is shown in Figure 31.

The steady state specific impulse of the first preigniter engine was 292 seconds at an O/F of 2.0 but the injector head soakback temperature was too high (450°F). Consequently, engine modifications were made to lower the engine operating temperatures, keep good performance and have good ignition characteristics. Table V lists the flow splits and injector parameters of the engines built during this time. The best engine was chosen as the PFRT configuration. This engine was almost identical to the replaceable fuel tube injector shown in Figure 31.

TABLE III

FIRST PREIGNITER HYDRAULICS

Case	Preigniter Flow			Main Flow		Total Flow $W_T$	Pressures		
	$W_{p_f}$	$W_{p_o}$	$W_p$	$W_{m_f}$	$W_{m_o}$		$P_p$	$P_c$	$(\Delta P/P)_p$
I	19.8	32.1	28.0	147.5	139.6	170	0	0	-
II	23.9	38.5	33.6	126.1	118.4	155	0	0	-
III	8.8	14.1	12.5	154.2	152.5	166	48	10.0	.21
IV	14.5	23.2	20.3	137.0	134.1	155	80	16.3	.33
V	13.2	19.8	17.6	86.8	80.2	100	109	95	.17

Case Configurations:

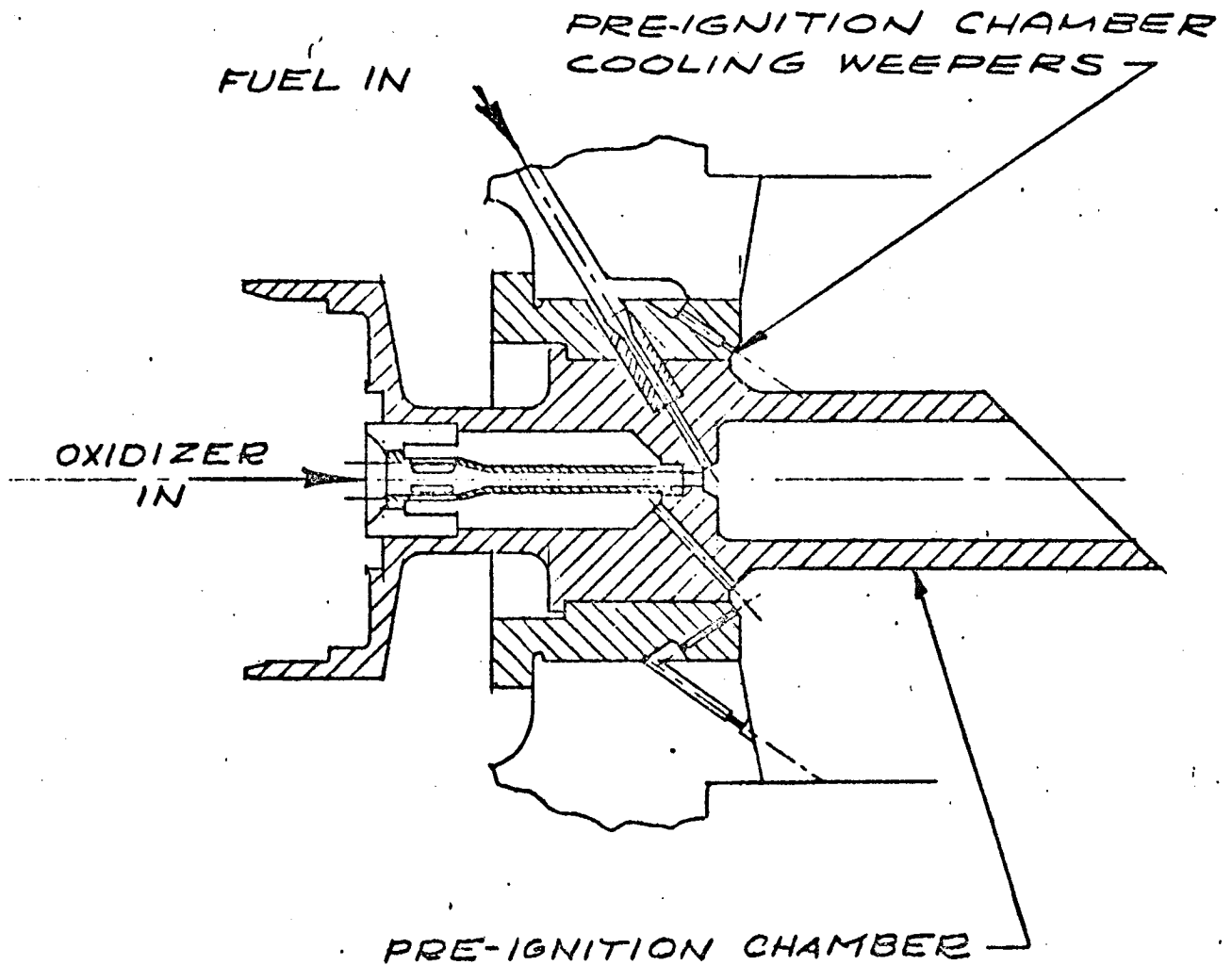
- I Preigniter Cold, Manifolds Empty
- II Preigniter Cold, Manifolds Full
- III Preigniter Hot, Manifolds Empty
- IV Preigniter Hot, Manifolds Full
- V Preigniter Hot, Engine Lit

Flows are expressed as a percentage of steady-state values, which are:

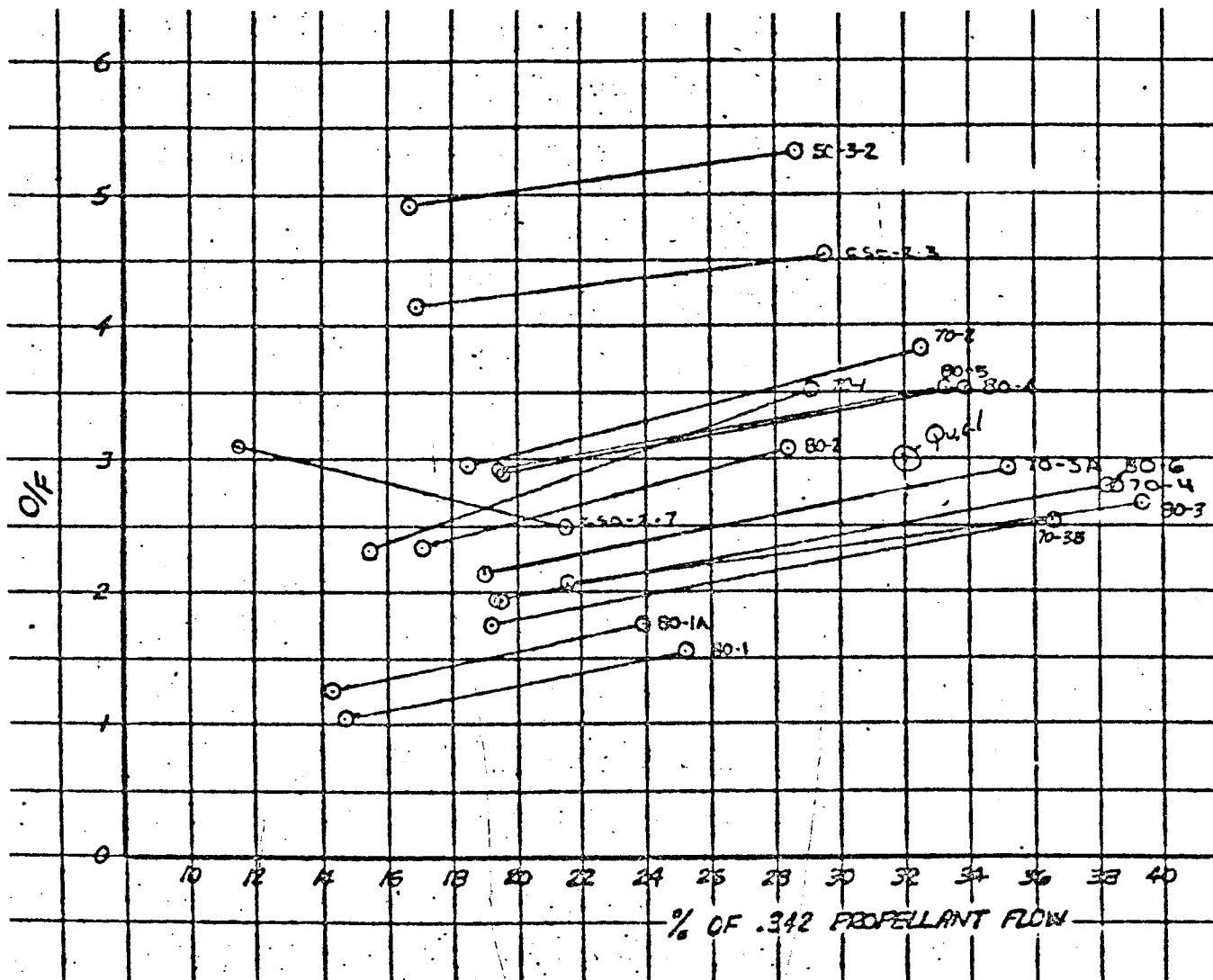
Fuel Flow	0.114 pps
Oxidizer Flow	0.228 pps
Total Flow	0.342 pps

FIRST PRE-IGNITOR INJECTOR

T-10650



RANGE OF O/F's AND TOTAL PROPELLANT FLOWS TESTED



% OF .342  $\dot{W}_p$

VS.

O/F<sub>RT.</sub>

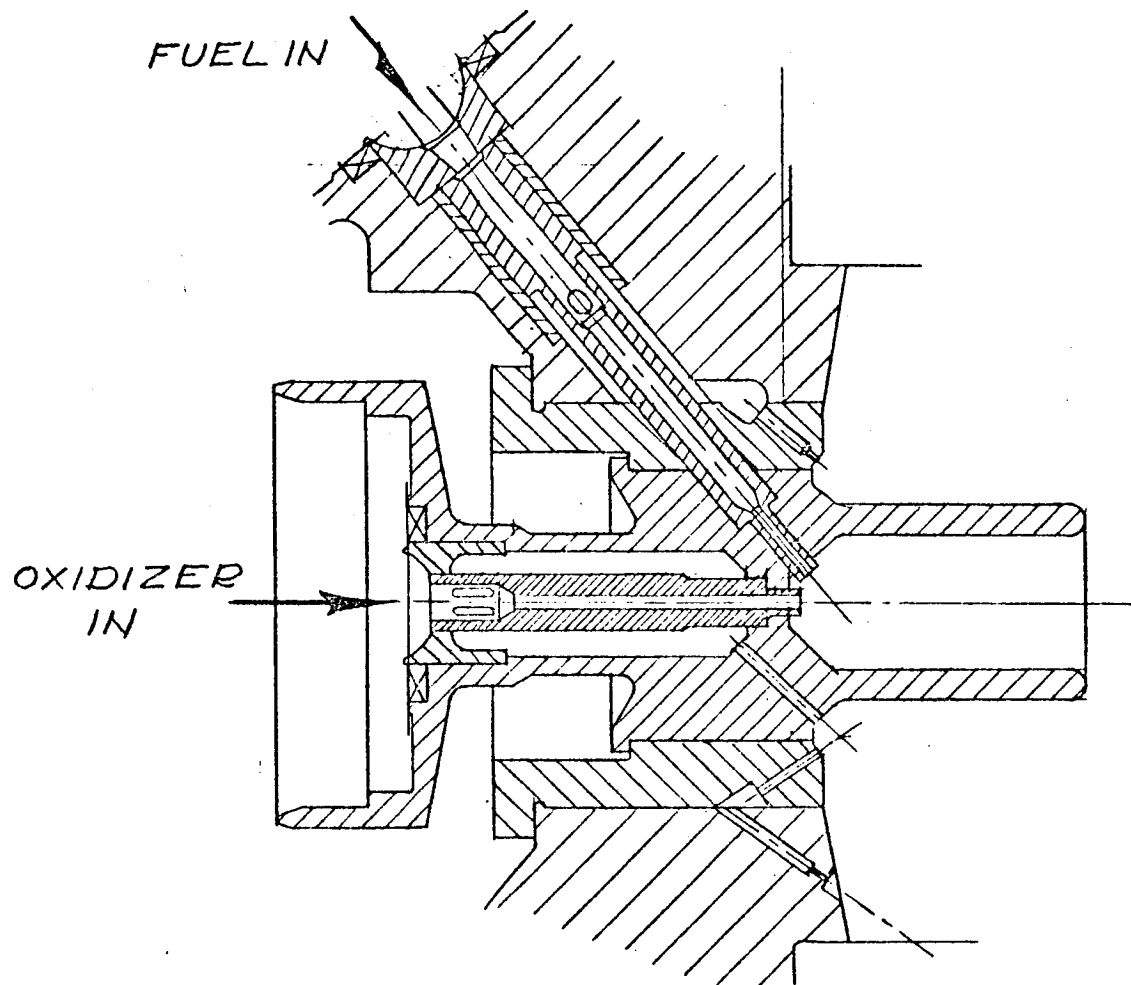
FOR CASES 1 & 9

O- LEAD

TABLE IV  
PREIGNITER TEST SUMMARY

Firing No.	Pre-igniter Tubes	Pre-igniter Lighting			Pre-igniter Chugging			Pre-igniter Not Conditions			Spikes Cold Conditions			No. of Runs/ Starts	Spikes at Normal P <sub>2</sub>	Spikes at Low P <sub>2</sub>	Spikes at High P <sub>2</sub>	Bz % Case 1 0. Lead
		Hot Conditions	Cold Conditions	Lead	Hot Conditions	Cold Conditions	Lead	Hot Conditions	Cold Conditions	Lead	Hot Conditions	Cold Conditions	Lead					
10650-1-3	.047 .028	G	G	G	M	P	M	G	G	G	G	G	G	25/49	0	3	0	4.15
10650-1-7	.047 .028	G	G	G	P	P	M	G	G	G	G	G	G	12/115	1	4	1	3.11
10650-1-2	.047 .0265	-	M	G	-	P	P	G	G	G	G	G	G	79/79	0	0	0	4.92
10670-1-1	.045 .022	M	M	P	G	G	G	G	G	G	G	G	G	134/134	4	0	0	2.51
10670-1-2	.045 .022	-	-	P	-	-	G	-	-	-	-	-	-	75/75	30	0	0	2.95
10670-1-3	.045 .024	G	G	G	P	G	G	G	G	G	G	G	G	185/187	5	1	0	1.76
10670-1-4	.047 .028	G	G	G	G	G	G	G	G	G	G	G	G	157/231	7	7	0	1.85
10680-1-1	.035 .026	-	G	G	-	P	M	-	-	-	G	G	G	79/79	10	0	0	1.05
10680-1-2	.041 .023	G	G	M	G	G	G	G	G	G	G	G	G	77/77	13	-	-	2.34
10680-1-3	.044 .028	G	G	M	P	P	M	G	G	G	G	G	G	170/225	15	2	1	2.08
10680-1-4	.044 .024	G	G	G	G	G	G	G	G	G	G	G	G	152/152	9	6	0	2.89
10680-1-5	.044 .024	-	-	G	-	-	G	-	-	-	G	-	-	27/27	4	1	-	2.91
10680-1-6	.048 .028	-	G	G	-	P	M	-	-	-	G	-	-	458/1287	23	-	-	1.94
														1975				
														3073				

LEGEND:  
G GOOD  
M MARGINAL  
P POOR



REPLACEABLE FUEL TUBE INJECTOR

TABLE V

EARLY PREIGNITER ENGINES

Engine	Doublet Diameter		Preigniter Diameter		Preigniter Cooling #1	Main Cooling	Window Diameter		Preigniter Flow		Preign. #1	Cooling Total	Main Cooling
	Fuel	Ox	Fuel	Ox			Fuel	Ox	Ox	Fuel			
T10650, S/N 001	.0256	.0354	.0283	.047	.010	.0118		.0186	27.8	14.2	-	10%	11.9
T10650, S/N 002-1, 2, 3, 4, 5	.0303	.0355	.0260	.047	.010	.0120		.0186	27.5	11.0	-	10%	10.1
T10650, S/N 003-1, 2, 3	.0256	.0354	.0283	.0395	.010	.0118	.0062	.0186	20.5	14.2	-	10%	11.9
T10650, S/N 002-6, 7	.0256	.0355	.0220	.0450	.010	.0118	.0095	.0145	26.8	14.5	-	10%	12.8
T10670, S/N 0001-1, 2	.0256	.0355	.0280	.0470	.010	.0120	.0062	.0186	27.7	15.6	-	10%	16.4
T11110, S/N 001-1	.0256	.0355	.0260	.0450	.010	.0118	.0085	.0186	27.3	20.2	-	11.0%	20%
T10670, S/N 001-3	.0250	.0410	.0290	.0470	.010	.015	.00916	.0186	23.5	20.5	-	10%	16.4
T10700, S/N 001	.0256	.0410	.0280	.0470	.010	.0120	.0062	.0186	27.7	15.6	-	10%	12.3
T11110, S/N 001-2	.0256	.0410	.0260	.0350	.010	.0118	.0095	.0186	25.5	11.6	~4%	11.7	21.3
T10680, S/N 001	.0256	.0410	.0219	.0441	.020	.018	.0062	.0182	28.5	14.3	~4%	11%	22.5
T10650, S/N 002-8	.0256	.0355	.0283	.0470	.020	.0185	.0095	.0186	25.5	12.0	~4%	11%	22.0
T11111, S/N 001-1	.0256	.0410	.0219	.0441	.020	.018	.0045	.0080	14.3	17.3	-	10%	13.1
T10680, S/N 001-2	.0256	.041	.0228	.0406	.010	.0118	.0060	.0081	27.9	21.7	-	10%	10.9
T10680, S/N 001-3	.0256	.041	.0280	.0447	.010	.0118	.0079	.0079	27.1	14.2	-	10%	11.6
T10680, S/N 001-4	.0256	.041	.0240	.0440	.010	.0118	.0062	.0186	25.9	14.2	~4%	10.8	23.5
T10650, S/N 002-9, 10	.0256	.041	.0283	.047	.020	.0185	.0110	.0186	27.6	21.8	-	10%	11.4
T10670, S/N 001-4	.0256	.0355	.0240	.040	.010	.0118	.00760	.00760	26.6	15.3	-	10%	12.2
T10680, S/N 001-5	.0256	.041	.0280	.048	.010	.0118	.0110	.0186	25.3	18.2	-	10%	11.7
T10680, S/N 001-6	.0256	.041	.024	.044	.010	.0118	.0076	.0076	27.5	14.4	-	10%	12.1
T10680, S/N 001	.0256	.0354	.028	.048	.010	.0186	.0061	.0186	28.1	23.7	-	10%	20.8
T10670, S/N 001-5	.022	.041	.0241	.044	.020	.0158	.0670	.0761	28.5	16.9	~4%	15.9	19.4
T11200, S/N 0001-1	.0256	.041	.025	.044	.010	.0118	.0076	.0076	27.5	16.2	-	10%	12.1
T10680, S/N 001-9	.025	.0354	.0249	.043	.020	.0186	.0123	.0076	28.8	15.6	~4%	11.8	27.0
T10670, S/N 001-6	.0256	.041	.025	.044	.010	.0118	.0076	.0076	24.6	16.5	-	8.3	12.2
T10680, S/N 001-10	.0256	.0354	.025	.044	.020	.0186	.0076	.0076	24.6	15.6	~4%	11.8	27.7
T10670, S/N 001-7	.0256	.0354	.0248	.044	.020	.0186	.0076	.0076	27.0	14.5	~4%	11.8	27.8
T10670, S/N 001-8	.0256	.0354	.0255	.044	.020	.0186	.0076	.0076	28.0	16.9	~4%	11.8	25.3
T10670, S/N 001-9, 10	.0256	.0354	.0255	.044	.020	.0186	.0076	.0076	27.7	15.4	~4%	12.2	24.6
T10670, S/N 002-1	.0256	.0354	.0255	.044	.020	.0186	.0076	.0076	27.7	15.4	~4%	12.2	24.6
T10670, S/N 002-2, 3	.0256	.0354	.0255	.044	.020	.0186	.0076	.0076	27.7	15.4	~4%	12.2	24.6

PFRT



The first engine to have both good steady state performance and good pre-igniter action had 100# thrust. However, the production tolerances on orificing and window sizes were such that all production engines could not have 100# thrust. Consequently, the nominal thrust was reduced to 95# to ensure a reasonable variation from engine to engine in thrust. NAA concurred with this decision. Later the thrust was increased to a nominal of 100# since the LM vehicle needs the extra thrust. The thrust was increased by increasing the oxidizer window area in the preigniter tube.

When it was decided to increase the thrust from 95# to 100#, the oxidizer window size was increased. The performance of the engine did not change significantly from the PFRT's performance and ignition tests showed that it still eliminated ignition overpressures. In another way the thrust was increased by enlarging the oxidizer doublet diameter from .0355 to .0365 as well as a small increase in the oxidizer window diameter. The performance of this engine was about 3-5 seconds higher than from the window increase alone and the ignition characteristics were still good. However, because there was more experience with the enlarged window engine, that configuration was selected as the Qualification injector.

In order to lower the heat lost from the vehicle to space through the engine and consequently lower the power requirement to keep the engine panel warm, a Passive Thermal Control program was undertaken. An analysis showed that by increasing the thermal resistance between the fuel valve and the injector, a significant reduction in the heat lost could be achieved. Consequently, a fuel standoff was designed and incorporated into the Qualification engine. Figure 1 is a drawing of this engine.

### III. INJECTOR DESIGN CRITERIA

#### Unlike Doublets

Except for the early work with a vortex injector all of the Apollo engines have been unlike doublets. The injector is the controlling element for performance and the thermal characteristics. During the development of the R-4D engine, significant relationships have been found between multiple unlike doublets and these performance characteristics.

To achieve good steady state performance it is important to have an even or constant mixture ratio across the injector face, to have good liquid-liquid mixing, to create small drops of propellant and to avoid separation of the two streams at the impingement due to the rapid reaction of the two hypergolic propellants. To achieve good thermal characteristics it is necessary to provide the chamber with fuel film cooling and thermally isolate the critical injector and valve components from the hot chamber.

### Steady State Performance

In developing the multiple doublet injector the number of doublets tested included 1, 4, 6, 8, 12 and 24. It is intuitively obvious that the specific impulse should increase as the number of doublets increase, since the streams are smaller which should result in better mixing. Also, smaller streams should produce smaller drop sizes. Another phenomenon being studied is the effect of the two hypergolic propellants reacting at the impingement point, blowing apart and consequently lowering performance because of poorer liquid-liquid mixing. It has been shown that unlike doublets of greater than 15-20 lbs. thrust will blow apart and result in a reduction in performance. Marquardt's experience has shown, for probably a combination of the reasons discussed above, that the specific impulse increased as the number of doublets increased (Figure 32).

Another important design goal for an unlike doublet injector is to have a uniform mixture ratio distribution in the resultant spray. Jack Rupe of JPL empirically determined such a relationship. Nonreactive fluids (water and an immiscible fluid) were used to simulate propellants. For a doublet the mixing ratio is optimum when the momentum ratio of the two streams equal the diameter ratio or

$$\frac{\rho_1 V_1^2}{\rho_2 V_2^2} = \frac{D_1}{D_2}$$

This can be rearranged to the following form

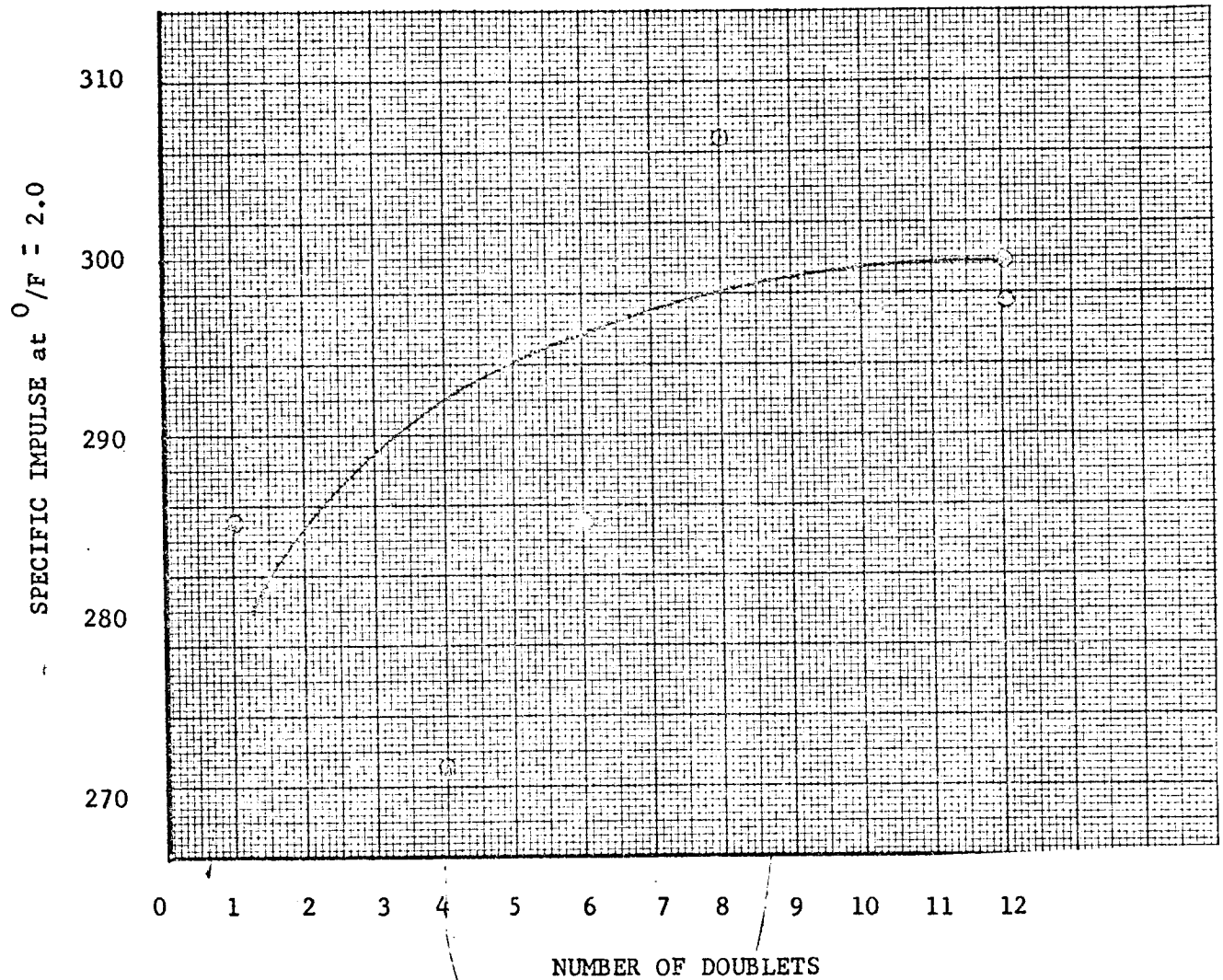
$$\frac{1}{(O/F)^2} \cdot \left( \frac{D_o}{D_f} \right)^3 \frac{\rho_{ox}}{\rho_f} = 1.0$$

which is more convenient to use when correlating Rupe's criteria with test data.

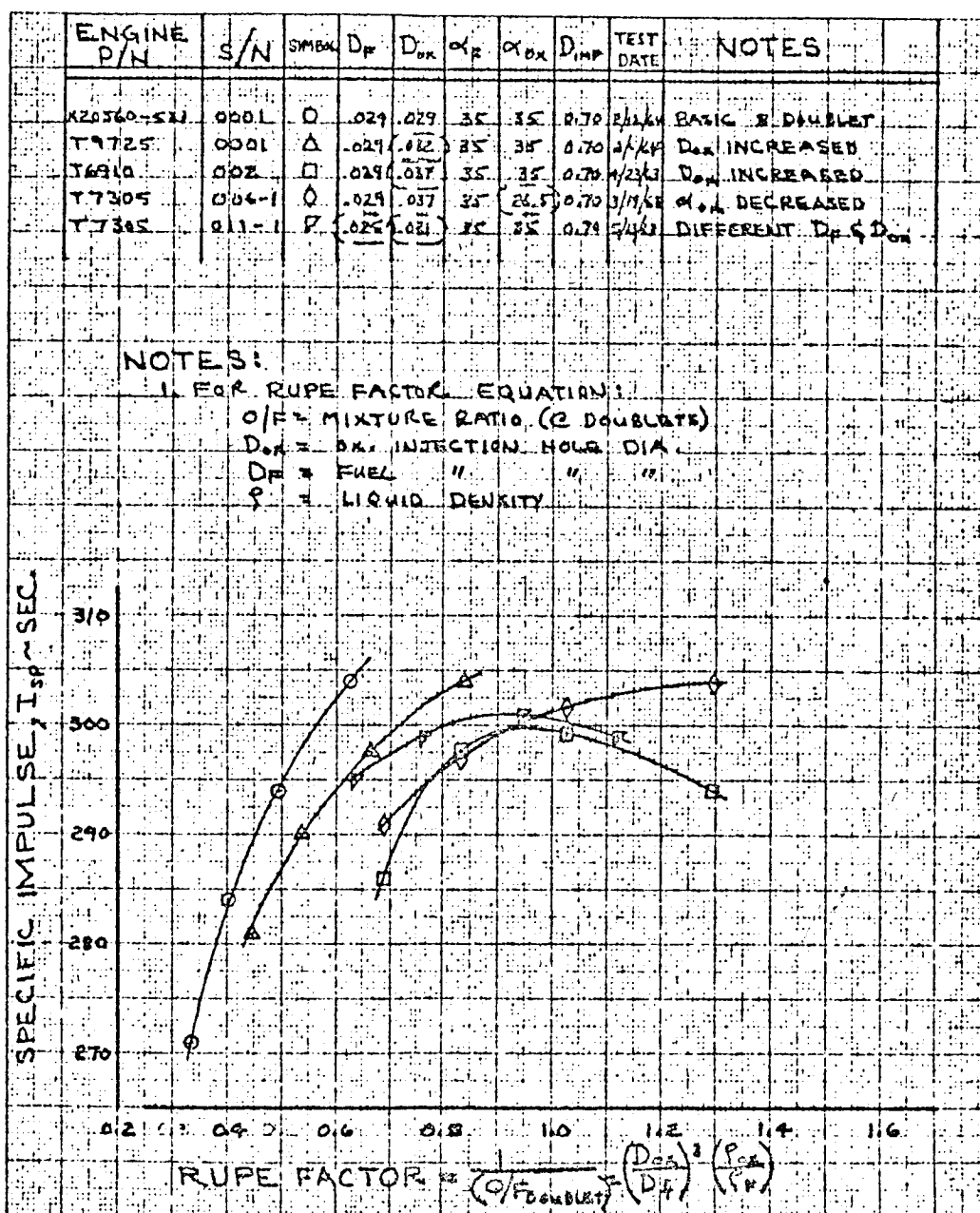
Figure 33 shows the specific impulse peaks out at the predicted value of 1.0. In this figure the Rupe factor was calculated using the overall mixture ratio. In Figures 34 and 35, the fuel film cooled engine and the preigniter engine, the criteria was calculated based on the doublet O/F. These figures also show that the best performance occurs at the optimum value for the Rupe criteria.

In addition to an even or constant mixture ratio distribution in the spray of each doublet, it is also important to have a constant mixture ratio across the face of the injector or at each doublet. In the present R-4D engine, the mixture ratio at each doublet varies as shown in Figure 36.

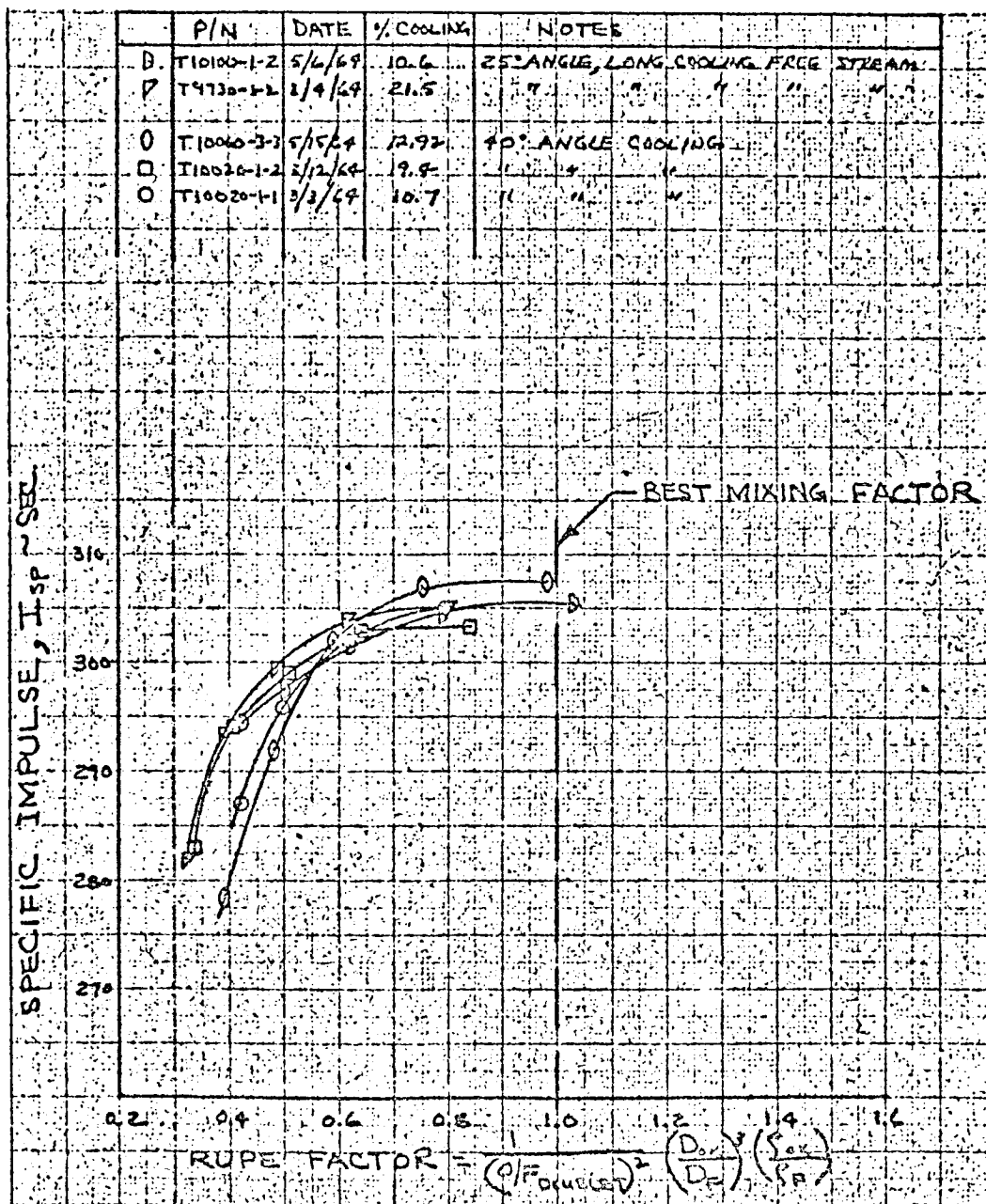
SPECIFIC IMPULSE vs NUMBER OF DOUBLETS



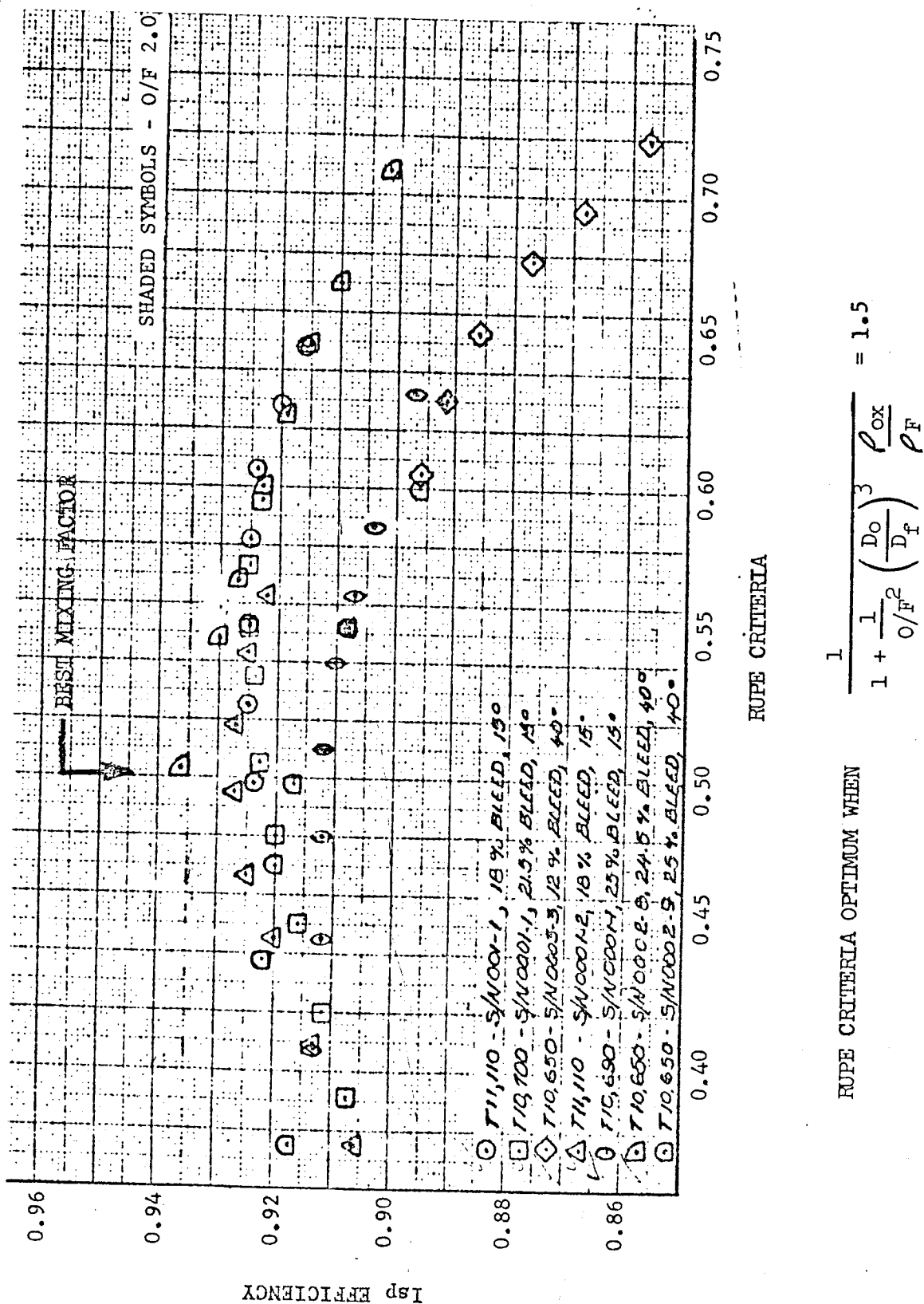
NON-FILM-COOLED - NONPREIGNITER  
SPECIFIC IMPULSE VS. RUPE FACTOR  
8 DOUBLET INJECTORS



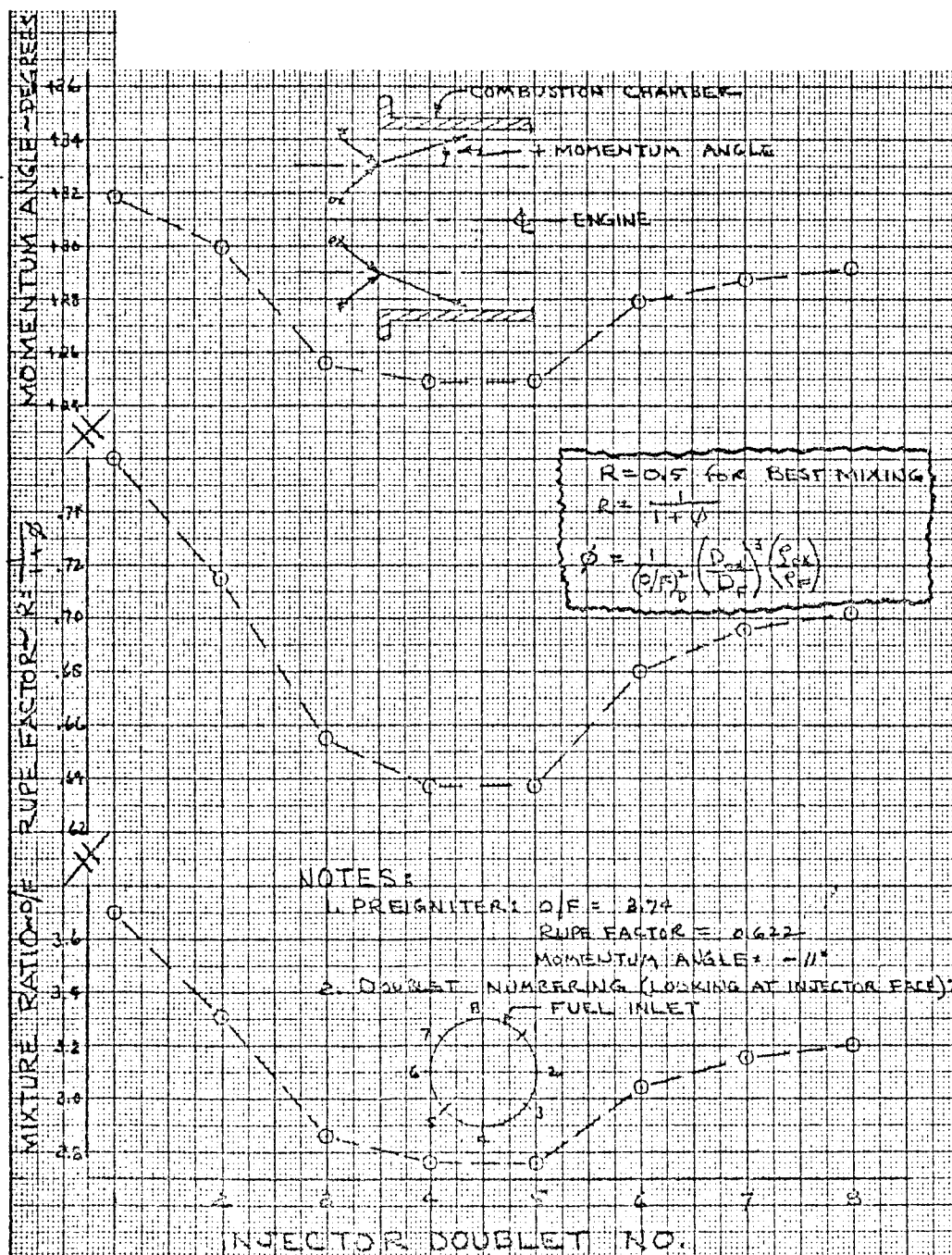
SPECIFIC IMPULSE VS. RUPE FACTOR  
FUEL FILM-COOLED, NONPREIGNITER 8 DOUBLET



$I_{sp}$  EFFICIENCY vs. RUPE CRITERIA  
PREIGNITER ENGINES



PREIGNITER INJECTOR DOUBLET  
MIXTURE RATIO, RUPE FACTOR, MOMENTUM ANGLE  
FOR CASE V STEADY STATE BURNING



Since the variation in main oxidizer doublet flow from hole to hole is less than 1%, most of the variation in O/F is due to the variation in the fuel flow caused by the static pressure profile in the fuel annulus. The static pressure in the annulus is lowest at the fuel valve and highest, 180° opposite the fuel valve.

A company funded eight doublet nonpreigniter fuel cooled engine was built with a specially designed fuel annulus to provide a uniform static pressure profile. The specific impulse was 300 seconds with 27 percent of the fuel cooling the chamber. This dramatically demonstrates the importance of uniform mixture ratio at each doublet.

The decrease in specific impulse with the addition of fuel film chamber cooling was small. Figure 37 shows decrease in specific impulse with fuel film cooling. With no film cooling the specific impulse was 298 seconds. When the film cooling was increased to 10-12%, the specific impulse dropped by 2 seconds to 296 seconds. With 20-22% film cooling, it dropped another 2 seconds to 294 seconds.

Splash plates were tried with the single doublet injectors but they usually decreased the performance. Also, a 12 doublet engine was tested with the chamber walls forming circumferencial splash plates. The doublets had a large outward momentum angle so that the resultant spray impinged on the chamber wall. The specific impulse of this engine was poor (280 seconds). Splash plates are not necessary to obtain good performance.

In summary, good steady state performance for unlike doublets can be achieved by keeping the thrust per element to 10-15 lbs., optimizing Rupe's criteria, and by having the same mixture ratio at each doublet. Fuel film cooling decrease the specific impulse by 2 to 4 seconds which is a very small loss to pay for the advantage of fuel cooling.

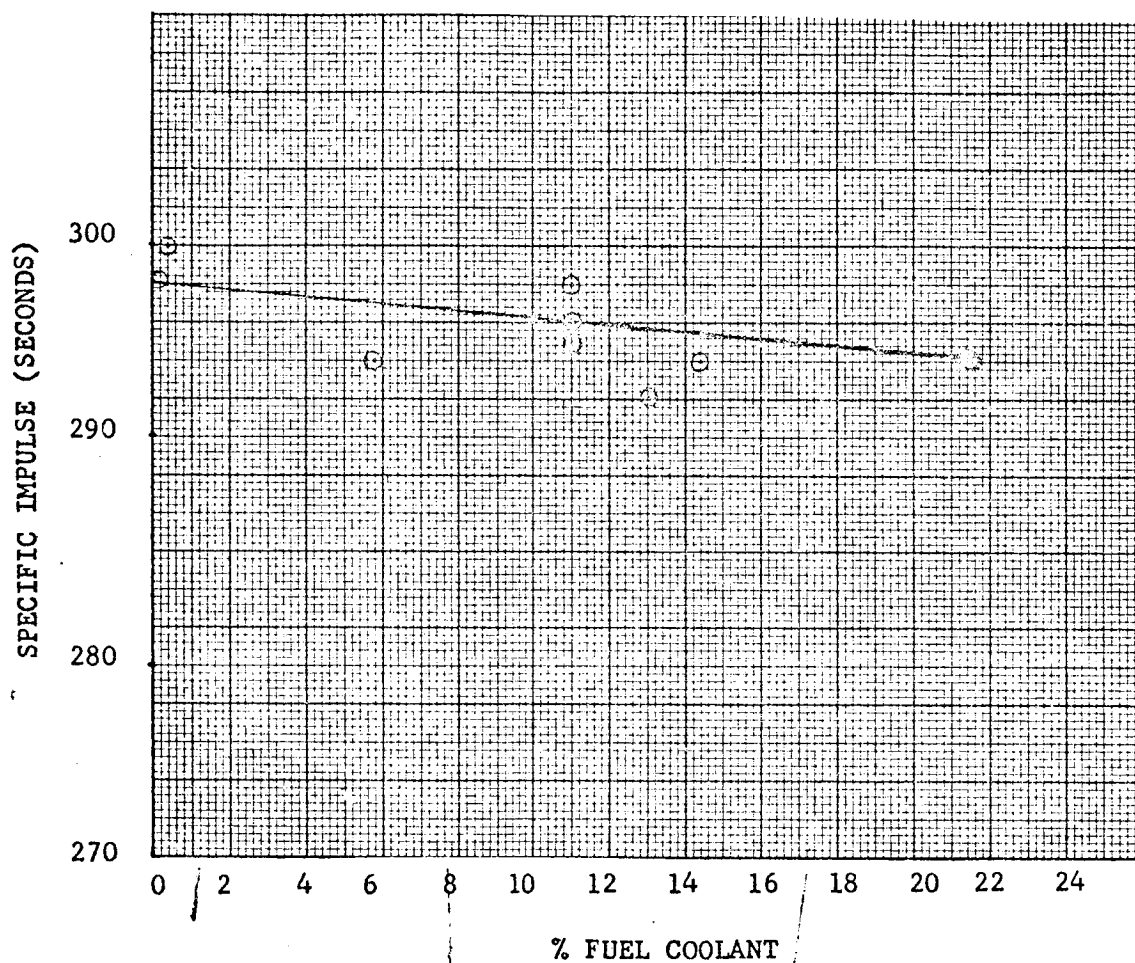
#### Thermal Performance

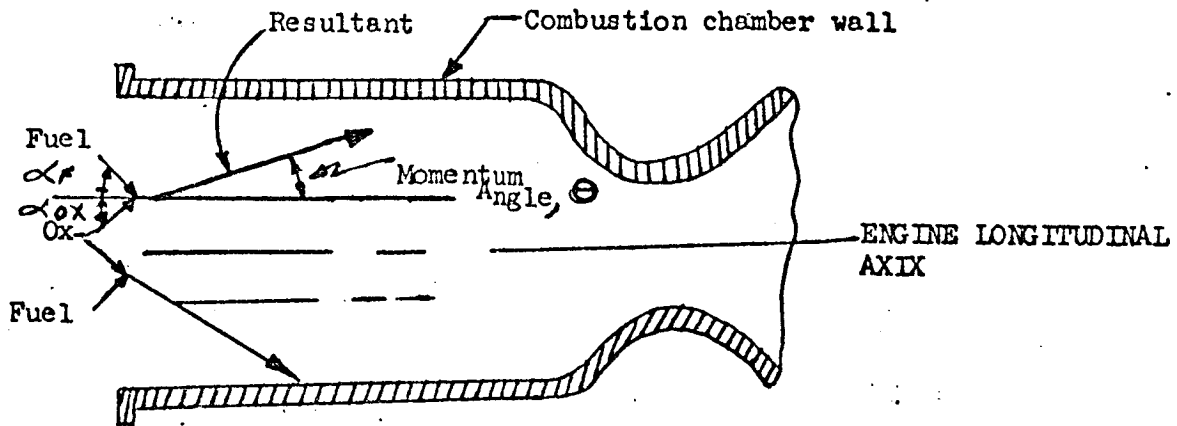
The throat temperature of the non fuel cooled engines was 2800 to 3000°F and the flange temperature was 1800° to 2200°F. This throat temperature was acceptable. However, the flange temperature led to other problems. The injector head, propellant valves and injector head to chamber seal were too hot. These problems were finally overcome by fuel film cooling but before fuel cooling, engine temperatures were effected to a small extent by the momentum angle of the spray formed by the two impinging propellant streams.

The momentum angle is determined from the following formula. The angle has been defined as positive if it is directed outwards towards the chamber wall.



SPECIFIC IMPULSE vs PERCENT FUEL COOLING





MOMENTUM RESULTANT ANGLE SCHEMATIC

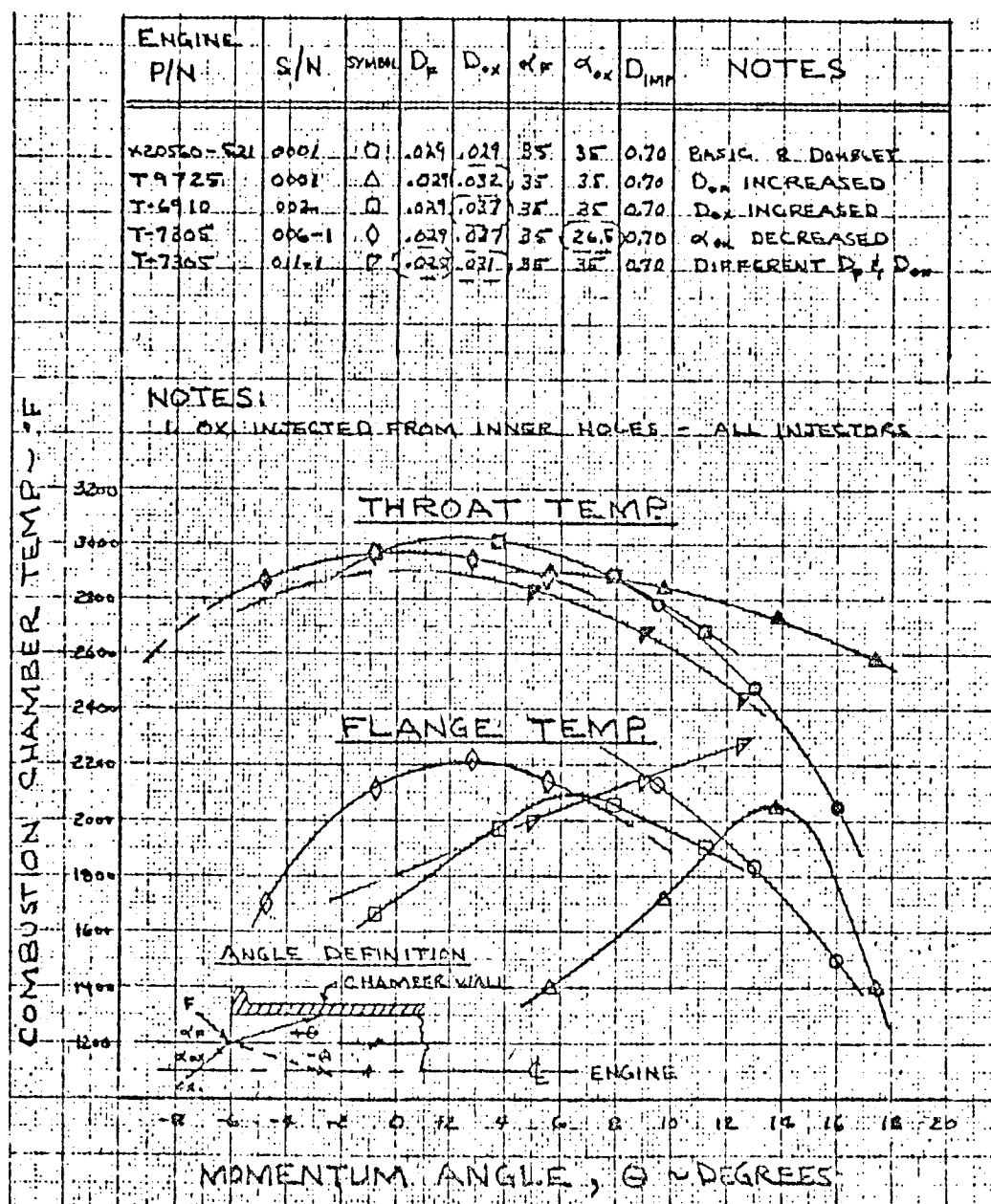
$$\tan \theta = \frac{\sin \alpha_{ox} - \left( \frac{W_f}{W_{ox}} \right)^2 \frac{\alpha_{ox}}{\alpha_F} \left( \frac{D_{ox}}{D_F} \right)^2 \sin \alpha_F}{\cos \alpha_{ox} + \left( \frac{W_f}{W_{ox}} \right)^2 \frac{\alpha_{ox}}{\alpha_F} \left( \frac{D_{ox}}{D_F} \right)^2 \cos \alpha_F}$$

Combustor temperatures for the non fuel cooled engines are shown on Figure 38 as a function of the doublet momentum angle. The range of angles tested,  $-5^\circ$  to  $+18^\circ$ , did not lower the chamber temperatures to an acceptable level, but the flange temperature was lower at the positive angles.

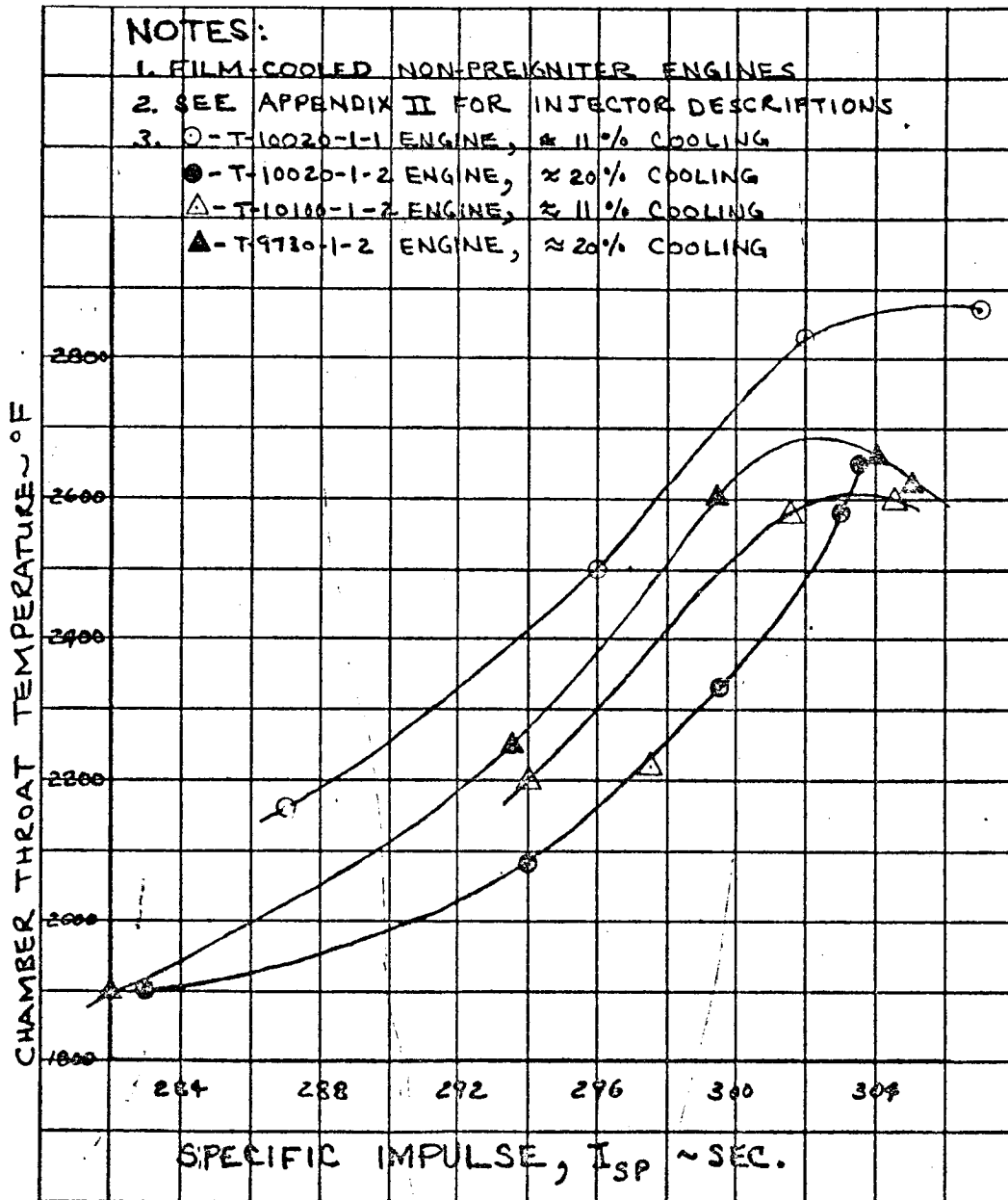
The fuel cooled engine was originally designed for operation at an O/F of 1.6 without any chamber cooling and then chamber fuel cooling holes were added. Originally, without any fuel cooling, the momentum angle was  $8^\circ$  and Rupe's Factor was 0.95 at the design O/F of 1.6. When the fuel cooling holes were added and the engine operated at an O/F of 2.0, the Rupe number was 0.5 and the momentum angle increased to  $22^\circ$ . Since most of the fuel cooled injectors were identical to this configuration, except for the amount of fuel used as a coolant, the variation in momentum angle and Rupe Factor was small. Also, the momentum angle was always greater than  $6^\circ$  even at an O/F of 1.4 so that no comparison was made in thermal characteristics between negative and positive momentum angles.

A relationship exists between the throat temperature and specific impulse for the fuel cooled engines as shown in Figure 39. Throat temperature increases with specific impulse.

NON-FILM COOLED - NONPREIGNITER  
FLANGE & THROAT TEMP. VS. MOMENTUM ANGLE  
8 DOUBLET INJECTORS



THROAT TEMPERATURE VS. SPECIFIC IMPULSE

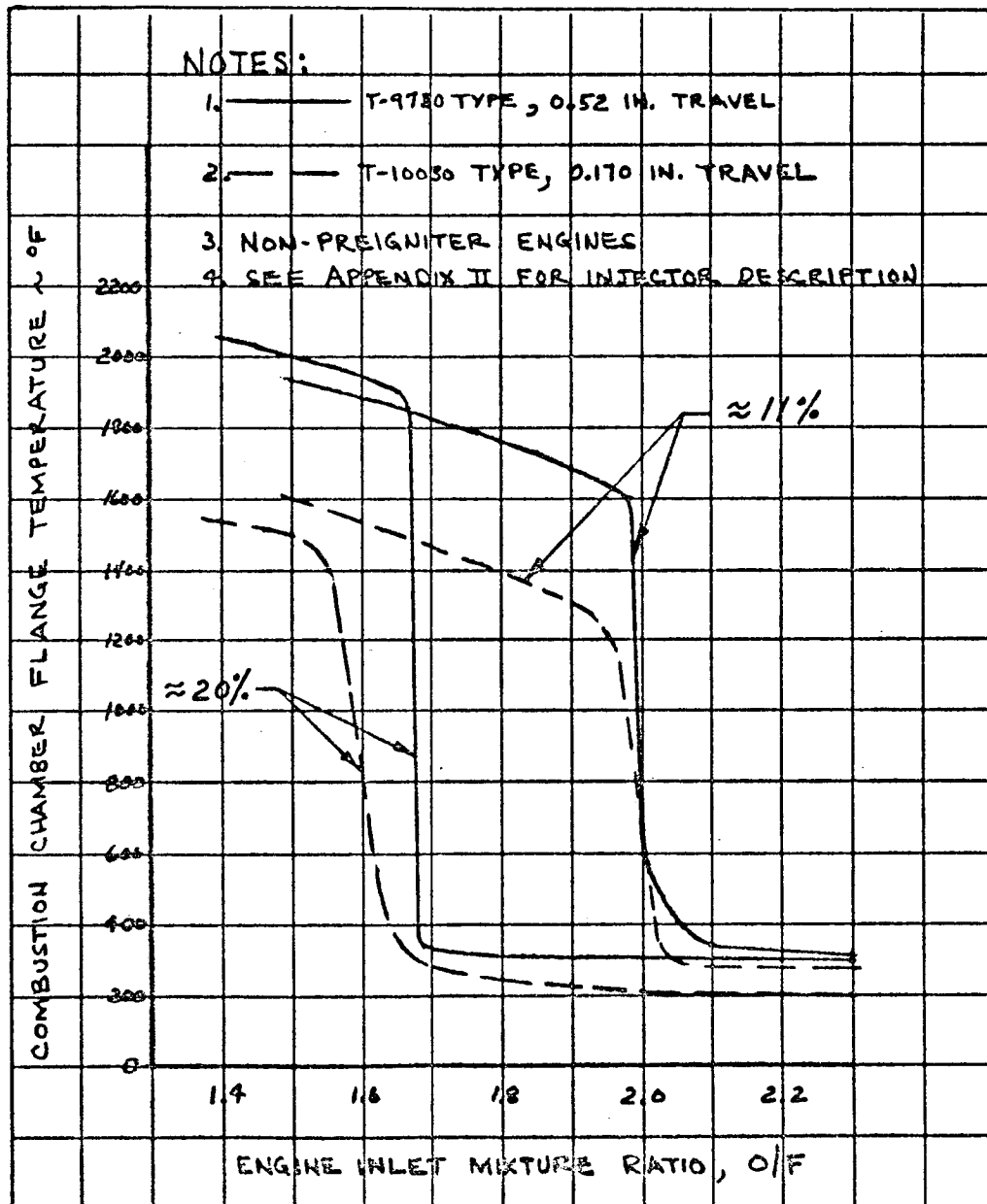


The two significant chamber temperatures are the flange and throat temperature. Of these, the flange temperature has been the most critical because of the chamber to injector seal and heat transferred to the injector through the flange. Testing of the fuel cooled engines has shown that the flange either runs cool (less than 500°) or hot (1500° to 2200°F) depending on the amount of coolant, coolant hole angle, free stream travel, and the mixture ratio. This is explained by nucleate boiling heat transfer at the lower temperature and film boiling heat transfer at the higher temperature. At low wall temperatures, nucleate boiling of the cooling fuel directed onto the chamber wall occurs keeping the flange and upper chamber wall near 300°F. As the throat temperature increases, additional heat is conducted up the chamber wall until a heat flux is reached which cannot be sustained by nucleate boiling. When this happens, a gaseous film is formed between the liquid coolant and the chamber wall which decreases the heat transfer to the coolant and causes a rapid increase in wall temperature (film cooling). Shown on Figure 40 is the flange temperature vs. mixture ratio for the two nominal film coolant flows of 10% and 20%. The step to the higher flange temperature occurs between an O/F of 1.8 and 2.0 for 10% and 1.6 to 1.8 for 20% film cooling.

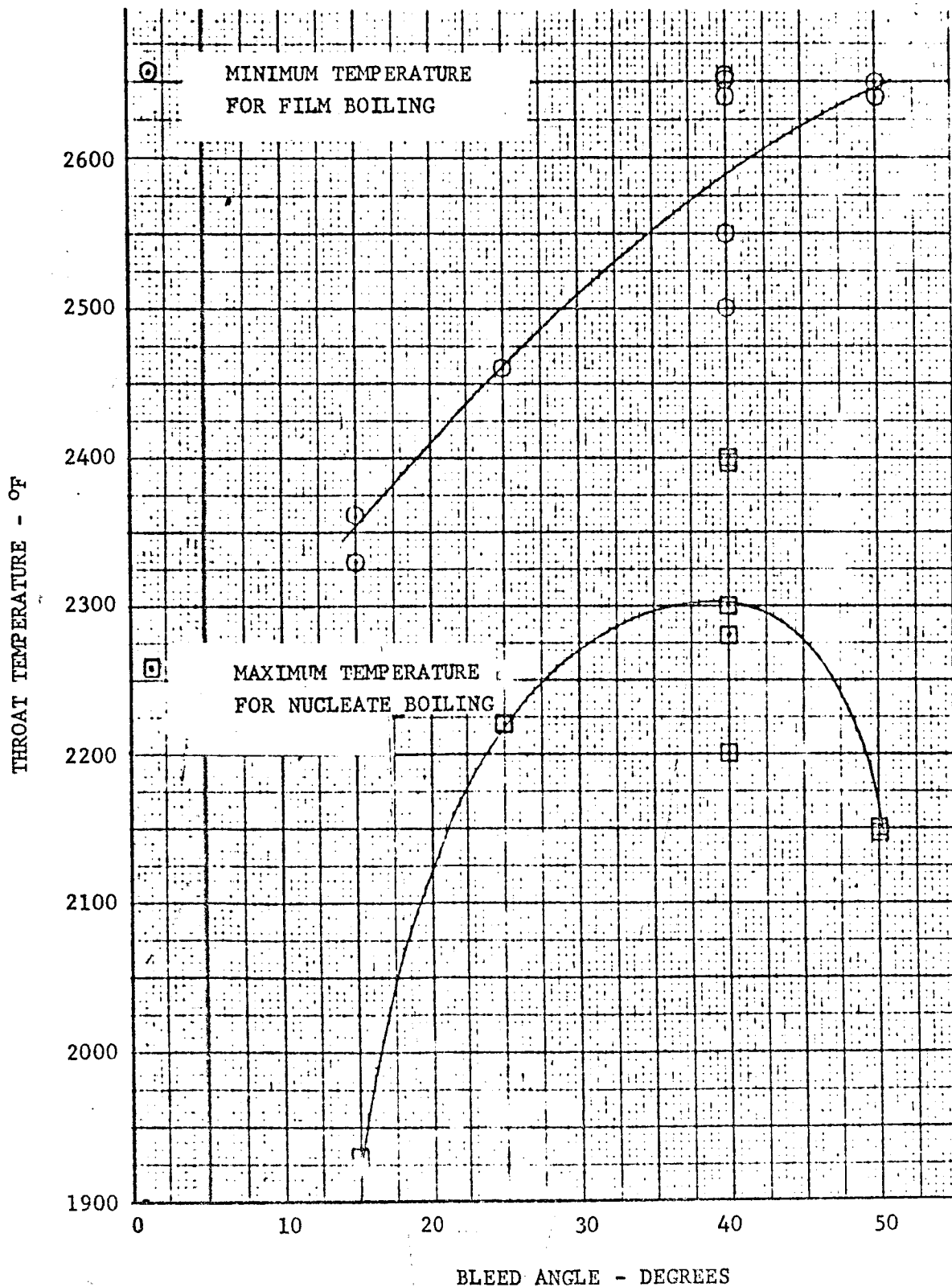
The transition from nucleate to film boiling is a function of time and chamber throat temperature. An examination of non-preigniter engine test data has led to an evaluation of the throat temperatures at which the transition from one cooling mode to the other can be expected for 60-90 second runs. These results are shown in Figure 41 where the throat temperature at both the top and bottom of the transition region are shown as a function of the angle of the coolant flow on the chamber wall. From this figure it can be seen that nucleate boiling, and thus a cool flange, can be maintained to the highest throat temperature (2300°F) with a bleed angle of 40°.

The effect of the amount of fuel film cooling on the throat temperature is shown in Figure 42 for the non-preigniter engines and the preigniter engines. The non-preigniter throat temperature was reduced from 2800-3000° with no film cooling, to 2000-2300° with 12% fuel film cooling. The throat temperature did not continue to decrease when the percent fuel cooling was increased beyond 12% to 15%. The throat temperature of the preigniter engine was not cooled to 2200-2400° until the fuel film cooling percentage was increased to 24% indicating that the addition of the preigniter significantly increased the engine temperatures.

FLANGE TEMPERATURE VS. MIXTURE RATIO  
FOR 11% & 20% FUEL FILM COOLING



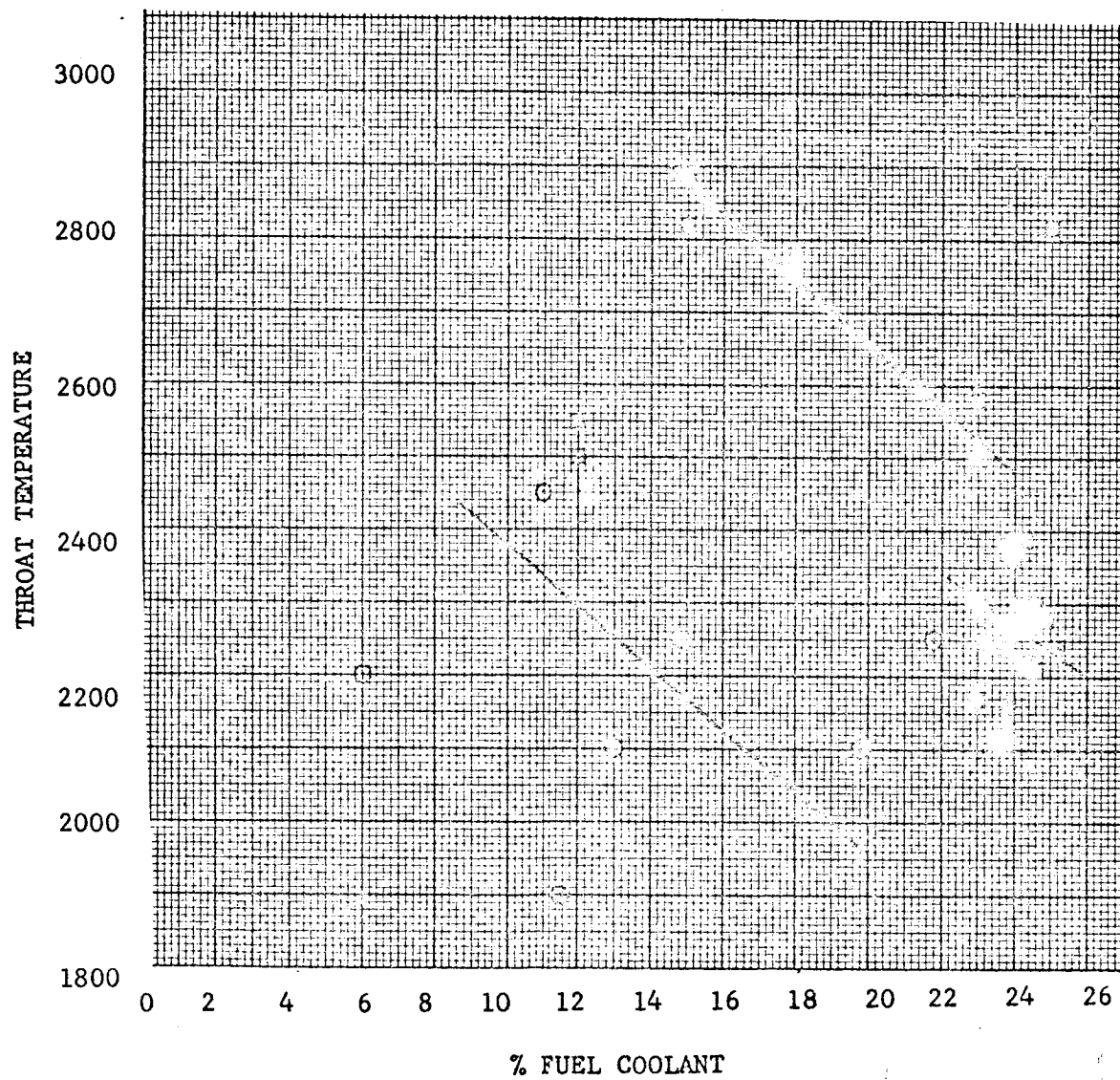
EFFECT OF BLEED ANGLE AND THROAT  
TEMPERATURE UPON THE TRANSITION  
FROM NUCLEATE TO FILM BOILING OF COOLING FLUID



THROAT TEMPERATURE vs PERCENT  
FUEL COOLING

○ NON PREIGNITER ENGINES

□ PREIGNITER ENGINES





CHAPTER 11

THRUST CHAMBER DESIGN

BY

J. C. REEVES

TABLE OF CONTENTS

	<u>Page</u>
I INTRODUCTION	11-1
II MATERIAL & COATING DEVELOPMENTS	11-1
A. Thrust Chamber Material Development	11-1
B. Materials and Coatings	11-5
C. 90TaLOW-Tungsten	11-6
D. Cb Alloy Program	11-17
E. Torch Testing of Coated Substrates	11-18
F. Comprehensive Molybdenum Evaluation Program	11-19
III THRUST CHAMBER CHRONOLOGICAL DEVELOPMENT	11-38
IV CHAMBER LIFE	11-58
A. Coating Loss Mechanism	11-63
B. Analysis and Discussion	11-71
C. Conclusions	11-78
REFERENCES	11-79
BIBLIOGRAPHY	11-79

# LIST OF ILLUSTRATIONS

<u>Figure Number</u>	<u>Title</u>	<u>Page</u>
1	0.5% Ti Molybdenum Riveted Tailpipe	11-3
2	25 Pound Thrust Motor	11-4
3	Coating Thickness vs. Time	11-7
4	Effect of Improper Edge Preparation	11-8
5	Effect of Disilicide Coating on the Surface Finish	11-9
6	Thermal Expansion Coefficients of Molybdenum and Molybdenum Disilicide	11-10
7	Hardness vs. Temperature	11-11
8	Tensile Strength of Molybdenum vs. Molybdenum Disilicide	11-12
9	Effect of Disilicide Coatings on Ultimate Tensile Strength	11-13
10	Effect of Disilicide Coating on Tensile Ductility	11-14
11	Effect of Disilicide Coating on Creep and Rupture	11-15
12	Time to Failure at 3000°F	11-16
13	Molybdenum Bar Stock After 3100°F Test	11-25
14	Molybdenum Forgings After 3100°F Test	11-26
15	Molybdenum Sheet Stock After 3100°F Test	11-27
16	Molybdenum Bar Stock After 3200°F Test	11-28
17	Molybdenum Forgings After 3200°F Test	11-29
18	Molybdenum Sheet Stock After 3200°F Test	11-30
19	Photomicrographs of Unalloyed Molybdenum Bar Stock	11-31
20	Photomicrographs of Unalloyed Molybdenum Forged Stock	11-32
21	Photomicrographs of Unalloyed Molybdenum Sheet Stock	11-33
22	Comparative Life of Forgings, Bar, Sheet Stock	11-37
23	Original Engine	11-41
24	Flo-Turn Lathe	11-42
25	Flo-Turn Molybdenum Combustion Chambers	11-43
26	Chamber Chronology	11-44
27	Drawing of First Combustor X18711	11-45
28	Engine With Ribbed One Piece Combustor	11-46
29	Two Piece Chamber 228128	11-47
30	Engine With Two Piece Chamber	11-48
31	Necked Down Chamber	11-50
32	Spherical Chamber	11-51
33	Coated 90TA-10W Thick Wall Combustion Chamber Post Fired	11-52
34	Coated 90TA-10W Thick Wall Combustion Chamber Post Fired	11-53
35	90TA-10W Combustion Chamber	11-54
36	90 Tantalum-10 Tungsten Alloy Thrust Chamber Welded Construction	11-55
37	Tensile Properties of TZM Alloy Sheet	11-56
38	Stress to Produce 2% Plastic Creep & Creep Rupture	11-57

LIST OF ILLUSTRATIONS (continued)

<u>Figure Number</u>	<u>Title</u>	<u>Page</u>
39	TZM Chamber T10085	11-59
40	Extra Thick Moly	11-60
41	Columbium Combustor After Pressure Check at 8600 psia	11-61
42	Engine With Columbium Chamber	11-62
43	Coating Life vs. Maximum Chamber Wall Temperature	11-64
44	Synopsis of Temperature and Oxygen Effects on Oxidation Protective Behavior of MoSi <sub>2</sub> and Mo <sub>5</sub> Si <sub>3</sub>	11-65
45	Growth and Depletion of Mo <sub>5</sub> Si <sub>3</sub> and MoSi <sub>2</sub>	11-69
46	Vapor Pressure of Three Gas Forming Transformations	11-70
47	Regression Rate of Surface in Hard Vacuum Due to Sublimation	11-73
48	Predicted Coating Life vs. Maximum Wall Temperature	11-74
49	Maximum Wall Temperature vs. Time	11-76
50	Apollo Cooling Cycle	11-77

LIST OF TABLES

<u>Number</u>	<u>Title</u>	<u>Page</u>
I	Early Columbium Data	11-18
II	Summary of Coated Alloys Evaluated	11-20
III	Time to Failure (in minutes) of Tested Substrates and Coatings	11-21
IV	Coating Thickness	11-22
V	Times to Initial Failure for Coated Molybdenum	11-23
VI	Average Coating Thickness	11-24
VII	Metallogical Thickness Data Sheet Stock at 3100°F	11-34
VIII	Metallogical Thickness Data Sheet Stock at 3200°F	11-34
IX	Metallogical Thickness Data Bar Stock at 3100°F	11-35
X	Metallogical Thickness Data Bar Stock at 3200°F	11-35
XI	Metallogical Thickness Data Forged Stock at 3100°F	11-36
XII	Metallogical Thickness Data Forged Stock at 3200°F	11-36
XIII	Properties of Unalloyed Molybdenum	11-39

## THRUST CHAMBER

### I. INTRODUCTION

The Apollo S/M RC engine was qualified by The Marquardt Corporation on December 31, 1965. Qualification, which consisted of 1000 seconds of running time at temperatures to 2200°F (I.D. throat), interrupted by 10,000 pulsing starts at temperatures from 40°F to 2200°F, was achieved after 3 1/2 years of comprehensive design, development and engine testing of the Apollo engine.

The problems associated with the design and development of a rocket engine are many and varied in nature. Setting aside all the complex factors of propellant valving, sealing, sophisticated injection systems, instrumentation, etc., the prime critical component of any rocket engine is the combustion chamber. The combustor is required to sustain vacuum ignition shock loadings, withstand extremely high pressures and operating temperatures during initial hypergolic reaction and burning of the fuel and oxidizer, be relatively impervious to the hot gases of combustion, and deliver the required thrust reliably throughout all phases of the duty cycle.

The thrust chamber used on the Apollo engine is fabricated from unalloyed molybdenum. The chamber is oxidation resistant coated with Durak B disilicide, and it is capable of sustaining elevated temperatures to 3000°F for extended time periods.

Unalloyed molybdenum exhibits excellent strength characteristics to 3000°F, however, as with all refractory metallics, this material has little oxidation resistance above 1600°F. To protect against catastrophic oxidation a disilicide coating is diffused into the substrate, with penetration and buildup being approximately the same. The Apollo thrust chamber of two-piece construction, incorporates an L-605 bell aft of the throat section and is attached by means of a Waspaloy nut (PH nickel base alloy). The use of L-605 and Waspaloy is permitted by lower operational throat temperature, i.e., from the original 3000°F to approximately 2000-2200°F. The cylindrical section of the combustor incorporates ribbed reinforcement to prevent localized over-pressuring during initial vacuum ignition.

### II. MATERIAL & COATING DEVELOPMENTS

#### A. Thrust Chamber Material Developments (Background)

In the beginning of the design phase for Apollo, the guidelines pertained only to the elevated temperature capability of the combustor. The original chamber was fabricated from pressed-sintered and forged unalloyed molybdenum and

incorporated a 0.030" wall. This combustor applied the technology derived from the Advent program, i.e., how to fabricate (machine) and disilicide coat molybdenum. Later developments in the Apollo program dictated the need to reinforce the cylindrical and throat section of the combustor, investigate the effects of localized force impact, institute redesign to soften vacuum ignition starting, and introduce film cooling to lower the interior wall surface temperatures. These items will be discussed in greater detail later on in this chapter.

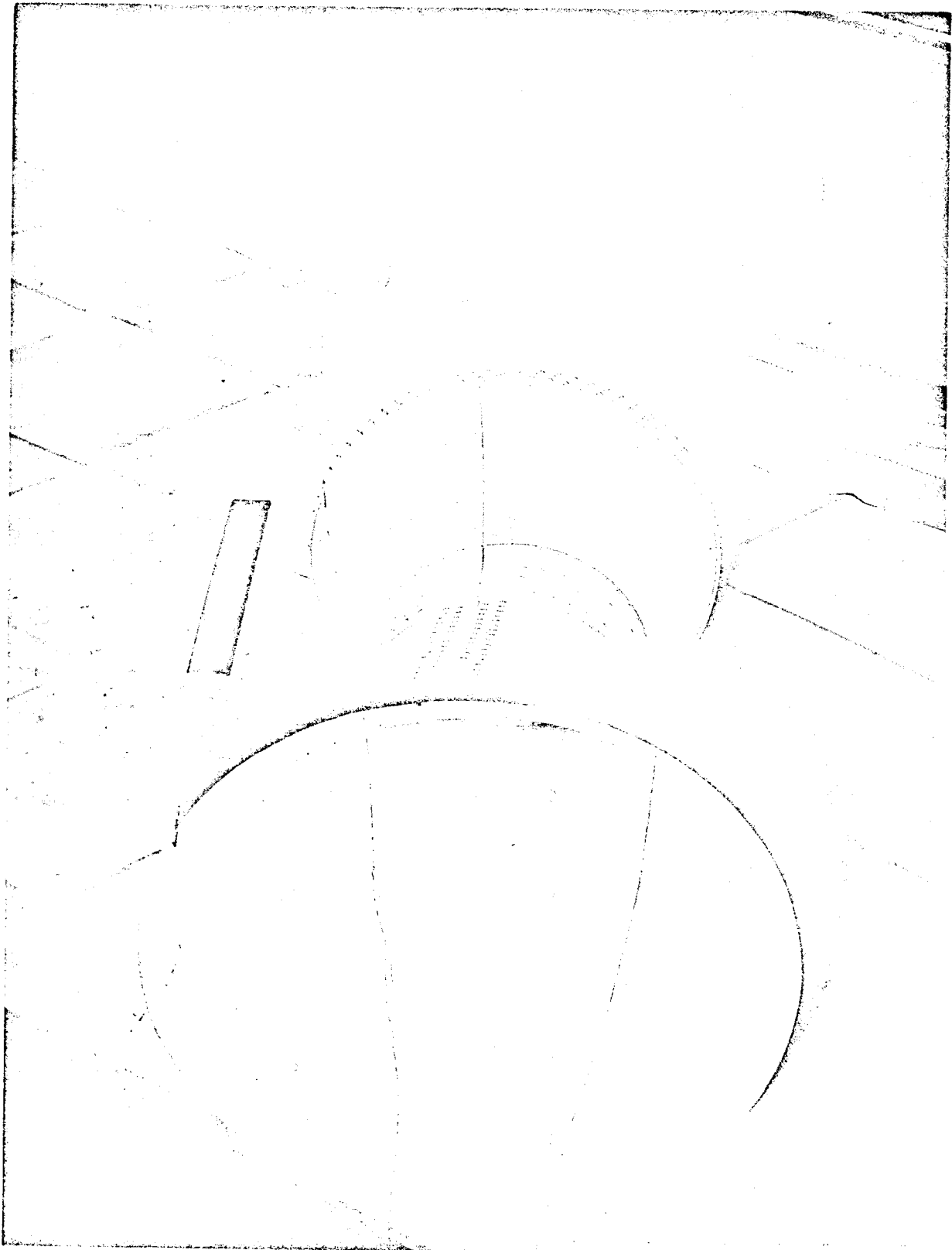
The forerunner of the Apollo program was the Air Force funded Advent Program. The know-how in refractory alloys, highlighting molybdenum, and disilicide coatings developed from 1955 to 1958, and which was partially applied by forming and riveting three (3) Hyperjet (ramjet-rocket) tailpipes (Figure 1), enabled TMC to approach the manufacture of a rocket engine combustor with confidence. The Hyperjet (Air Force) had been fabricated from 0.5 TiMo sheet alloy and coated with W-2 disilicide with actual application performed by the Chromalloy Corp., White Plains, New York.

For the 1960 Advent program, the utilization of bar stock 0.5 TiMo was a logical selection, but the higher operational temperatures required the use of a more sophisticated disilicide coating and as a result the W-2 was discarded in favor of a Durak B disilicide applied by the Chromizing Corp., L.A.

The Advent combustor (Figure 2) was machined from 0.5 TiMo bar stock. As noted above, the completed combustor was disilicide coated with Durak B which permitted long time operation at 2800°F, provided protection from the oxidizing products of combustion and performed extremely well overall.

This utilization of 0.5 TiMo on the Advent program and its successful operation at 2800°F, when protectively coated with Durak B disilicide, made this alloy a prime candidate for Apollo combustor application. However, as shown in Figure 2, the Advent combustor was only a 25# thrust version which was considerably smaller in the cylinder and skirt (3" dia.) sections than the Apollo 100# combustor which incorporated a flaring exit skirt cone 6" in diameter.

The 6" diameter of the Apollo combustor presented a significant material selection problem. The usage of 6" diameter bar was practically out of the question because of current unavailability and extreme waste if made available. These two (2) factors led to the designation of a forging preform. Again problems were encountered because 0.5 TiMo could not be preformed by the forging process. Fortunately for TMC, the General Electric Company, Cleveland, Ohio Division, had recently completed the sophistication of a process for producing pressed-sintered unalloyed molybdenum which could be readily forged into the preform configuration required for the Apollo combustor. Accordingly, this material was tentatively designated as the prime candidate for Apollo combustor application.



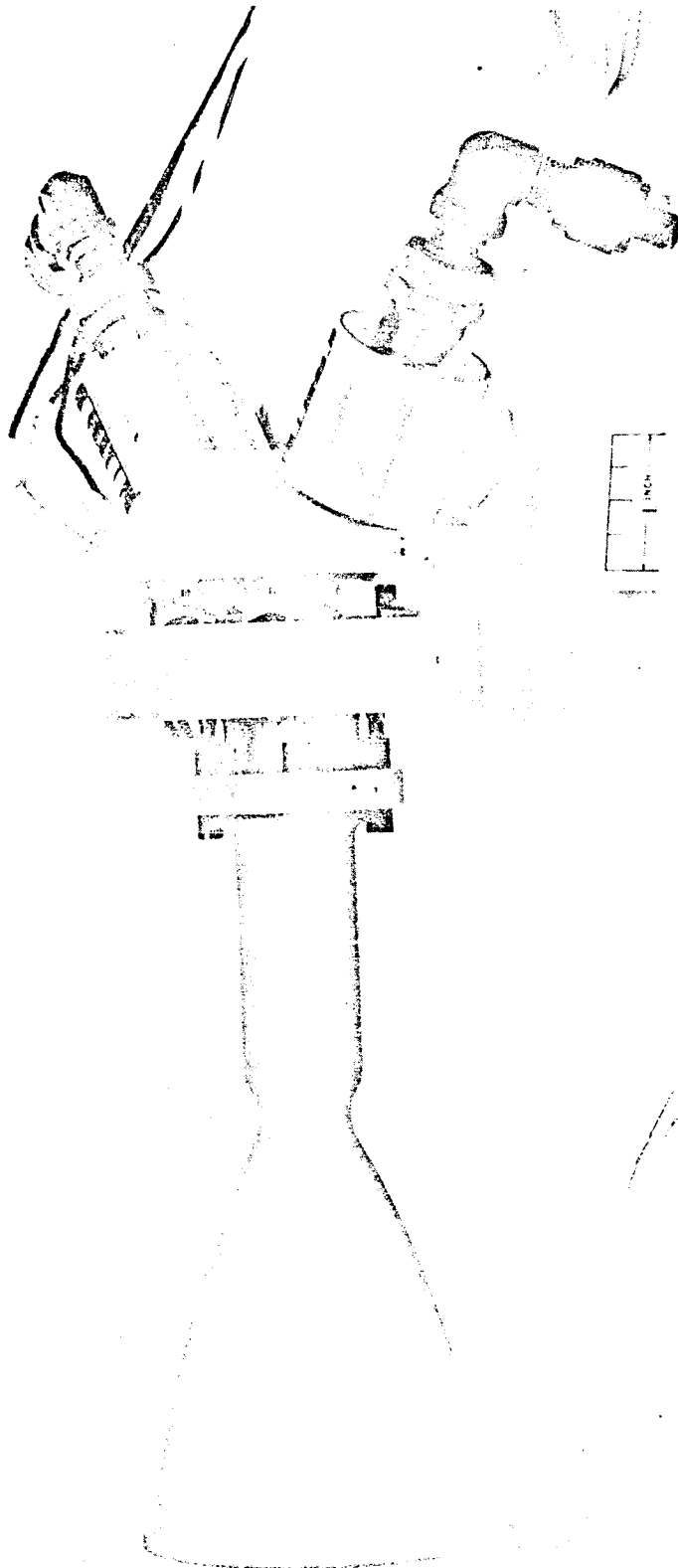
NEG. 1824-2

0.5% Ti Molybdenum Riveted Tail Pipe

11-3

Figure 1





NEG. 3864-1

25-Pound Thrust Motor

## B. Materials & Coatings

In the utilization of materials for high temperature application the primary emphasis must be placed on the ability of the base metal to sustain the operational temperatures to be imposed. The service temperatures of the Advent and Apollo combustors were initially established in the 2800°F - 3000°F range. These extreme elevated temperatures precluded the usage of the conventional super alloys and required the designation of one or more of the available metallic refractories, i.e., molybdenum, columbium, tantalum or tungsten.

These four refractory metallics and/or their alloys exhibit the capability to sustain temperatures far in excess of 3000°F, if suitably protected from an oxidizing environment. In essence, the refractory metallics will catastrophically oxidize at temperatures above 1500°F and all require an oxidation resistant coating. Therefore, in the selection of a suitable refractory alloy for the Apollo combustor in 1962, the only family of materials with a suitable oxidation resistant coating available were the molybdenum and molybdenum alloys. Of course, during the subsequent years, oxidation resistant coatings were developed for the other refractory metallics and these were evaluated accordingly.

Thus, the pressed-sintered unalloyed molybdenum became the prime candidate Apollo combustor material of application. For comparative purposes, the 0.5 TiMo alloy was given additional extensive evaluation. The initial step, of course, was to determine the suitability of applying the Durak B disilicide to unalloyed molybdenum. To accomplish this goal, an analysis was performed of the Durak B Pack Cementation process and consisted primarily of determining both the procedural requirements of the coating operation and the preparation of the molybdenum for disilicide application. Accordingly, a step analysis was setup and the general areas of interest are enumerated as follows:

1. Overall coating operation
2. Preparation of materials for coating
  - (a) Cleaning procedure - chemical
  - (b) Cleaning procedure - mechanical
3. Heating cycle
4. Designing for disilicide coating
5. Stripping, lapping and recoating
6. Torch testing to determine elevated temperature capability.

Suitable quantities of both unalloyed and 0.5 TiMo were prepared and subjected to the coating cycles. From these efforts much data was generated on the diffusion characteristics of Durak B disilicide at various hold-times at temperatures, the effects of a properly radiused edge, etc., are shown in Figures 3 through 12. These figures are separately discussed as follows:

Figure 3 displays the variations in coating thickness versus coating retort time/temperature. 1950°F for 12 hours appears to provide the maximum coating protection. The total coating thickness is measured from the interface of the diffused zone to the average of the buildup. Figure 4 illustrates the difference between a properly and improperly radiused edge for disilicide coating application.

Figure 5 tabulates effect of Durak B on surface finish of 0.5 TiMo and unalloyed molybdenum.

Figures 6 and 7 list the difference in Coefficient of Thermal Expansion of molybdenum and molybdenum disilicide, and the hardness of the mo-disil at elevated temperatures. Excessive variations in Coefficient of Thermal Expansion ( $\alpha$ ) can cause crazing. Crazing can be defined as superficial surface discontinuities.

Figure 8 shows the difference in tensile strength of 0.5 TiMo versus the disilicide at temperatures to 2500°F.

Figures 9, 10, 11 present data related to effect of disil on UTS of 0.5 TiMo, on the ductility, and on the creep, stress rupture properties.

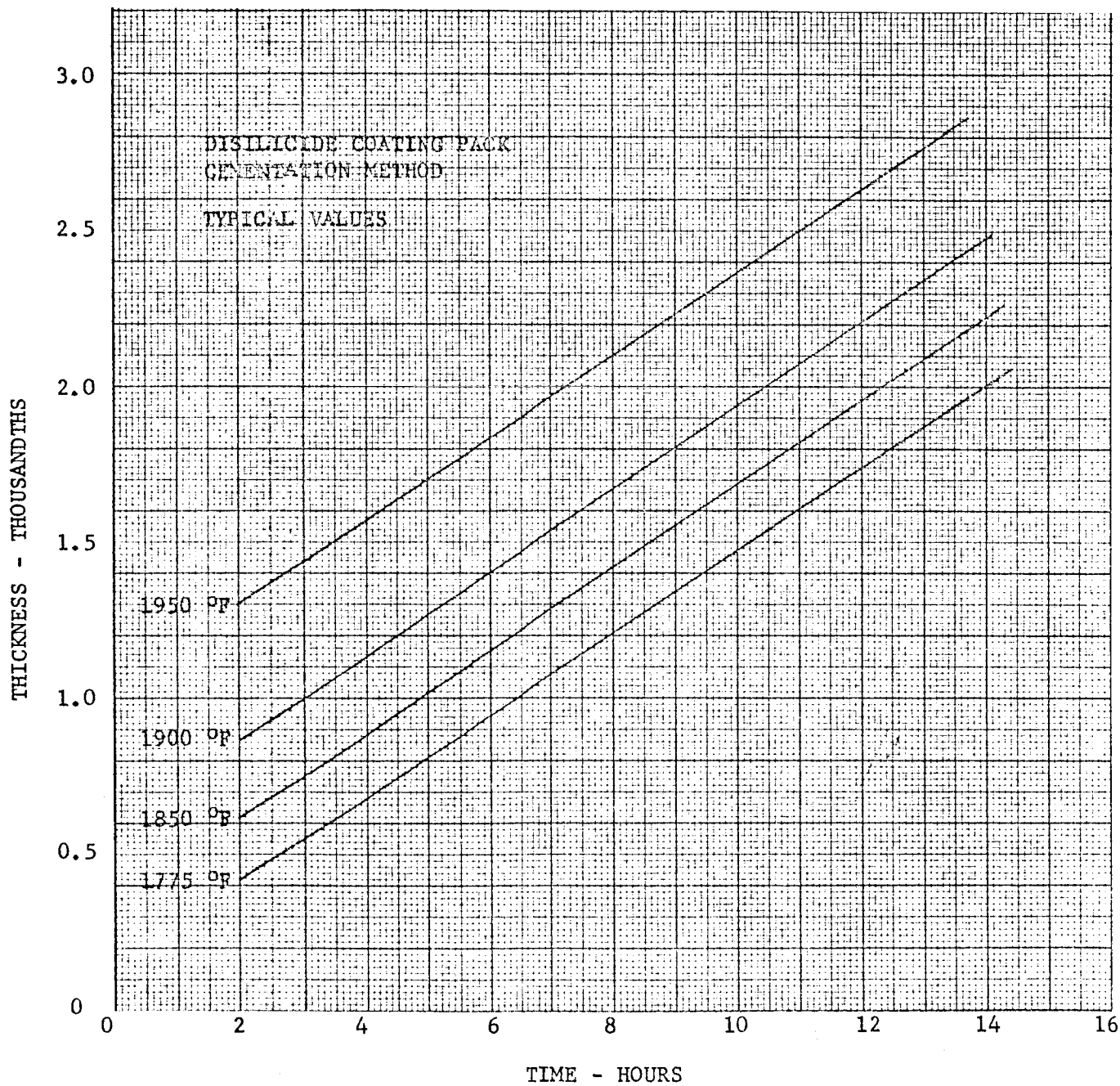
Figure 12 reports on torch test results. These tests were performed on 2" x 2 1/2" x 0.050 thick panels coated with disilicide and oxy-acetylene torch tested at 3000°F. As shown, one panel lasted 2 hours and 10 minutes before failure.

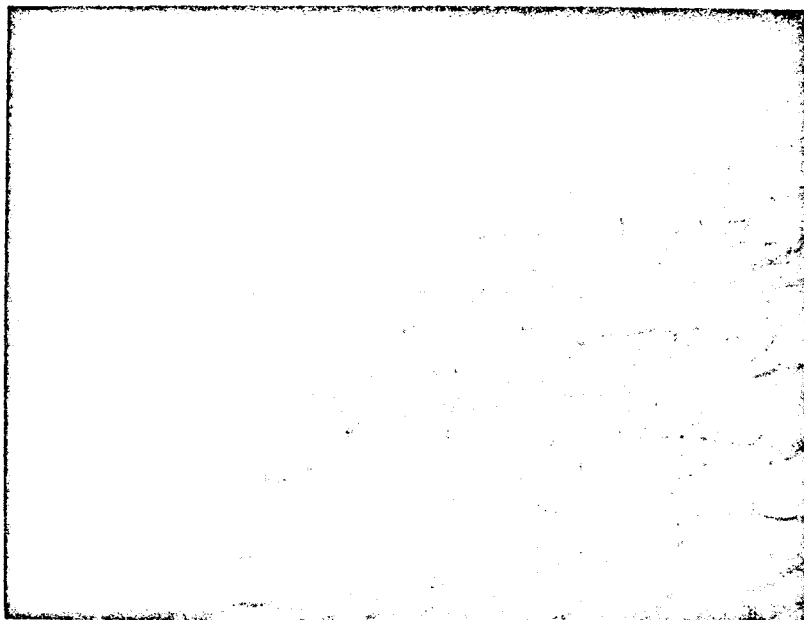
Prior to, during, and following the foregoing evaluation phases for disilicide coating and testing unalloyed molybdenum and 0.5 TiMo, research into the availability and capability of the other refractory alloys was continuing. Other prime reasons for the selection of unalloyed molybdenum, aside from a suitable oxidation resistant coating, was its availability, low cost, high strength at extreme elevated temperatures and fabrication characteristics. These factors permitted TMC to commence the fabrication of thrust chambers and to perform actual rocket engine firing tests, thereby permitting the generation of a comprehensive backlog of experience in this field. As other refractory alloys and coatings became available, extensive investigations were performed and the results compared with those of unalloyed molybdenum. In effect, molybdenum became the thrust chamber standard on which to base other refractory metallics and coating capability under rocket engine firing conditions.

#### C. 90Ta10W-Tungsten

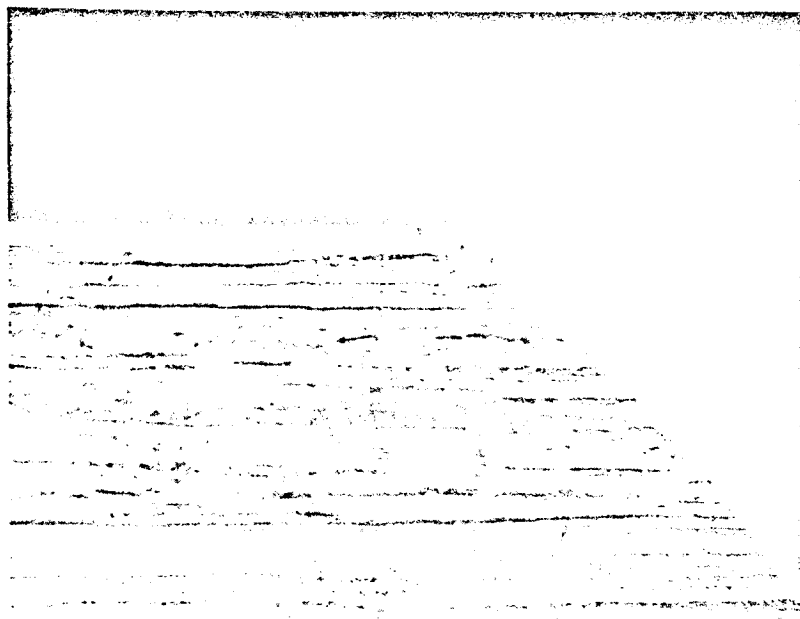
In 1962, TMC and the Air Force jointly initiated an anti-oxidation coating research program. As part of this Contributing Engineering Program, a survey of technical literature and different coating vendors was performed to determine capability and availability of 90Ta10W and Tungsten along with suitable high temperature protective coatings.

COATING THICKNESS VS TIME  
SHOWING EFFECT OF COATING TEMPERATURE





EDGE PROPERLY RADIUSSED



EDGE RADIUSSED BUT IMPROPERLY BLENDED  
INTO FACE ---NOTE DISCONTINUITY IN  
COATING

11-8

Figure 4

\*EFFECT OF DISILICIDE COATING ON THE SURFACE FINISH  
OF 0.5% Ti Molybdenum

Surface Finish, RMS

Before Coating

After Coating

4	20
6	14
6	17
8	10
8	12
8	15
8	18
10	12
10	15
15	15
16	25
20	30
23	32
23	35
30	40
30	40
32	47
45	60
50	70
50	75
65	110
80	110
80	120
85	110
110	135
120	170
220	235

Profilometer readings, typical values.

\*Same for unalloyed molybdenum.

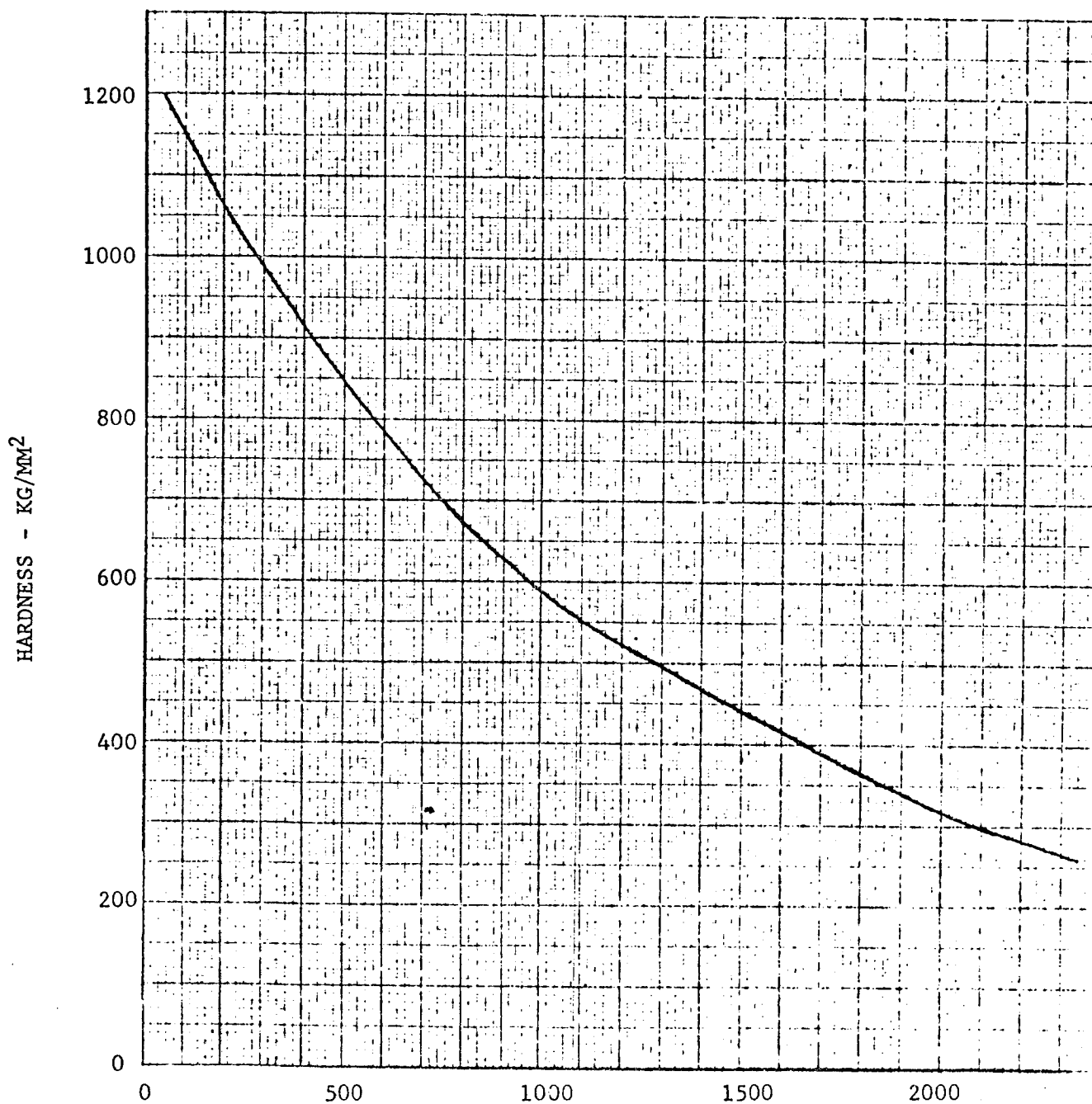
THERMAL EXPANSION COEFFICIENTS  
of  
MOLYBDENUM AND MOLYBDENUM DISILICIDE

Mean Linear Expansion Coefficients ( $10^{-6}$  ins/in./°F)

<u>Temperature Range °F</u>	<u>*0.5% Ti Molybdenum Alloy</u>	<u>MoSi<sub>2</sub></u>
80-200	2.77	4.0
80-400	2.88	3.8
80-600	2.98	4.0
80-800	3.00	4.2
80-1000	3.08	4.3
80-1200	3.12	4.3
80-1400	3.21	4.4
80-1600	3.26	4.41
80-1800	3.34	4.42
80-2000	3.41	4.48
80-2200	3.46	4.58
80-2400	3.54	4.70
80-2600	3.61	4.80
80-2750	3.66	4.91

\*Approximately the same for unalloyed molybdenum.

HARDNESS VS TEMPERATURE  
OF MOLYBDENUM DISILICIDE



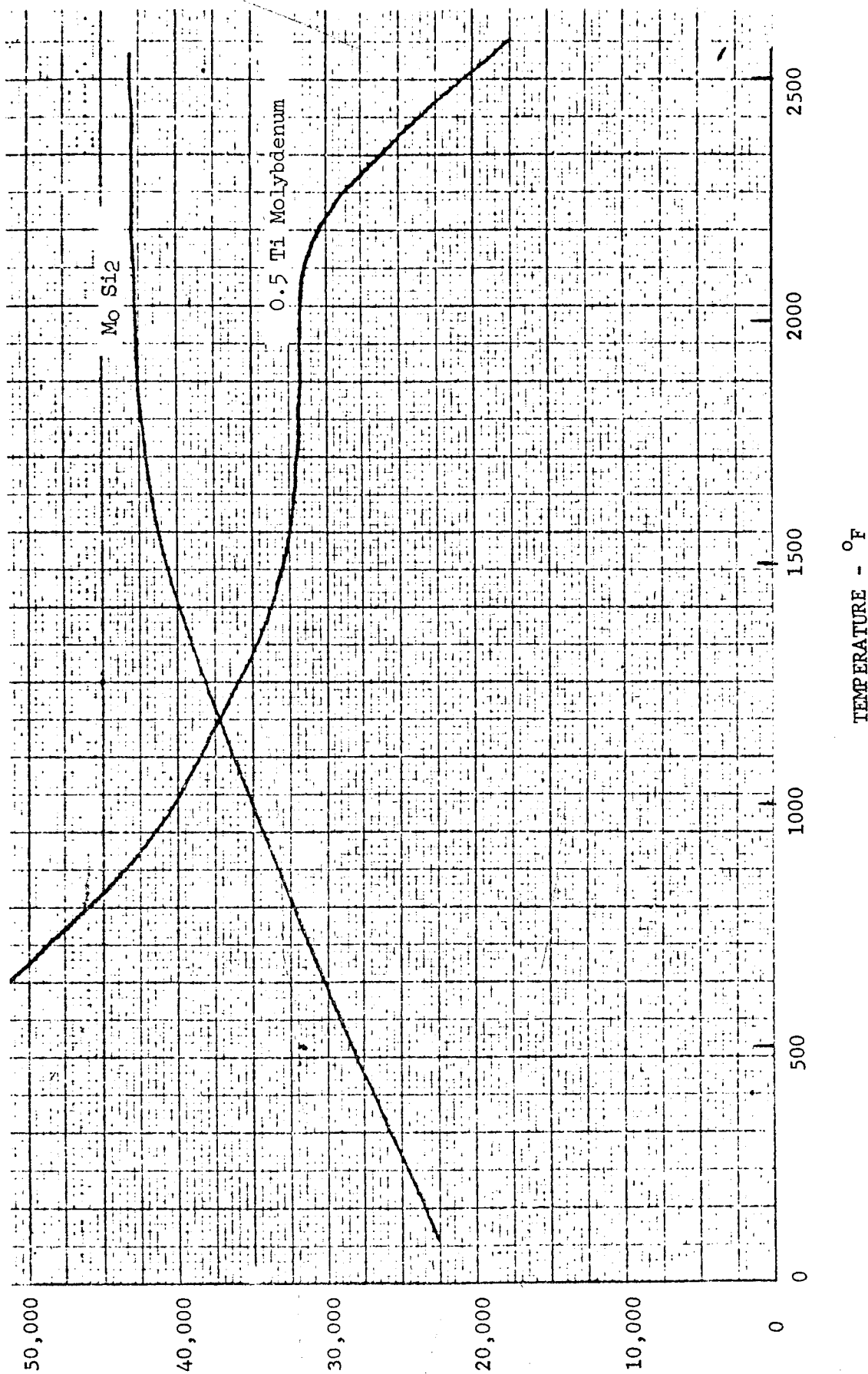
TEMPERATURE - °F

11-11

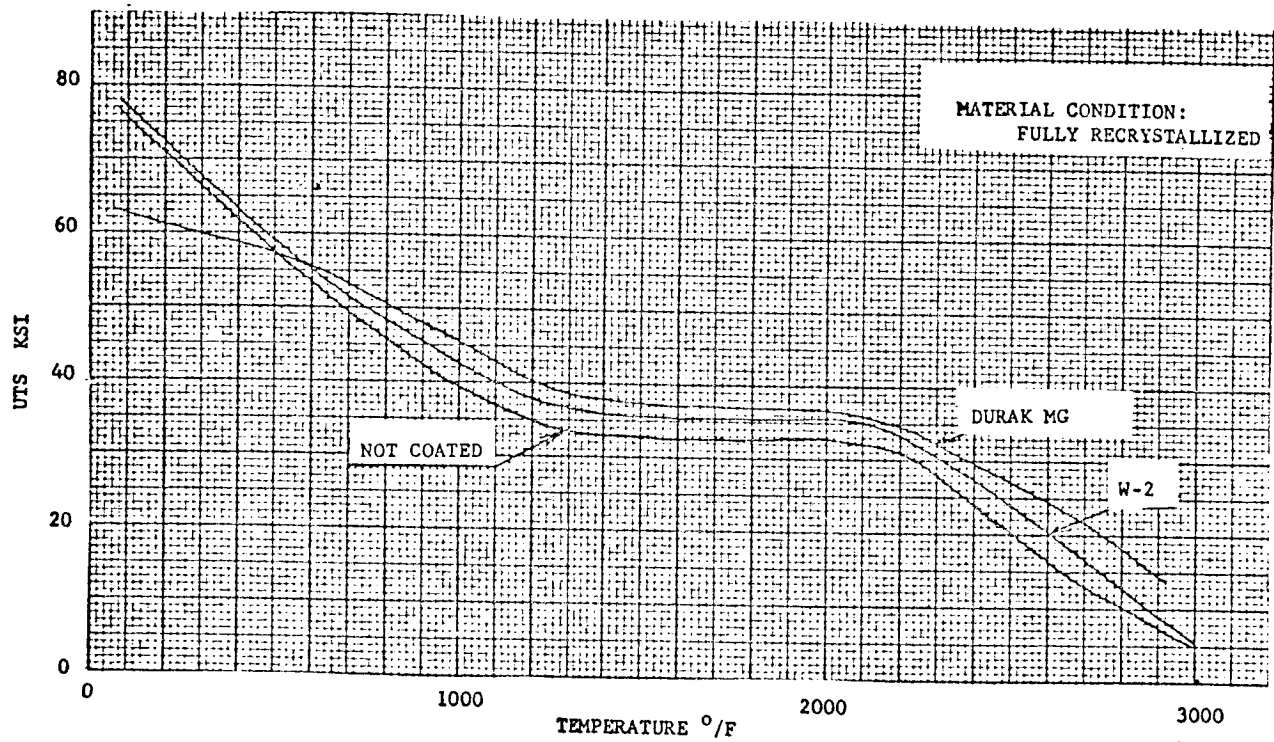
Figure 7



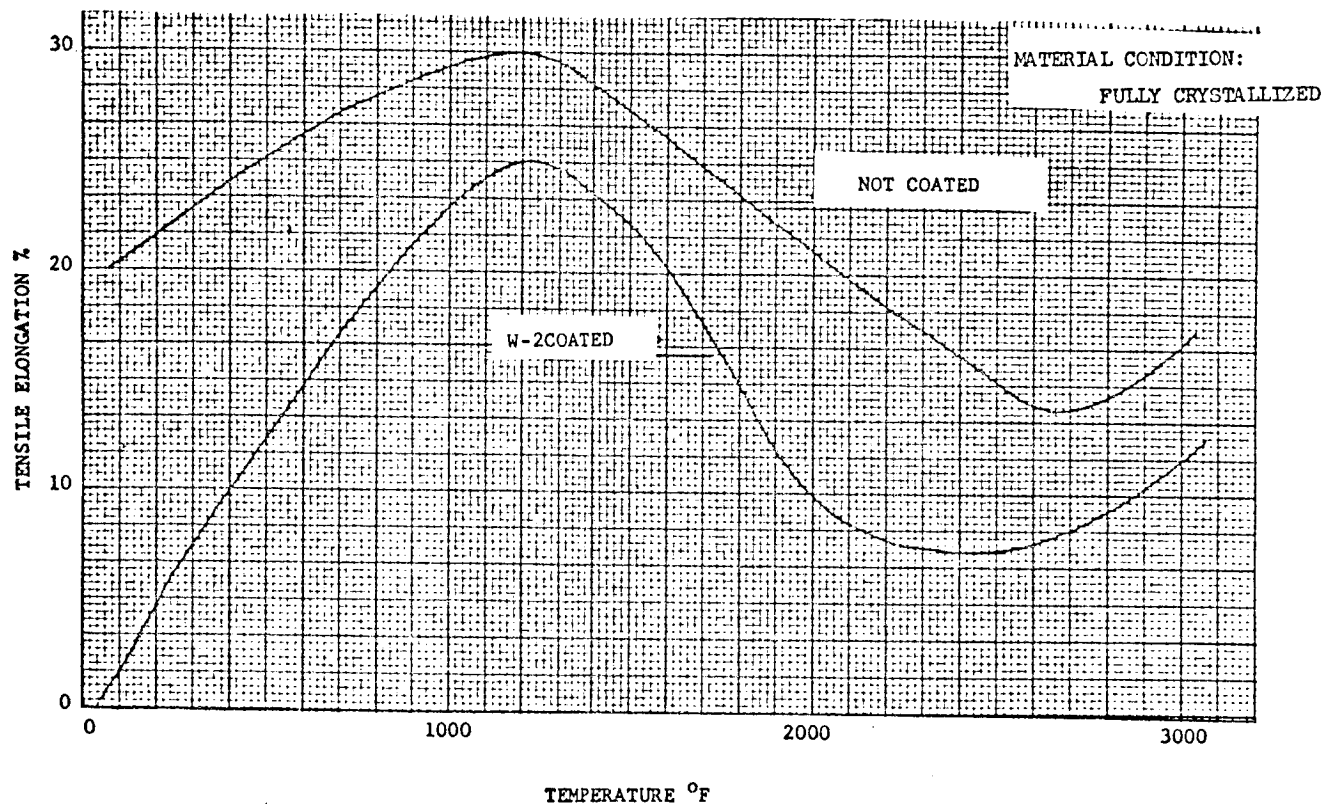
TENSILE STRENGTH OF  
MOLYBDENUM VS MOLYBDENUM DISILICIDE



EFFECT OF DISILICIDE COATINGS  
ON  
ULTIMATE TENSILE STRENGTH  
OF  
0.5% Ti MOLYBDENUM ALLOY



EFFECT OF DISILICIDE COATING  
ON  
TENSILE DUCTILITY



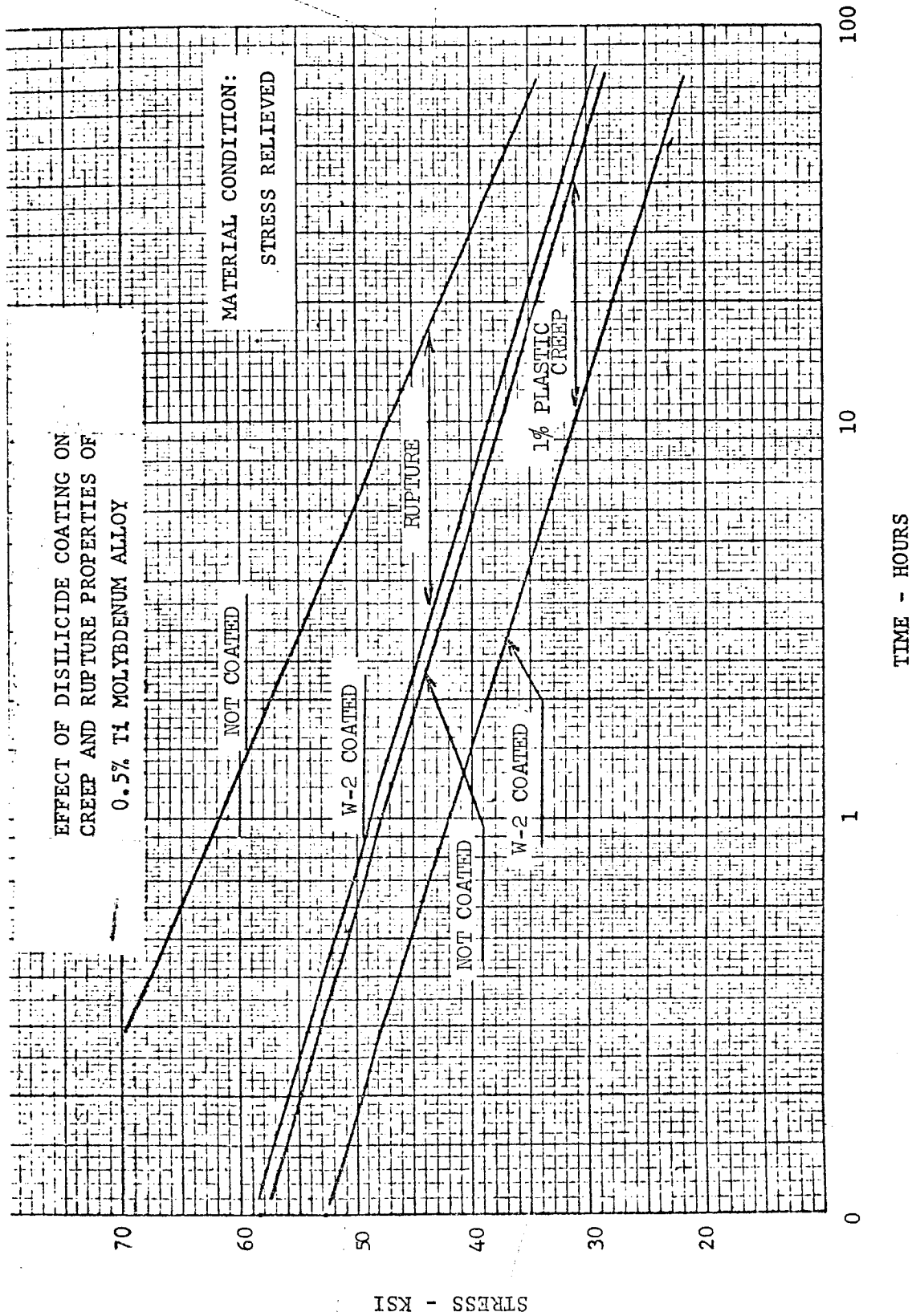
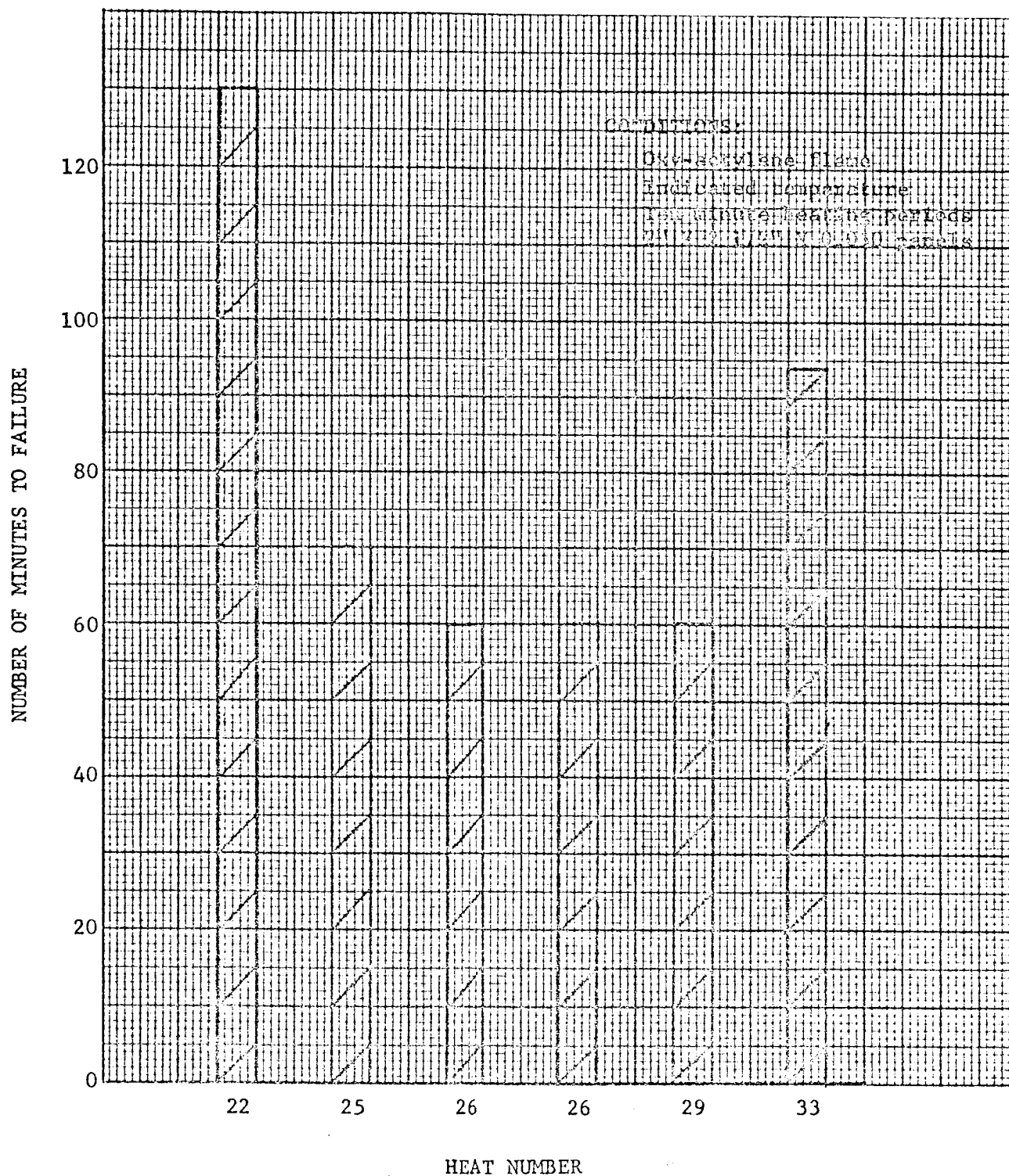


Figure 11

TIME TO FAILURE  
AT 3000° F OF  
TMC DISILICIDE PACK CEMENTATION COATINGS  
ON 0.5% TI MOLYBDENUM SHEET



Concurrent with this survey, The Marquardt Corporation, on other programs, was investigating anti-oxidant coating techniques for improved consistency and reliability, and was testing "in-house" coatings as well as vendor's coatings. Comparative test results favored "in-house" coatings because they were more consistently reliable and able to perform for longer times and at higher temperatures before failure. Therefore, "in-house" coatings were selected by the year's end (1962) for the portion of the program.

These test programs were specifically conducted to permit TMC to keep abreast of all current developments in the field of refractory metals other than molybdenum and the prime alloys were 90TalOW and pure tungsten.

Based on comparative test results, optimized TMC and outside source developed coating techniques were employed to produce anti-oxidation protective coating of disilicide, tin-aluminide, and silicon carbide types on tungsten and 90 TalOW alloy tensile specimens. Both metals received the disilicide coating. Tin-aluminide (GT&E, Long Island, N.Y.) was used only on 90 TalOW alloy while silicon carbide was used only on tungsten. The coated specimens were subjected to tensile, creep-rupture, and cyclic tests at elevated temperatures using the Marquardt TM-1 machine. The tin-aluminide coated 90 TalOW withstood 3500°F, in an air environment for 5 minutes prior to tensile testing. The disilicide coated tungsten and 90 TalOW withstood 2 minutes at 3500°F prior to tensile testing. The silicon carbide coated specimens smoked 30 seconds after heating to only 3000°F. The relative order of merit is therefore clearly defined, as the 90 TalOW with tin-aluminide coating demonstrated complete superiority over the other coated substrate systems.

The disilicide coating on tungsten was 0.003"-0.004" in thickness, while the coating on 90 TalOW was only 0.0009" thickness. The tin-aluminide coating was 0.0031"-0.0041". The silicon carbide coating on tungsten was 0.0015" - 0.002" thickness.

The disilicide type coatings for tungsten and for 90 TalOW were considered capable of application to hardware for use in air up to 3200°F. The tin-aluminide coating for 90 TalOW was useful to 3500°F, or possibly higher, but required additional development and testing. The test results of silicon carbide coating on tungsten were not conclusive.

#### D. Cb Alloy Program

Studies were performed in 1963 on candidate Cb alloys, and protective coating utilized was silicide (TMC's version). Tensile and creep rupture tests were conducted to 2600°F. Braze specimens were also tested. Braze alloys used were C.P. titanium and B120VCZ (Vanadium-Chrome-Aluminum) titanium alloy.

Table I lists the alloys, composition, thickness and source, as well as the braze alloys and form.

TABLE I

EARLY COLUMBIUM DATA

Alloy	Composition	Thickness	Source
D-36	Cb-10 Ti-5Zr	0.031 inch	DuPont
B-66	Cb-5 Va-5Mo-1Zr	0.031 inch	Westinghouse
FS-85	Cb-27 Ta-12W-0.5Zr	0.030 inch	Fansteel
SCb-291	Cb-10 Ta-10W	0.043 inch	Stauffer

Two brazing alloys were investigated:

<u>Alloy</u>	<u>Composition</u>	<u>Form</u>
Ti-75A	Commercially Pure Ti	0.060 wire
Bl20VCA	Ti-11Cr-13V-3Al	0.060 wire and 0.002 in. thick foil

The coatings were evaluated by oxy-acetylene torch testing. Results were inconclusive, although capability to 2600°F was demonstrated by the oxidation resistant coated columbium alloys.

E. Torch Testing of Coated Substrates

A thermal testing program was initiated in 1964 to collate all candidate refractory and super alloy substrate and coating know-how. The object was to coat these materials with the best known oxidation-thermal resistant coatings and evaluate the system by exposing to maximum allowable elevated temperatures. Method of heating was by oxy-propane torch. Table II summarizes the substrates; type of form, coating and coating types evaluated in this program. The results are as follows:

1. Disilicide coated, unalloyed molybdenum afforded two (2) hours minimum oxidation protection at 3000°F.
2. Oxidation protection supplied by coated TZM at 2600°F, and higher, was extremely poor (40 minutes maximum).
3. Four commercially available coatings supplied oxidation protection to 90Ta10W in the 2800°F-3000°F range.

4. Metallographic evaluation of 90Ta10W coatings showed varying degrees of intergranular oxidation of the substrate, with the exception of Sylcor's R508C coating. That coating remained uniform and continuous after thermal exposure.
5. No coatings for C-103 substrate were evaluated above 2700°F because the alloy lasted only 57 minutes at that temperature.
6. Coated L-605 failed in one (1) hour at 2400°F and therefore was not tested at higher temperatures.

Tables III and IV tabulate the pertinent data on torch testing of the candidate substrates and coatings. As can be seen, unalloyed molybdenum coated with Durak B silicide is far superior to any of the other coated substrates. Based on these tests the following conclusions and recommendations were made.

1. Disilicide coated unalloyed molybdenum afforded the best oxidation protection at 3000°F.
2. Coated TZM did not afford adequate oxidation protection above 2600°F.
3. 90 Ta-10W alloy should be considered as the best back-up material for coated unalloyed molybdenum.
4. Work on coated unalloyed molybdenum should be continued.

#### F. Comprehensive Molybdenum Evaluation Program

The thermal testing program initiated in 1964 to collate all data (Sub Section E) was beneficial in the generation of comparative data; however, all trends pointed toward unalloyed molybdenum remaining the prime candidate for thrust chamber fabrication. To reinforce the selection of unalloyed molybdenum, life cycle tests were performed on three (3) forms of unalloyed molybdenum. These forms were forgings, bar and sheet, all suitably coated with Durak B disilicide.

Table V reports the results of testing the three forms of unalloyed molybdenum (Durak B) at 3100°F and 3200°F. An oxy-acetylene torch was utilized to apply and maintain temperature.

Table VI tabulates the results of average coating thickness on bar, forged and sheet stock molybdenum after exposure at 3100°F and 3200°F. Figures 13 through 18 represents life tests on Durak B coated bar, forging and sheet stock of unalloyed molybdenum. All figures are self-explanatory.



Figures 19 through 21 represent photographs of the various zones of temperature encountered during torch testing of the specimens. Tables VII through XII present the results of metallographic examinations which measured the thickness through the coatings at the three zones.

Figure 22 summates the comparative life of forging, bar and sheet unalloyed molybdenum.

TABLE II

SUMMARY OF COATED ALLOYS EVALUATED

Substrate	Type of Stock	Coating Vendor	Coating Type
90Ta-10W	Sheet	Chromizing	MGF, 1-cycle (modified disilicide)
90Ta-10W	Sheet	Chromizing	MGF, 2-cycle (modified disilicide)
90Ta-10W	Sheet	Pfautler	PFR-50 (modified disilicide)
90Ta-10W	Sheet	Sylcor	W* + R508C (modified disilicide)
90Ta-10W	Sheet	Brooktronics	Ir Plate
90Ta-10W	Sheet	North American Rockwell	NAA-85 (aluminide)
TZM	Bar	Chromizing	Durak B (modified disilicide)
TZM	Sheet	Chromizing	Durak B (modified disilicide)
TZM	Sheet	TMC	Disilicide
C-103	Sheet	North American Rockwell	NAA-85 (aluminide)
L-605	Sheet	Brooktronics	Ir Plate with Ni Flash
Unalloyed Moly.	Sheet	Chromizing	Durak B (modified disilicide)

\*Vapor plated diffusion barrier.

TABLE III

TIMES-TO-FAILURE (in minutes) OF TESTED SUBSTRATES AND COATINGS

Temp.	Coating Vendor	90 Ta-10W	TZM Sheet	TZM Bar	C-103	L-605	Unalloyed Molybdenum
3,000°F	Sylcor	100 <sup>(1)</sup>					
	Pfautler	57					
	Chromizing 1-cy.	65					
	No. American	40					
	Rockwell						
	Brooktronics	10					
	Chromizing 2-cy.	29	10	10			120 <sup>(4)</sup>
	TMC		3				
2,900°F	Chromizing 1-cy.	60					
	No. American	40					
	Rockwell						
2,800°F	Sylcor	150 <sup>(1)</sup>					
	Pfautler	79					
	Chromizing 1-cy.	72					
	No. American	150 <sup>(1)</sup>					
	Rockwell						
	Chromizing 2-cy.	50	10				
	TMC		3				
2,700°F	Chromizing 1-cy.	110					
	No. American				57		
	Rockwell						
	Chromizing 2-cy.		40	40			
2,600°F	Sylcor	150 <sup>(2)</sup>					
	Pfautler	130 <sup>(1)</sup>					
	Chromizing 1-cy.	150 <sup>(2)</sup>					
	Brooktronics	23					
	Chromizing 2-cy.		34				
2,500°F	No. American				128		
	Rockwell						
	Brooktronics	60					
2,400°F	Chromizing 2-cy.		150 <sup>(2)</sup>	150 <sup>(2)</sup>		60	
2,200°F	Brooktronics	10 <sup>(3)</sup>				90 <sup>(2)</sup>	

(1) Failure questionable

(2) Not failed.

(3) Heat treated in static air and failed.

(4) Average is based on four (4) samples; 2 failed, 2 did not fail.

TABLE IV

COATING THICKNESS

Substrate	Vendor/Coating	Coating Thickness ( $10^{-3}$ in.)	
		Metallographic	Micrometer
90 Ta-10 W	Sylcor - W + R508C	3.1 - 6.8	6.5
90 Ta-10 W	Pfautler - PFR-50	2.4 - 2.8	2.4
90 Ta-10 W	NAA-85	2.1 - 2.2	2.0
90 Ta-10W	Chromizing/MGF 2-cy.	1.9 - 2.0	1.1
90 Ta-10W	Chromizing/MGF 1-cy.	1.4 - 1.5	0.7
90 Ta-10W	Brooktronics	0.1	-
TZM Bar	Chromizing - Durak B	-	1.6
TZM Sheet	Chromizing - Durak B	2.8 - 4.1	1.6
TZM Sheet	TMC Disilicide	2.2 - 2.4	1.7
Unalloyed Molybdenum	Chromizing Durak B	3.1 - 3.2	1.7
C-103	NAA-85	1.8 - 2.2	2.8
L-605	Brooktronics	-	0.6

TABLE V  
Times to Initial Failure for Coated Molybdenum  
Exposed at 3100°F and 3200°F

Exposure Temperature	Bar Stock		Forged Stock		Sheet Stock	
	Sample #	Time to Failure	Sample #	Time to Failure	Sample #	Time to Failure
3100°F	B-16	6 hrs 30 min	F-1*	6 hrs	S-16	4 hrs 50 min
	B-20	6 hrs	F-15*	4 hrs	S-20	4 hrs 10 min
	B-12	5 hrs 40 min	F-15	4 hrs	S-12	3 hrs 20 min
	B-6	5 hrs 30 min	F-11*	3 hrs 10 min	S-6	2 hrs
	B-11	3 hrs	F-12*	3 hrs	S-11	2 hrs
3200°F	B-19	3 hrs 20 min	F-8*	3 hrs	S-19	1 hr 40 min
	B-14	3 hrs	F-13	1 hr 10 min	S-1	1 hr 10 min
	B-1	2 hrs 50 min	F-19	1 hr	S-8	1 hr 10 min
	B-5	2 hrs	F-14	1 hr	S-14	50 min
	B-8	50 min	F-5	50 min	S-5	40 min

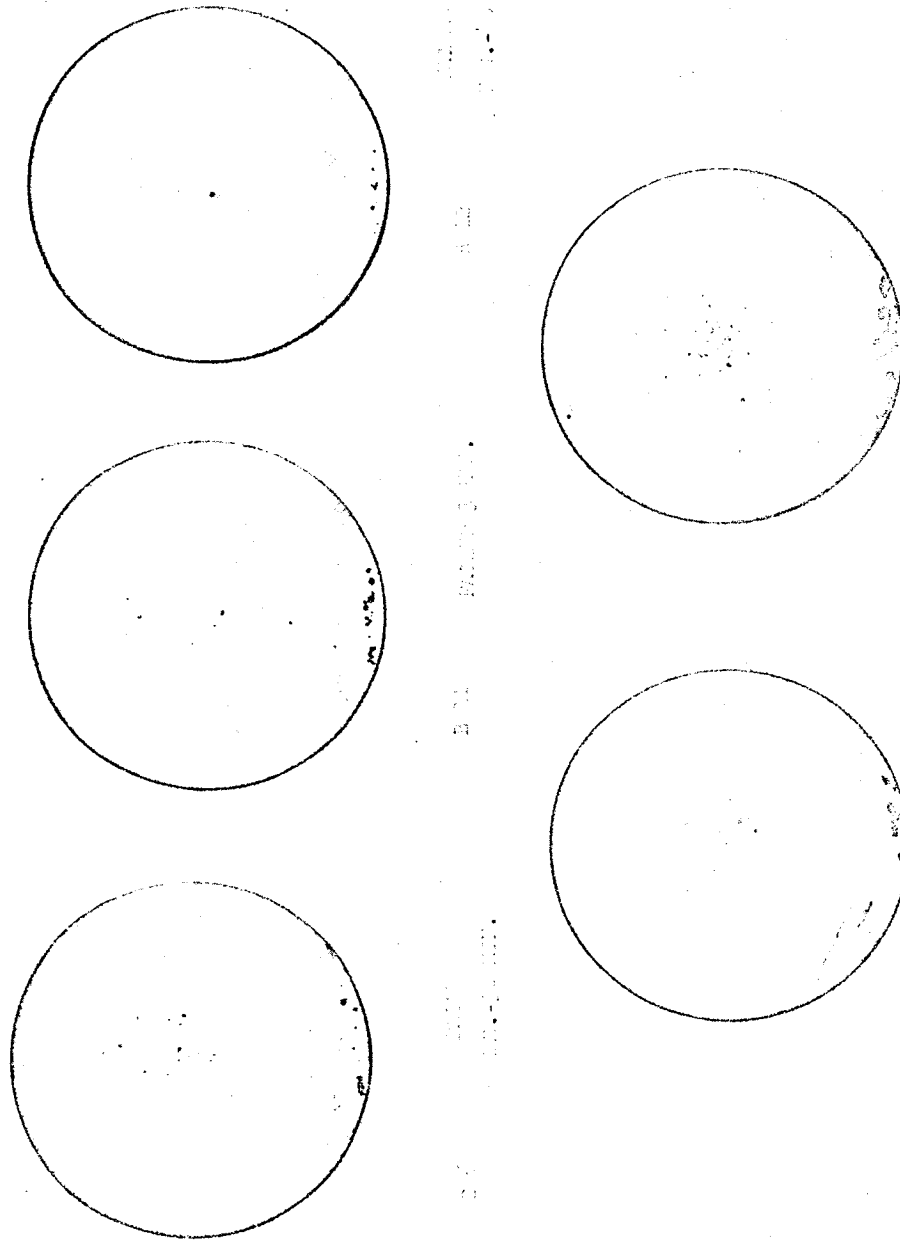
\*Exposure of these samples was continued to "burn through." (F-11, 5 hrs; F-1, 9 hrs 10 min; F-12, 5 hrs 50 min; F-19, 3 hrs; F-8, 4 hrs 50 min)

TABLE VI

Average Coating Thickness Measured on Specimens  
After Exposure to 3100°F and 3200°F

Exposure Temperature	Bar Stock	Forged Stock	Sheet Stock
	Average Coating Thickness	Average Coating Thickness	Average Coating Thickness
3100°F	0.0045	0.0045	0.0048
	0.0043	0.0049	0.0042
	0.0041	0.0045	0.0037
	0.0043	0.0040	0.0038
	0.0037	0.0043	0.0035
3200°F	0.0043	0.0045	0.0042
	0.0043	0.0037	0.0039
	0.0040	0.0041	0.0036
	0.0041	0.0040	0.0038
	0.0038	0.0038	0.0035

NEG. 5095-5



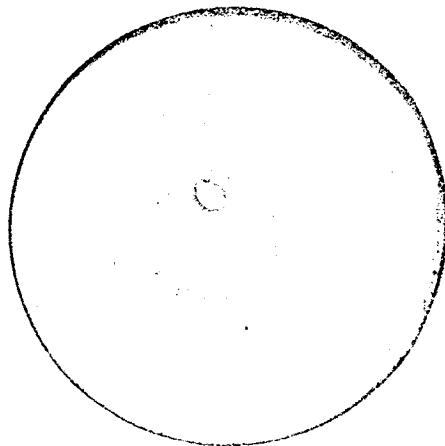
Molybdenum Bar Stock after 3100°F Test

11-25

Figure 13

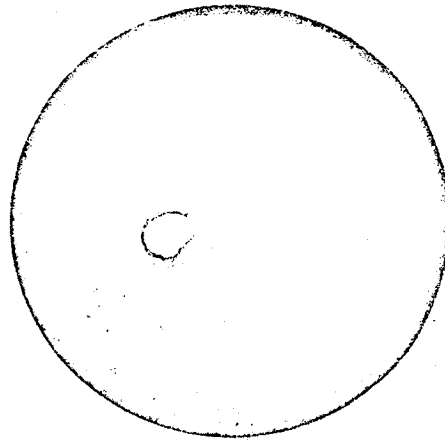
NEG. 5095-1

CHRYSLER CORP. 1/16" THICK 3100°F  
FABRICATION TRUE TEMPERATURE



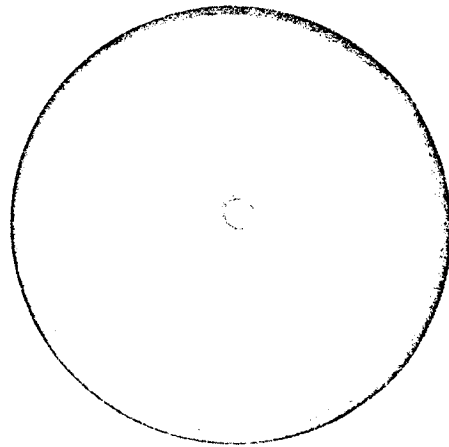
FAILED 6 HRS.  
BURN THRU  
3 HRS-10 MIN.

F-10



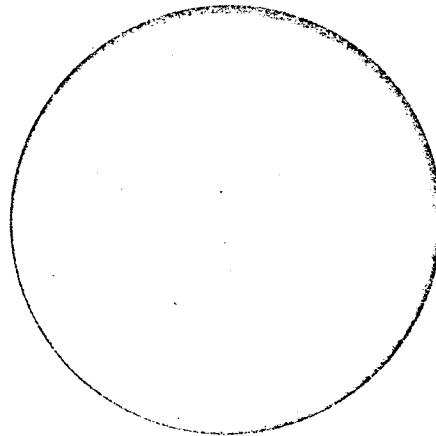
FAILED  
3 HRS-10 MIN.  
BURN THRU 5 HRS.

F-11



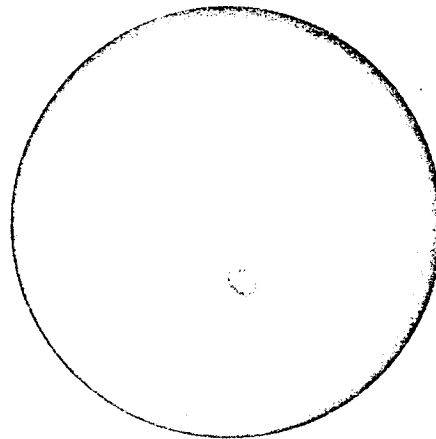
FAILED 3 HRS.  
BURN THRU  
5 HRS-50 MIN.

F-12



FAILED 4 HRS.

F-15



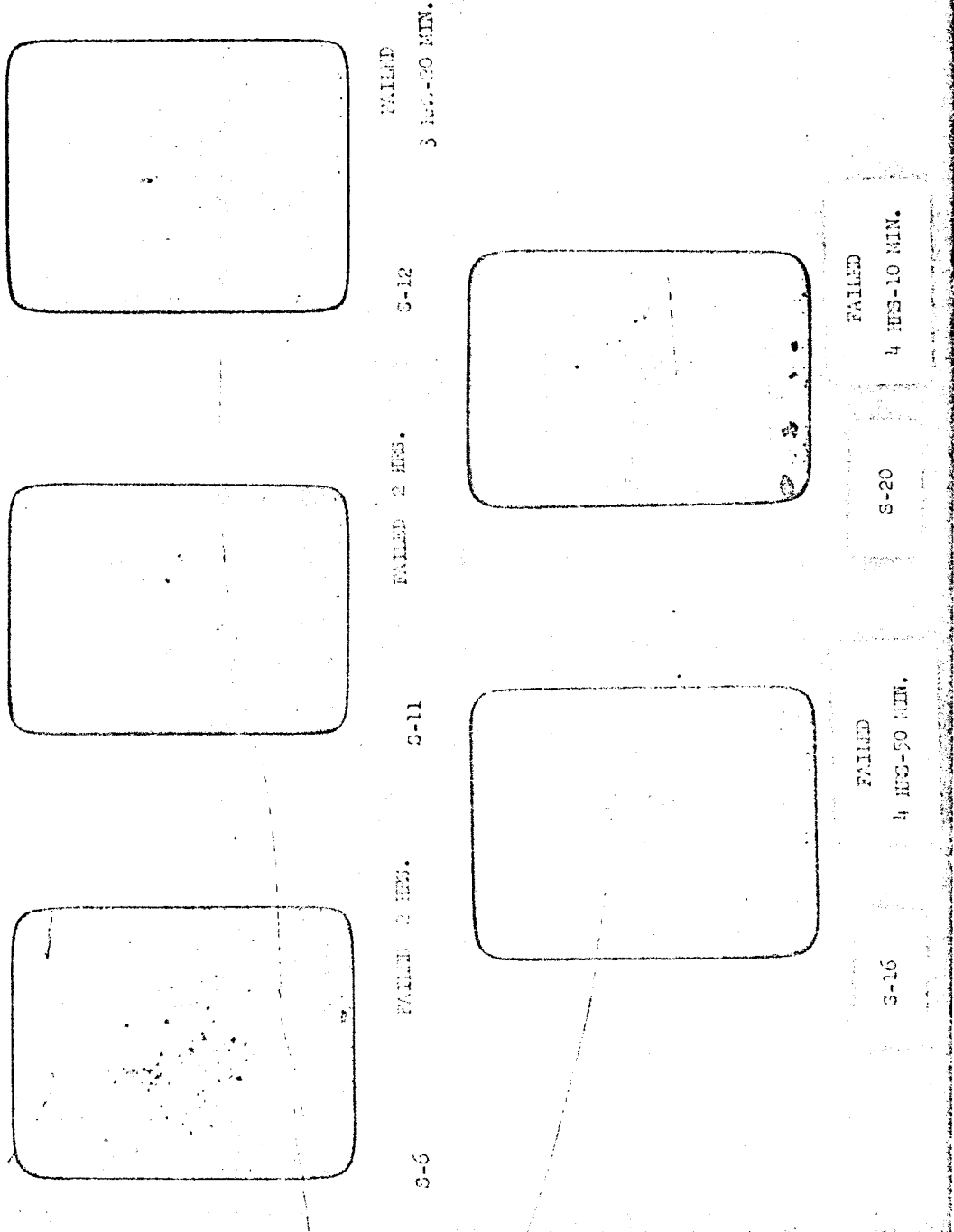
FAILED 4 HRS.  
BURN THRU 7 HRS.

F-16

Molybdenum Forgings after 3100°F Test

NEG. 5095-3

CHROMIUM CORP. 1/16" THICK 3100°F  
NOS. 2 SHEET STOCK TRUE TEMPERATURE



Molybdenum Sheet Stock after 3100°F Test

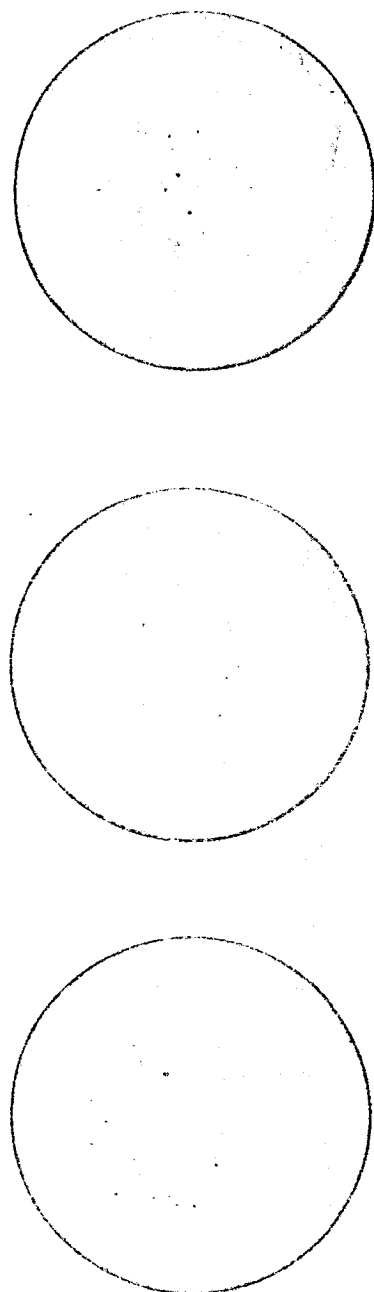
11-27

Figure 15

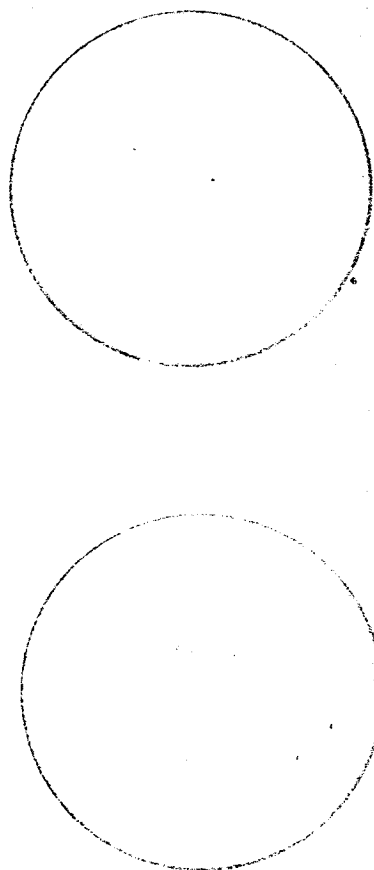


NEG. 5095-6

CHROMIUM CARB. 1/16" THICK  
MOLYB  
TWO SPECIMENS



B 1 FAILED 2 HRS.-30 MIN.  
B 5 FAILED 2 HRS.  
B 8 FAILED 30 MIN.



B 14 FAILED 3 HRS.  
B 19 FAILED 3 HRS.-20 MIN.

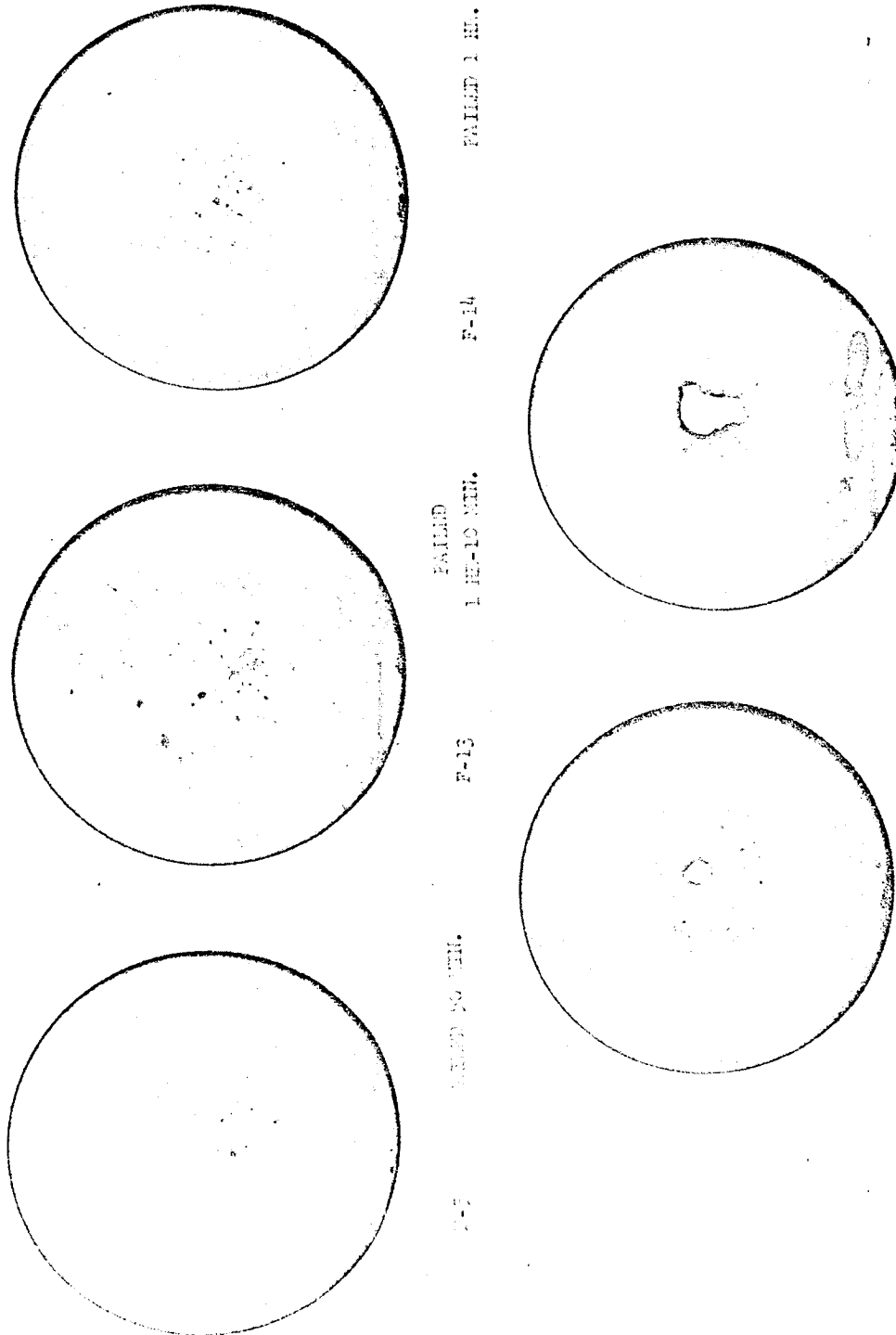
Molybdenum Bar Stock After 3200°F Test

11-28

Figure 16

NEG. 5095-2

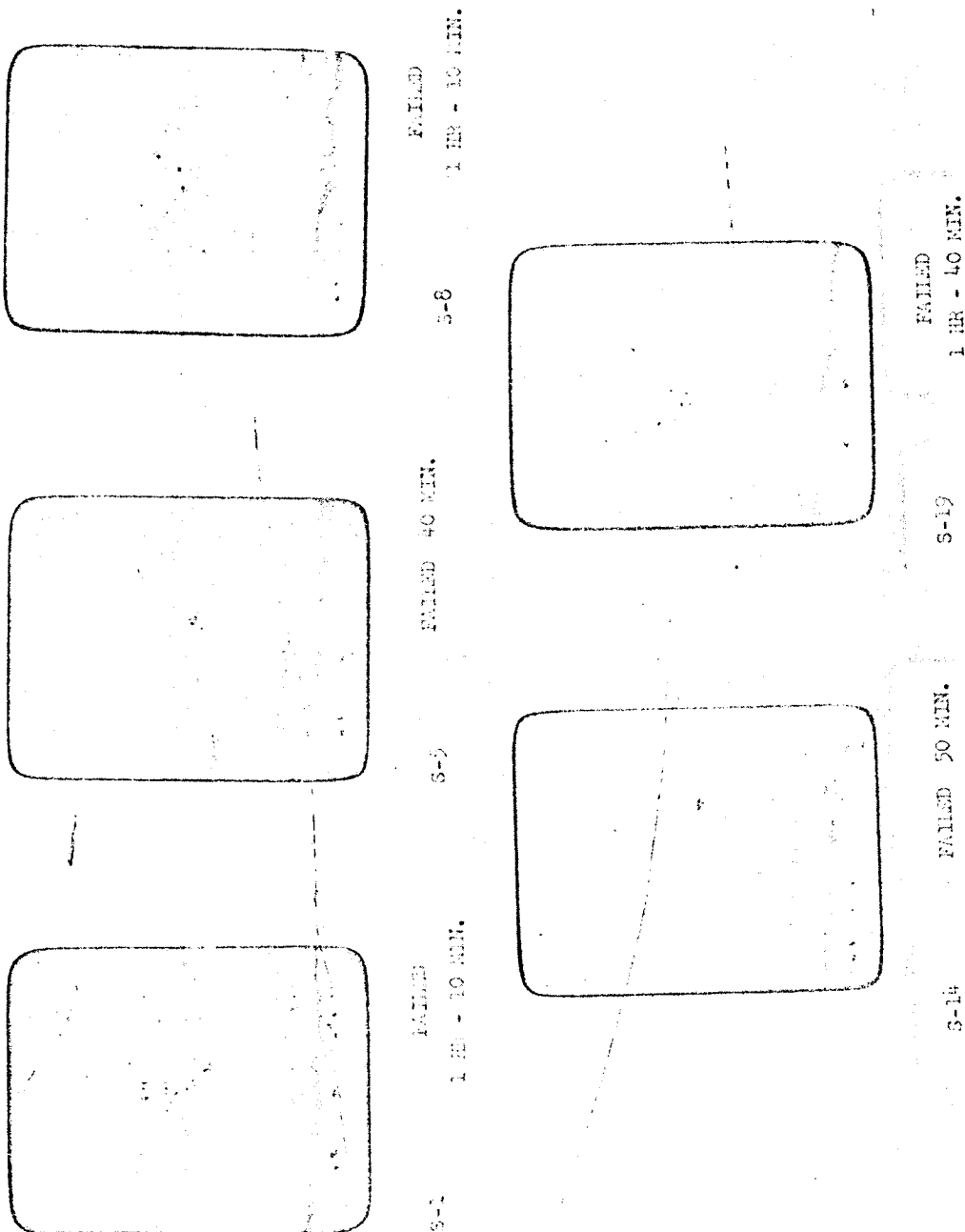
3200°F  
TRUE TEMPERATURE  
1/16" THICK  
FORGINGS



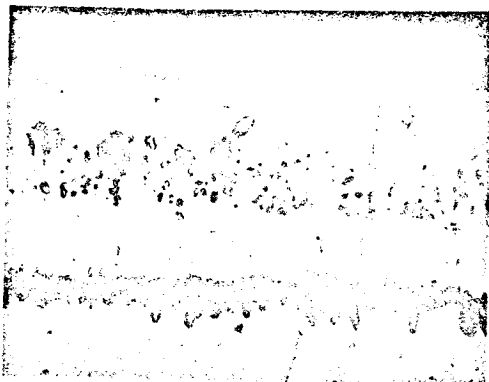
Molybdenum Forgings after 3200°F Test

NEG. 5095-4

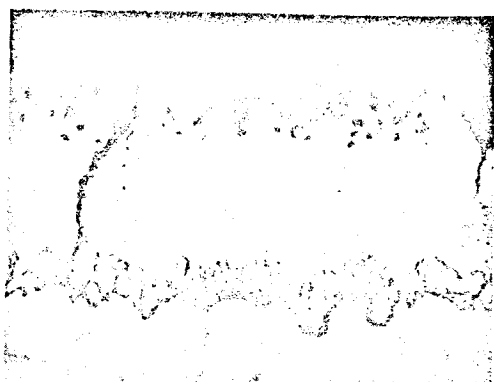
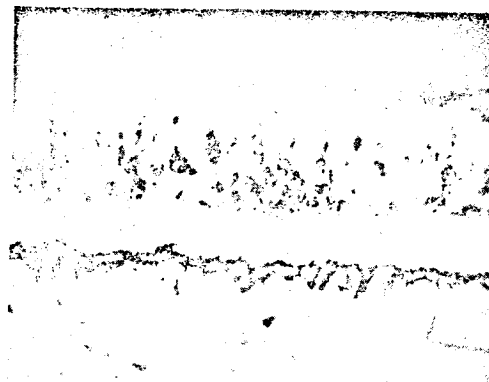
CHRYSLER CORP. 1/16" THICK 3200°F  
SHEET STOCK TRUE TEMPERATURE



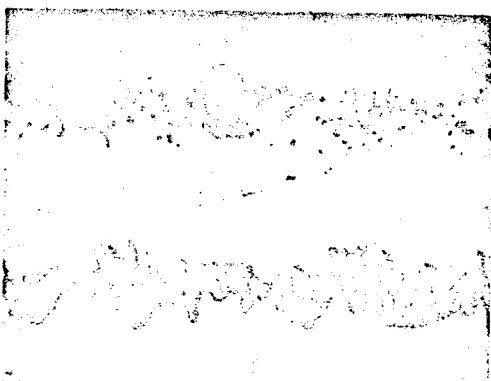
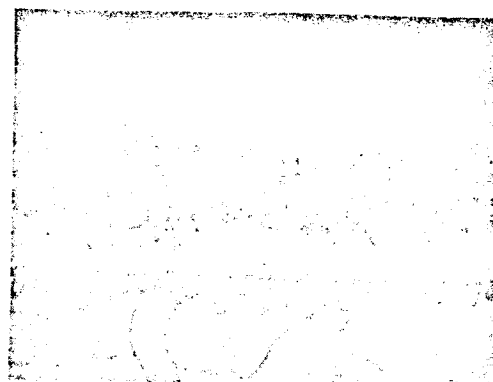
Molybdenum Sheet Stock after 3200°F Test



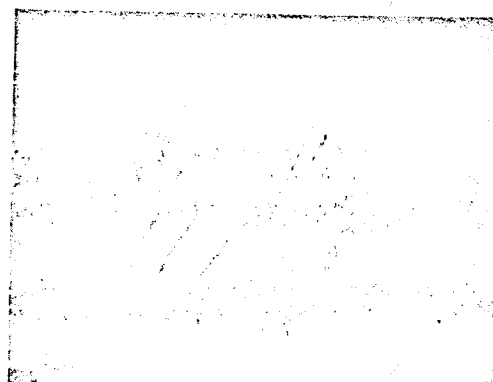
COLD  
ZONE



INTERMEDIATE  
ZONE



HOT  
ZONE

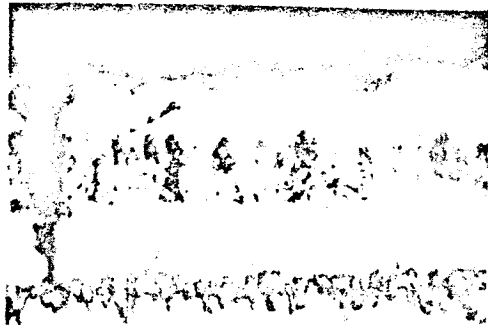


3100°F  
SAMPLE NO. B-16  
POLISH - ETCH - BUFF

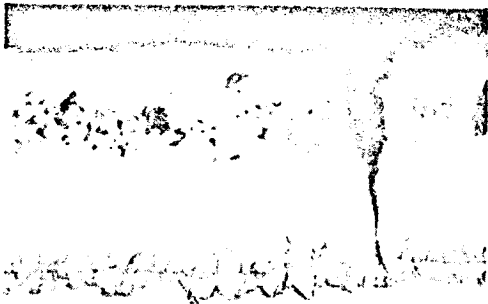
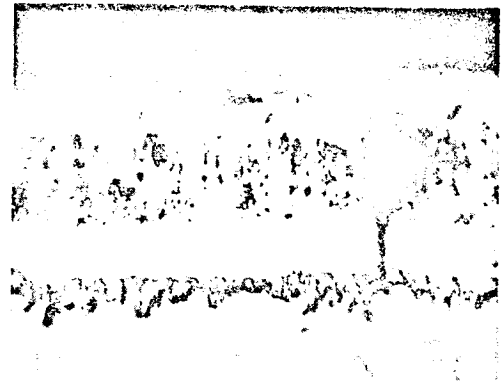
3200°F  
SAMPLE NO. B-8  
MAGNIFICATION X500

NEG. C5095-7

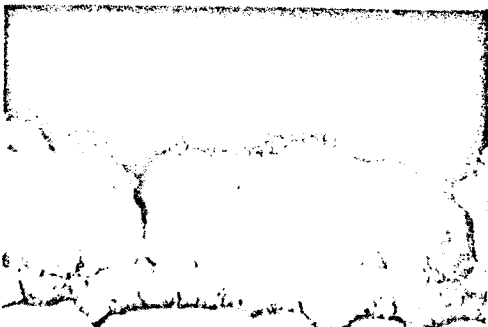
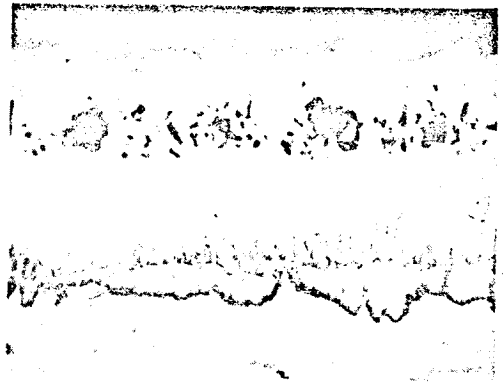
PHOTOMICROGRAPHS OF UNALLOYED  
MOLYBDENUM BAR STOCK



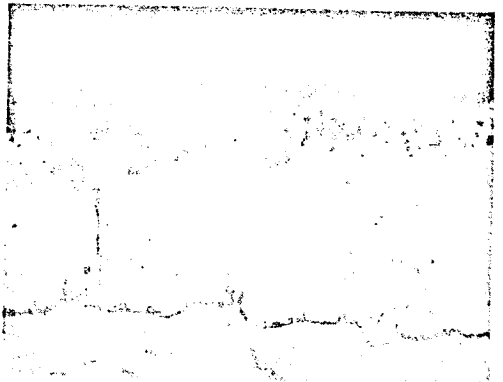
COLD  
ZONE



INTERMEDIATE  
ZONE



HOT  
ZONE



NEG. C5095-8

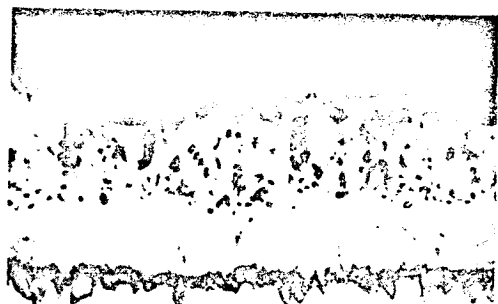
3100°F  
SAMPLE NO. F-1  
POLISH - ETCH - BUFF

3200°F  
SAMPLE NO. F-8  
MAGNIFICATION X500

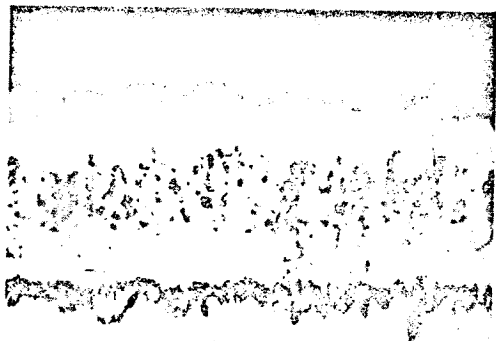
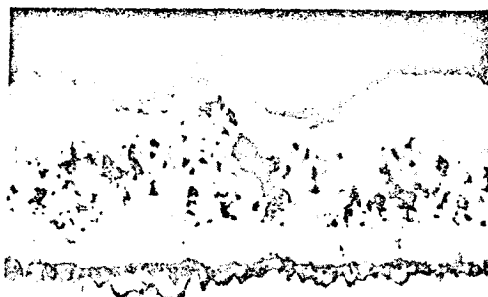
PHOTOMICROGRAPHS OF UNALLOYED  
MOLYBDENUM FORGED STOCK

11-32

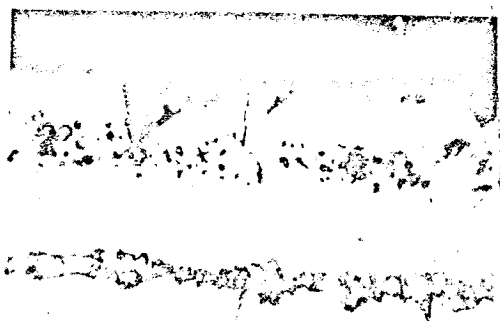
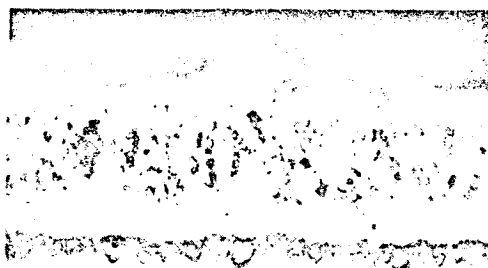
Figure 20



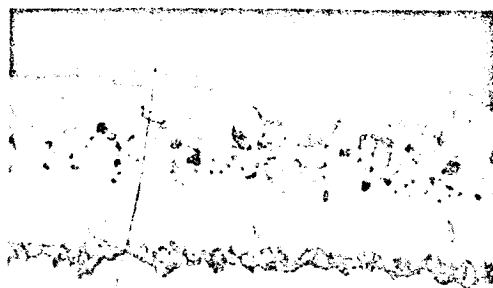
COLD  
ZONE



INTERMEDIATE  
ZONE



HOT  
ZONE



3100 F  
SAMPLE NO. S-6  
POLISH - ETCH - BUFF

3200°F  
SAMPLE NO. S-5  
MAGNIFICATION X500

PHOTOMICROGRAPHS OF UNALLOYED  
MOLYBDENUM SHEET STOCK

TABLE VII

Metallographic Thickness Data

Sample #	Molybdenum Sheet Stock After Exposure at 3100°F					
	Z O N E					
	Cold	Medium	Hot	Hot	Hot	Cold
S-16	0.0048	0.0049	0.0049	0.0047	0.0049	0.0048
S-20	0.0044	0.0043	0.0039	0.0042	0.0043	0.0040
S-12	0.0037	0.0038	0.0038	0.0037	0.0038	0.0035
S-6	0.0036	0.0040	0.0038	0.0037	0.0038	0.0039
S-11	0.0035	0.0036	0.0033	0.0034	0.0036	0.0034

TABLE VIII

Metallographic Thickness Data

Sample #	Molybdenum Sheet Stock After Exposure at 3200°F					
	Z O N E					
	Cold	Medium	Hot	Hot	Hot	Cold
S-19	0.0044	0.0042	0.0041	0.0043	0.0042	0.0042
S-1	0.0035	0.0037	0.0039	0.0039	0.0041	0.0039
S-8	0.0034	0.0033	0.0035	0.0037	0.0037	0.0038
S-14	0.0038	0.0039	0.0038	0.0035	0.0040	0.0039
S-5	0.0035	0.0034	0.0036	0.0036	0.0036	0.0036

TABLE IX  
Metallographic Thickness Data

Molybdenum Bar Stock After Exposure at 3100°F						
Z O N E						
Cold	Medium	Hot	Hot	Hot	Medium	Cold
0.0045	0.0047	0.0046	0.0048	0.0046	0.0041	0.0042
0.0041	0.0043	0.0044	0.0045	0.0044	0.0041	0.0040
0.0038	0.0040	0.0041	0.0040	0.0041	0.0043	0.0042
0.0043	0.0042	0.0042	0.0042	0.0043	0.0044	0.0043
0.0035	0.0035	0.0036	0.0036	0.0039	0.0039	0.0038

TABLE X  
Metallographic Thickness Data

Molybdenum Bar Stock After Exposure at 3200°F						
Z O N E						
Cold	Medium	Hot	Hot	Hot	Medium	Cold
0.0041	0.0043	0.0043	0.0043	0.0046	0.0041	0.0044
0.0041	0.0041	0.0042	0.0045	0.0045	0.0045	0.0045
0.0036	0.0040	0.0040	0.0040	0.0040	0.0041	0.0040
0.0038	0.0039	0.0040	0.0041	0.0041	0.0043	0.0043
0.0038	0.0036	0.0038	0.0039	0.0039	0.0038	0.0038



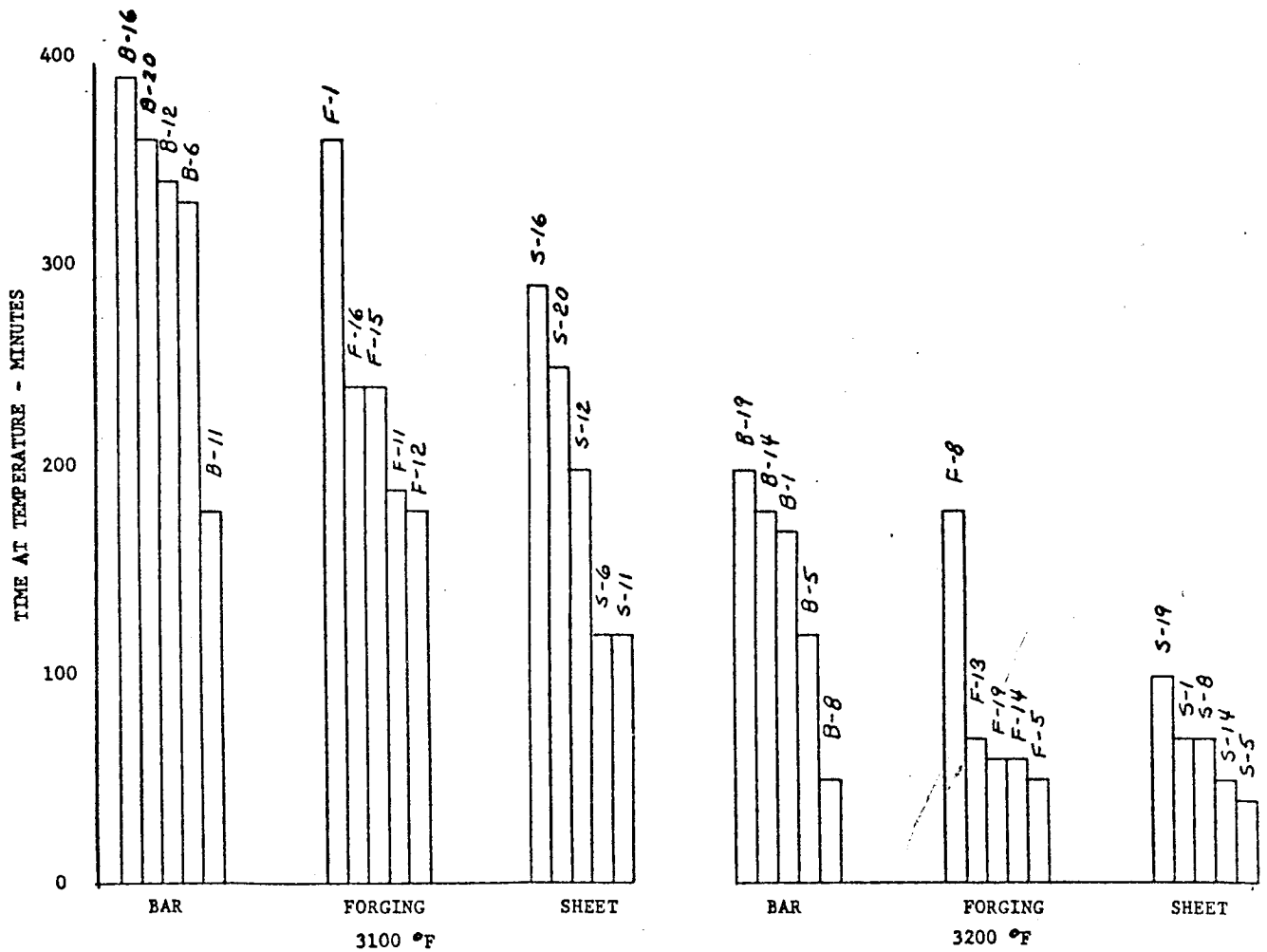
TABLE XI  
Metallographic Thickness Data

Molybdenum Forged Stock After Exposure at 3100°F									
Z O N E									
Cold		Medium		Hot		Medium		Cold	
0.0040	0.0041	0.0041	0.0041	0.0047	0.0036	0.0051	0.0053	0.0050	0.0048
0.0045	0.0045	0.0050	0.0050	0.0053	0.0049				
0.0044	0.0044	0.0047	0.0048	0.0046	0.0043	0.0043	0.0043	0.0043	0.0042
0.0039	0.0039	0.0038	0.0040	0.0043	0.0043	0.0041	0.0040	0.0038	0.0037
0.0040	0.0042	0.0045	0.0044	0.0047	0.0047	0.0044	0.0040	0.0041	0.0041

TABLE XII  
Metallographic Thickness Data

Molybdenum Forged Stock After Exposure at 3200°F									
Z O N E									
Cold		Medium		Hot		Medium		Cold	
0.0044	0.0044	0.0044	0.0045	0.0047	0.0048	0.0048	0.0044	0.0041	0.0041
0.0037	0.0038	0.0039	0.0037	0.0036	0.0040	0.0034	0.0037	0.0034	0.0034
0.0038	0.0038	0.0040	0.0042	0.0044	0.0043	0.0041	0.0040	0.0041	0.0043
0.0039	0.0037	0.0035	0.0040	0.0041	0.0043	0.0040	0.0041	0.0041	0.0042
0.0037	0.0040	0.0036	0.0037	0.0038	0.0036	0.0036	0.0039	0.0039	

COMPARATIVE LIFE  
OF FORGING, BAR, SHEET STOCK  
AT 3100°F & 3200°F TRUE TEMPERATURE



The conclusions drawn from this life cycle program may be stated as follows:

1. Increasing the temperature from 3100°F to 3200°F, lessens the "time-to-failure" by a factor of two.
2. Decreasing coating thickness will decrease the time to failure.
3. Forgings and bar are superior to sheet molybdenum.
4. Unalloyed molybdenum, coated with Durak B disilicide is satisfactory to 3100°F for long periods of time.

Tables XIII reports on typical properties (General Electric Data) of P/S unalloyed molybdenum at various temperatures in cold worked (Stress relieved) and Annealed (Recrystallized) conditions.

### III. THRUST CHAMBER CHRONOLOGICAL DEVELOPMENT

The original combustor on an early engine is shown in Figure 23. The smooth cylindrical section and integral bell were fabricated from a press-sintered-forged preform-floturned molybdenum and coated with moly disilicide. This is one of the first experimental high purity moly thrust chambers made by Viking Forge and analyzed by General Electric Company, Cleveland, Ohio, for TMC. The success of the flow-turn (shear spinning) operation on unalloyed molybdenum forging convinced TMC to order and install a Flow Turn machine at the Van Nuys Facility (Figures 24 and 25).

The chronological development of the R-4D chamber is shown in Figure 26. The first altitude chambers (Figure 27) were unalloyed molybdenum coated with molydisilicide. The inside dimensions, throat, chamber length from injector face to throat and expansion bell are identical to the present chamber. In February, 1964, ribs were added to strengthen the chamber (Figure 28) so it would better withstand the ignition overpressures that had broken several non-ribbed chambers. After the preigniter was successfully developed, the ribbed configuration was maintained. To avoid possible handling problems and to increase its strength, the bell material was changed from molybdenum to L-605 stainless steel while the combustor material remained molybdenum (Figure 29). The combustor and chamber were fastened together with a Waspaloy nut. Ribs were added to the L-605 bell in September, 1964, to increase its strength without an increase in weight. The final two piece chamber is shown in Figure 30.

TABLE XIII

PROPERTIES OF P/S UNALLOYED MOLYBDENUM

Modulus of Elasticity

<u>Temperature</u>	<u>E x 10<sup>6</sup> P.S.I.</u>
Room	48
500°C	44
1000°C	40
1200°C	38
1400°C	36
1600°C	34

Tensile Test Data (Wrought-stress relief at 925°C).

<u>Temperature</u>	<u>U.T.S.</u>	<u>.2% Y.S.</u>	<u>% Elongation in 1"</u>
70°F	118,400	93,900	16%
600°F	90,990	71,200	11%
1000°F	78,100	61,600	6%
1600°F	67,600	46,800	5%
2200°F	17,140	6,950	54%
2600°F	10,690	5,320	63%
2800°F	9,020	4,660	58%

Tensile Test Data (recrystallized)

<u>Temperature</u>	<u>U.T.S.</u>	<u>.2% Y.S.</u>	<u>% Elongation in 1"</u>
70°F	77,900	72,400	42%
600°F	54,650	49,050	40%
1000°F	38,800	13,000	39%
1600°F	30,900	9,475	46%
2200°F	15,100	6,210	65%
2600°F	9,410	3,990	74%
2800°F	7,790	3,930	36%

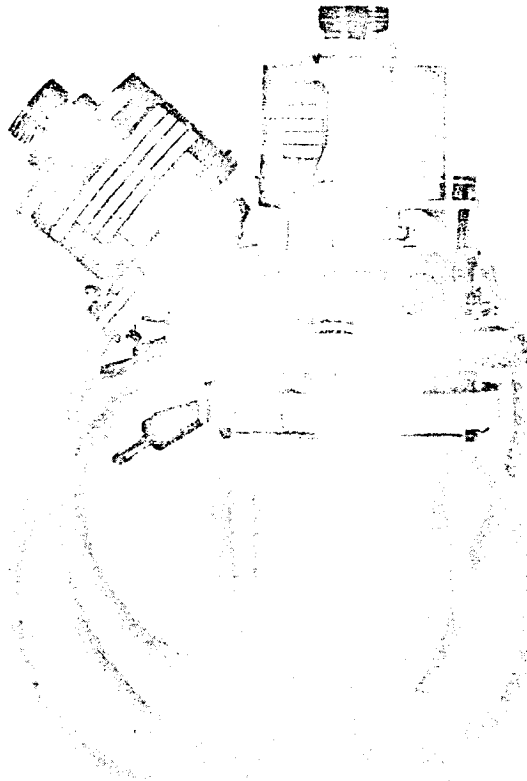
1. Above values are typical values and may vary depending on test conditions and material history.
2. Strain rate (room temperature to 1900°F) 0.005 in/in/min. to 0.6% offset, 0.05 in/in/min. to fracture.
3. Strain rate (2000°F to 2900°F) 0.01 in/in/min. to 0.6% offset, 0.10 in/in/min. to fracture.

TABLE XIII (continued)

Impact Resistance Pure Molybdenum

<u>Material Condition</u>	<u>Temperature</u>	<u>Impact Resistance (Ft.-Lbs.)</u>
Annealed	Room	30.0 ±
Annealed } Stress	0°C	18.0 -- 30.00
Annealed } - Relieved	-97°C	8.00-- 12.00
R x Y-	Room	1.0 -- 4.0
R x Y,	0°C	1.0 -- 2.0
R x Y,	-97°C	1.0 -- 2.0
20%-30% R x Y.	Room	5.0 -- 8.0

1. Above values obtained on un-notched standard Izod type specimens using 24" fall, (11.4 ft./sec.) and 15 lb. bob.
2. Values are averages or typical ranges of values that can be expected.
3. These values are representative of both rolled plate and forged parts made by a good metallurgical practice.



NEG. 6839-2

Original Engine

11-41

Figure 23

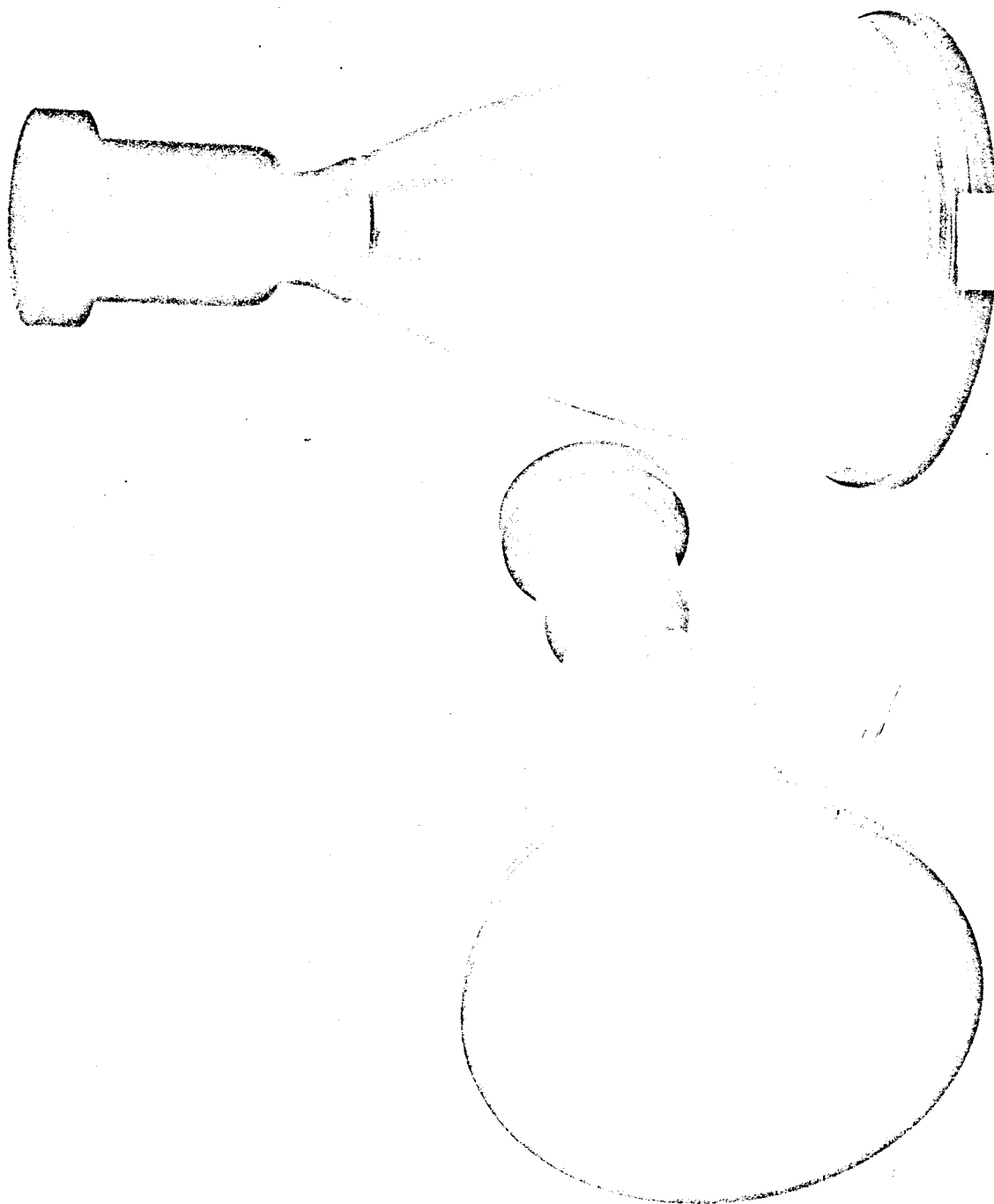


NEG. 4651-28

Flo-Turn Lathe

11-42

Figure 24

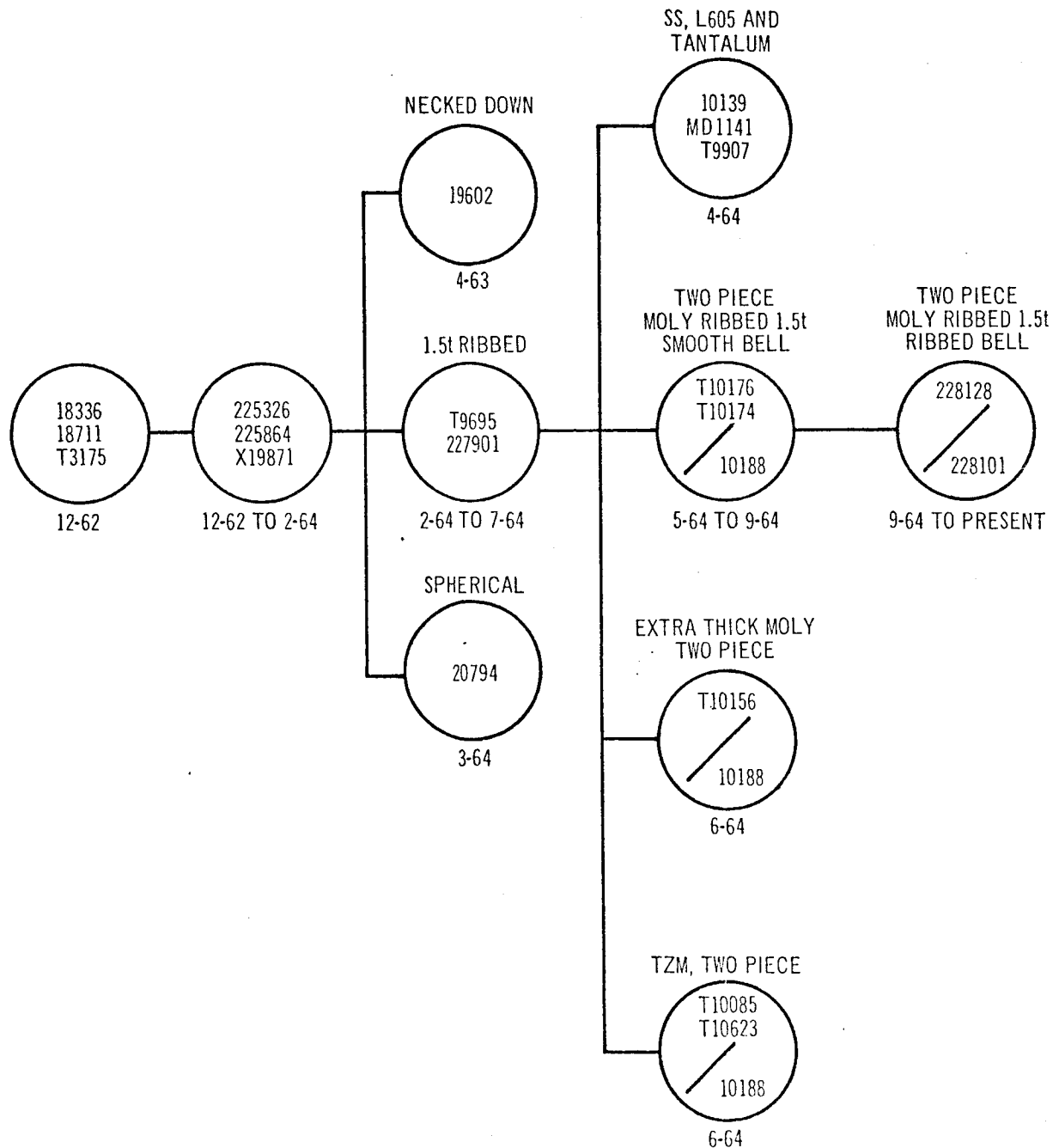


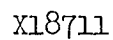
NEG. 4799-1

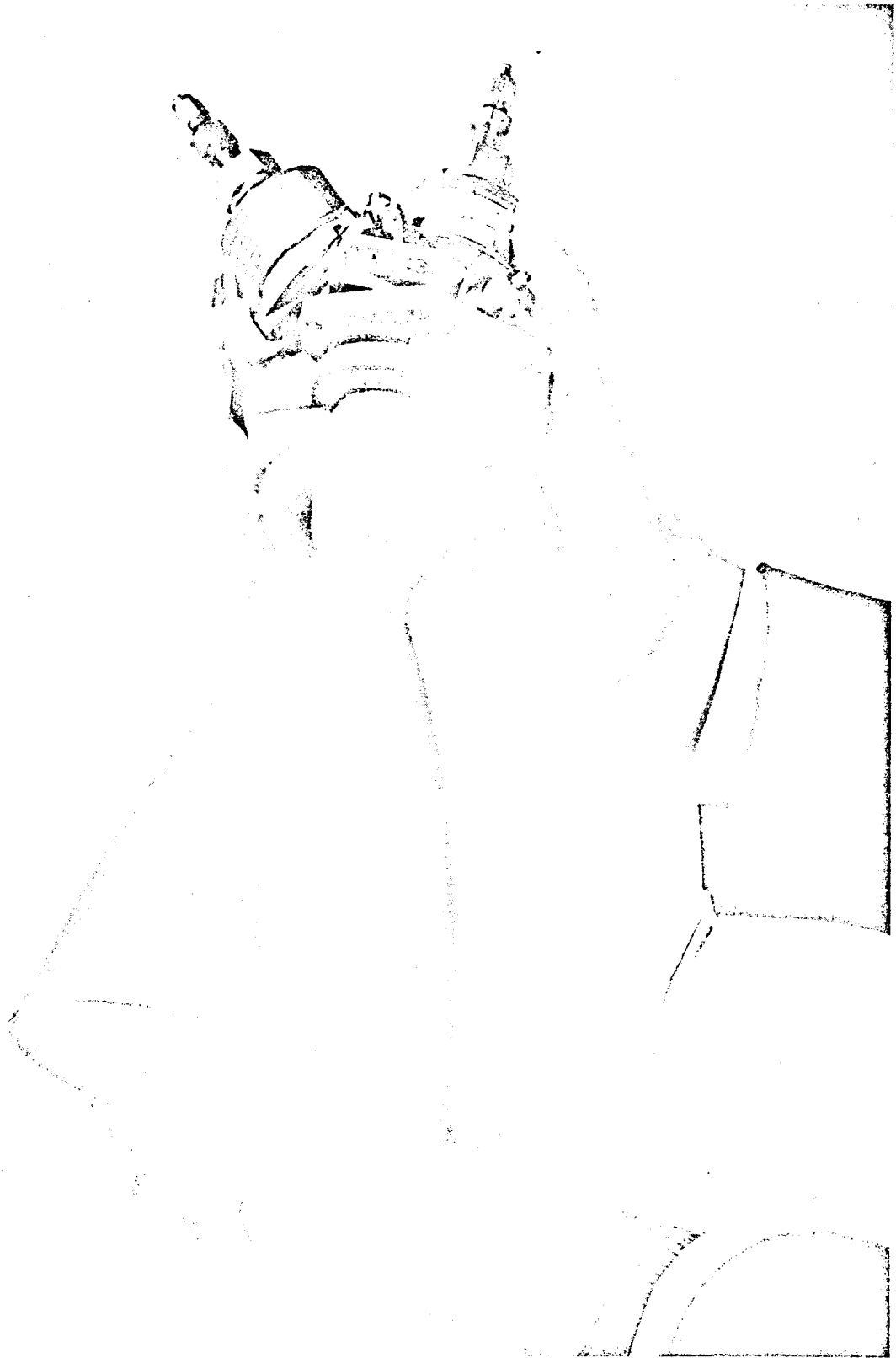
Flo-Turn Molybdenum Combustion Chambers



## CHAMBER CHRONOLOGY

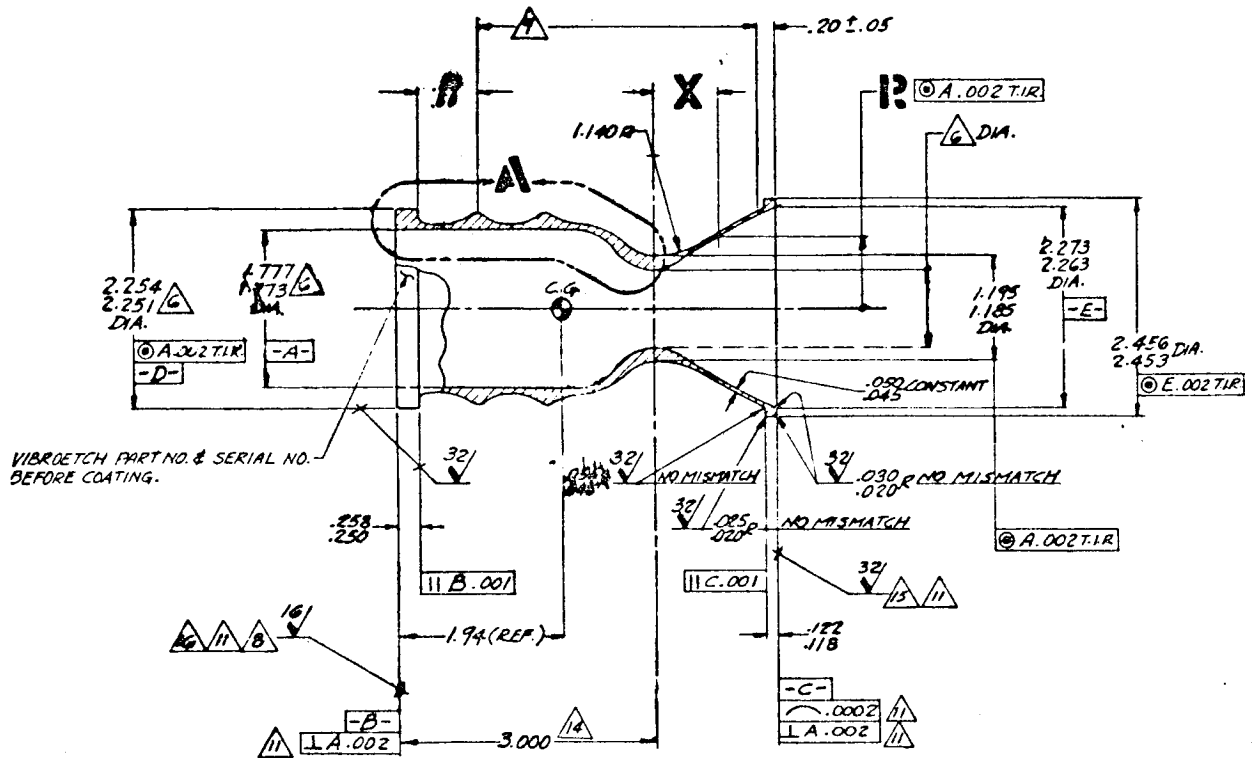






NEG. 6028-1

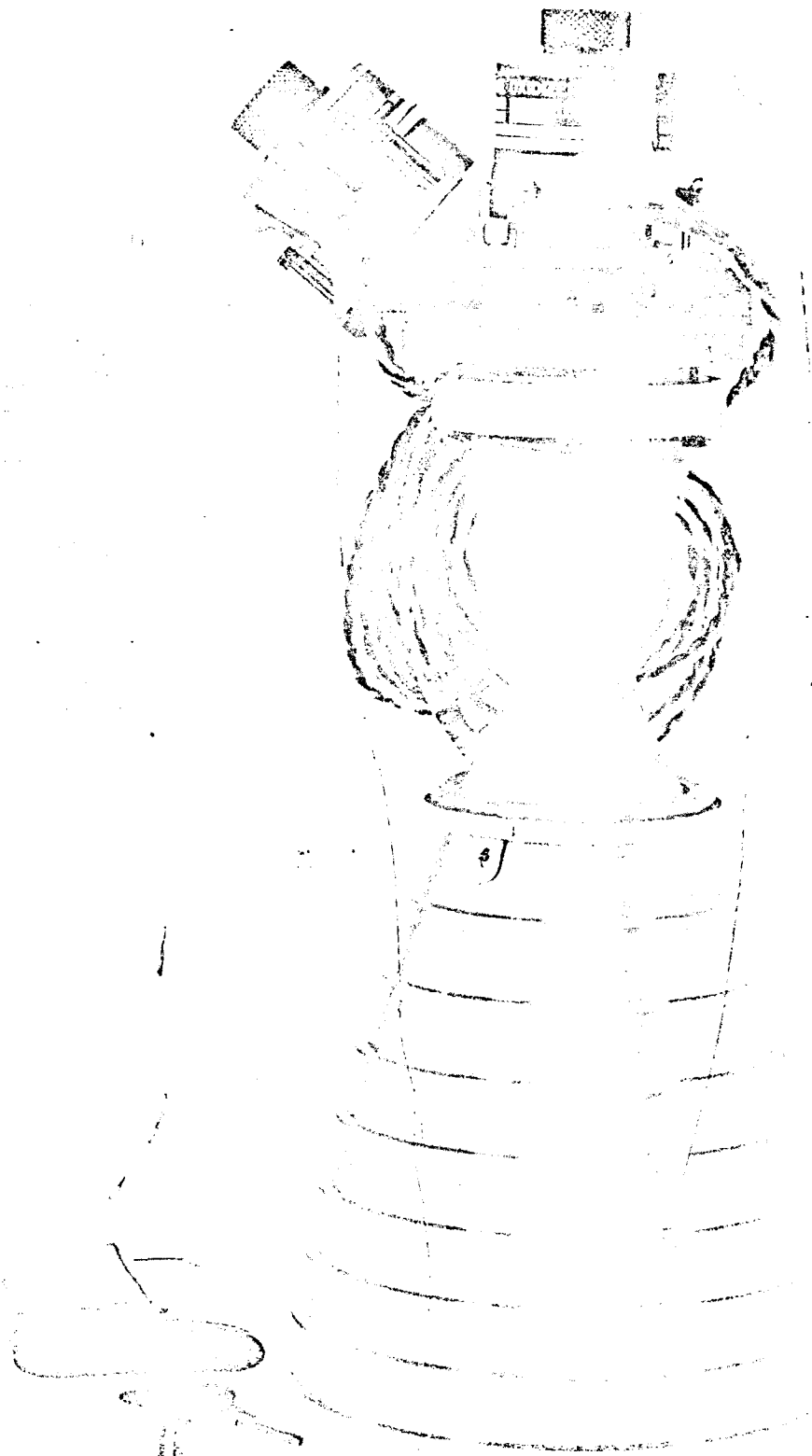
Engine with Ribbed One Piece Combustor



X BASIC	R	R ± TOL.
.000	.434	.0020
.270	.513	.0025
.474	.635	.0025
.812	.832	.0025
1.339	1.106	.0025
1.400	1.134	.0025

TWO PIECE CHAMBER

228128



NEG. 6839-3

Engine with Two Piece Chamber  
11-48

Figure 30

Other chamber configurations were also built and tested but dropped because they did not have an advantage over the R-4D chamber at that time or the lack of experience compared to the R-4D's outweighed a possible advantage. A chamber with a necked down area at the injector face (Figure 31) tested in April 1963, did not improve the performance as was hoped. A spherical chamber, Figure 32, tested in January 1964, did not eliminate ignition overpressures and it also ran hotter. The spherical chamber was tried because the ignition overpressure appeared to be gas-vapor phase detonations traveling from the throat toward the injector face that might be suppressed or eliminated by the shape of the spherical chamber.

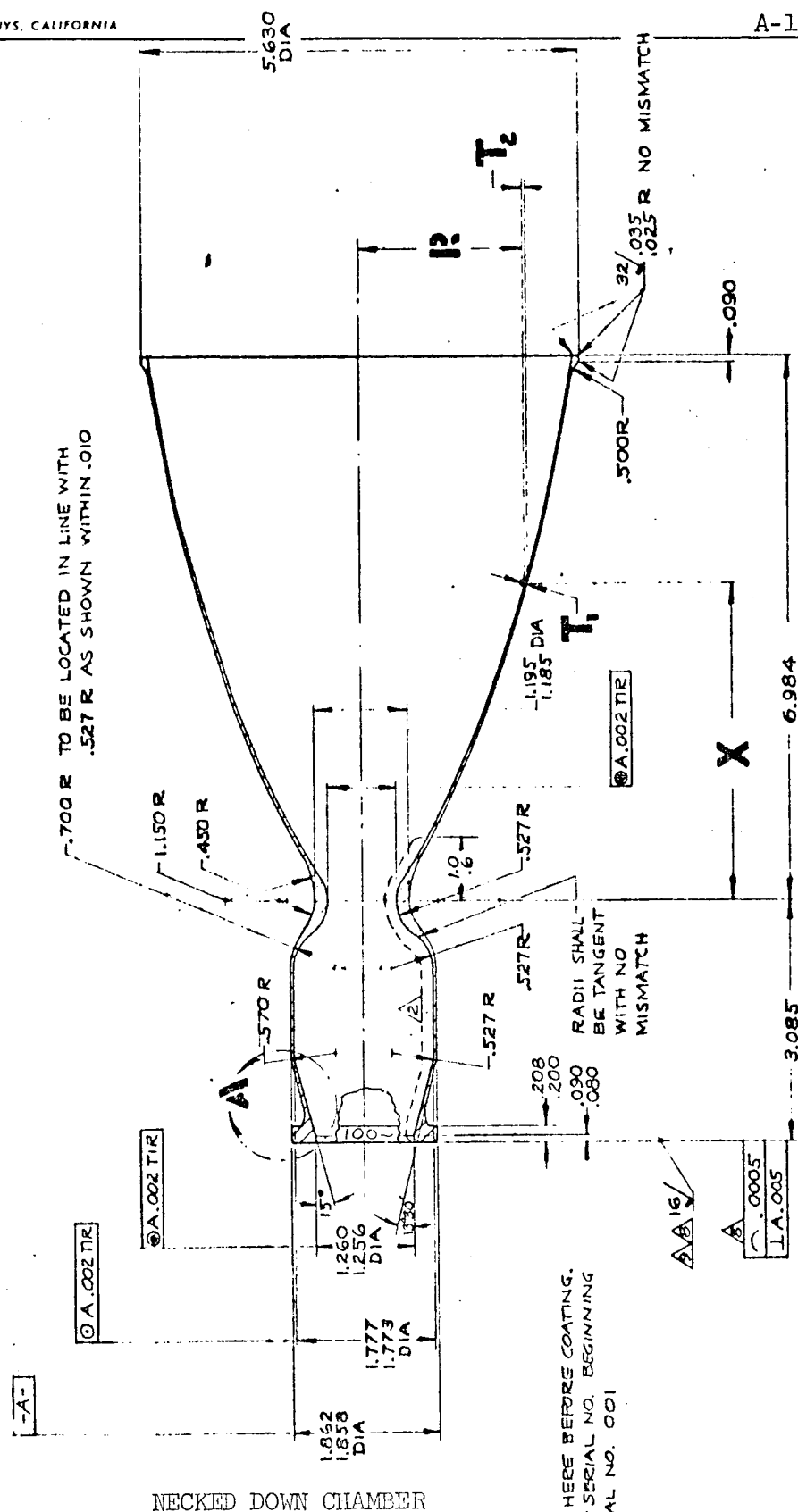
Ignition pressures were eliminated as a problem by the preigniter concept in June 1964. However, prior to and during the preigniter development, attempts were made to overcome the ignition problem by building stronger chambers either with materials other than molybdenum or by making a thicker and stronger molybdenum chamber.

Because fuel film cooling had reduced the combustion chamber temperatures significantly, steel was tested as a chamber material. The margin of safety between the operating temperature (2000°F) and melting temperature was not large enough so steel was dropped as a candidate.

The data generated from the material investigation resulted in TMC initiating an evaluation program on 90 Ta10W. At about this period of time (early 1964) the Chromizing Corporation had introduced a Durak MGF disilicide coating for 90 Ta10W and as a backup to molybdenum, a combustor was fabricated and coated.

Also in early 1964, the Sylcor Corporation, L.I., N.Y., introduced a tin-aluminide coating designated R505C. A chamber (welded construction) was fabricated, coated and tested. The walls were of relatively heavy construction. Subsequent test firing of both 90 Ta10W chambers were inconclusive. The key drawback to utilizing Ta alloys is the high density of the material - to the other of 0.608 lb.in<sup>3</sup>, versus only 0.369 for molybdenum. Photos of the chambers are shown in Figures 33, 34, 35, and 36.

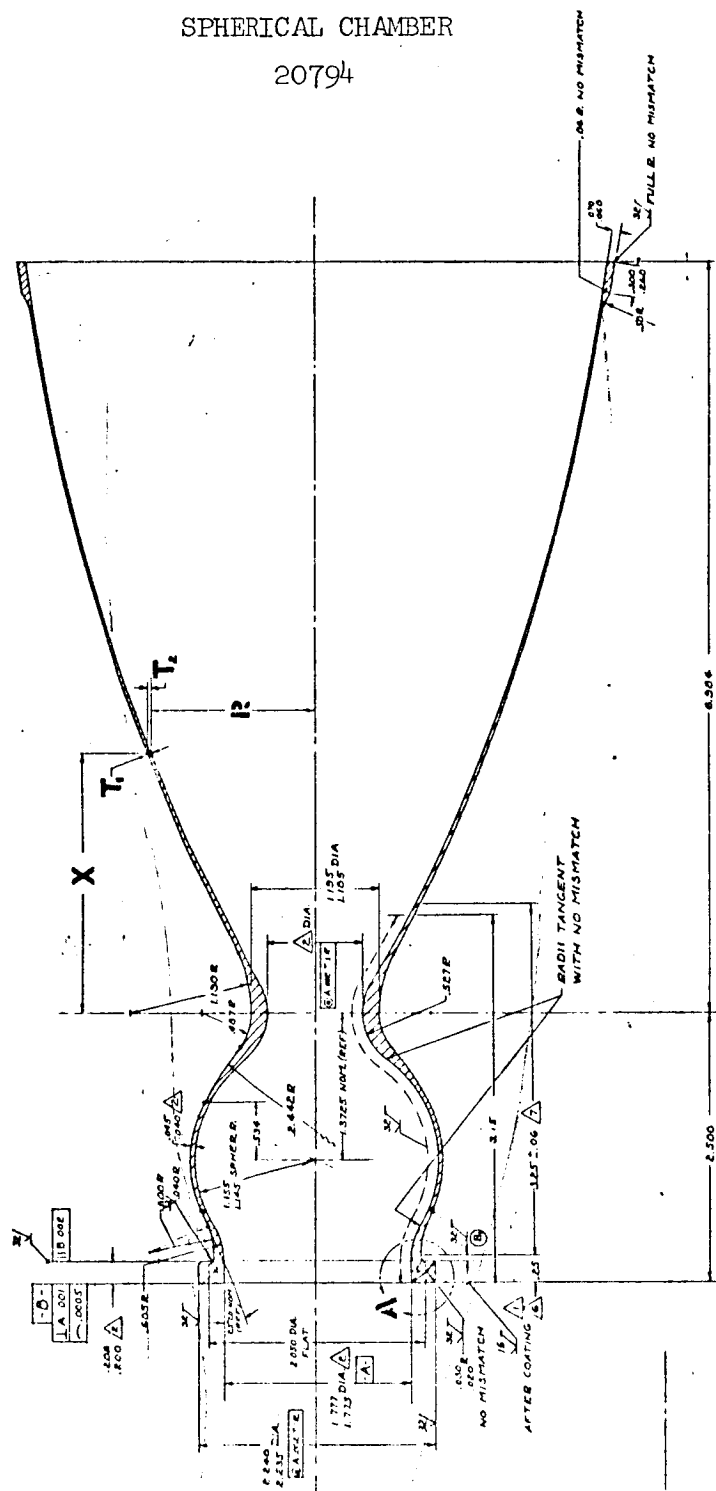
Consideration of two-piece chamber construction required a reevaluation of the materials of application. The proven success of disilicide coated unalloyed molybdenum required retention of the coating but not necessarily of the molybdenum forging which incorporated the skirt. As a result, a program was initiated to evaluate TZM bar. Since the combustion section of the thrust chamber (no integral bell) was 3", off-the-shelf TZM bar was available for use. TZM was also selected because of its high recrystallization temperature (2650°F) and the anticipation of retaining its high strength properties after the coating cycle. See Figures 37 and 38 for tensile and creep-rupture properties. It should be noted that un-



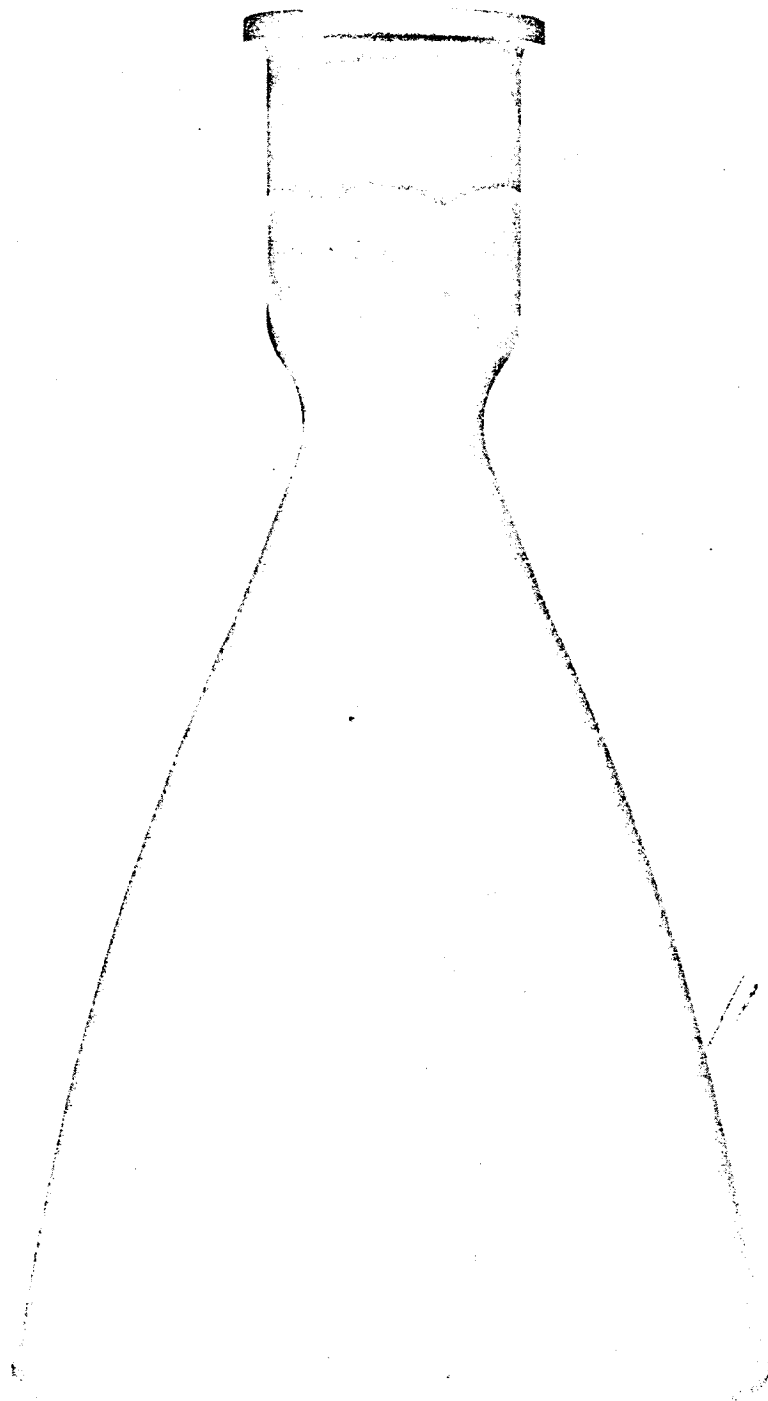
IDENTIFY HERE BEFORE COATING.  
PART NO. & SERIAL NO. BEGINNING  
WITH SERIAL NO. 001

## SPHERICAL CHAMBER

20794

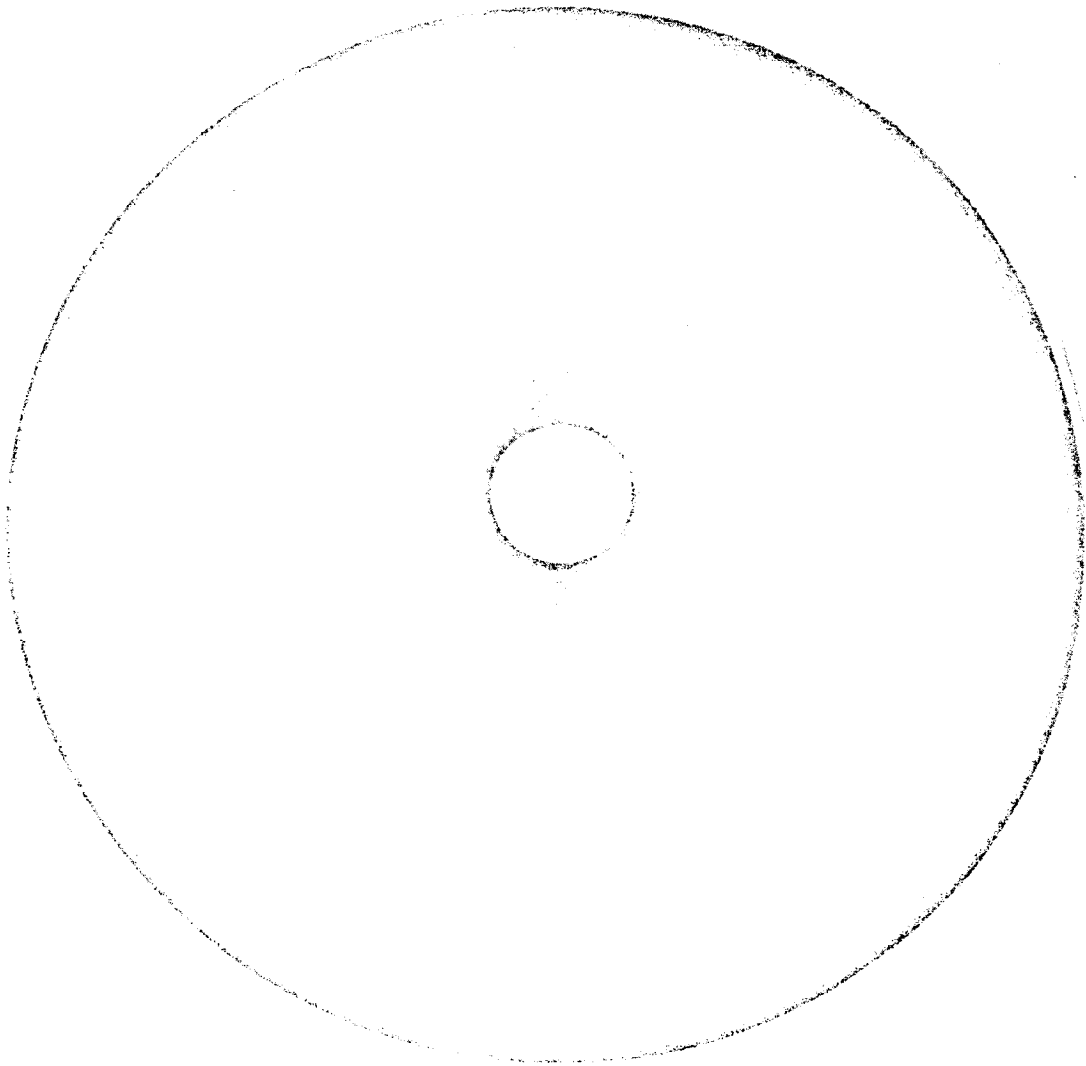






NEG. T3106-156

Coated 90 Ta-10W Thick Wall Combustion Chamber Post Fired

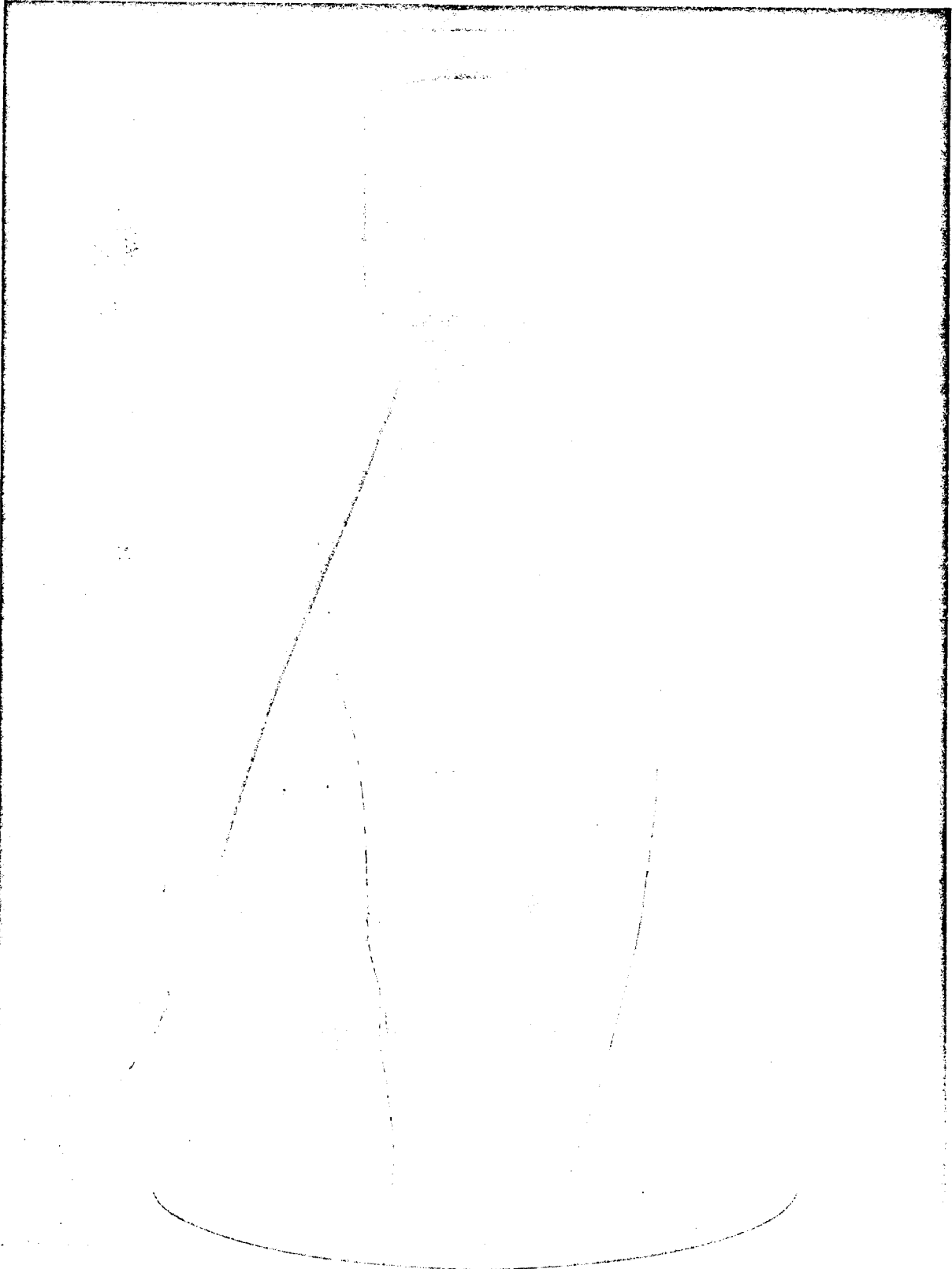


NEG. T3106-161

Coated 90Ta-10W Thick Wall Combustion Chamber Post Fired

11-53

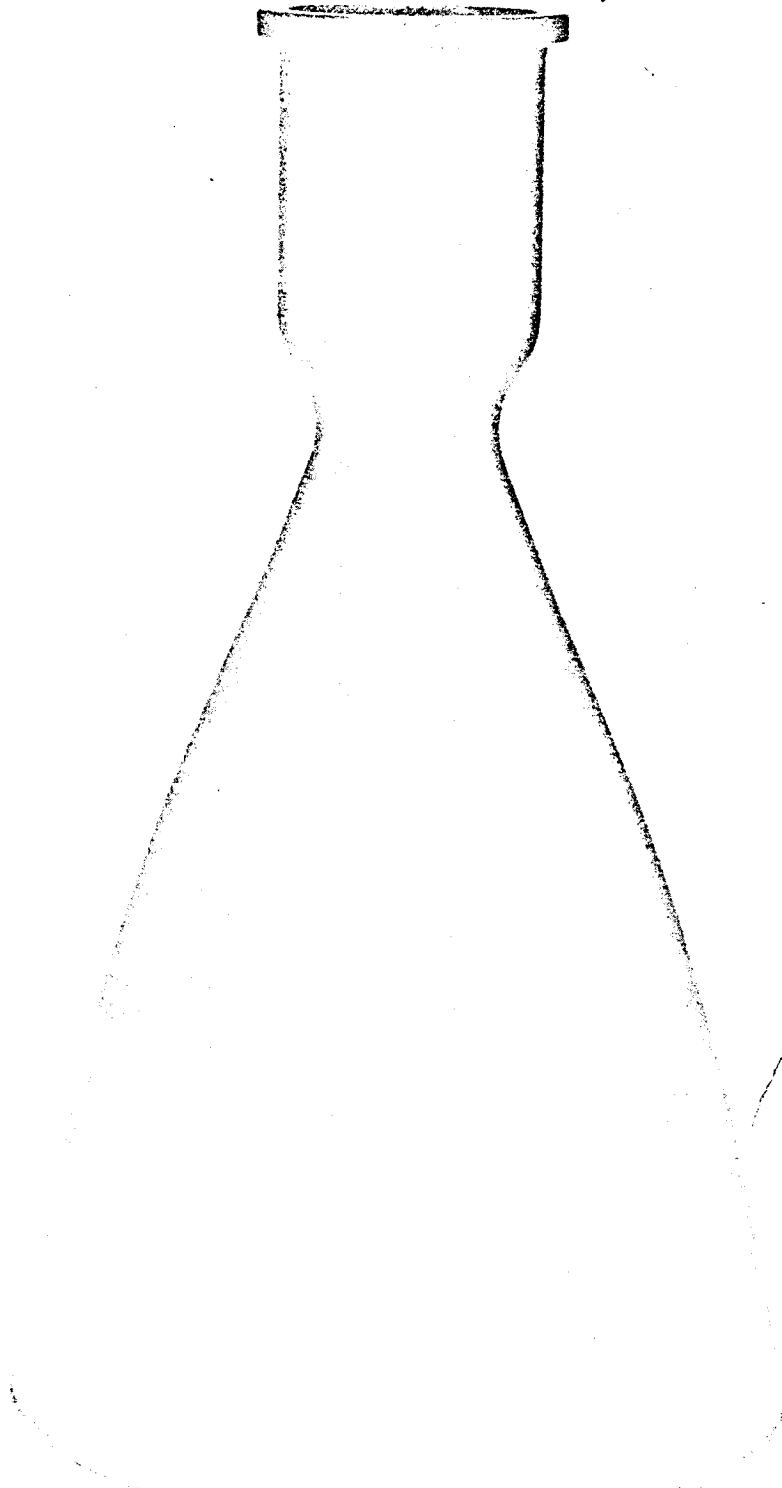
Figure 34



90 Ta-10W Combustion Chamber

11-54

Figure 35



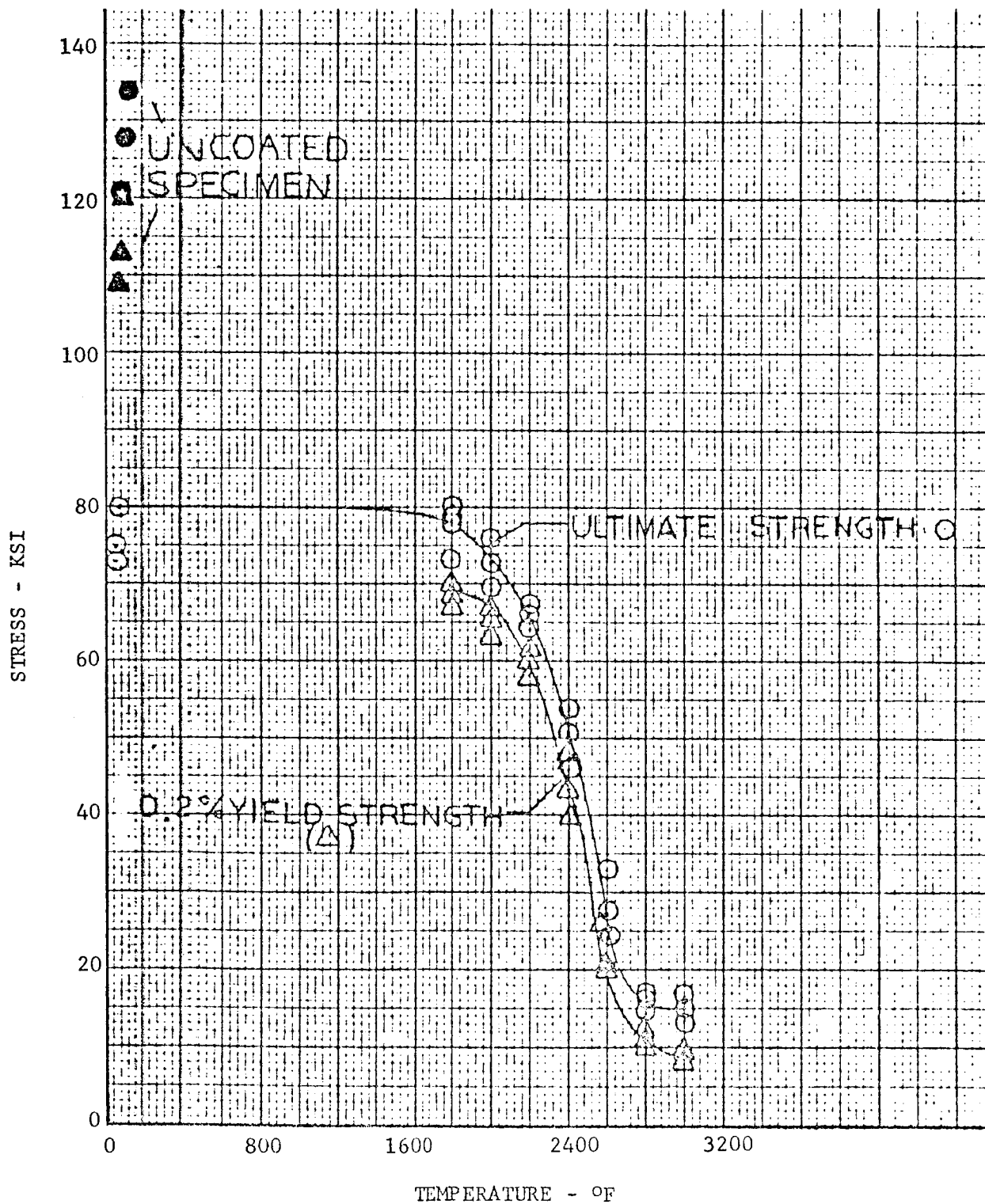
NEG. 6064-1

90 Tantalum - 10 Tungsten Alloy Thrust Chamber Welded Construction

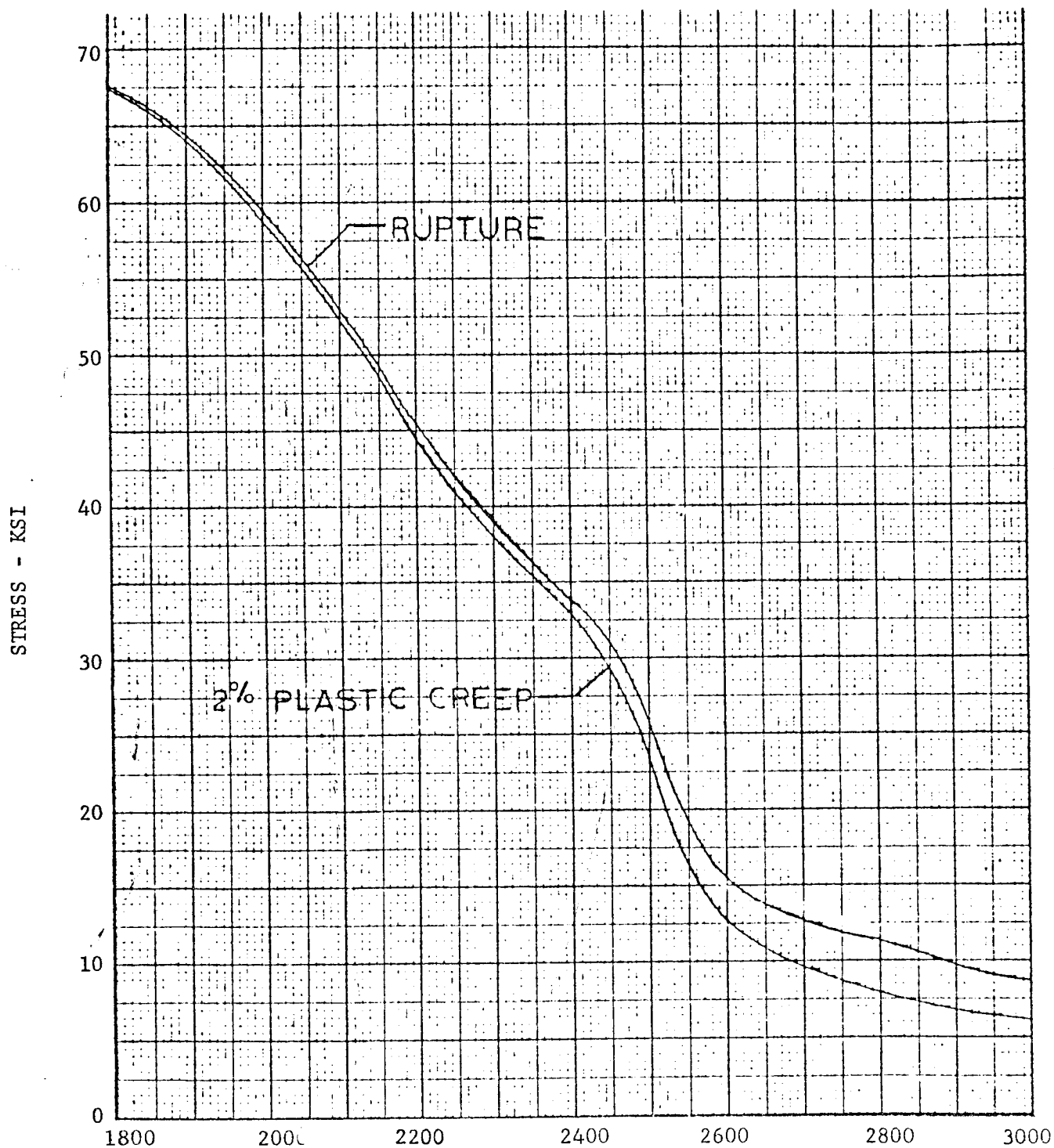
11-55

Figure 36

TENSILE PROPERTIES OF TZM ALLOY SHEET  
GRIT BLASTED AND DISILICIDE COATED



STRESS TO PRODUCE 2% PLASTIC CREEP & CREEP RUPTURE  
IN 30 MINUTES FOR TZM ALLOY SHEET  
(GRIT BLASTED & DISILICIDE COATED)



alloyed molybdenum forgings were still considered the prime material, and Marquardt was merely following its traditional policy of constantly seeking alternate or better materials throughout the program.

A two-piece thrust chamber was designed, with the thrust chamber section fabricated from TZM bar (disilicide coated with Durak B), and the skirt (bell) section flo-turned and machined from an L-605 forging (Figure 39). The skirt was held on to the combustor by a Waspaloy (PH Ni Base) nut. Rocket engine tests followed and were highly successful.

Although the TZM thrust chamber performed exceedingly well, the decision was made to stay with molybdenum forgings. The decision was based on the proven history for obtaining high purity reproducible quality material and the fact that many unknowns remained about TZM's chemical and mechanical properties.

An extra thick walled molybdenum chamber (Figure 40) was tested in June, 1964. The test was a performance, steady state and pulse, and life test which the chamber completed successfully. This combustor was heavier than the ribbed molybdenum chamber so that the chamber held more heat in it after a firing and consequently the injector head soakback temperature was higher. Because of the higher soakback temperature and greater weight, testing of this chamber was discontinued.

After the qualification of the preigniter engine work continued on a chamber that would be stronger than molybdenum. As a result a columbium chamber (C-103) with a Sylvania R-512A silicide coating has been developed. This chamber is an improvement over the moly chamber because it is ductile and will better withstand ignition overpressure that would fail the moly chamber. For example, Figure 41 is a picture of a columbium chamber that has been pressure checked to 8600 psia. Note how the chamber has ballooned out indicating its ductility.

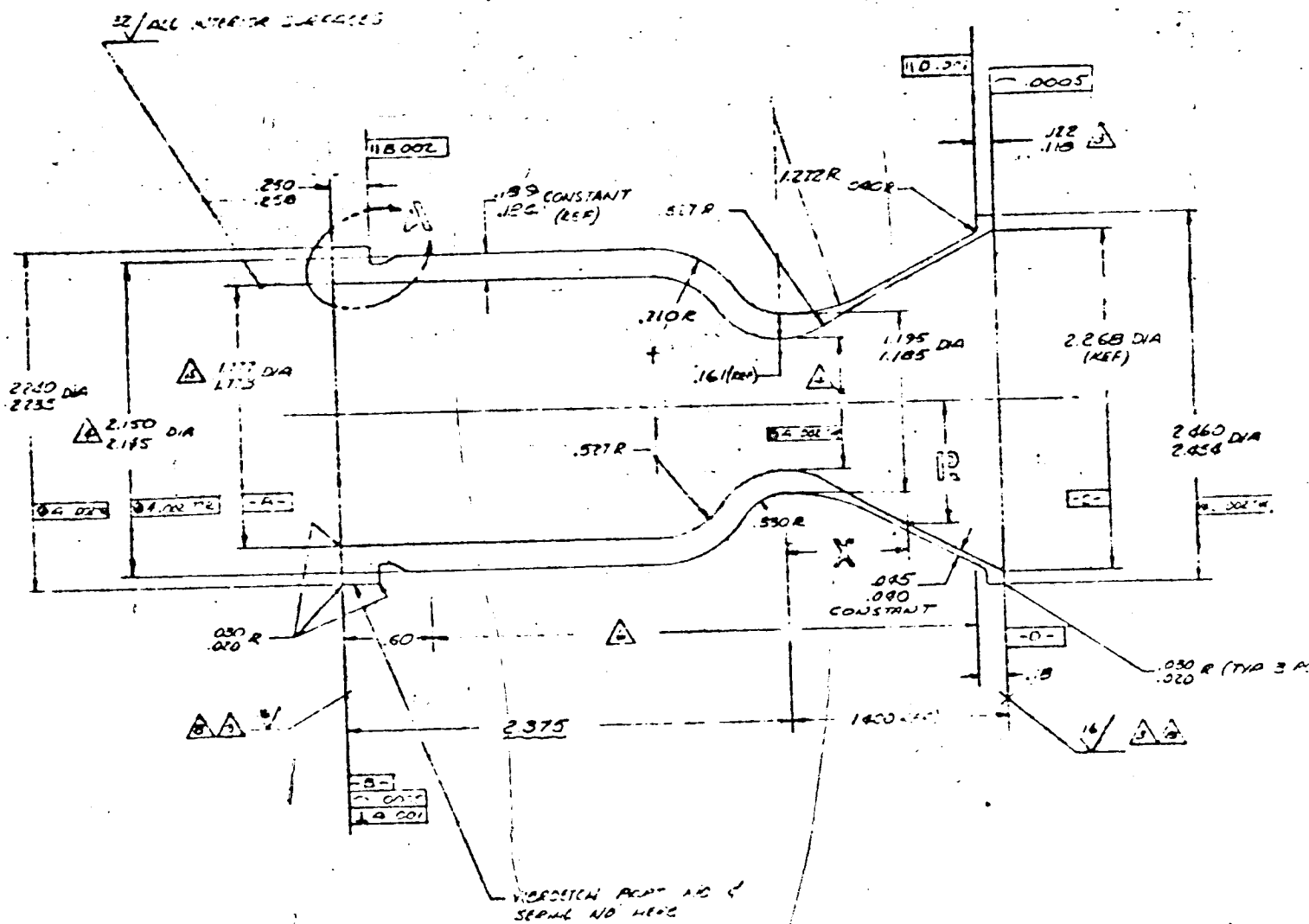
Figure 42 is a picture of the R-4D engine with the columbium chamber. Six of these engine configurations have accumulated 22,636 seconds of burn time and 38,441 starts.

#### IV. CHAMBER LIFE

The life of the molybdenum chamber is unlimited compared to the mission requirements. At the operating temperature of 2000-2200°F the chamber life is greater than 200 hours or almost 10 days of steady state firing. The mission requirements are that one engine fire for no more than 1000 seconds or 1/3 of an hour.

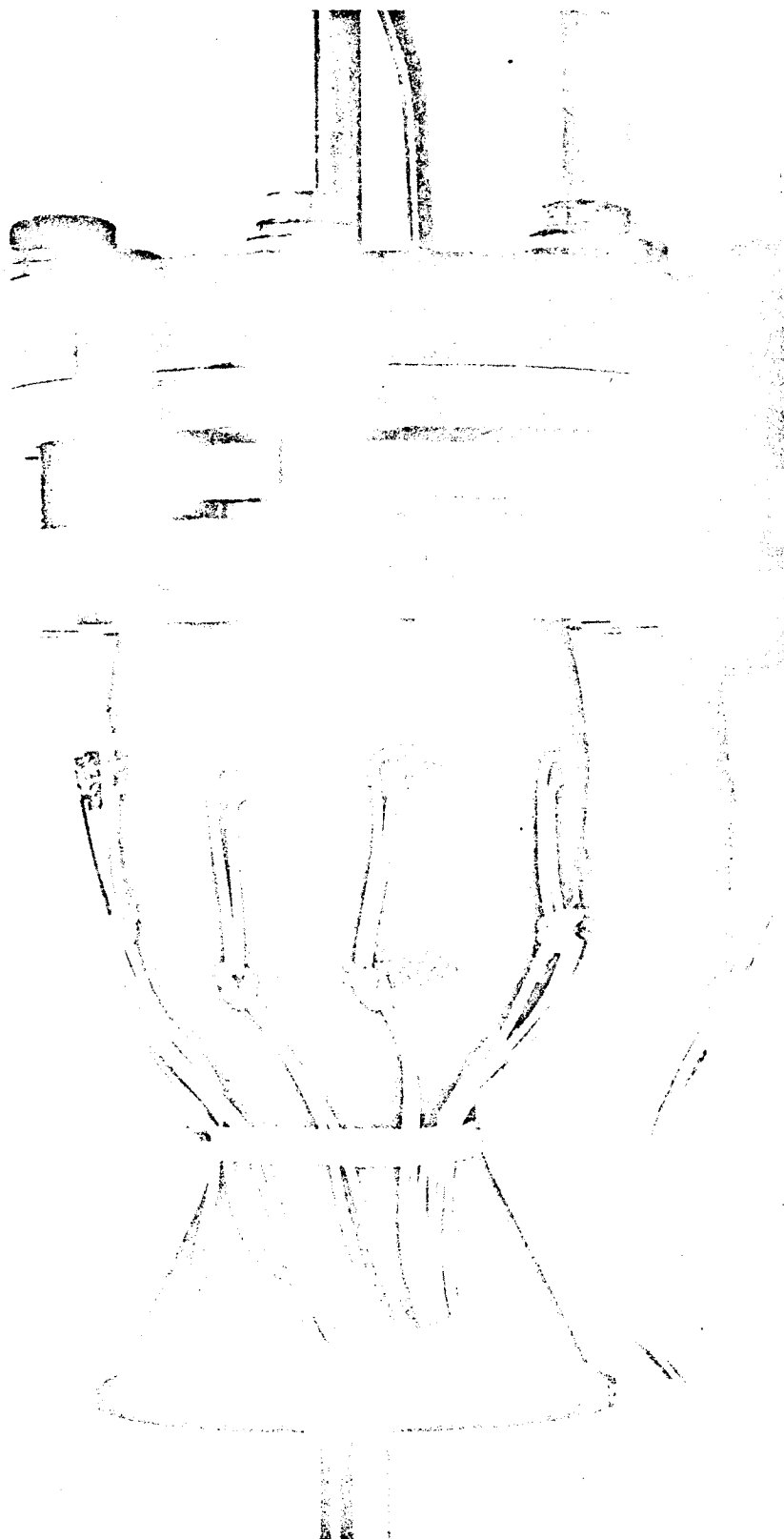






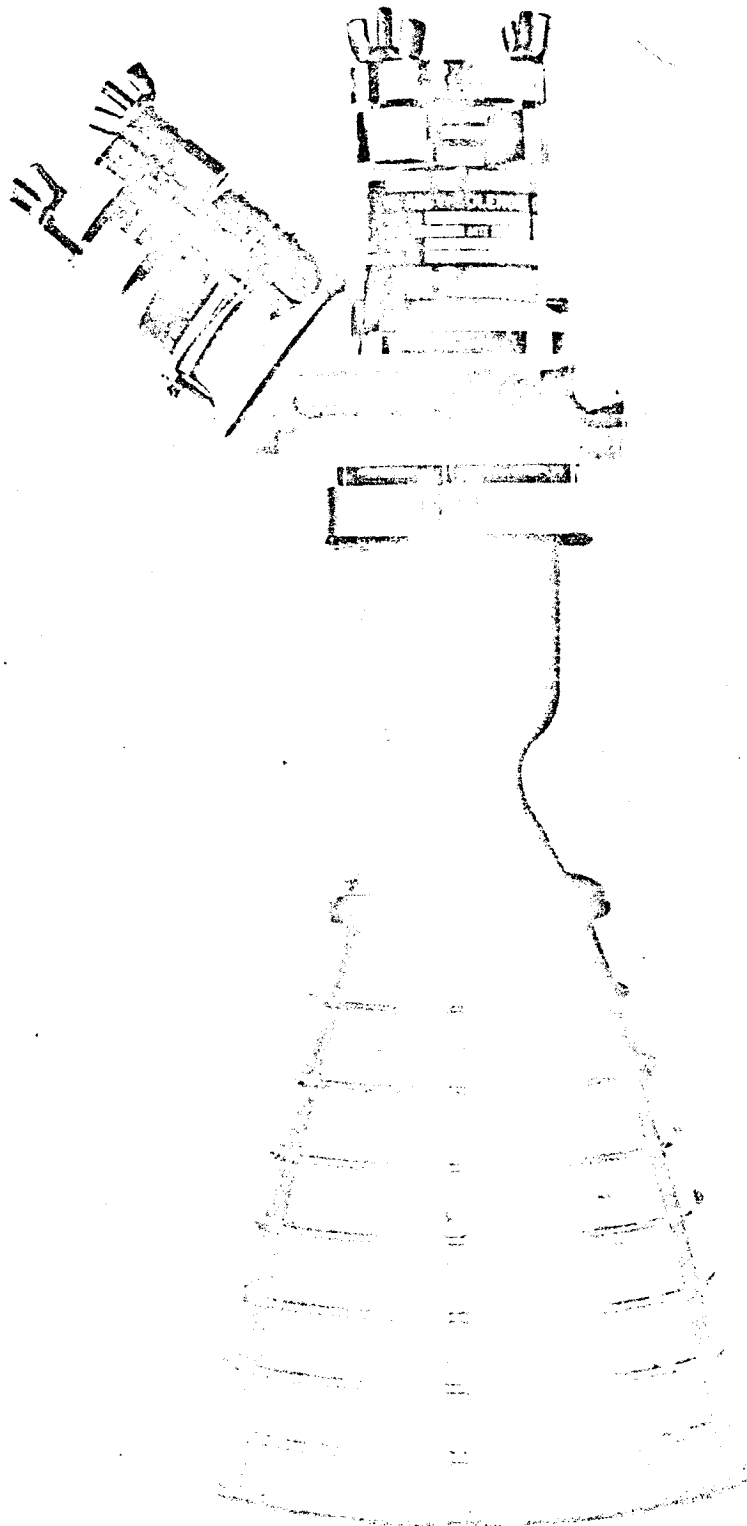
EXTRA THICK MOLY

T 10156



NEG. 8504-2

Columbiu Combustor After Pressure Check at 8600 psia



NEG. CAT3419-9

Engine with Columbian Chamber

11-62

Figure 42

The molybdenum chamber is coated with an oxidation resistance coating of molybdenum disilicide. If this coating, which is approximately .003 inches thick, should fail the molybdenum chamber would quickly be oxidized by the combustion gases and a hole would be burned in the chamber. To determine what the chamber life is, chambers were tested until they failed and molybdenum coupons, coated in the same way as the combustors, were torch tested as described previously. An analytical model was also developed to describe the coating wearout.

Shown on Figure 43, is the test data from the combustion chambers. Most of the testing has been done in the 2700°F to 3100°F range for several reasons. Until the addition of fuel film chamber cooling the combustion chamber temperature was between 2700°F and 3100°F. Also below 2700°F the test becomes prohibitively expensive because of the long time required to reach a failure. Also shown on the figure is the predicted life line based on the analysis discussed below.

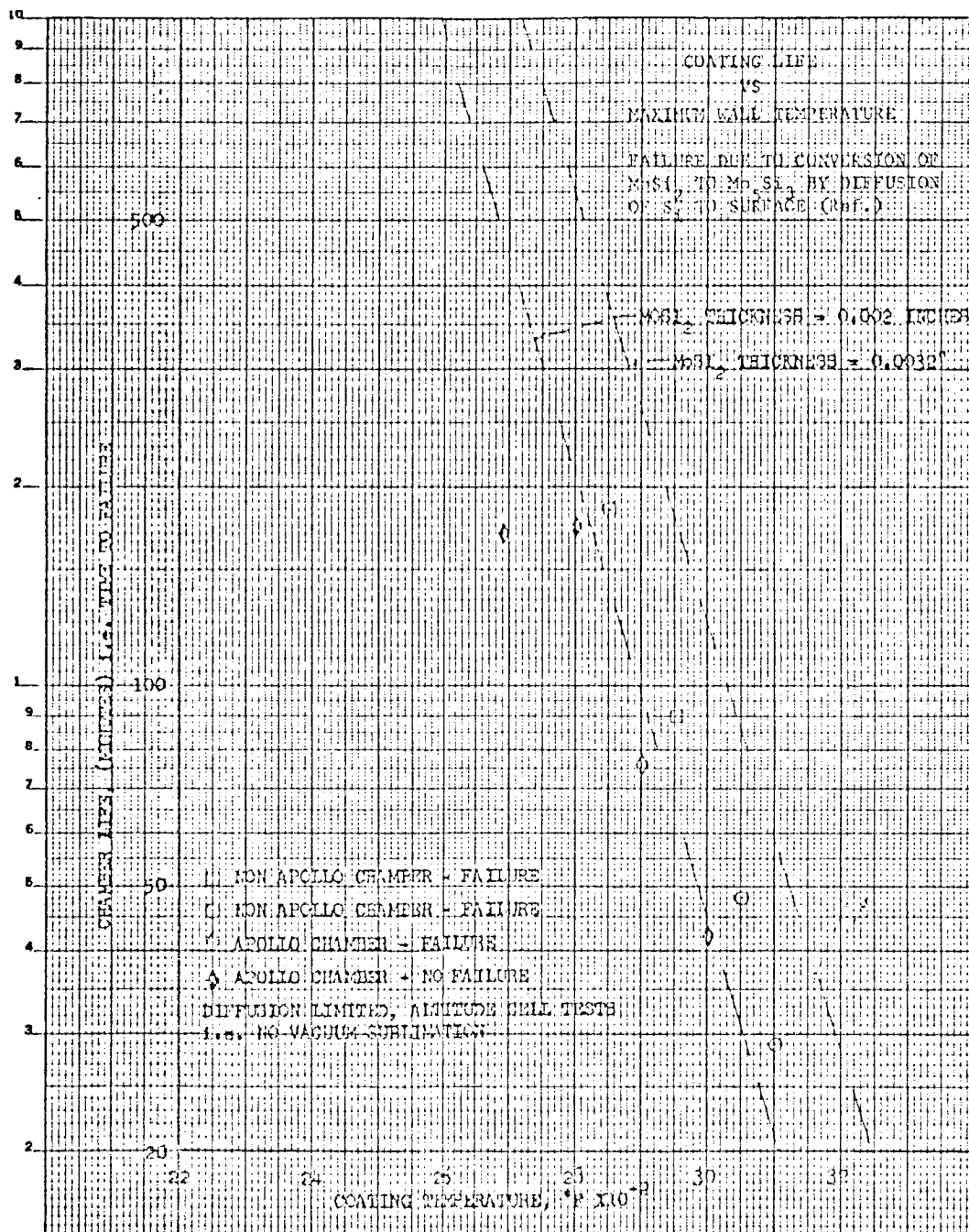
The use of refractory metals and alloys in aerospace vehicles requires oxidation protection coatings when subjected to the environments of combustion gases and air. Many types of oxidation protection coatings are available but the best coating presently available for the protection of molybdenum, which is used for the Apollo RCS combustion chamber, is the disilicide  $\text{MoSi}_2$ . This coating is formed by the diffusion of silicon into the molybdenum to form  $\text{MoSi}_2$ . The disilicide, on contact with air or an oxidizing atmosphere, will in most cases be characterized by growth of a continuous adherent oxide film ( $\text{SiO}_2$ , Figure 1, Reference 1). Below 600°C (1100°F), nucleation and growth of amorphous  $\text{SiO}_2$  particles and small single crystals of  $\text{MoO}_3$  occur on the oxide film. Both of these oxides are nonadherent and constitute the silicide "Pest." At low pressures and high temperatures the coating will not form a passive  $\text{SiO}_2$  film but will instead form  $\text{SiO}$ . In the case of the Apollo RCS combustion chamber or similar chamber, the pressure is high enough during the oxidizing phase that the protective  $\text{SiO}_2$  coating is always formed except in the regions of the chamber below about 1100°F. Then the formation of "Pest" will be found. The outside of the chamber during testing in the altitude chamber is still in the region of the formation of the passive film (Figure 44). During the actual mission, the outside wall is in a hard vacuum and thus the need for a passive film is eliminated.

#### A. Coating Loss Mechanisms

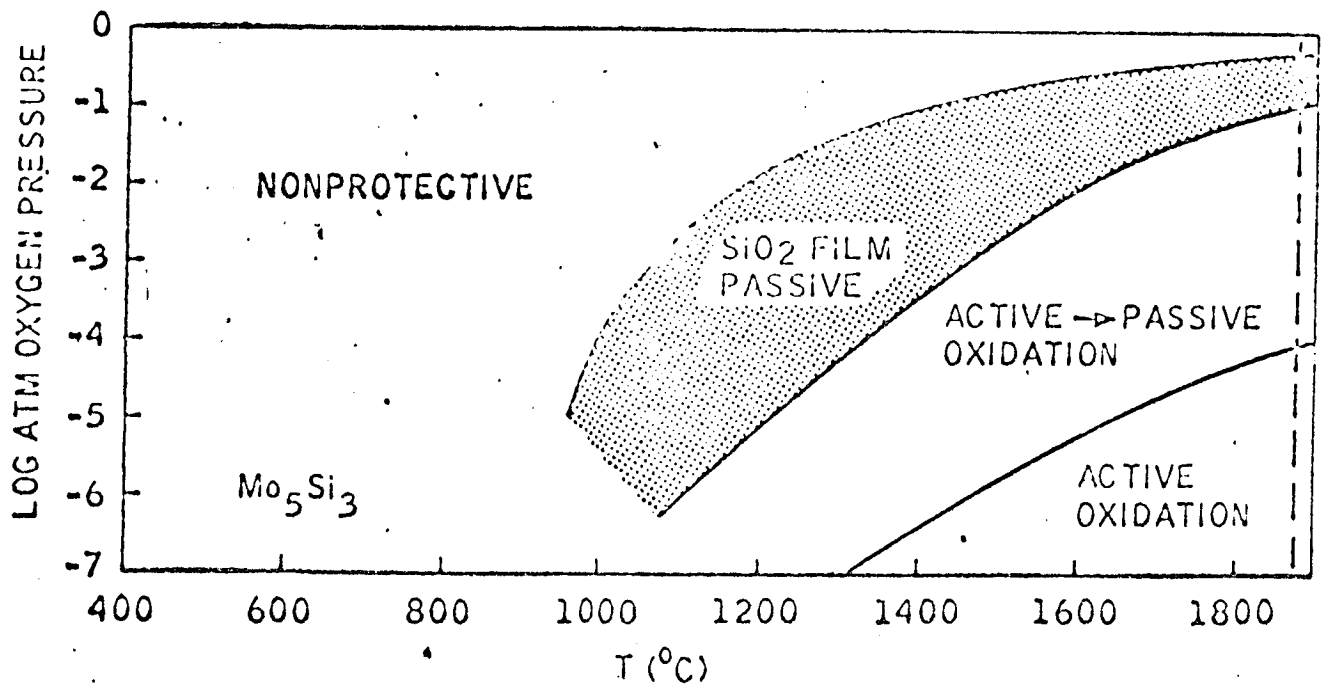
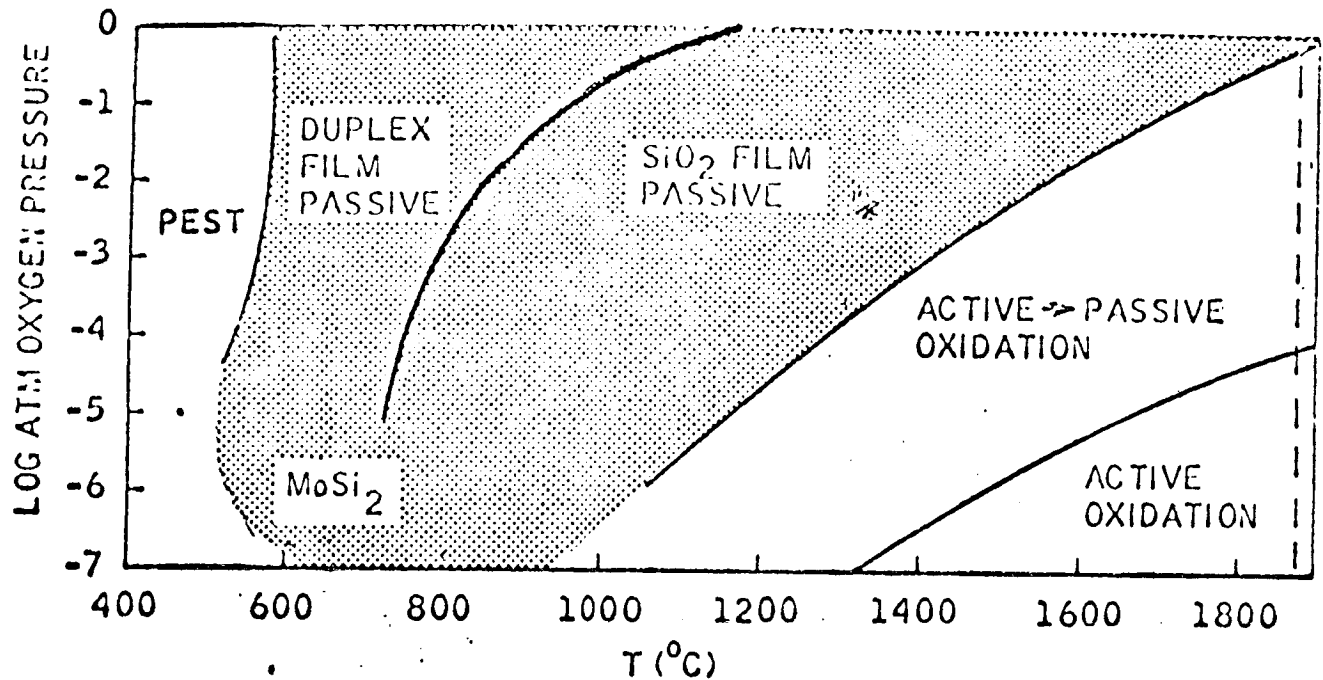
##### Diffusion

During the use of silicide coated molybdenum at high temperature, diffusion of  $\text{MoSi}_2$  occurs and, since the silicon source is absent, causes growth of lower silicide compounds and depletion of the disilicide. The lower silicides are less effective than the disilicide in forming a protective oxide film and failure of the coating usually coincides with complete conversion of the disilicide phase.

# COATING LIFE VS. MAXIMUM WALL TEMPERATURE



SYNOPSIS OF TEMPERATURE AND OXYGEN EFFECTS ON  
OXIDATION PROTECTIVE BEHAVIOR OF  $\text{MoSi}_2$  AND  $\text{Mo}_5\text{Si}_3$  (Ref.#1)



There are three intermetallic compounds in the molybdenum-silicon system:  $\text{MoSi}_2$ ,  $\text{Mo}_5\text{Si}_3$ , and  $\text{Mo}_3\text{Si}$ . The growth kinetics is dependent on the diffusion controlled reactions between a finite disilicide layer that is eventually consumed, a complex phase between the disilicide and the substrate, and the semi-infinite metal substrate. Depletion of the  $\text{MoSi}_2$  layer and growth of the  $\text{Mo}_5\text{Si}_3$  layer begins when diffusion is initiated. As long as the  $\text{MoSi}_2$  is present the growth of  $\text{Mo}_3\text{Si}$  is negligible. At the time the  $\text{MoSi}_2$  is eliminated, the  $\text{Mo}_3\text{Si}$  phase is consumed. The movement of the phase boundaries and the growth of the intermediate silicides are a result of the diffusion of silicon and molybdenum in these phases.

The diffusion in each element is

$$j_{ik} = D_{ik} \frac{\partial C_{ik}}{\partial x_k}$$

where  $j_{ik}$  is the flux,  $D_{ik}$  is the diffusion coefficient and  $C_{ik}$  is the concentration difference between phase boundaries of the  $i^{\text{th}}$  element and the  $k^{\text{th}}$  phase and  $x_k$  is the thickness of the  $k^{\text{th}}$  phase. The resulting equations for the four phases of the molybdenum-disilicide-molybdenum system are (Reference 1).

1. Depletion of  $\text{MoSi}_2$  (Phase I)

$$\frac{dx}{dt} \text{MoSi}_2 = - \frac{8}{7} \left( \frac{M}{\rho} \right)_{\text{MoSi}_2} \frac{\tilde{D}_{II} \Delta C_{II}}{\Delta x_{II}}$$

Growth of  $\text{Mo}_5\text{Si}_3$  (Phase II)

$$\frac{dx}{dt} \text{Mo}_5\text{Si}_3 = \left( \frac{M}{\rho} \right)_{\text{Mo}_5\text{Si}_3} \left\{ \frac{10}{7} \frac{\tilde{D}_{II} \Delta C_{II}}{\Delta x_{II}} - \frac{\tilde{D}_{III} \Delta C_{III}}{\Delta x_{III}} \right\}$$

Growth of  $\text{Mo}_3\text{Si}$  (Phase III)

$$\frac{dx}{dt} \text{Mo}_3\text{Si} = \left( \frac{M}{\rho} \right)_{\text{Mo}_3\text{Si}} \left\{ 3 \frac{\tilde{D}_{III} \Delta C_{III}}{\Delta x_{III}} - 2 \frac{\tilde{D}_{II} \Delta C_{II}}{\Delta x_{II}} \right\}$$

# Depletion of Mo (Phase IV)

$$\frac{dx}{dt} \text{ Mo} = -4 \left( \frac{M}{\rho} \right)_{\text{Mo}} \frac{\tilde{D}_{\text{III}} \Delta C_{\text{III}}}{\Delta X_{\text{III}}}$$

The growth of  $\text{Mo}_5\text{Si}_3$  and the depletion of  $\text{MoSi}_2$  is the most important aspect in the combustion chamber since  $\text{Mo}_5\text{Si}_3$  is easily oxidized and it can be assumed that as soon as the  $\text{MoSi}_2$  is used that failure of the coating will occur. This can be seen in Figure 44 where the various temperature pressure envelopes of protection are shown for  $\text{Mo}_5\text{Si}_3$ . There is no oxidation protection at the Apollo RCS chamber pressure (i.e., 90 psia). Therefore, the equations can be simplified since the growth of  $\text{Mo}_3\text{Si}$  is negligible before the disappearance of  $\text{MoSi}_2$ .

$$\frac{dx}{dt} \text{ Mo}_3\text{Si} \approx 0$$

Therefore,

$$\frac{\tilde{D}_{\text{III}} \Delta C_{\text{III}}}{\Delta X_{\text{III}}} = \frac{2}{3} \frac{\tilde{D}_{\text{II}} \Delta C_{\text{II}}}{\Delta X_{\text{II}}}$$

and

$$\frac{dx}{dt} \text{ Mo}_5\text{Si}_3 = \frac{16}{21} \left( \frac{M}{\rho} \right)_{\text{Mo}_5\text{Si}_3} \frac{\tilde{D}_{\text{II}} \Delta C_{\text{II}}}{\Delta X_{\text{II}}}$$

Upon integration, a parabolic equation for the growth of  $\text{Mo}_5\text{Si}_3$  in terms of the average diffusion coefficient of  $\text{Mo}_5\text{Si}_3$  ( $\tilde{D}_{\text{II}}$ ) results

$$\Delta X_{\text{Mo}_5\text{Si}_3} = \left\{ \frac{32}{21} \left( \frac{M}{\rho} \right)_{\text{Mo}_5\text{Si}_3} \tilde{D}_{\text{II}} \Delta C_{\text{II}} \right\}^{1/2} t$$

where

$$(\tilde{D}_{\text{II}} \Delta C_{\text{II}})_{\text{Mo}_5\text{Si}_3} = 1.3 \quad -(\Delta E/RT)$$

and  $E = 87.0 \text{ Kcal/mole}$



The loss of  $\text{MoSi}_2$  is

$$-\Delta X_{\text{MoSi}_2} = 1.86 \left( \frac{M}{\rho} \right)_{\text{MoSi}_2} \left( \frac{\rho}{M} \right)_{\text{Mo}_5\text{Si}_3}^{1/2} \left( \bar{D}_{\text{II}} \Delta C_{\text{II}} \right) t^{1/2}$$

Figure 43 shows the results of this analysis. As shown, a good correlation is found between the loss of  $\text{MoSi}_2$  due to the diffusion rate and the actual engine failures. The assumption is that during this time, the  $\text{SiO}_2$  in contact with the oxidizing surface did not sublime. The rate of loss of  $\text{SiO}_2$  on the surface, after the engine is shut down, due to sublimation into the hard vacuum is much smaller than the diffusion rate ( $\text{MoSi}_2 - \text{Mo}_5\text{Si}_3$ ) for an Apollo type duty cycle. This is illustrated in Figure 45 which depicts the loss and growth rate of  $\text{MoSi}_2$  and  $\text{Mo}_5\text{Si}_3$ . As shown, the loss of disilicide on the outside surface due to sublimation is small compared to the diffusional loss, but as time progresses the diffusion rate decreased ( $\sqrt{\text{time}}$ ) while the sublimation rate is constant and eventually the sublimation rate is faster.

#### "Pest" Formation

At temperatures below  $1100^\circ\text{F}$ , it is increasingly difficult for self-limiting oxide film to develop on  $\text{MoSi}_2$  inside the combustion chamber.

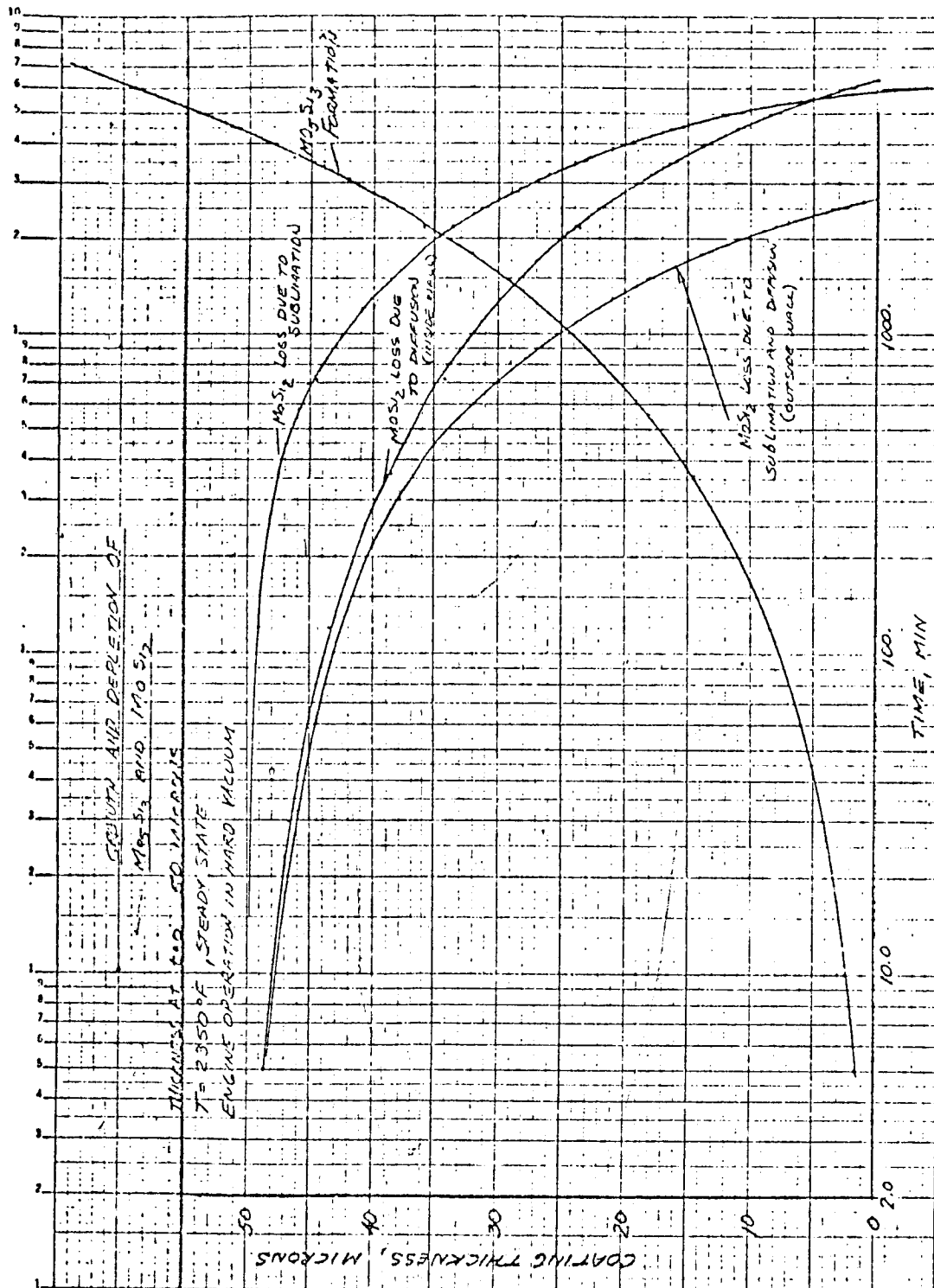
Although  $\text{MoO}_3$  is subliming at these temperatures, the sublimation rate is slow and net weight increases can be expected. After several hours, an oxide product (Silicide "Pest" Oxide) is usually visible to the unaided eye. It usually appears as randomly scattered mounds of nonadherent white or yellow powder. Exposure for several days at temperatures near  $1100^\circ\text{F}$  causes complete disintegration of  $\text{MoSi}_2$  samples and severe oxidation. The "Pest" oxide formed on  $\text{MoSi}_2$  is a mixture of small  $\text{MoO}_3$  crystals and colloidal sized amorphous particles of  $\text{SiO}_2$ . Individual films formed in the  $900$ - $1200^\circ\text{F}$  range are not uniform in density even when amorphous. Usually they are fine speckled in appearance but they may be opaque, or look like wrinkled carbon films. The data obtained in Reference 1 shows that in two hours the "Pest" was visible to the eye and in 30 hours, loose clusters were found. This would indicate that the formation of the "Pest" at location where the temperature is  $900$  to  $1100^\circ\text{F}$  could become the controlling mode of thermal failure for life times greater than 20-30 hours.

#### Sublimation of Coating

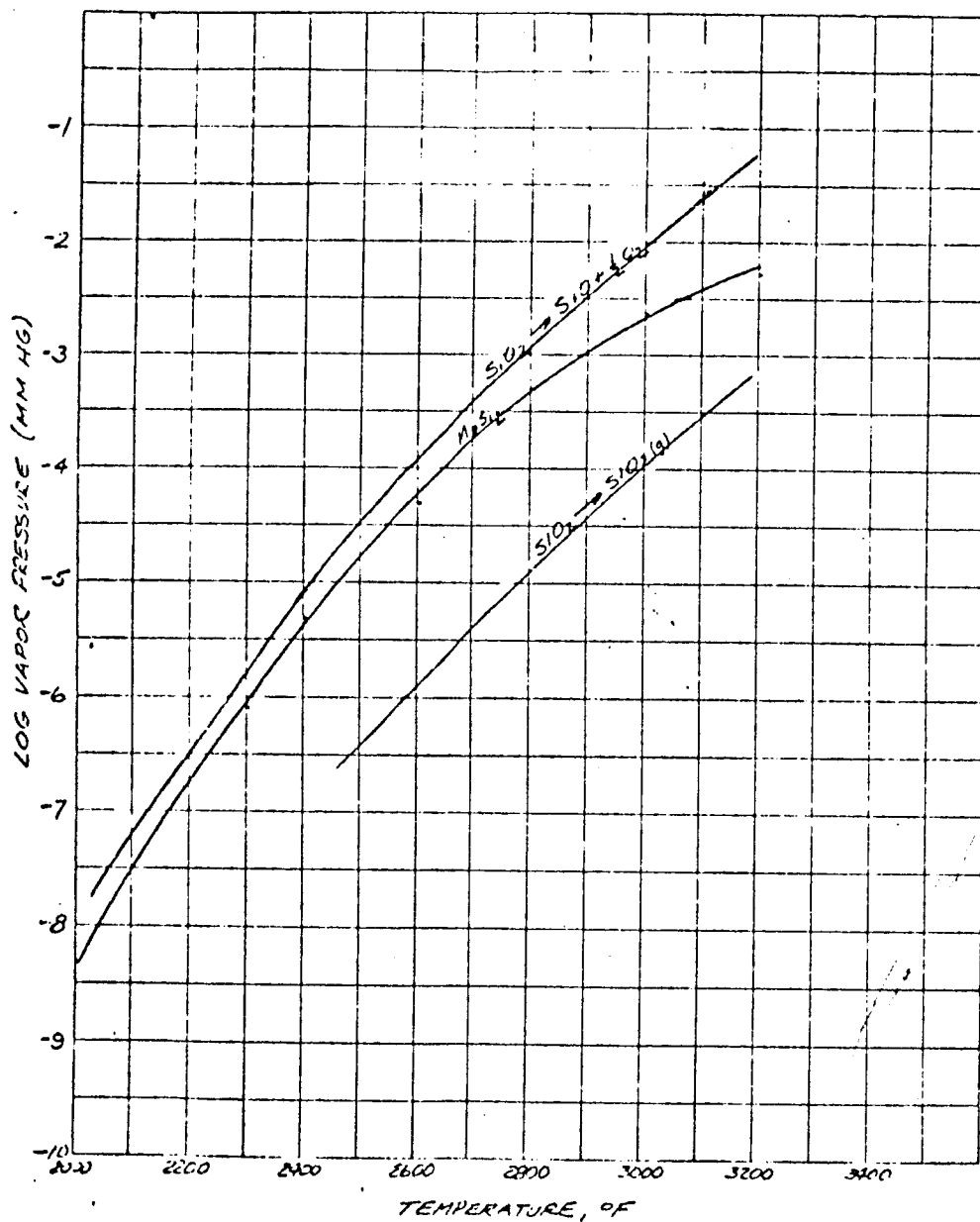
The sublimation rate of  $\text{MoSi}_2$  surface as a function of pressure on the outside of the combustion chamber and the  $\text{SiO}_2$  on the inside walls of the chamber can be determined from vapor pressure data (Figure 46) and the equation for loss of molecules from a plate in free molecular flow. From Reference 2

$$\dot{w} = \frac{1}{4} n \bar{u}$$

GROWTH & DEPLETION OF  $\text{Mo}_5\text{Si}_3$  &  $\text{MoSi}_2$



VAPOR PRESSURE OF THREE GAS FORMING  
TRANSFORMATIONS INVOLVING SILICON



Where  $\eta$  is the molecule concentration and

$$\bar{u} = \sqrt{\frac{8KT}{\pi m}}$$

This equation can be reduced to

$$\dot{w} = 0.0011125 P \sqrt{\frac{M}{T}}$$

where  $P$  = pressure, mm hg  
 $M$  = molecular weight  
 $T$  = temperature °R  
 $\dot{w}$  = flow rate #/in<sup>2</sup> sec.

## B. Analysis and Discussion

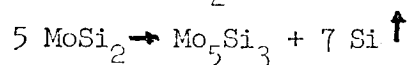
The loss of disilicide coating from the inside and outside of the Apollo RCS combustion chamber including the effects due to multiple restarts in a hard vacuum was investigated. It was reported in Reference 2 that the loss of coating was negligible if sublimation of the coating were the only consideration. However, the diffusion of the  $\text{MoSi}_2$  in the substrate to form  $\text{Mo}_5\text{Si}_3$  on the inside of the chamber must be considered. On the outside, even if the coating diffuses to  $\text{Mo}_5\text{Si}_3$ , there would be no failure due to the absence of an oxidizing atmosphere. The use of a  $\text{MoSi}_2$  coating on the outside of the engine has no effect on molybdenum life other than the fact that the  $\text{Mo}_5\text{Si}_3$  could have a lower emittance value than the disilicide which could result in a higher equilibrium wall temperature and a reduction in the coating life on the inside walls of the chamber. The main reason for the use of the coating on the outside wall is to protect the molybdenum during acceptance testing in altitude cells where the oxidizing atmosphere is present.

### Coating Loss Mechanisms

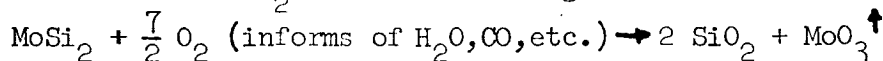
A coating degradation on the inside and outside of the wall is a combination of two processes and the basic reactions are shown below.

#### Inside Surface

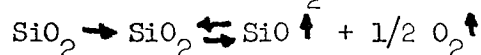
1. Loss of  $\text{MoSi}_2$  by diffusion



2. Reaction of  $\text{MoSi}_2$  at surface during combustion

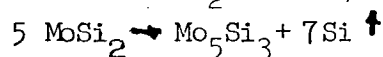


3. Sublimation of  $\text{SiO}_2$  in hard vacuum

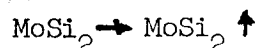


#### Outside Surface

1. Loss of  $\text{MoSi}_2$  by diffusion



2. Sublimation of  $\text{MoSi}_2$



#### Coating Loss Rate on Inside and Outside Nozzle

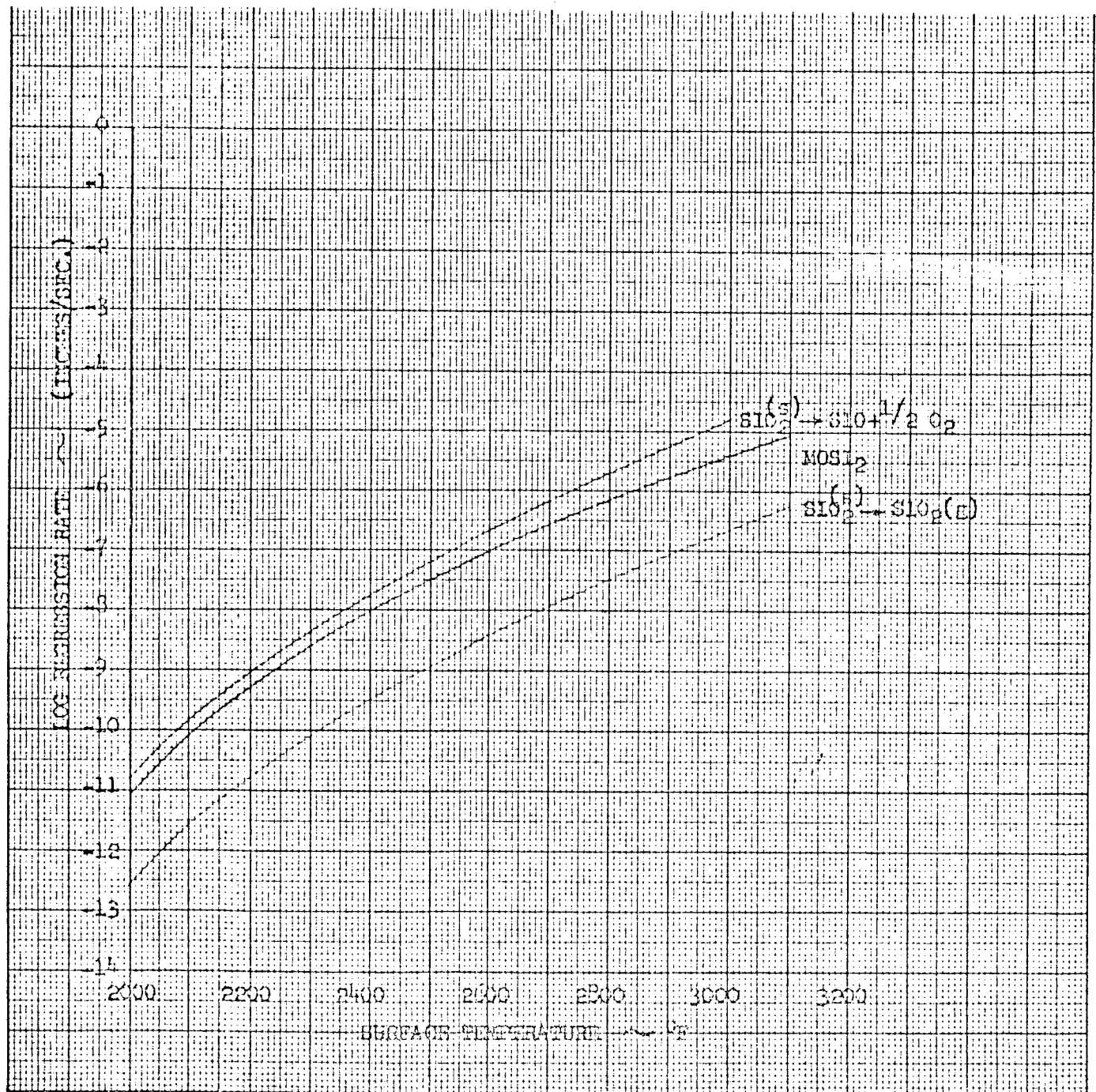
##### Outside Wall

Figure 47 shows the loss of disilicide and silica in inches/seconds vs. temperature. From this figure for any given wall temperature rise or decay rate, the loss of coating due to sublimation may be determined. The initial losses from the outside wall are a combination of diffusion of the  $\text{MoSi}_2$  to  $\text{Mo}_5\text{Si}_3$  and at the same time, sublimation of  $\text{MoSi}_2$ . When the  $\text{MoSi}_2$  disappears, a coating of  $\text{Mo}_5\text{Si}_3$  remains which in turn diffuses to  $\text{Mo}_3\text{Si}$  and sublimes. Since an oxidizing atmosphere is not present, we do not have any problem with oxidation of the molybdenum on the outside, however, the emittance of the  $\text{Mo}_5\text{Si}_3$  could change and increase or decrease the wall temperature. It is probable, based on test experience, that the emittance of the coating would not change to any large degree. Therefore, coating sublimation on the outside surface will not effect engine life. As shown on Figure 48, the loss of coating from the outside wall is much larger at steady state operation than from the inside. This is due to the addition of the sublimation of the  $\text{MoSi}_2$  on the outside wall. On the inside wall, the sublimation of the  $\text{SiO}_2$  is not expected due to the high chamber pressure.

##### Inside Wall

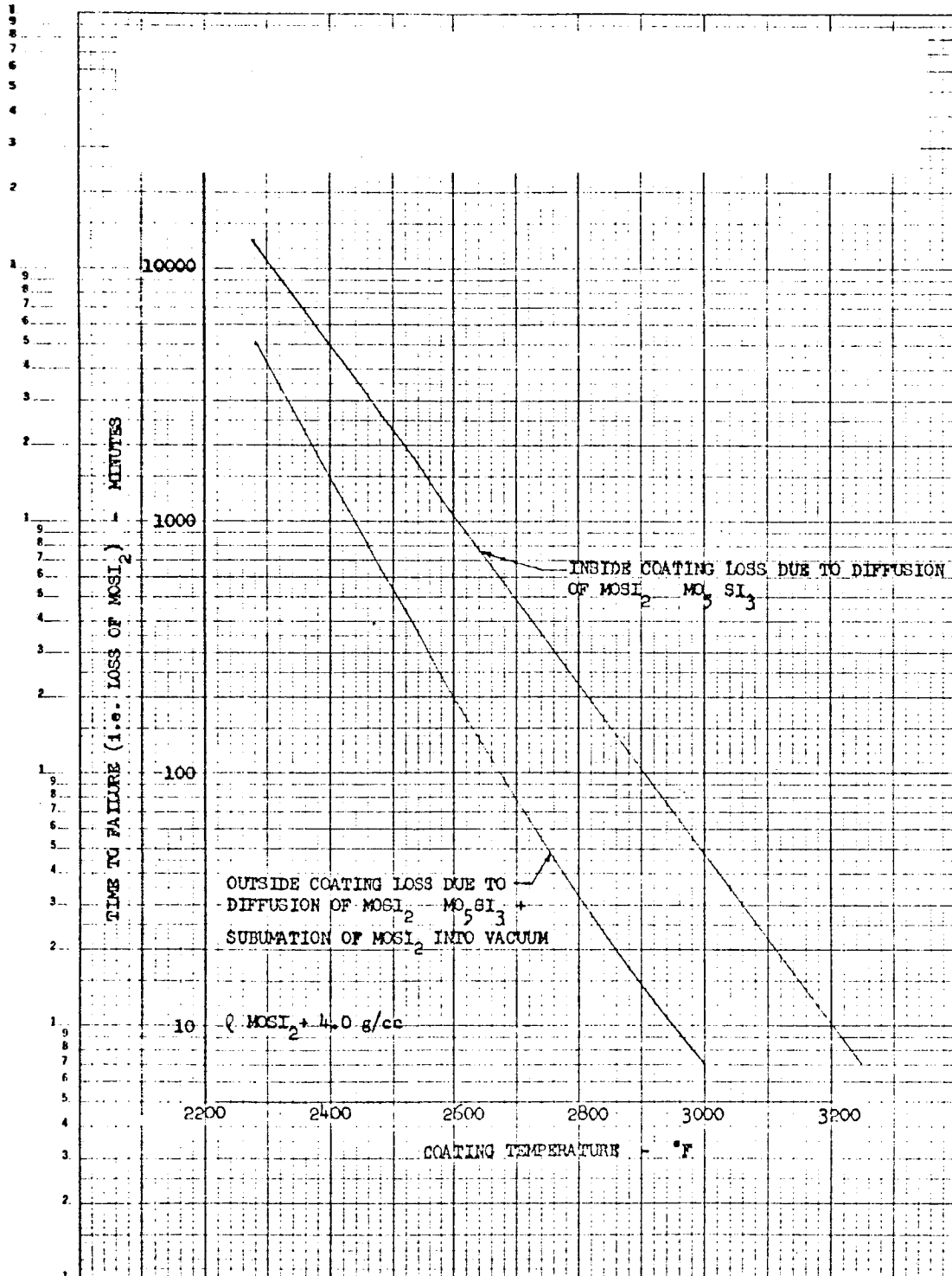
The loss of coating from the inside is a combination of diffusion of the  $\text{MoSi}_2$  and sublimation of the  $\text{SiO}_2$  when the engine is shutdown (i.e., hard vacuum). During long steady state runs, the loss can be predicted from the equations given in the text and the predicted life shown in Figure 48, however, when the engine is pulsed the addition of  $\text{SiO}_2$  sublimation must be taken into account. It was found, however, that the coating life increased for the same on time when the engine is pulsed. This is due to the fact that in a transient mode (pulsing) the engine is not operating at as high an average temperature.

REGRESSION RATE OF SURFACE  
IN HARD VACUUM DUE TO SUBLIMATION



PREDICTED COATING LIFE VS. MAXIMUM WALL TEMPERATURE  
STEADY STATE

$\text{MoSi}_2$  COATING -  $2.0 \times 10^{-3}$  INCHES  
ENGINE OPERATING IN HARD VACUUM



Thus, the transient nature of the pulse, which means that the engine does not run at the equilibrium wall temperature for the entire pulse, results in a lower coating loss than for steady state run. Therefore, it can be concluded that there is no engine operating condition worse than a steady state operation. Examples of the coating loss for various duty cycles are shown below. The following duty cycles were considered.

1. NAA duty cycle (mission time of 168 hours, 19 minutes with 5648 pulses for a total time of 529 seconds.
2. Worst duty cycle (30 minutes on time).
3. Steady state run of 30 minutes.

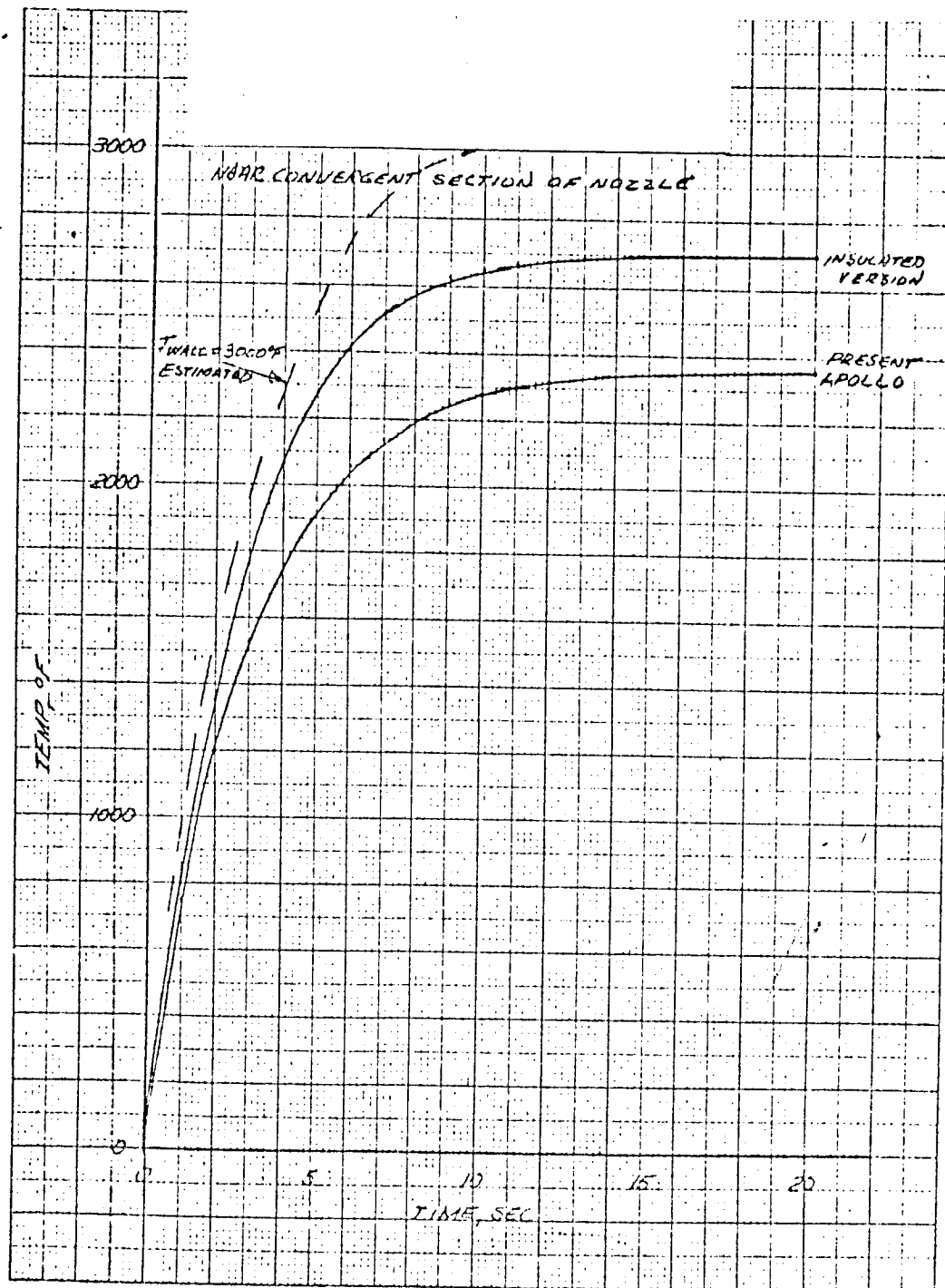
The heating and cooling transients are shown in Figures 49 and 50 for equilibrium wall temperatures of 2350°F, 2700°F, and 3000°F.

COATING LOSS FOR VARIOUS DUTY CYCLES

			Wall Temperature At Equilibrium °F	Coating Loss (inches)	Percentage of Total Coating Loss (Initial Thick- ness $2 \times 10^{-3}$ " )
<u>NAA Duty Cycle</u> (10 Min.On)			2350	$2.905 \times 10^{-9}$	.000145
<u>"Worst" Duty Cycle</u> (30 Min.On)					
ON	OFF	# Pulses			
5.5	4.3	328	2350	$6.5 \times 10^{-5}$ ( $2.3 \times 10^{-6}$ due to $\text{SiO}_2$ sublimation)	0.325
4.0	5.4	450	2700	$3.56 \times 10^{-4}$ ( $7.9 \times 10^{-5}$ due to $\text{SiO}_2$ sublimation)	1.78
Steady State (30 minutes) (no $\text{SiO}_2$ sublimation)			2350	$1.27 \times 10^{-4}$	6.35
			2700	$6.05 \times 10^{-4}$	30.25
			3000	$1.72 \times 10^{-3}$	86.00



APOLLO RCS ENGINE  
MAXIMUM METAL TEMPERATURE  
VS.  
TIME



APOLLO COOLING CYCLE  
RCS ENGINE

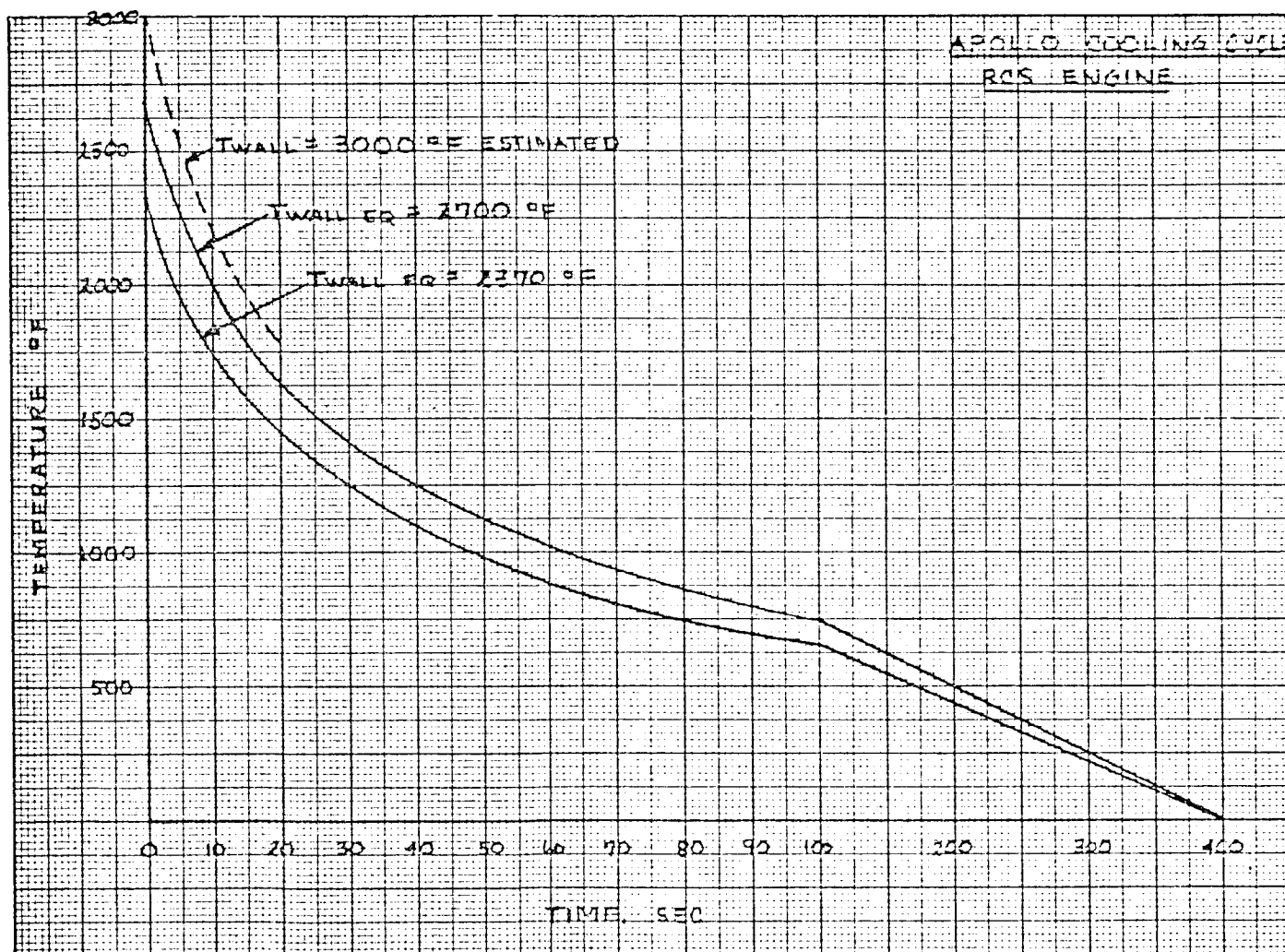


Figure 50

The results above indicate that the duty cycle is very important in determining engine life. We can consider engine failure to occur when the  $\text{Mo}_5\text{Si}_3$  coating is exposed thus, resulting in large increase in oxidation rate and no protective coating. The NAA duty cycle, which consists of short on times (milliseconds) and long off times (seconds-minutes) means that the chamber temperature is low ( $<1000^\circ\text{F}$ ) most of the on time and only a few cycles are essentially steady state runs. The loss of coating is essentially zero and would be the same for most duty cycles of this type.

The "worst" duty cycles and the steady state runs result in coating losses which are still insignificant for the range below  $2700\text{-}2800^\circ\text{F}$  equilibrium wall temperatures (based on 30 minute life). As the temperature of the chamber approaches the  $3000^\circ\text{F}$  range, examination of each individual duty cycle must be made. The NAA duty cycle would not result in significant losses at  $3000^\circ\text{F}$ , however, the "worst" duty cycle and steady state runs would result in significant loss of the coating at  $3000^\circ\text{F}$ .

### C. Conclusions

1. The disilicide coating life on molybdenum combustion chambers can be predicted from diffusion and sublimation data.
2. Good correlation between engine failure and loss of coating due to diffusion (for steady state runs) has been found.
3. Intermittent sublimation of the  $\text{SiO}_2$  from the inside wall to the hard vacuum during pulsing operation will not significantly contribute to engine coating loss.
4. The loss of coating from the outside of the engine will not affect engine operation.
5. Inside wall coating loss is negligible when subjected to duty cycles involving milliseconds "on" time and seconds-minutes "off" time for chambers which have equilibrium wall temperatures up to  $3000^\circ\text{F}$  (30 minutes total "on" time).

REFERENCES

1. Philco, Investigation of Mechanisms for Oxidation Protection and Failures of Intermetallic Coatings for Refractory Metals, Quarterly Progress Reports 4, U2239, 15 July 1963; 5, U2325, 15 October 1963; 6, U2492, 15 January 1964; 8, U2675, 15 July 1964; 9, U2885, 15 October 1964.
2. IOM to S.J.Minton from C.Stechman; Subject, "Sublimation of Disilicide from Molybdenum Combustion Chambers, " dated 22 April 1965.

BIBLIOGRAPHY

1. Marquardt Report PR 281-3Q4, "Stability and Emittance of Molybdenum Disilicide Coating Under Varying Temperatures and Pressures," March 1, 1963.
2. ASD-TDR-63-753 (Part I) "Investigation of Mechanisms for Oxidation Protection and Failure of Intermetallic Coatings for Refractory Metals," July, 1964.
3. ASD-TDR-63-753 (Part II) Ibid, June, 1963.
4. Thompson Ramo Wooldridge Report TM3320-67; Advancement of High Temperature Protective Coatings for Columbium Alloys, 26 October 1963.
5. Lockheed Missiles and Space Company, "Coatings for Refractory Metals in Aerospace Environments," Report 2-84-63-2, Second Quarterly Progress Report.
6. Ibid, Report No. 2-04-64-1.
7. NASA TND-2040, "A Study of Several Oxidation Resistant Coatings on Mo-0.5 Ti Alloy Sheet at 2500°F.
8. NASA TND-2039, "Diffusion Studies of Several Oxidation Resistant Coatings on Mo-0.5 Ti Molybdenum Alloy at 2500°F," August, 1964.
9. ASD TDR-62-934, "Advancement of High Temperature Protective Coatings for Columbium Alloys," April, 1964.
10. "Test Program to Study the Vaporization of Durak "B" in Vacuum at Elevated Temperature," Hughes Aircraft Report P63-41, August, 1963.
11. Refractory Molybdenum Silicides, Climax Molybdenum Company Bulletin Cdb-6A.